10/12-2-91 JSO (1)

SANDIA REPORT

SAND89—1639 • UC—814
Unlimited Release
Printed October 1991

Yucca Mountain Site Characterization Project

Yucca Mountain Project Thermal and Mechanical Codes First Benchmark Exercise Part III: Jointed Rock Mass Analysis

Laurence S. Costin, Stephen J. Bauer

Prepared by
Sandia National Laboratories
Albuquerque, New Mexico 87185 and Livermore, California 94550
for the United States Department of Energy
under Contract DE-AC04-76DP00789

DISTRIBUTION OF THIS DOCUMENT IS UNLIMITED

"Prepared by Yucca Mountain Site Characterization Project (YMSCP) participants as part of the Civilian Radioactive Waste Management Program (CRWM). The YMSCP is managed by the Yucca Mountain Project Office of the U.S. Department of Energy, DOE Field Office, Nevada (DOE/NV). YMSCP work is sponsored by the Office of Geologic Repositories (OGR) of the DOE Office of Civilian Radioactive Waste Management (OCRWM)."

Printed in the United States of America. This report has been reproduced directly from the best available copy.

Available to DOE and DOE contractors from
Office of Scientific and Technical Information
PO Box 62
Oak Ridge, TN 37831

Prices available from (615) 576-8401, FTS 626-8401

Available to the public from
National Technical Information Service
US Department of Commerce
5285 Port Royal Rd
Springfield, VA 22161

NTIS price codes
Printed copy: A11
Microfiche copy: A01

SAND--89-1639

DE92 003611

SAND89-1639
Unlimited Release
Printed October, 1991

YUCCA MOUNTAIN PROJECT
THERMAL AND MECHANICAL CODES
FIRST BENCHMARK EXERCISE
PART III: JOINTED ROCK MASS ANALYSIS

Laurence S. Costin and Stephen J. Bauer

Geotechnical Design Division, 6314
Sandia National Laboratories
Albuquerque, NM

ABSTRACT

Thermal and mechanical models for intact and jointed rock mass behavior are being developed, verified, and validated at Sandia National Laboratories for the Yucca Mountain Site Characterization Project. Benchmarking is an essential part of this effort and is one of the tools used to demonstrate verification of engineering software used to solve thermomechanical problems. This report presents the results of the third (and final) phase of the first thermomechanical benchmark exercise. In the first phase of this exercise, nonlinear heat conduction codes were used to solve the thermal portion of the benchmark problem. The results from the thermal analysis were then used as input to the second and third phases of the exercise, which consisted of solving the structural portion of the benchmark problem. In the second phase of the exercise, a linear elastic rock mass model was used. In the third phase of the exercise, two different nonlinear jointed rock mass models were used to solve the thermostructural problem. Both models, the Sandia compliant joint model and the RE/SPEC joint empirical model, explicitly incorporate the effect of the joints on the response of the continuum. Three different structural codes, JAC, SANCHO, and SPECTROM-31, were used with the above models in the third phase of the study. Each model was implemented in two different codes so that direct comparisons of results from each model could be made. The results submitted by the participants showed that the finite element solutions using each model were in reasonable agreement. Some consistent differences between the solutions using the two different models were noted but are not considered important to verification of the codes.

This work was performed under WBS 1.2.4.2.3.1. The SNL Quality Assurance Program Plan (including Department 6310 QAPP specific to the YMP) was in effect during the course of this work. Criteria 1-7 and 15-18 of the QAPP applied to this work. Department Operating Procedures 2-4, 3-2, and 3-3 were specifically used to assure quality in the conduct of these analyses. The analysis definition was developed interactively through interactions with the participants. This report was reviewed by two technical peers, line management, and was reviewed for policy concerns by the YMP Office. The future application of the exercise detailed in this report will be considered quality affecting. More discussion of the specific QA requirements are in Section 4.1 of this report.

TABLE OF CONTENTS

TABLE OF CONTENTS (Concluded)

LIST OF FIGURES

LIST OF FIGURES (Continued)

LIST OF FIGURES (Continued)

LIST OF FIGURES (Continued)

LIST OF FIGURES (Continued)

LIST OF FIGURES (Continued)

LIST OF FIGURES (Continued)

LIST OF FIGURES (Continued)

LIST OF FIGURES (Continued)

LIST OF FIGURES (Continued)

LIST OF FIGURES (Continued)

LIST OF FIGURES (Concluded)

LIST OF TABLES

1.0 INTRODUCTION

1.1 Background

Computer software that incorporates thermal and structural models for intact and jointed rock mass behavior is being developed, verified and validated at Sandia National Laboratories (SNL) for the Yucca Mountain Site Characterization Project (YMP), administered by the Nevada Operations Office of the U.S. Department of Energy. Scientific and engineering software used in substantiating a license application for a potential radioactive waste repository must meet certain requirements intended to satisfy the Nuclear Regulatory Commission as to the the quality of the software. Software verification is addressed in this report. In this context, a distinction between software and models needs to be made. A model is a mathematical representation of a physical process. Software is a numerical tool used to solve the equations associated with the model. Thus, software verification addresses the correctness of the implementation of the model equations and numerical techniques used to solve those equations.

One means of demonstrating verification and assessing the characteristics of engineering software is benchmarking, defined here as the comparison of the results obtained using one piece of software with those obtained using other software applied to identical problems. One advantage of benchmarking is that many parameters are available for independent comparison. In a benchmarking exercise, numerous mechanical and thermal parameters (stresses, strains, strain rates, displacements, joint motion, temperatures, etc.) can be compared over the entire analysis region. With the exact specification of geometry and material properties, many uncertainties in the comparison of results can be removed.

1.2 Objectives and Scope of the Benchmark Exercise

In the first thermomechanical benchmark exercise, a specific thermomechanical boundary value problem is solved. The problem is a generic extraction of a typical problem likely to be run by design analysts. However, the analyses performed as part of this exercise should not be considered to represent any type of "reference" analysis for repository design. The benchmark exercise as specified by Problem Definition Memo 71-032 (Appendix A of Costin and Bauer, 1989) includes three separate comparative analyses: a thermal analysis (Costin and Bauer, 1989), a structural analysis using a linear elastic rock mass model (Bauer and Costin, 1990), and a structural analysis using two different nonlinear continuum joint rock mass models (this report). The two structural analyses use, as inputs, the temperature histories resulting from the thermal analysis. Each of the three analyses were performed by several different analysts using a number of different codes. The participating analysts and the codes used in this exercise are discussed in Section 3.

The codes and models to be used for this problem were chosen so that several comparisons could be made. For the thermal analysis, one comparison was among the results of several thermal codes solving the same problem. This comparison assisted in documenting the verification of the thermal codes. In addition, the results obtained by different analysts using the same code were compared to document the variability in results that can be expected solely as the result of the analysts' preferences in meshing and running a problem (Costin and Bauer, 1989). In the second part of the benchmark exercise, the results of the structural calculations using a linear elastic rock mass model (denoted linear elastic analysis) were compared. This comparison assisted in demonstrating verification of the structural codes for their intended use within the YMP and will provide baseline results for assessment of the results from the nonlinear analyses. The final analysis, a thermomechanical analysis using nonlinear continuum rock mass models, compares results from two different models as well as results from different codes using the same model. Thus, further code verification will be achieved as well as verification of the implementation of these new models. In addition, a direct comparison of the results of both models run with the same codes will provide a means of assessing the differences in the response predicted by the two models. The two continuum joint models to be used are the compliant joint model (CJM) (Chen, 1987) and the joint empirical model (JEM) (Blanford and Key, 1989). These models are essentially different mathematical descriptions and implementations of the same physical processes; that is, joint closure under normal stress and joint shear as a result of normal and shear stresses are explicitly addressed in both models.

The codes and models used in this benchmark exercise are only a subset of those being considered for use in repository design. Other codes, such as those based on discrete block motion rather than continuum principles, have been developed and reported in the literature. This class of model is also under consideration for use in the project.

1.3 Report Outline

The remainder of this report will be limited, as much as possible, to discussions and results of the third part of the benchmark problem, the jointed rock mass analysis. In Section 2, a general description of the benchmark problem will be presented. The structural portion of the problem will be discussed in some detail. The participant groups, analysts, codes, and models used for the jointed rock mass solutions are presented in Section 3. An overview of the benchmarking process is given in Section 4, along with a discussion of the the specific control procedures and requirements specified in the problem definition memo. These controls were instituted to ensure that project quality assurance requirements were met. Section 5 presents the comparison of the results from all participants in graphical form. Three separate sets of analyses were performed during the jointed rock mass analysis phase of the benchmark exercise. The initial attempt at a solution was suspended after some participants reported difficulties in obtaining solutions beyond the first few time steps. Such difficulties are not unusual when attempting to solve nonlinear problems. After meeting to discuss and resolve the problems, a second attempt at completing the solution was successfully completed by all participants. During this analysis, it was noted that some improvements to the numerical method used in the CJM to solve the joint stress-strain equations could be easily implemented. Thus, a new release of the CJM was produced. Further, the differences were noted between solutions using the same model. In order to investigate the reasons for these differences and to provide a benchmark comparison of the revised CJM, a third analysis was performed. Comparative results of all three analyses, as well as discussion of the decisions and evaluations made during the course of this portion of the benchmark exercise, are given in Sec ion 5. The results from the latter two analyses, which were completed, are evaluated in Section 6. Section 7 presents conclusions of the authors based on their review of the results.

2.0 PROBLEM FORMULATION

2.1 Problem Selection

The benchmark problem was designed to be a generic representation of a typical repository design analysis. For this reason, the drift dimensions, rock properties, and nominal in situ stresses were taken to be identical with those listed in the YMP Reference Information Base (RIB), Version 2.002 (draft). The rationale for using a geometry and material properties typical of those expected in waste emplacement panels at Yucca Mountain was to make the benchmark problem typical of the kind of problem that the codes being benchmarked would be required to solve as part of the license application design process. The principal investigators (PI) thought that it was highly desirable to provide evidence and documentation of code verification efforts that were specific to the intended use of the particular codes involved.

The initial problem was formulated and issued to the participants on November 2, 1987, in the form of a draft problem definition memo (PDM). The participants had several weeks to review the draft and prepare comments. On December 13, 1987, a meeting of the PIs and participants was held to review the comments. As a result of this review, several minor changes to the draft were made, and a final PDM was issued under a cover letter dated December 23, 1987 (Appendix A, Costin and Bauer, 1989). The PDM completed management review and was sent to the participants on January 4, 1988.

2.2 Problem Definition

The problem is described in detail in Problem Definition Memo 71-032 (Appendix A, Costin and Bauer, 1989). Only a brief summary of the important features of the problem definition is presented here.

2.2.1 General Description

The problem geometry is a two-dimensional idealization of an infinite series of drifts with the approximate dimensions of the proposed design for vertical emplacement of nuclear waste at Yucca Mountain (Figure 2-1). From symmetry, the region to be analyzed can be reduced to a vertical strip extending from the centerline of the drift to the centerline of the adjacent pillar. Plane strain conditions were assumed for the structural calculations. The analyses were to be performed in three phases: thermal solution (using thermal codes only - documented in Costin and Bauer, 1989) thermomechanical solution using the linear elastic rock mass model (mechanical codes with input from the thermal solutions documented in Bauer and Costin, 1990) and thermomechanical solution using jointed rock mass models (mechanical codes with input from the thermal solutions). After each phase was completed, a letter report and results from each participant were to be forwarded to the PIs for review and comparison of results. This report discusses the results of the third phase (jointed rock mass analysis) only.

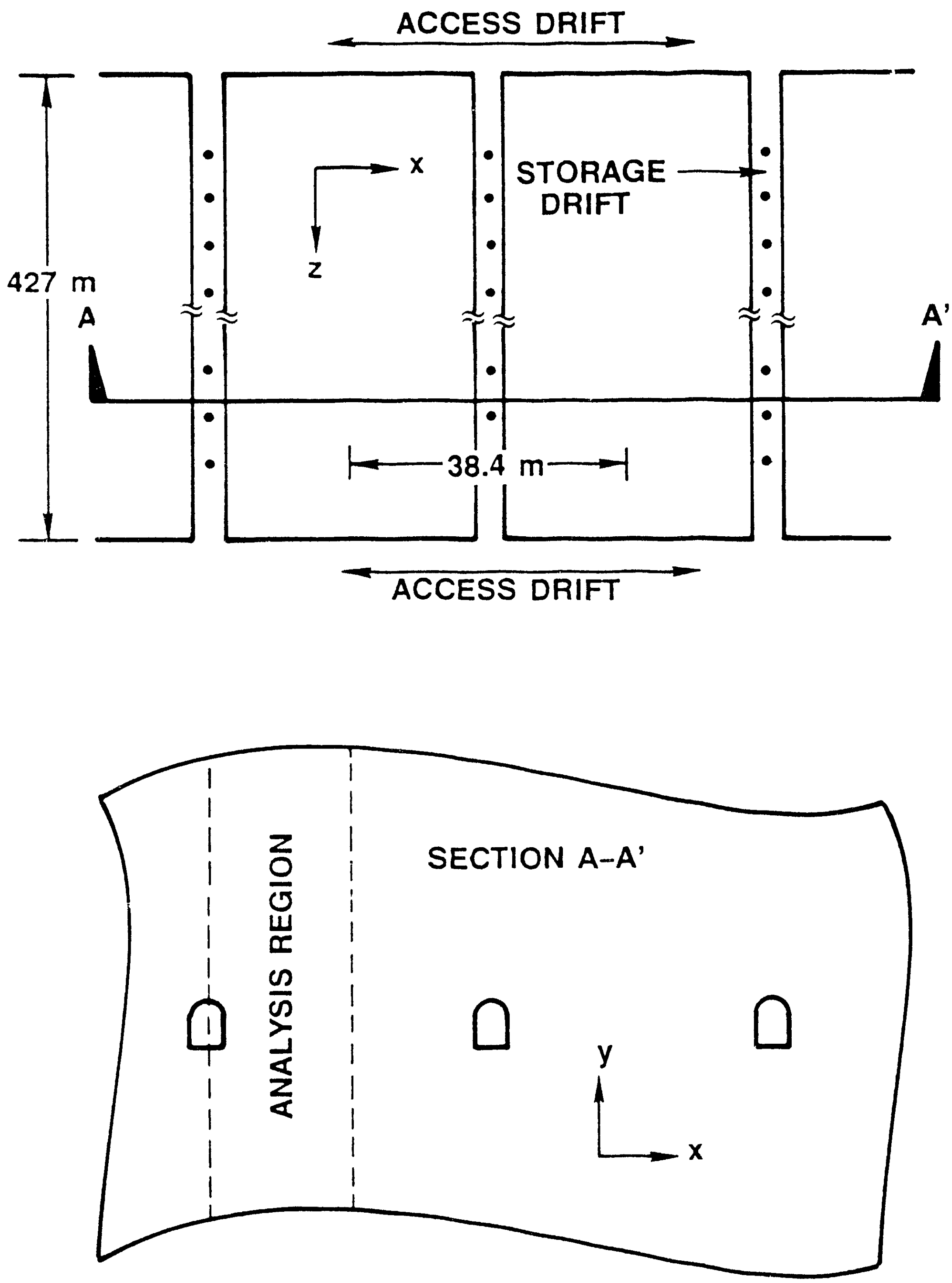

Figure 2-1. Sketch of the Panel in the Vertical Emplacement Configuration and the Analysis Region for the Benchmark Problem

2.2.2 Jointed Rock Mass Analysis

The structural analysis using jointed rock mass models was conducted with three finite element codes: JAC (Biffle, 1984), SPECTROM-31 (Key and Labreche, 1990), and SANCHO (Stone et al, 1985). Two different jointed rock mass models were used. The CJM (Chen, 1987) was implemented in both JAC and SANCHO whereas the JEM (Blanford and Key, 1989) was implemented in SPECTROM-31 and SANCHO.

2.2.2.1 Geometry, Boundary Conditions, and Loads

The problem geometry and boundary conditions are shown in Figure 2-2. The region analyzed is a strip that is bounded by the centerline of the drift on the left and by the centerline of the pillar on the right. The rock mass is assumed to be uniform and homogeneous throughout. The drift has a horizontal floor, a vertical side wall, and an arched roof. The roof is formed by a circular sector with a radius of 2.74 m. The intersection of the floor with the side wall is rounded with a radius of 0.3 m. This was done to reduce the stress concentration at the corner of the drift. The floor of the drift is located 311 m below the surface, and the lower boundary of the modeled region extends 100 m below the drift floor.

A line of heat sources was simulated as being buried 3.05 m below the center of the drift floor. Details of the thermal phase of the benchmark problem are given in Costin and Bauer (1989). The temperature histories of each nodal point in the finite element mesh resulting from the thermal calculations were used as input to the structural analyses (both the linear elastic and the nonlinear jointed rock analyses). The thermal solutions generated in part 1 of the benchmark exercise were close enough that they do not cause discrepancies in results generated in Part 3 of the benchmark exercise. For the structural analyses, the heated region was assumed to have the same mechanical properties as the surrounding rock.

The analysis region was defined as a vertical slice taken from an infinite array of emplacement drifts. The vertical boundaries of the region extend through the centerline of the drift and the centerline of the pillar. The vertical extent of the modeled region extends 100 m above and below the floor of the drift (Figure 2-2). The vertical extent of the analysis region is somewhat smaller for the structural calculations than was the case for the thermal calculations. This is because the thermal problem required that the boundaries be farther away from the drift to avoid having them affect the thermal solution in the region to be used for the structural analysis. To account for the overburden load of the rock and soil over the modeled region, an overburden pressure of 4.72 MPa was applied to the top of the region. This pressure was calculated from the thickness and density of the overlaying strata as given in the RIB (see Appendix A of Costin and Bauer, 1989). A vertical body force equivalent to the gravitational loading of the rock in the modeled region has also been applied. In the PDM the ratio of initial horizontal to vertical in situ stress in the modeled region was specified as 0.5. Thus, both the horizontal and vertical in situ stresses increased with depth in the modeled region. The bottom of the modeled region (100 m below the floor of the drift, 411 m below the earth's surface) has been constrained from

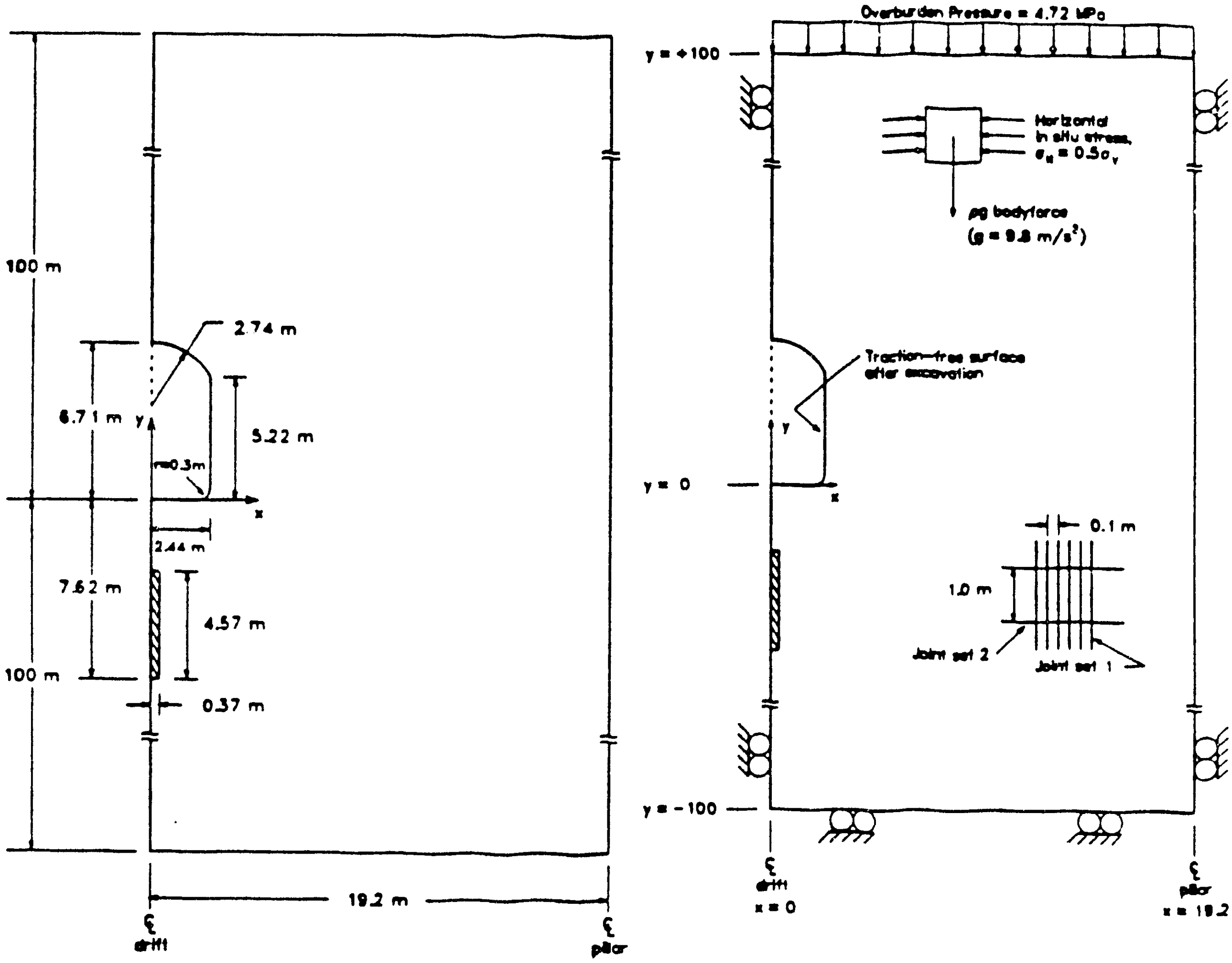

a. Analysis Region

b. Boundary Conditions

Figure 2-2. Analysis Region and Boundary Conditions vertical displacement. Because of the assumed symmetry, horizontal displacements are constrained to be zero along the vertical boundaries (Figure 2-2). Plane-strain conditions were assumed to exist so that strains parallel to the drift are zero.

The solution was to start at a problem time of zero years and run through a problem time of 101 yr. The drift was assumed to be mined instantaneously at a time of 0.5 yr. The heat source became active at a problem time of 1 yr.

2.2.2.2 Material Characterization

Both the thermal and mechanical properties were assumed to be uniform throughout the rock mass. The value of each property or material model parameter used in the solution was taken from the RIB Version 2.002 (draft), assuming the drift was located in the TSw2 thermal/mechanical unit. Specific values assigned each parameter are given in Table 2-1. Because two different jointed rock mass models were used in this phase of the benchmark analysis, two sets of material parameters for the jointed rock mass were identified. Care was taken to ensure that the values assigned to the material parameters of each model were such that the behavior of the models would be as nearly equivalent as possible. Completely equivalent behavior, of course is not possible because of the somewhat different assumptions about the physical behavior of joints that are incorporated into the models (Section 3). The judgment on equivalent behavior was based on making the normal closure versus normal stress and the shear displacement versus shear stress (at constant normal stress) curves for joints in each model as nearly the same as possible. The JEM contains an empirical method for scaling joint properties, as measured on laboratory samples, to the equivalent field-scale joint properties. The CJM assumes that laboratory and field properties are equivalent. Thus, the scaling parameters in the JEM were set such that laboratory and field scales were the same. Further, the JEM allows for dilatation of the joint resulting from slip displacement. The CJM does not contain this feature, so no joint dilatation was used in the JEM.

2.2.2.3 Output Specifications

Specific information concerning the calculations and the results was required in order to completely evaluate the benchmark exercise and the codes and models used. In addition, the results provided by each participant was to be sent in a specific format so that direct comparisons could be made easily. All results were transmitted by a letter report to the PIs along with a computer-readable copy (magnetic tape or floppy disk) of the source code and required plot files.

Each participant was required to provide the following information for their solution:

- problem run time (CPU seconds);
- computer used;

TABLE 2-1

MATERIAL PROPERTIES USED IN THE JOINTED ROCK MASS MODEL BENCHMARK ANALYSIS

Material/Model	Parameter	Value
Intact Rock		
	Young's modulus	30.4 GPa
	Poisson's ratio	0.24
Rock Mass		
	Density	2.32 Mg/m^3
	Coefficient of thermal expansion	8.8 X 10^{-6} K^{-1} (T < 200°C) 24.0 X 10^{-6} K^{-1} (T > 200°C)
	Joint spacing	0.1 m (vertical joints) 1.0 m (horizontal hoints)
Compliant Joint Model		
	Joint cohesion	0.1 MPa
	Joint friction coefficient	0.54
	Unstressed aperture	0.030 mm
	Half closure stress	2.0 MPa
	Shear stiffness (G_s)	1.0 X 10^6 MPa/m
	Shear hardening (G_{sp})	1.0 X 10^4 MPa/m
Joint Empirical Model		
	Unstressed aperture	0.030 mm
	Half closure stress	2.0 MPa
	JRC_o	9.0°
	JRS_o	171.0 MPa
	Base (residual) friction angle	28.4°
	Joint dilatation	None
	Laboratory joint length (L_o)	0.1 m (both sets)
	Characteristic (block) length (L_n)	0.1 m (both sets)

- convergence criteria and tolerance used for the solution; and

- mesh statistics:
  - figure showing the undeformed mesh,
  - the number of nodes,
  - the number and type of elements,
  - the number of degrees of freedom, and
  - the minimum and maximum node spacing.

Three sets of solution results were required. First, the displacement histories of three points on the perimeter of the drift were required. These displacement histories included the vertical and horizontal displacements of Point B (shown in Figure 2-3) and the vertical displacement at Points A and E. Second, displacement profiles along Lines 1 and 3 (Figure 2-3) were required. The vertical displacement as a function of position along Line 1 and the horizontal displacement along Line 3 were required for problem times 0.5, 1, 6, 11, 26, 76, and 101 yr. Finally, stress profiles along Lines 1, 2, 3, and 4 were required at times 0.5, 6, 11, 26, 76, and 101 yr. Specifically, plots of the horizontal and vertical normal stress components along Lines 1 and 2, the vertical normal stress and the in-plane shear stress along Line 3, and the horizontal normal stress along Line 4 were required. These results produced 60 different plots from each solution that could be compared.

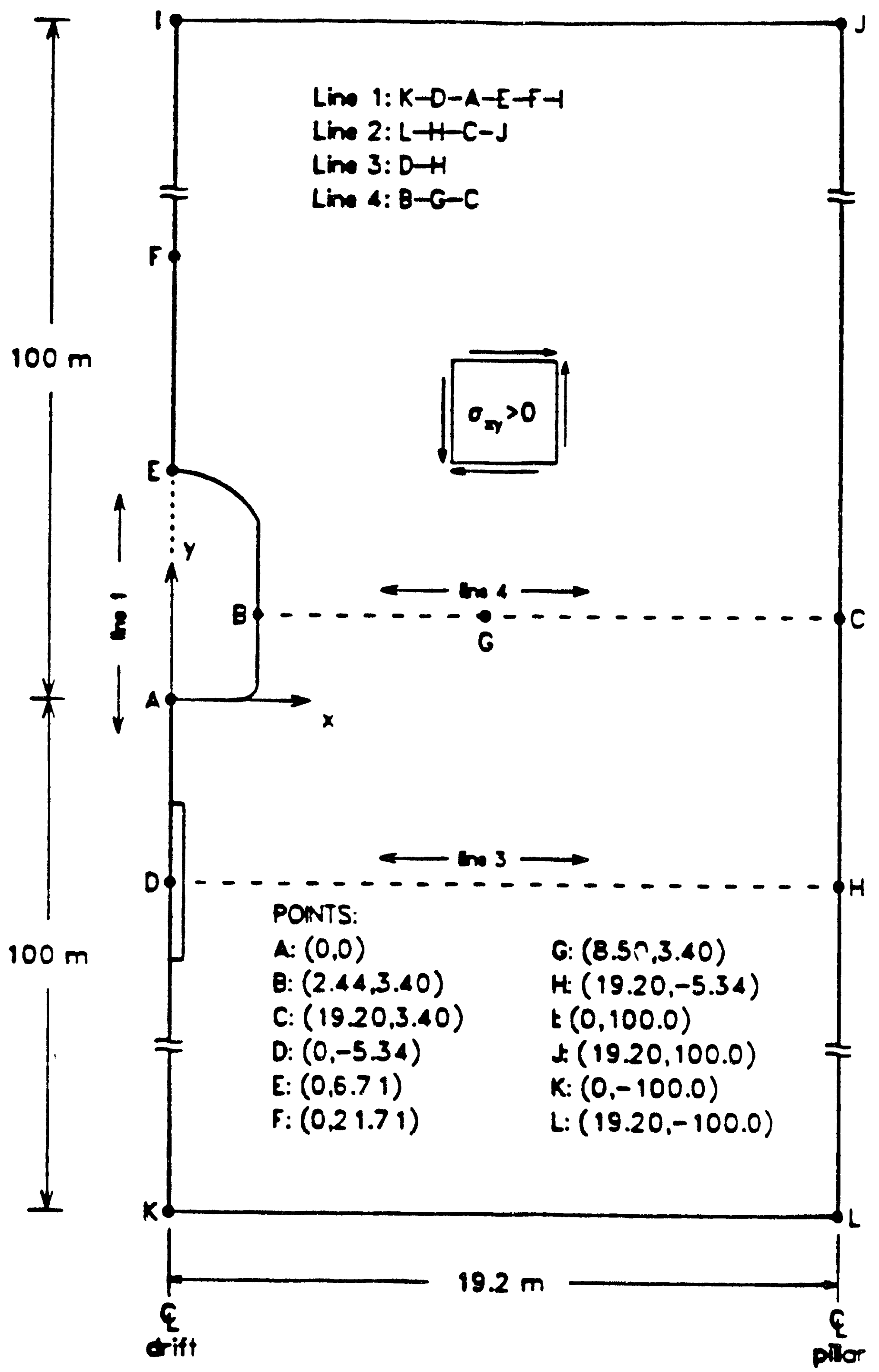

Figure 2-3. Locations and Conventions Used in Reporting the Results of the Benchmark Exercise

3.0 PARTICIPANTS

3.1 Participant Identification

The participant groups, specific analysts assigned, and the structural codes used are shown in Table 3-1. Three organizations are participating in the exercise: J.F.T. Agapito & Associates, Inc. (JFTA&A), located in Grand Junction Colorado; SNL's Applied Mechanics Division (Division 1523); and RE/SPEC Inc. (RSI), located in Albuquerque, New Mexico. Because of the number of thermal and structural code combinations being used in the benchmark exercise, SNL and RSI each assigned two analysts to the problem so that each analyst would be responsible for only one thermal and mechanical code combination.

The thermal codes used to generate the temperature histories that were in turn used as input to the structural calculations are discussed in a previous report (Costin and Bauer, 1989). In that report, the results from the three thermal codes (DOT, COYOTE, and SPECTROM-41) used as input for the present calculations were shown to be nearly identical. Thus, any differences in results from the structural calculations should not be a result of using temperature histories from different codes.

The code designator given each analyst-code combination listed in Table 3-1 is used to identify the results from that run in the figures presented in Section 5.

TABLE 3-1

PARTICIPANT ORGANIZATIONS, ANALYSTS, AND CODES USED

Participant Organization	Analyst	Structural Code/Version	Joint Model	Designation
JFTA&A	Asgian	JAC v2.01[a]	CJM	DOT/JAC/CJM
SNL	Holland	JAC v2.0[a]	CJM	COY/JAC/CJM
	Koteras	SANCHO v1.0[b]	CJM	COY/SANCHO/CJM
RSI	Petney	SANCHO v1.03[b]	JEM	SP41/SANCHO/JEM
	Labreche	SPECTROM-31 v3.09	JEM	SP41/SP31/JEM

a. JAC v2.01 is identical to JAC v2.0 except for modifications required to run on the JFTA&A computer.

b. SANCHO v1.03 is identical to SANCHO v1.0 except for modifications required to run on the RSI VAX system.

3.2 Code and Model Descriptions

In this section, the three codes and two material models used in the jointed rock mass model solution portion of the benchmark exercise are briefly described.

3.2.1 JAC

JAC (Biffle, 1984) uses the nonlinear conjugate gradient procedure to solve iteratively quasistatic nonlinear mechanics problems. A set of continuum equations is used that is very convenient for use with the conjugate gradient method and accurately describes nonlinear mechanics involving large rotation and strain. The method is exploited in a two-dimensional plane-strain or axisymmetric setting while using various methods for accelerating convergence. Sliding interface conditions are also implemented using a master-slave algorithm. A four-node Lagrangian uniform strain element with single point integration is used with orthogonal hourglass viscosity to control the zero energy modes. The program is vectorized to make optimal use of the CRAY 1 computer architecture.

3.2.2 SANCHO

SANCHO (Stone et al., 1985) was developed to solve the quasistatic, large deformation, inelastic response of two-dimensional solids. The element used is a bilinear isoparametric quadrilateral with a constant bulk strain. The equilibrium solution strategy uses an iterative scheme designed around a self-adaptive dynamic relaxation algorithm. The iterative scheme is based on explicit central difference pseudo-time integration with artificial damping. The code is explicit in nature so that no stiffness matrix is formed or factorized, which reduces the amount of computer storage necessary for execution. A sliding interface capability, based on a master-slave algorithm, is also incorporated in SANCHO.

3.2.3 SPECTROM-31

SPECTROM-31 (Key and Labreche, 1990) is a finite element method computer program designed to calculate the large deformation, elastic and inelastic, static and quasistatic response of two-dimensional solids. To accommodate a wide variety of applications, finite strain calculations are incorporated. Spatially, the program uses an eight-node isoparametric quadrilateral element. In time, the program solves for equilibrium using a modified Newton-Raphson iteration. Because the time-stepping scheme is sensitive to material nonlinearities and geometric changes, the program continuously monitors the number of iterations per load step and adjusts the load step to keep the calculation stable. Fixed or moving displacement boundary conditions are provided. Pressure and shear boundary loadings are allowed. Thermal loads are implemented via a predefined temperature history. Body forces resulting from gravity are incorporated. Initial stress conditions tailored to the in situ stresses common in geologic analyses are a feature of the code. The program functions entirely in core using a symmetric linear equation solver that stores only active column heights.

3.2.4 Compliant Joint Model

The CJM is a continuum constitutive model for describing the behavior of jointed media (Chen, 1987). A two-dimensional version of the model was numerically implemented in the form of a subroutine called ORTHO.UPD. This subroutine is used by the JAC and SANCHO codes to solve structural problems. The current numerical model (ORTHO.UPD) allows for two different sets of joints oriented orthogonally to each other with their strikes normal to the plane of interest. The model is a continuum approximation based on summing the discontinuous displacements across a number of joint planes contained within a representative elementary volume. The continuum approximation captures the gross response of the rock by smearing the individual responses of the joints. The approximation yields satisfactory results when the least dimension of the representative rock volume is approximately five to ten times larger than the joint spacings so that enough joints exist in the representative volume to validate the averaging process. The constitutive description of the rock mass assumes a linear elastic rock matrix with nonlinear normal and shear joint behavior between the joint planes. The deformation response normal to each joint is assumed to be nonlinear elastic. Joint shear response (shear stress versus shear displacement) is treated as linear elastic before attaining a critical stress level governed by the Coulomb friction criterion. Beyond the critical stress value, a linear relationship, analogous to strain-hardening plasticity, governs the shear stress versus joint slip displacement relationship. In this model there is an explicit coupling between joint slip and the normal stress on the joint through the Coulomb criterion. However, there is no coupling between slip displacement and normal displacement (i.e., shear induced dilation or compaction of the joint is not accounted for). All material parameters in the model, with the exception of the joint aperture, which should be measured on in situ joints, can be obtained from laboratory experiments on single-joint specimens.

3.2.5 Joint Empirical Model

The JEM (Blanford and Key, 1989) is a continuum numerical model that can be used in finite element based stress analyses. The model was developed under the assumption that joints are contact discontinuities; that is, the stress normal to the joint surface and the shear stress parallel to the joint surface are continuous across the joint. Because of the continuum approximations, the joint spacing is assumed to be small compared to a representative volume of material. The implementation is fully three-dimensional and allows for up to four sets of joints to be specified. However, when used with a two-dimensional code, the orientations of the joints are restricted by dimensional and symmetry considerations. The matrix rock is assumed to be linearly elastic and isotropic. The behavior of individual joints is based on Barton's (1982) empirical relations that were developed from field and laboratory experiments on joints. The joint normal behavior is assumed to be nonlinear elastic (identical to the CJM). The shear behavior of the joints is assumed to be governed by Amonton's law of friction (Bowden and Tabor, 1954), which is similar to the Coulomb slip criterion used in the CJM. However, in the JEM, a joint sustains any shear stress up to its current shear strength without displacement. The shear strength is proportional to the normal stress acting across the joint. The shear strength is also a complex function of geometry (joint roughness coefficient, JRC), strength (joint compressive strength, JCS), and scaling (ratio of field to laboratory-scale lengths) parameters. Thus, some attempt is made to scale laboratory measurements of joint slip to the behavior of in situ joints based on measurements of in situ joint apertures and roughnesses. Finally, dilation of the joint resulting from shear displacement is characterized by a dilatation angle, the tangent of which is the rate of change in normal displacement with respect to shear displacement. The dilatation angle is a function of the roughness (JRC) and the applied normal stress.

4.0 CONTROL PROCEDURES

4.1 Quality Assurance Requirements

This benchmark exercise is being conducted under the procedures detailed in Nuclear Waste Repository Technology (NWRT) Department Operating Procedures for Analysis Control and Verification (DOP 2-4) and for Analysis Definition (DOP 3-3). For the work done, the data transmission procedures are described in Section 4.3; no interface procedural controls were in place at the time the work was done. The analysis was defined in a PDM that completely described the problem to be solved and the reporting requirements (Appendix A of Costin and Bauer, 1989). A draft of the PDM was first issued so that the participants could review the problem and submit comments on it. The participants then met to review and resolve all comments to their satisfaction so that a final PDM could be issued. DOP 2-4 requires that the conduct and results of the benchmark analyses be subjected to independent technical review. This requirement is being met by documenting fully each phase of the exercise in a report and submitting the report to technical and management review before release. In addition, it is intended that the results of this benchmark exercise be subjected to a peer review by a panel composed of technical experts not directly connected with the YMP.

Department operating procedures also specify requirements for control and documentation of the software used in the analyses (DOP 3-2, Rev. A). These procedures did not come into force before the start of the benchmark analyses. However, for the jointed rock mass analysis phase of the benchmark exercise, all requirements for software configuration management and certification had been met. The specific versions of the codes certified for use at the beginning of this portion of the exercise are given in Table 3-1. To ensure that a complete record of the codes and procedures used in the benchmark exercise is maintained, the PDM required each participant to submit a computer-readable version of each code used, the input files for the code, and the required output files.

During the course of the initial analyses using the CJM an error in the way the model subroutine (ORTHO.UPD versions 1.0 and 1.01) calculated the unloading shear behavior was discovered. In addition, several improvements to the numerical solution routines used in the model were suggested by the participants. The error was corrected and the improvements were implemented using the procedure given in NWRT DOP 3-2. As a result, a new release of ORTHO.UPD was produced for use in the remainder of the benchmark exercise. During the time the model was being modified, a second set of analyses was authorized by the PIs. For these analyses, the participants were instructed (through a revision to the PDM) to use the original model (ORTHO.UPD versions 1.0 and 1.01) and set the shear hardening parameter (G_{sp}) to zero. This allowed the calculations to be completed with the original model without invoking the portion of the subroutine that contained the error. After modification, a new release of ORTHO.UPD was issued for use (version 1.1 for SNL and version 1.02 for JFTA&A). A third set of calculations was then performed using the new version of the model. Thus, three separate analyses were performed for the jointed rock mass portion of the benchmark exercise. A complete history and comparison of results of each analysis is given in Section 5.

4.2 Communication with Participants

All communication regarding the benchmark exercise was distributed through the PIs. Because each analyst, who was assigned a specific code to use, was expected to work the problem with no outside assistance, the PDM specifically required that the analysts not communicate among themselves. This also applied to analysts working for the same participant organization but using different codes. This requirement was invoked because of the desire to simulate conditions that occur during normal analyses. That is, the analyst was expected to follow the PDM exactly and contact only the PI for clarification, if required.

4.3 Transmission and Verification of Data

When each phase of the benchmark exercise was completed, the participants were required to submit a letter report that included how the analysis was conducted, any problems encountered, and hard copy and plots of the results. In addition, seven computer files of results (for the jointed rock mass analysis) were submitted on magnetic tape or floppy disk in ASCII format. These files were then read into the SNL VAX computer system and processed for comparison plots. Each set of computer results was plotted using the SNL system and compared with hardcopies of the plots provided by each participant. This allowed the PIs to verify that the data was transmitted and read correctly. No problems were encountered in transferring data to the PIs. Once the data was verified, a series of plots was prepared that compared the results from all participants. These results are discussed in the next section.

5.0 RESULTS

Although the PDM required that only a single analysis be completed by each participant using the assigned code and model combination, certain difficulties encountered during the analysis effort and the desire to document, as completely as possible, the effect on the results of certain analyst-controlled variables such as mesh size and convergence tolerance, three sets of analyses were actually completed and reported. In this section, the results of each analysis are presented separately along with observations concerning the comparisons of results. In addition, a narrative of the entire process is included to help the reader understand the progression of events and to document the rationale for the decisions made during this part of the benchmark exercise.

5.1 Results from the Initial Analysis

The initial analysis of the third part of the benchmark exercise began in May 1988. Several weeks later, an informal review of progress on the analyses revealed that several analysts were having difficulty completing the calculations. The analysts at RSI reported that their calculations using the JEM were proceeding very slowly, and they were having difficulties achieving global convergence of the solution at each time step. Similar problems were reported by Holland of SNL using the JAC code with the CJM. The two remaining analysts reported minor difficulties in getting solutions beyond 80 yr of problem time. As a result, the PIs decided that the effort should be suspended, and the results of the analyses, even though not complete in most cases, should be submitted in a letter report as prescribed in the PDM. After the results were compiled and compared, a review meeting was held on August 25 and 26, 1988, to discuss the problems encountered, review the results obtained thus far, and decide whether or not to continue the analysis. The results of this initial effort are given below in Sections 5.1.1 through 5.1.4.

5.1.1 Mesh Statistics and Computer Usage, Initial Analysis

Only one of the five analysts was successful in completing the calculation to the final problem time of 101 yr. The remaining four analyses were terminated before completion for various reasons. Table 5-1 gives a summary of the extent to which each calculation was completed, the computer time (CPU time) used, and the reason for suspending the calculation. Computer usage was not reported by JFTA&A for the initial analysis using DOT/JAC/CJM.

As part of the reported results, each participant was also required to provide some general information regarding the finite element mesh used. Table 5-2 lists the mesh statistics required by the PDM and discussed in Section 2.2.2.3 of this report. A mesh typical of those used by all finite element analyses is shown in Figure 5-1. The mesh shown in the figure is for the DOT/JAC/CJM computation. Meshes used by other analysts were quite similar, differing only in degree of coarseness or fineness near the drift.

TABLE 5-1

PROBLEM STATUS AND COMPUTER USAGE FOR INITIAL ANALYSIS

Code/Model	Computer	CPU Time (sec)	Last Problem Time Solved (yr)	Reason for Suspension
SP41/SANCHO/JEM	CRAY XMP	54,0001	7.125	Excessive CPU time
COY/SANCHO/CJM	CRAY XMP	49,9209	6.1	Convergence failure
SP41/SP31/JEM	VAX 11/750	892,800	6.0	Convergence problems
COY/JAC/CJM	CRAY XMP	53,580	29	Convergence failure
DOT/JAC/CJM	IBM PC/AT	-------	101	------------

TABLE 5-2

MESH STATISTICS FOR INITIAL ANALYSIS

Number of Nodes	Nodes/Degrees of Freedom	Type of Element	Number of Elements	Spacing (m)	
				Minimum	Maximum
SP41/SANCHO/JEM	981/1962	4-node quad	903	0.13	13.11
COY/SANCHO/CJM 9	2762/5524	4-node quad	2624	0.2959	2.608
SP41/SP31/JEM	2181/4362	8-node quad	682	0.02	12.7
COY/JAC	2144/4288	4-node quad	2068	0.185	5.469
DOT/JAC/CJM	851/1702	4-node quad	760	0.15	9.08

5.1.2 Displacement Histories at Selected Points, Initial Analysis

The vertical displacement histories at Points A and E (Figure 2-3) and the vertical and horizontal displacement histories at Point B from each code are compared in Figures 5-2 through 5-5, respectively. The predictions of vertical displacement at Points A, B, and E are all in reasonable agreement, except for the SP41/SP31/JEM calculation, which is obviously different at Points A and E. In addition, the COY/SANCHO/CJM calculation shows a large oscillation at Point E after about 60 yr. There is considerably more scatter in the predictions of horizontal displacement at Point B. The three CJM calculations show the same trend as do the two JEM calculations. However, the CJM calculations appear to converge at later times whereas the JEM results appear to diverge.

5.1.3 Displacements Along Selected Paths at Seven Times, Initial Analysis

The vertical displacements along Line 1 (from Point K through Point I on Figure 2-3) at 0.5, 1, 6, 11, 26, 76, and 101 yr are shown in Figures 5-6 through 5-12. Because Point K was restrained from vertical motion, the displacement at this point should be zero. The results at both 0.5 and 1 yr were requested to see if any effects of the instantaneous mining of the drift would show up in the results. The "ND" attached to the end of a code and model designator in the figures signifies that no data were available from that code and model combination for that plot time (i.e., the analysis was terminated before the time shown on the plot). Although the SANCHO/CJM calculation only ran through 96 yr, the final (96 yr) results are plotted for comparison on the 101-yr plots. The three CJM solutions agree quite well through 6 yr. At 11 and 26 yr the two JAC/CJM solutions are in good agreement with a small difference observed between those solutions and the SANCHO/CJM solution. Beyond 26 yr, the DOT/JAC/CJM and the COY/SANCHO/CJM solutions (the only two that went that far) are in good agreement, except for some oscillations in the COY/SANCHO/CJM solution near the drift. The two JEM solutions do not agree with each other and are different from the CJM solutions at 0.5 and 1 yr. At 6 and 11 yr, the SANCHO/JEM solution is in agreement with the three CJM solutions; but, the SP31/JEM solution is not in agreement at 6 yr, and no results are available at 11 yr.

Predictions of horizontal displacement along Line 3 (from Point D to Point H in Figure 2-3) are compared in Figures 5-13 through 5-19. Because of the symmetry conditions, the horizontal displacement at the two end points of Line 3 should be zero. The three CJM solutions are in good agreement through 26 yr, except for some oscillations in the DOT/JAC/CJM solution near the heat source (zero position on Line 3). At 76 and 101 yr, the DOT/JAC/CJM and the COY/SANCHO/CJM solutions are significantly different. The two JEM solutions predict somewhat larger displacements than those using the CJM. In addition, the two JEM solutions show a progressive divergence from 0.5 through 6 yr.

5.1.4 Stress Components Along Selected Paths at Six Times, Initial Analysis

Comparisons of predicted vertical and horizontal normal stresses along Line 1 (from Point K to Point I in Figure 2-3) at 0.5, 6, 11, 26, 76, and 101 yr are given in Figures 5-20 through 5-31. For the vertical stress, the agreement among the three CJM solutions up to 26 yr is good. The only differences occur in the heater region just below the floor of the drift. The SANCHO/CJM solution does differ slightly from the two JAC/CJM solutions near the drift. At late times the SANCHO/CJM solution has large oscillations near the drift. The near drift region is where the stress and displacement gradients are expected to be most severe. The oscillations in some of the solutions indicates that, locally, equilibrium is not being satisfied by the solution, although globally the measure of equilibrium may well be better than the required solution tolerance. The horizontal stress predictions are in better agreement overall, although oscillations in the SANCHO/CJM solution are evident at late times.

Figures 5-32 through 5-43 present the comparison of predicted vertical and horizontal stresses along Line 2 (from Point L to Point J in Figure 2-3) at the same times as the comparisons for Line 1. The results are somewhat better than those for Line 1 in that better agreement was achieved among codes using the same model. Because of its distance from the drift and heater, the stress gradients along Line 2 are less severe than those along other paths shown. Note that the oscillations in the solutions evident along Line 1 are not present along Line 2.

Along Line 3 (Point D to Point H in Figure 2-3) the PDM requested that the participants report both the vertical normal stress and the in-plane shear stress. These results are compared in Figures 5-44 through 55. Consistent with the previous results, there was good agreement among the predictions of vertical stress (Figures 5-44 through 5-49) for the two models beyond about 5 m from the heater. Within 5 m of the heat source, the solutions vary somewhat with sharp oscillations evident in some solutions. The predictions of shear stresses (Figures 5-50 through 5-55) show some variations in the reported results. The two JEM solutions appear to agree at 0.5 and 6 yr. The three CJM solutions also agree up to 26 yr with the exception of the DOT/JAC/CJM solution predicting lower stresses near the heat source. At 76 and 101 yr, the DOT/JAC/CJM and the SANCHO/CJM solutions are in total disagreement.

The horizontal normal stress predicted along Line 4 (Point B to Point C in Figure 2-3) from each code is compared in Figures 5-56 through 5-61. Because of the traction-free boundary at Point B (Figure 2-3), the horizontal stress should be zero at that point. Again, the three CJM solutions show some disagreement near the drift (4- to 10-m region along Line 4) but are in agreement farther from the drift. The two JEM solutions show just the opposite trend.

5.1.5 Evaluation and Discussion of Results from the Initial Analysis

In general, the results from all code and model combinations were in agreement. The exception was the SP31/JEM solution, which contained an input error resulting from the analyst's incorrect interpretation of the input parameters given for the JEM in the PDM. Specifically, the wrong scale factor (ratio of laboratory joint length to field-scale length) was used. It should be noted that the JEM and CJM showed the same trends in displacements and stresses, with the JEM tending to predict somewhat larger displacements than the CJM. Vertical stresses and displacements tended to be similar to the elastic solution (Bauer and Costin, 1990). The elastic solution used a rock mass modulus that was one-half of the intact rock modulus used in the present calculations. Thus, it appears that the 1-m spacing for horizontal joints, along with the proscribed joint properties is approximately equivalent to reducing the intact modulus by 50%. Horizontal displacements and stresses, especially near the heat source and the drift, tended to be more varied and, generally, larger than those predicted by the elastic solution. At later times (76 and 101 yr) large differences between the SANCHO/CJM and the DOT/JAC/CJM solutions were noted in some places.

One problem experienced by all analysts was the excessive amount of computer time required to obtain solutions at each time step. The CJM required a substantial amount of time in the fourth order root solver to find the roots during each global solution iteration. This, combined with the fact that from 1,000 to 80,000 iterations were required for each solution step, resulted in a large amount of computer time being used. The JEM apparently also caused very slow convergence at each time step. The slow convergence was attributed to the fact that it is implemented as a three-dimensional model. Thus, additional calculations are being performed that are not necessary for a simplified, two-dimensional problem.

A review meeting with the participants was held on August 25-26, 1988, to discuss the results of the initial analysis effort and to decide what steps needed to be taken to complete the benchmark exercise. The discussion during the meeting focused on two issues: first, determining what steps should be taken to improve the numerics of the models (so that the class of problems represented by the benchmark problem can be solved more easily) and second, determining what needs to be done to complete the benchmark exercise.

Two deficiencies in the CJM (ORTHO.UPD code) were brought to light as a result of the initial analysis. First, the shear hardening as envisioned in the model is not correctly implemented; second, the fourth-order root solver algorithm needs improvement because a great deal of computational time is spent in this routine. As a result, a modification request (MOD) was submitted as required by DOP 3-2 to correct these two problems. A new version of the model was expected to be released after completing the MOD.

Several potential problems regarding the reasons analysts were having difficulties with solution convergence in the nonlinear calculations were discussed at the review meeting. It was noted that the convergence criteria of the different codes were all different. Further, there is no single convergence criterion for explicit codes, such as those used in this exercise, that is accepted as the best. That is, it is very difficult to formulate a method for judging whether equilibrium has been achieved. The result is that the analyst must apply a quality judgment as to whether reasonable equilibrium has been achieved. This is especially difficult in nonlinear problems because what represents an adequate equilibrium solution is highly problem-dependent. Finally, it was noted that problems that are driven principally by thermal strains are an especially difficult class of problems for explicit codes to solve because of the large rigid body motions that may occur.

Based on the results of the review meeting, the PIs directed that the analysis effort should continue in an effort to get a complete set of results from each code and model combination. The PDM was modified to allow those using the CJM to use a shear hardening parameter (G_{sp}) of zero. This would circumvent the problem with the error in the unloading behavior and not significantly affect the results. The analysts were allowed to use reasonable means to obtain a complete solution to 101 yr problem time, which may include coarsening the mesh and loosening convergence tolerances. Once the solutions using the current versions of the models were completed, the models could be revised to correct any errors found or to improve the numerical methods. A second analysis of the benchmark problem would then be run to document the verification of the new model versions. This course of action was taken because the models are thought to contain the correct physics, and the improvements and error correction required for the CJM should not alter the solution to the benchmark problem. In addition, a full comparison of results would provide a good basis for updating the models if that proves necessary.

5.2 Results from the Second Analysis

The results of this second analysis were submitted by letter report from the participants during November 1988. On December 12, 1988, a second review meeting was held to present and discuss the results. All analysts succeeded in obtaining a complete solution to the problem; i.e., all solutions went to 101 yr. Before going into the details of the results, a brief discussion is presented on the differences in approach and methodology used by each analyst in running the benchmark problem the second time versus the initial analysis.

Sharon Petney (RSI) performed the SP41/SANCHO/JEM analysis. In the initial analysis, an error tolerance of 0.1% was used up to a limit of 800 iterations. If the error was 0.35% or less after 800 iterations, the solution was accepted. The calculation was terminated at 17.1 yr because of the large amount of computer time used to that point (900 CPU minutes on the Cray-XMP). For the second run, the error tolerance was increased to 0.2% and the problem was restarted. The problem ran to completion with an additional 270 minutes of computer time. This indicated that, in the first attempt, a great deal of computer time was used in iterations where the error was less than 0.2% but greater than 0.1%.

Richard Koteras (SNL) performed the COY/SANCHO/CJM analysis. Although the analysis was supposed to be performed with the original version of the CJM (ORTHO.UPD version 1.0) and with the shear hardening parameter set to zero, the calculation was performed with the updated version of the model (ORTHO.UPD version 1.1), and the originally specified value of the shear hardening modulus was used. Because no change to the physics of the model was made in the updated version and the model behavior is very insensitive to the shear hardening modulus, there should be no difference between the results of this calculation and the others using the earlier version. For the second analysis, a convergence tolerance of 3.0% was used along with changing DXSCALE from the default value of 0.9 to 0.5 (DXSCALE multiplies the internal time step used in the central difference time integrator in SANCHO and allows the user some control over the stability of the integration scheme).

Duane Labreche (RSI) performed the SP41/SP31/JEM analysis. The initial calculations were terminated at the 6-yr problem time because of excessive computer usage and the small step size required to get convergence. After the results were compared with other solutions, an input error in the joint scaling parameter was discovered. For the second analysis, this error was corrected, double precision was used, and an enhanced Newton-Raphson iterative solution method in SPECTROM-31 was invoked.

John Holland (Technadyne, SNL) performed the COY/JAC/CJM analysis. In the initial analysis, the calculation run terminated after the 29-yr problem time because of a failure to converge on the next time step, even with zero shear hardening specified. The convergence failure was apparently a result of large displacements being predicted in the floor of the drift. These displacements were apparently the result of zero energy-mode (keystone) deformations. For the second analysis, the artificial viscosity, used to control keystone deformations, was increased from 10 to 100. This was the only change made. The convergence tolerances used were 0.001 on forces and 0.0001 on displacements. The problem ran to completion at 101 yr. Results from the second run compared with those from the initial analysis from zero to 26 yr showed very good agreement, which demonstrates that the increased viscosity used in the second run did not significantly alter the solution but did suppress the zero energy mode deformations that had stopped the first run.

Margaret Asgian (J.F.T. Agapito & Associates, Inc.) performed the DOT/JAC/CJM analysis. For the second analysis, no modifications to the mesh, time steps, or other user-defined control parameters were made. The only change was to set the shear hardening parameter to zero as required. The convergence tolerances for solutions at each time step were set to 0.003 on the forces and 0.001 on displacements. The artificial (keystone) viscosity was set to the default value of 1.0. A complete solution to 101 yr was obtained; however, some convergence problems were noted at some solution times greater than 20 yr (e.g., convergence on the displacement rather than on force balance after more than 2,000 iterations).

In the following sections, the results of the second analysis are presented in detail. For comparison, one of the elastic analysis solutions to the benchmark problem (Bauer and Costin, 1990) is plotted along with the present results. This solution is designated COY/JAC/LE on the plots. Note that the elastic analysis used a rock mass modulus of one-half the intact rock modulus.

5.2.1 Mesh Statistics and Computer Usage, Second Analysis

Computer usage for the second analysis is given in Table 5-3. The calculation time for the JEM appears to be significantly greater than that for the CJM, even for the same code run on the same machine. The new version the CJM, which was run for the SANCHO/CJM analysis and contains the simplified root solver, showed substantial improvement in run time.

TABLE 5-3

COMPUTER USAGE FOR SECOND ANALYSIS

Code/Model	Computer	CPU Time (sec)
SP41/SANCHO/JEM	CRAY XMP	70,740
COY/SANCHO/CJM	CRAY XMP	7,020
SP41/SP31/JEM	VAX 11/750	1,220,900
COY/JAC/CJM	CRAY XMP	10,560
DOT/JAC/CJM	IBM PC/AT	216,000

Table 5-4 lists the mesh statistics required by the PDM and discussed in Section 2.2.2.3 of this report. Only the mesh for the SP41/SP31/JEM calculation was modified for the second analysis.

TABLE 5-4

MESH STATISTICS FOR SECOND ANALYSIS

Number of Nodes	Nodes/Degrees of Freedom	Type of Element	Number of Elements	Spacing (m)	
				Minimum	Maximum
SP41/SANCHO/JEM	981/1962	4-node quad	903	0.13	13.11
COY/SANCHO/CJM	2762/5524	4-node quad	2624	0.2959	2.6089
SP41/SP31/JEM	2065/4130	8-node quad	646	0.02	15.2
COY/JAC/CJM	2144/4288	4-node quad	2068	0.185	5.469
DOT/JAC/CJM	851/1702	4-node quad	760	0.15	9.08

5.2.2 Displacement Histories at Selected Points, Second Analysis

The vertical displacement histories at Points A and E (Figure 2-3) and the vertical and horizontal displacement histories at Point B from each code are compared in Figures 5-62 through 5-65, respectively. The predictions of vertical displacement at Points A, B, and E are all in reasonable agreement. Minor deviations from the mean are noted for the

SANCHO/CJM solution at early times (1-10 yr) and for the SP31/JEM solution at late times (60-101 yr). In addition, the predicted displacements from the joint models are quite close to those from the elastic rock mass model. There is considerably more scatter in the CJM predictions of horizontal displacement at Point B (Figure 5-65). The three CJM calculations show the same trend, but there is a consistent 2- to 3-mm difference in the displacements predicted by the SANCHO/CJM and the COY/JAC/CJM solutions. The DOT/JAC/CJM is in good agreement with the COY/JAC/CJM solution at times less than 10 yr. After that the DOT/JAC/CJM solution deviates considerably from the two other CJM solutions. The two JEM solutions are in good agreement over the entire history of the calculation. Finally, the horizontal displacements at Point B predicted by both jointed rock models are considerably greater than those predicted by the elastic rock mass model.

5.2.3 Displacements Along Selected Paths at Seven Times, Second Analysis

The vertical displacements along Line 1 (from Point K through Point I on Figure 2-3) at 0.5, 1, 6, 11, 26, 76, and 101 yr are shown in Figures 5-66 through 5-72. Because Point K was restrained from vertical motion, the displacement at this point should be zero. The results at both 0.5 and 1 yr were requested to see if any effects of the instantaneous mining of the drift would show up in the results. The three CJM solutions agree quite well at all times except 6 yr where the SANCHO/CJM solution differs from the other two by as much as 30%. The two JEM solutions are in agreement through 11 yr but show increasing deviation from 26 through 101 yr. The JEM solutions also differ from the CJM solutions after the drift is mined (at 0.5 yr) but before heating begins (at 1 yr). After 1 yr, the two models appear to agree with each other and with the elastic solution, except for the SP31/JEM solution, which deviates from this trend after 26 yr.

Predictions of horizontal displacement along Line 3 (from Point D to Point H in Figure 2-3) are compared in Figures 5-73 through 5-79. Because of the symmetry conditions, the horizontal displacement at the two end points of Line 3 should be zero. The three CJM solutions are in good agreement for all times shown. Note that the oscillations that appeared in some of the initial analysis results are absent from these results. Also, the CJM solutions are in agreement with the elastic solution after the mining phase but predict larger displacements than the elastic solution after heating begins. The two JEM solutions consistently predict more positive displacements than the elastic solutions. The JEM solutions also predict larger displacements than the CJM solutions after heating begins. In addition, there is an apparent consistent difference between the the two JEM solutions that is most evident in the 3- to 10-m range from the heater.

5.2.4 Stress Components Along Selected Paths at Six Times, Second Analysis

Comparisons of predicted vertical and horizontal normal stresses along Line 1 (from Point K to Point I in Figure 2-3) at 0.5, 6, 11, 26, 76, and 101 yr are given in Figures 5-80 through 5-91. For the vertical stress, 101 yr are given in Figures 5-80 through 5-91. For the vertical stress, the two JAC/CJM solutions are in good agreement. The SANCHO/CJM solution is in general agreement with the JAC/CJM solutions except in regions below the drift, especially at 6 yr. The fact that the SANCHO/CJM solution does not approach the in situ stress at -100 m on Line 1 indicates that the equilibrium solution tolerance used in the computation may be too loose. The two JEM solutions are in agreement except for small differences in the first 10 m above the drift. None of the vertical stress profiles predicted by the jointed rock models is significantly different from that predicted by the elastic analysis. The horizontal stress predictions along Line 1 are all in good agreement overall, although small differences are noted in the SP31/JEM solution at late times. The jointed rock models predict stresses that are larger than those predicted from the elastic analysis and this difference increases over time. At 101 yr, the maximum horizontal stresses predicted by the jointed rock models are larger by nearly a factor of two than those predicted by the elastic analysis.

Figures 5-92 through 5-103 present the comparison of predicted vertical and horizontal stresses along Line 2 (from Point L to Point J in Figure 2-3) at the same times as the comparisons for Line 1. The results are somewhat better than those for Line 1 in that better agreement was achieved among codes using the same model. The one obvious exception is the predictions of vertical stress from the SANCHO/CJM analysis. As with the comparisons of vertical stresses along Line 1, the SANCHO/CJM solution does not converge to the in situ stress in the region well below the heater. This is a clear indication that the solution is not in equilibrium. The predictions of horizontal stress (Figures 5-98 through 5-103) are in good agreement except for the SP31/JEM solution, which predicts somewhat lower stresses at later times. As was noted with the stresses along Line 1, the vertical stress along Line 2, predicted from the jointed rock models, does not differ significantly from the elastic solution. However, the horizontal stresses are consistently larger than those from the elastic solution.

Along Line 3 (Point D to Point H in Figure 2-3) the PDM requested that the participants report both the vertical normal stress and the in-plane shear stress. These results are compared in Figures 5-104 through 5-115. Consistent with the previous results, there was good agreement among the predictions of vertical stress (Figures 5-104 through 5-109) for each model beyond about 5 m from the heater. Within 5 m of the heat source, the solutions vary somewhat with a large difference between the CJM and JEM solutions. The CJM solutions tend to predict larger stresses in this region and somewhat smaller stresses than the JEM at distances farther away from the heater. This is most likely because the JEM allows slip on the joints at lower stresses than the CJM, thus relieving some of the stress near the heater. The predictions of shear stresses (Figures 5-110 through 5-115) are consistent with this explanation. The three CJM solutions predict larger shear stresses than the two JEM solutions, especially in the region near the heater. The DOT/JAC/CJM solution predicts a somewhat different response than the other two CJM solutions, with the difference becoming more evident at later times. The JEM solutions are in quite consistent agreement over the span of Line 3. At 76 and 101 yr, some oscillations in the COY/JAC/CJM solution are evident near the heater (zero position on Line 3).

The horizontal normal stress predicted along Line 4 (Point B to Point C in Figure 2-3) from each code is compared in Figures 5-116 through 5-121. Because of the traction-free boundary at Point B (Figure 2-3), the horizontal stress should be zero at that point. At times, 0.5 through 26 yr, the two JAC/CJM solutions are in agreement but are different from the SANCHO/CJM solution. After 26 yr, the SANCHO/CJM and the DOT/JAC/CJM solutions show the same trend and are in general agreement, but the COY/JAC/CJM solution is quite different. The two JEM solutions show the same trend throughout with a slightly, but consistently increasing difference between them.

5.2.5 Evaluation and Discussion of Results from the Second Analysis

On December 12, 1988, a meeting between the PIs and the participants in the benchmark exercise was held to review and discuss the results from the second analysis. The following discussion is a summary of the evaluation of the results of the second analysis based on the consensus of those at the meeting.

In general, the results from different codes using the same material model were consistent. The differences noted between the SANCHO/CJM calculation and the two other analyses using the CJM were judged to be a result of using too loose a convergence tolerance. The fact that the SANCHO/CJM calculation was performed with the updated CJM (ORTHO.UPD version 1.1) probably did not contribute to the discrepancies. However, it was thought that this should be demonstrated with an additional analysis. The differences in the two solutions using the JEM were attributed primarily to differences in the degree of mesh refinement used near the drift. It was also thought that this conjecture should be investigated further.

Based on the evaluation of the results, the PIs decided that to complete the exercise a third analysis should be undertaken. The primary purpose of this analysis would be to benchmark the codes with the new version of the CJM because the updated version is the one expected to become the standard version for use in later analyses. In addition, mesh sensitivity should be explored by repeating one of the JEM calculations with a revised mesh that closely matches the mesh used by the other JEM calculation in the second analysis. Therefore, the following additional calculations were requested: (1) the SANCHO/CJM analysis would be rerun using the updated version of the CJM and a tighter tolerance on the equilibrium convergence criterion; (2) the COY/JAC/CJM analysis would be rerun using the updated CJM, and the artificial viscosity and convergence tolerances set to the values used by JFTA&A on the DOT/JAC/CJM analyses; (3) the DOT/JAC/CJM analysis would be rerun using the updated CJM; and (4) the SP31/JEM analysis would be rerun using a mesh nearly identical to that used for the second SANCHO/JEM analysis.

5.3 Results from the Third Analysis

The results of the third analysis effort were submitted by letter report from the participants during the first quarter of 1989. For the third analysis, new releases of ORTHO.UPD (CJM) were issued (version 1.1 for SNL and version 1.02 for JFTA&A) with the changes implemented through a Modification Request (DOP 3-2, Rev. A). The new release contains revisions to the root solver and shear hardening routine. All three CJM analyses were rerun using the new CJM and convergence tolerances and other control variables set so that the three analyses would use comparable values. For the JEM, only the SP31/JEM analysis was rerun using a mesh comparable to that used by the second SANCHO/JEM analysis.

5.3.1 Mesh Statistics and Computer Usage, Third Analysis

Computer usage for the third analysis is given in Table 5-5. The new version the CJM showed substantial improvement (factor of 10) in run time for the COY/JAC/CJM analysis. Table 5-6 lists the mesh statistics required by the PDM and discussed in Section 2.2.2.3 of this report. Only the mesh for the SP41/SP31/JEM calculation was modified for the third analysis.

5.3.2 Displacement Histories at Selected Points, Third Analysis

In all the figures reporting results from the third analysis, the "R" attached to the analysis designators in the legend indicates that the results plotted are from the (rerun) third analysis. Also included in each figure are the results of the second SANCHO/JEM analysis and one of the results from the previous elastic analyses (COY/JAC). The vertical displacement histories at Points A and E (Figure 2-3) and the vertical and horizontal displacement histories at Point B from each code are compared in Figures 5-122 through 5-125, respectively. The predictions of vertical displacement at Points A, B, and E for both jointed rock models are all in reasonable agreement. In addition, the predicted displacements from the joint models are quite close to those from the elastic rock mass model.

TABLE 5-5

COMPUTER USAGE FOR THIRD ANALYSIS

Code/Model	Computer	CPU Time (sec)
SP41/SANCHO/JEM*	CRAY XMP	70,740
COY/SANCHO/CJM	CRAY XMP	49,920
SP41/SP31/JEM	VAX 11/750	190,380
COY/JAC/CJM	CRAY XMP	780
DOT/JAC/CJM	IBM PC/AT	216,000

*Analysis was not repeated; results shown are for the second analysis.

TABLE 5-6

MESH STATISTICS FOR THIRD ANALYSIS

Number of Nodes	Nodes/Degrees of Freedom	Type of Element	Number of Elements	Spacing (m) Minimum	Maximum
SP41/SANCHO/JEM*	981/1962	4-node quad	903	0.13	13.11
COY/SANCHO/CJM	2762/5524	4-node quad	2624	0.2959	2.6089
SP41/SP31/JEM	1110/2220	8-node quad	341	0.12	24.4
COY/JAC/CJM	2144/4288	4-node quad	2068	0.185	5.469
DOT/JAC/CJM	851/1702	4-node quad	760	0.15	9.08

* Analysis was not repeated; the results shown are for the second analysis.

The horizontal displacements at Point B (Figure 5-125) predicted by the three CJM analyses show some differences (maximum of 3 mm), but the trend and magnitude of the predicted displacements over the 101-yr time span are in reasonable agreement. The two JEM calculations are in excellent agreement. Note that both jointed rock models predict considerably greater displacements than those predicted by the elastic rock mass model.

5.3.3 Displacements Along Selected Paths at Seven Times, Third Analysis

The vertical displacements along Line 1 (from Point K through Point I on Figure 2-3) at 0.5, 1, 6, 11, 26, 76, and 101 yr are shown in Figures 5-126 through 5-132. Because Point K was restrained from vertical motion, the displacement at this point should be zero. The results at both 0.5 and 1 yr were requested to see if any transitory effects of the instantaneous mining of the drift would show up in the results. For all times, the three CJM calculations are in agreement as are the two JEM calculations. The JEM predicts somewhat larger vertical displacements than the CJM just after mining the drift. However, these differences are negligible after heating is established (6-101 yr). After heating begins, both models are in agreement with the elastic solution.

Predictions of horizontal displacement along Line 3 (from Point D to Point H in Figure 2-3) are compared in Figures 5-133 through 5-139. Because of the symmetry conditions, the horizontal displacement at the two end points of Line 3 should be zero. The three CJM solutions are in good agreement for all times shown, as was the case for the second analysis. The two JEM solutions consistently predict more positive displacement than either the CJM or the elastic solutions. The two JEM solutions are in excellent agreement, indicating that the differences noted in the results from the second analysis are, in fact, a result of the differences in mesh refinement used in the second analysis.

5.3.4 Stress Components Along Selected Paths at Six Times, Third Analysis

Comparisons of predicted vertical and horizontal normal stresses along Line 1 (from Point K to Point I in Figure 2-3) at 0.5, 6, 11, 26, 76, and 101 yr are given in Figures 5-140 through 5-151. For the vertical stress, the results from both models show very good agreement within each set of calculations using the same model. Small differences are observed only in the region just above and below the drift where the vertical stress gradient is very large. Within a region of 30 m above and below the drift, the two models predict slightly different behaviors, with the JEM predicting lower stresses than the CJM. Note that the SANCHO/CJM solution is in much better agreement with the two JAC/CJM solutions than was observed for the second analysis, indicating that the loose convergence tolerance used in the second analysis was probably the cause of the differences in the results. The vertical stress profiles predicted by the jointed rock models are not significantly different from those predicted by the elastic analysis.

The horizontal stress predictions along Line 1 (Figures 5-146 through 5-151) are all in good agreement with both jointed rock models predicting approximately the same behavior. The jointed rock models predict stresses that are larger than those predicted from the elastic analysis, and this difference increases over time. At 101 yr, the maximum horizontal stresses predicted by the jointed rock models are larger by nearly a factor of two than those predicted by the elastic analysis.

Figures 5-152 through 5-163 present the comparison of predicted vertical and horizontal stresses along Line 2 (from Point L to Point J in Figure 2-3) at the same times as the comparisons for Line 1. For each model, the results using the different codes are quite consistent. For the vertical stress (Figures 5-152 through 5-157), the two models predict quite different behavior in the region near the elevation of the drift. The CJM predicts stresses larger than the elastic solution whereas the JEM predicts stresses somewhat smaller than the elastic solution. It should be noted that the SANCHO/CJM solution still shows some problems in achieving equilibrium at 11 and 26 yr, but the differences are substantially less than those resulting from the second analysis. The predictions of horizontal stress (Figures 5-158 through 5-163) are in good agreement both within each model group and between models. As was noted with the stresses along Line 1, the horizontal stresses predicted by the jointed rock models are consistently larger than those from the elastic solution.

Along Line 3 (Point D to Point H in Figure 2-3) the PDM requested that the participants report both the vertical normal stress and the in-plane shear stress. These results are compared in Figures 5-164 through 5-175. Consistent with the results from other lines, there was good agreement among the predictions of vertical stress (Figures 5-164 through 5-169) for each model beyond about 5 m from the heater. Within 5 m of the heat source, the solutions vary somewhat with the SANCHO/CJM solution predicting larger stresses than the other analyses. There is also a moderate difference between the CJM and JEM solutions. The CJM solutions tend to predict larger stresses in this region and somewhat smaller stresses than the JEM at distances farther away from the heater. This is most likely because the JEM allows slip on the joints at lower stresses than the CJM, thus relieving some of the stress near the heater. The predictions of shear stresses along Line 3 (Figures 5-170 through 5-175) are consistent with this explanation. The three CJM solutions predict larger shear stresses than the two JEM solutions, especially in the region near the heater. The CJM solutions are in good agreement except in the region near the heater where the stress gradients are large. Part of the difference seen in the solutions could be attributed to the inherent errors involved in reporting the average stress in elements (or averaging the stress computed at neighboring Gauss points) where the gradients are large. The JEM solutions show somewhat better agreement over the span of Line 3 than the CJM solutions.

The horizontal normal stress predicted along Line 4 (Point B to Point C in Figure 2-3) from each code is compared in Figures 5-176 through 5-181. Because of the traction-free boundary at Point B (Figure 2-3), the horizontal stress should be zero at that point. The three CJM solutions agree at early times but tend to disagree along the middle of the line for later times. The COY/JAC/CJM solution seems to diverge the most. The same solution for the second analysis agrees better with the other CJM results from the third analysis. This indicates that loosening the tolerance and reducing the artificial viscosity for the third analysis had some detrimental effects. The two JEM solutions show the same trend throughout with a slightly, but consistently increasing difference between them. This difference, although small, becomes more evident at later times.

5.3.5 Evaluation and Discussion of Results from the Third Analysis

A review of the comparison plots from the third analysis shows that the two JEM solutions are in quite good agreement. The differences observed in the result from the second analysis were apparently the result of the differences in mesh resolution. The revised (third) SP31/JEM calculation used 1110 nodes with 341 8-node elements whereas the second analysis used 2065 nodes and 646 elements. The SANCHO/JEM calculations used 981 nodes with 903 4-node elements. The effect of changing the mesh by approximately a factor of two changed the predicted maximum displacement along Line 3 by 15%. Smaller changes were noted in the horizontal and vertical stresses near the opening.

The results from the third analysis also showed better agreement among the three CJM solutions. Some differences remain, however, especially in the stresses along Line 4 where the stress predictions near the center of the line differ by 10 MPa at later times. The tighter convergence tolerance applied to the SANCHO/CJM solution resulted in much better agreement with the two JAC/CJM solutions. The revision to the COY/JAC/CJM solution was primarily one of reducing the antikeystoning viscosity and loosening the convergence tolerance slightly. This resulted in some oscillations in the solution, especially in the horizontal stress along

Line 4, that were not present in the second analysis solution. The DOT/JAC/CJM solution was arrived at with the identical viscosity and tolerance settings and does not show this oscillation. The major differences in the two calculations are that the DOT/JAC/CJM calculation used a much coarser mesh (760 elements versus 2068 elements) and was run on a PC instead of a CRAY.

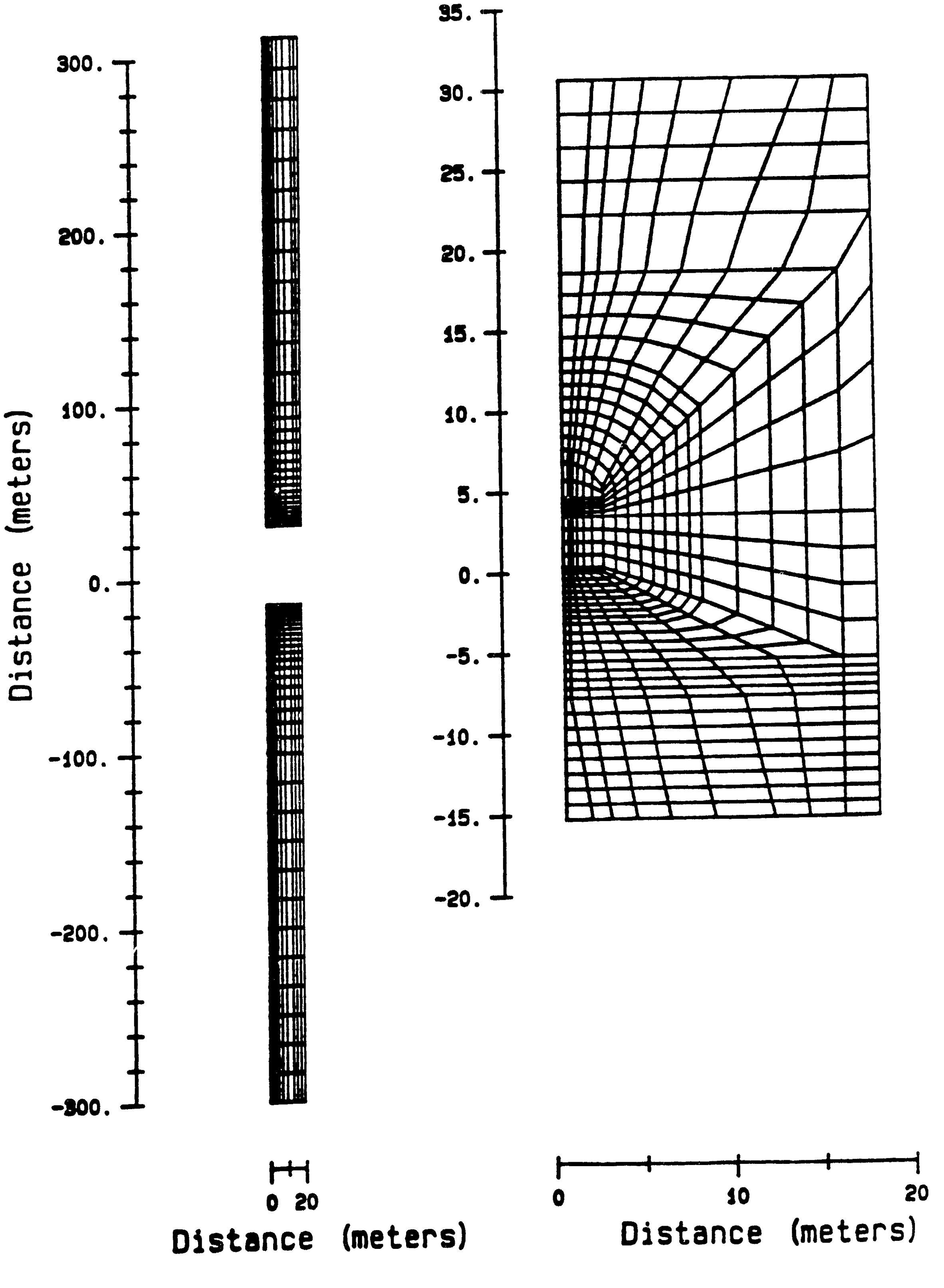

Figure 5-1. Finite Element Representation of the Thermomechanical Problem. (Mesh shown is from the DOT/JAC analysis.)

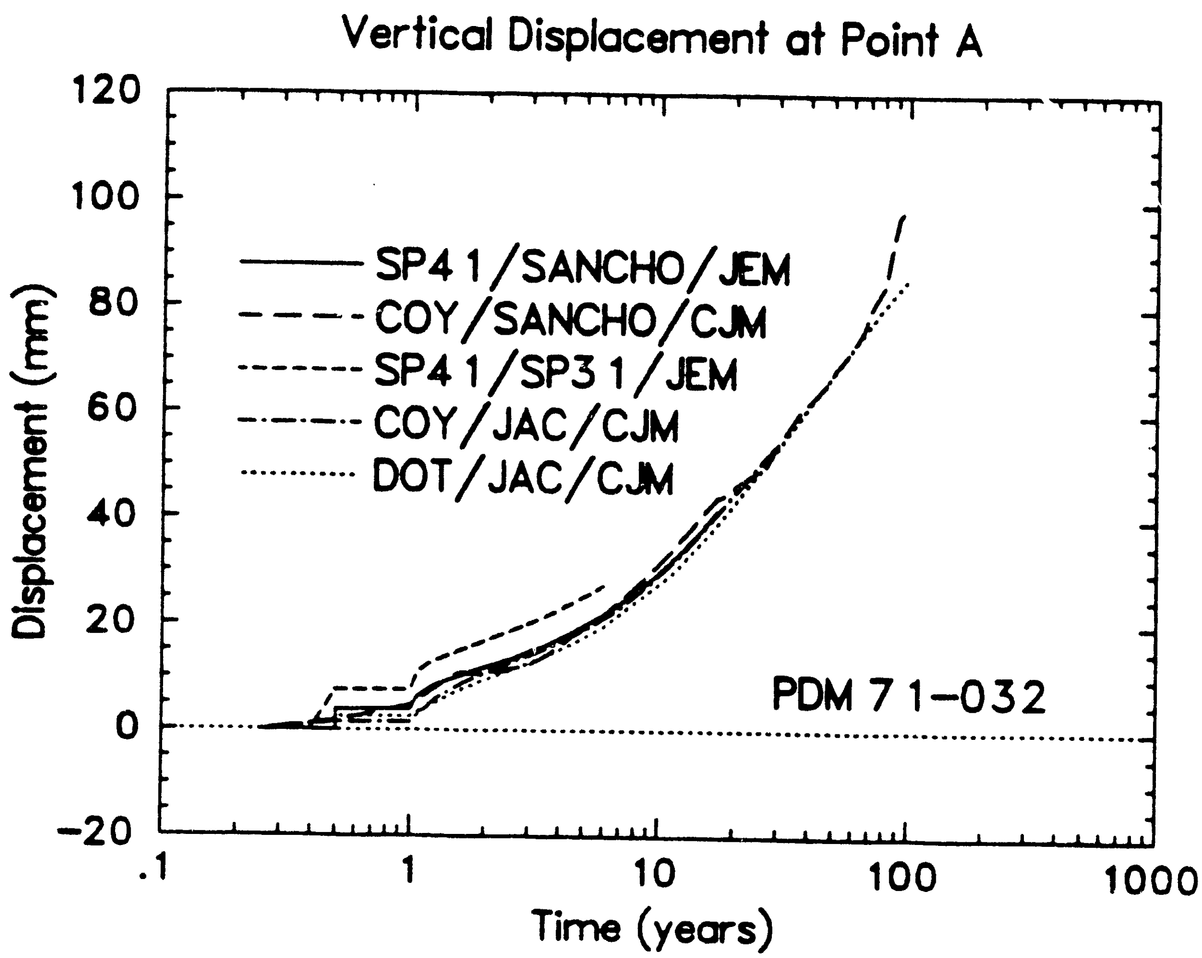

Figure 5-2. Comparison of Results for the Vertical Displacement History at Point A (Figure 2-3), Initial Analysis

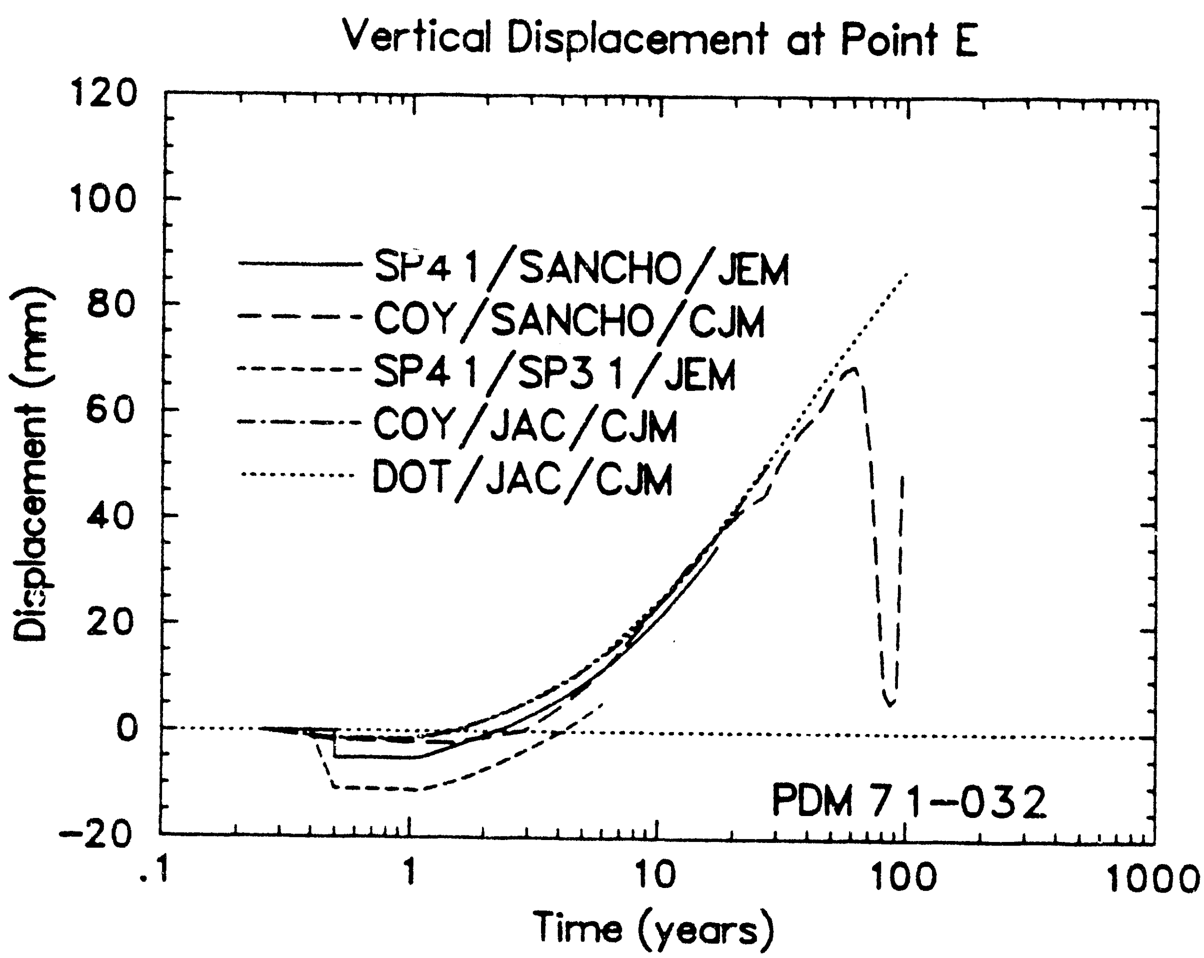

Figure 5-3. Comparison Results for the Vertical Displacement History at Point E (Figure 2-3), Initial Analysis

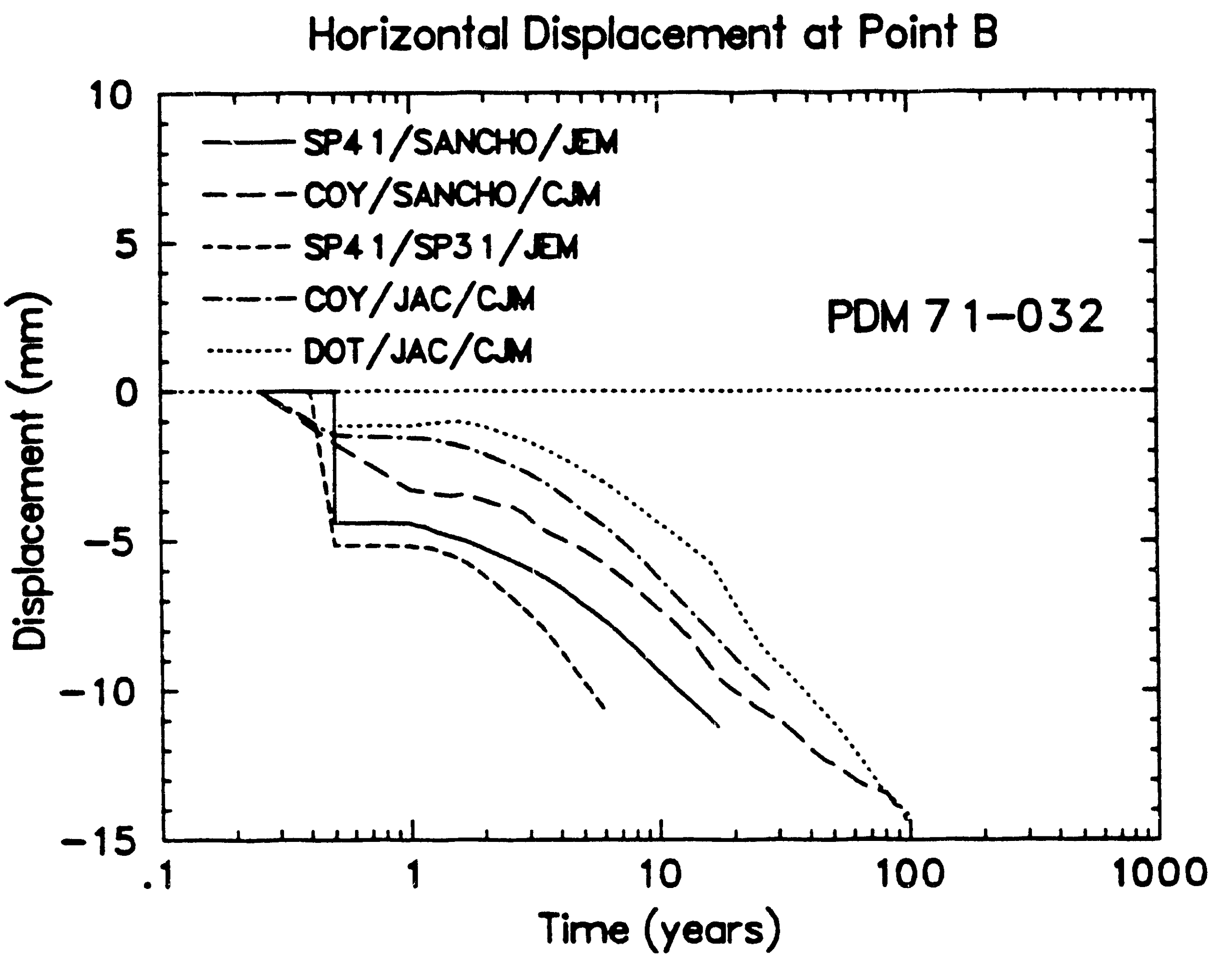

Figure 5-4. Comparison of Results for the Vertical Displacement History at Point B (Figure 2-3), Initial Analysis

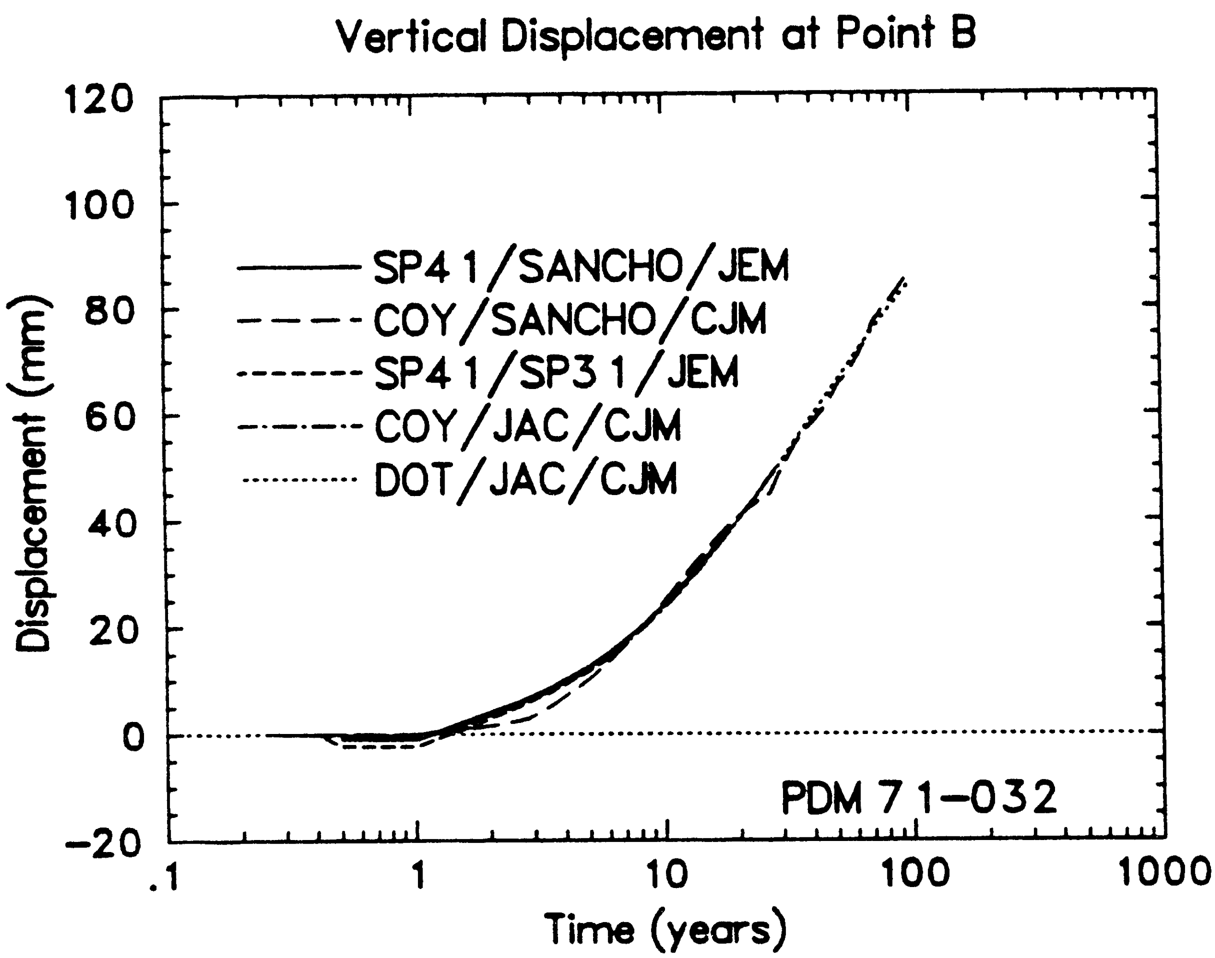

Figure 5-5. Comparison of Results for the Horizontal Displacement History at Point B (Figure 2-3), Initial Analysis

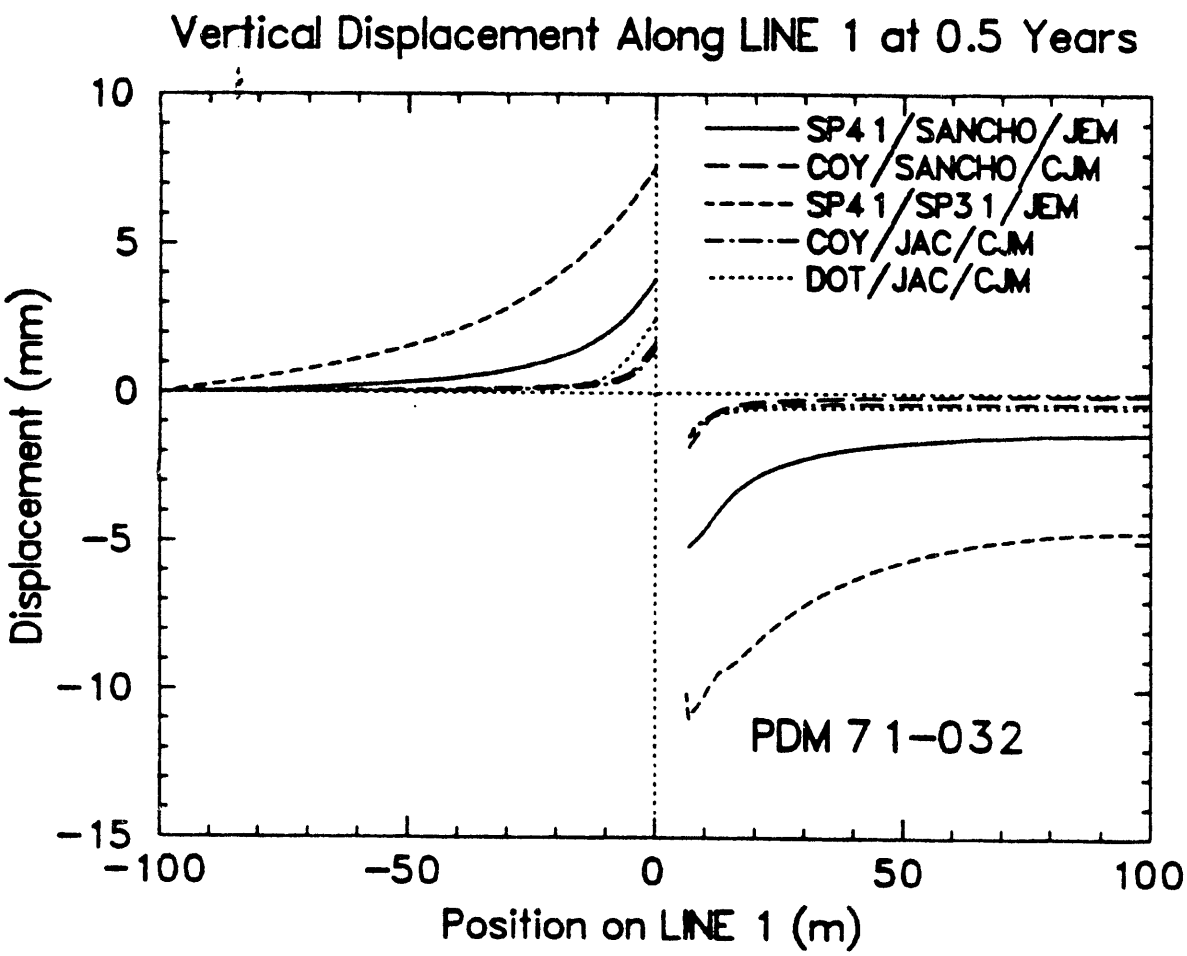

Figure 5-6. Comparison of Results for the Vertical Displacement Along Line 1 (Figure 2-3) at 0.5 Yr, Initial Analysis

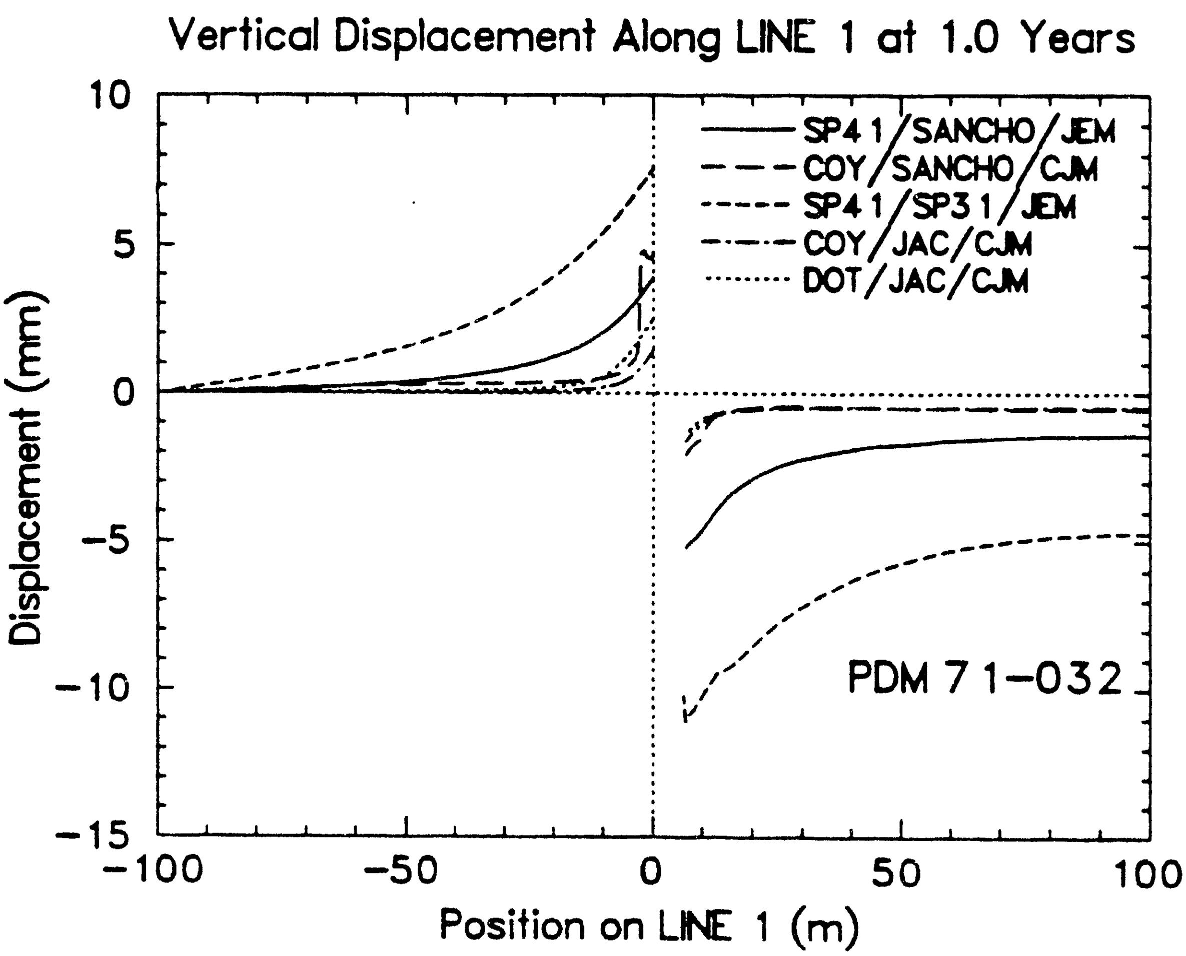

Figure 5-7. Comparison of Results for the Vertical Displacement Along Line 1 (Figure 2-3) at 1 Yr, Initial Analysis

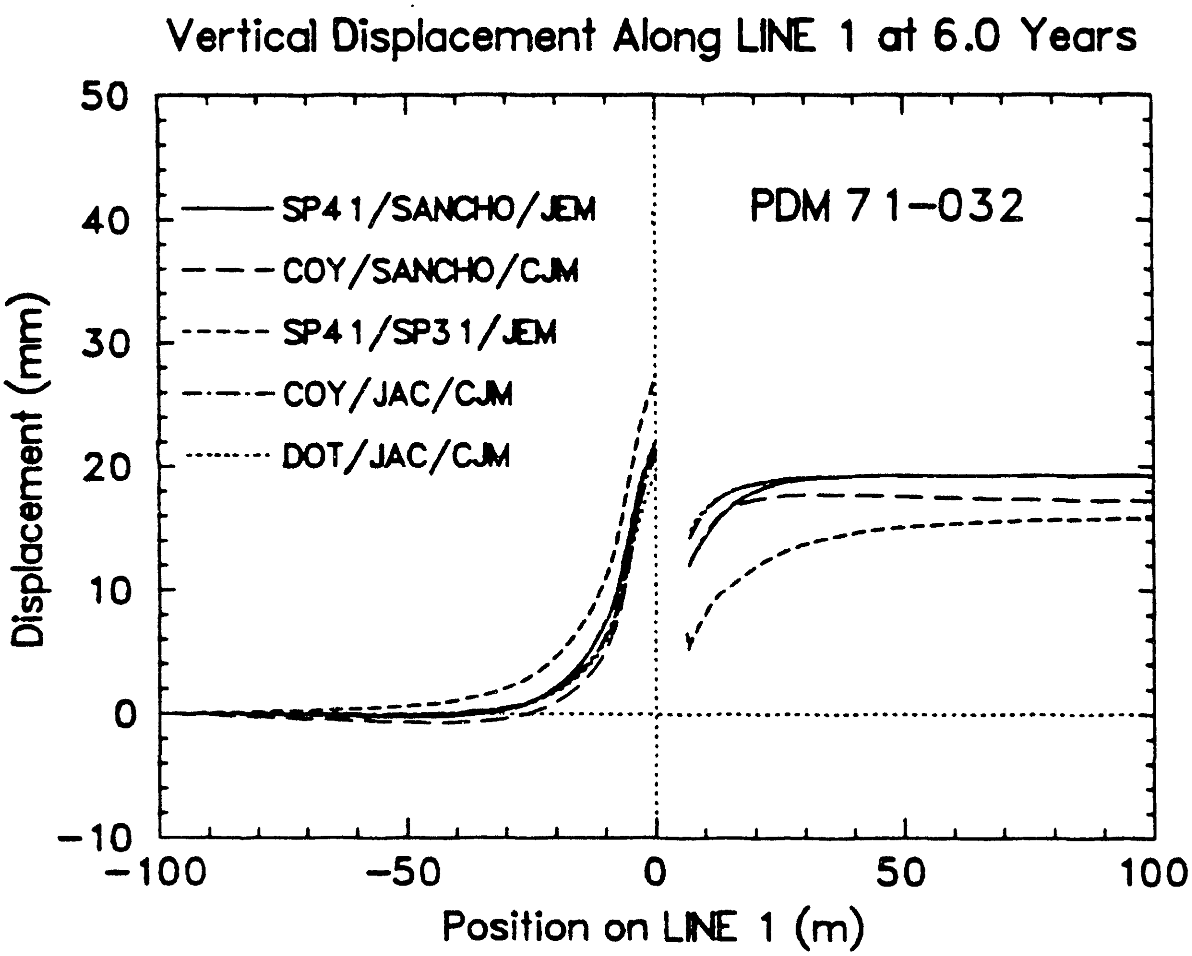

Figure 5-8. Comparison of Results for the Vertical Displacement Along Line 1 (Figure 2-3) at 6 Yr, Initial Analysis

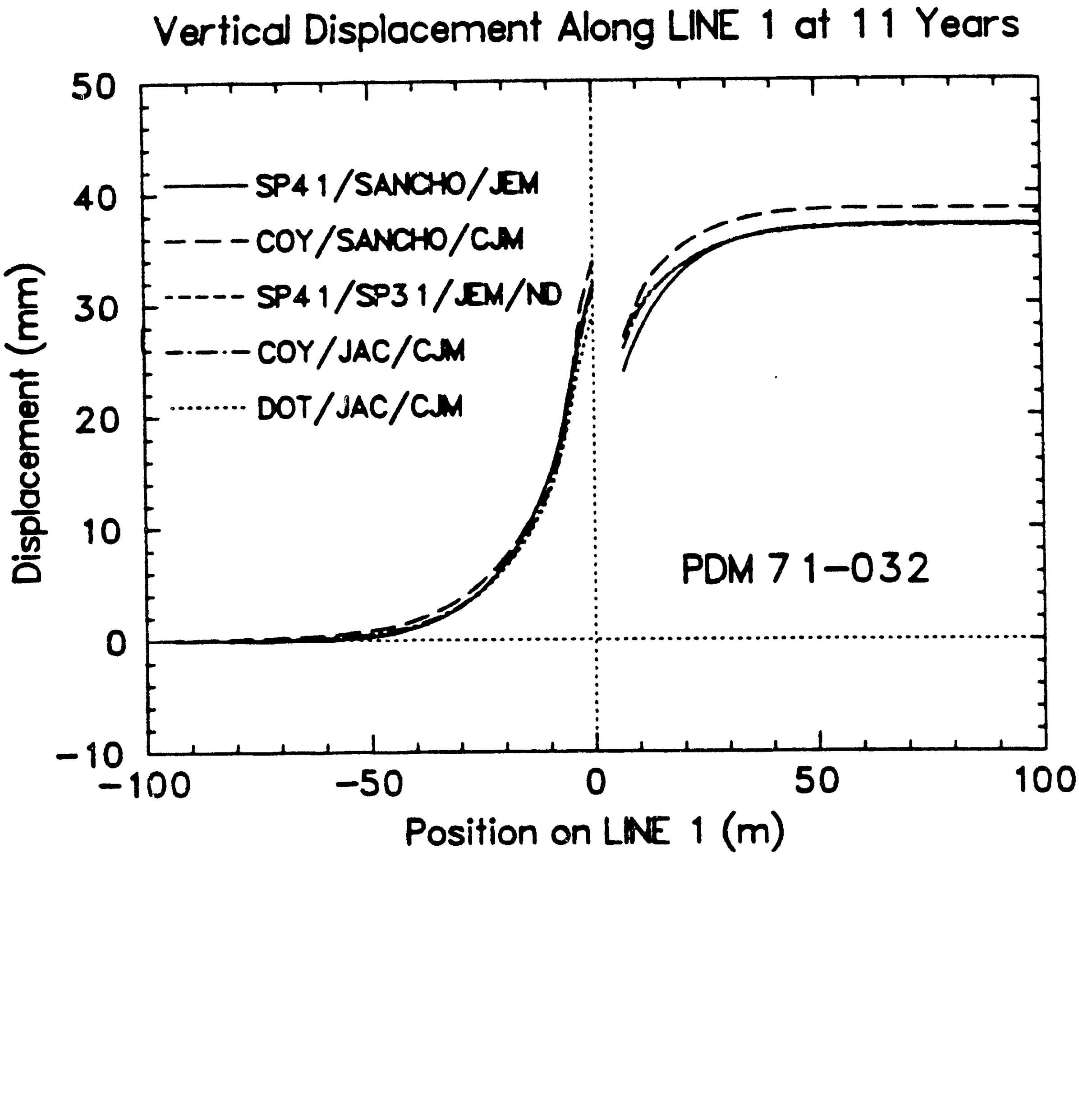

Figure 5-9. Comparison of Results for the Vertical Displacement Along Line 1 (Figure 2-3) at 11 Yr, Initial Analysis

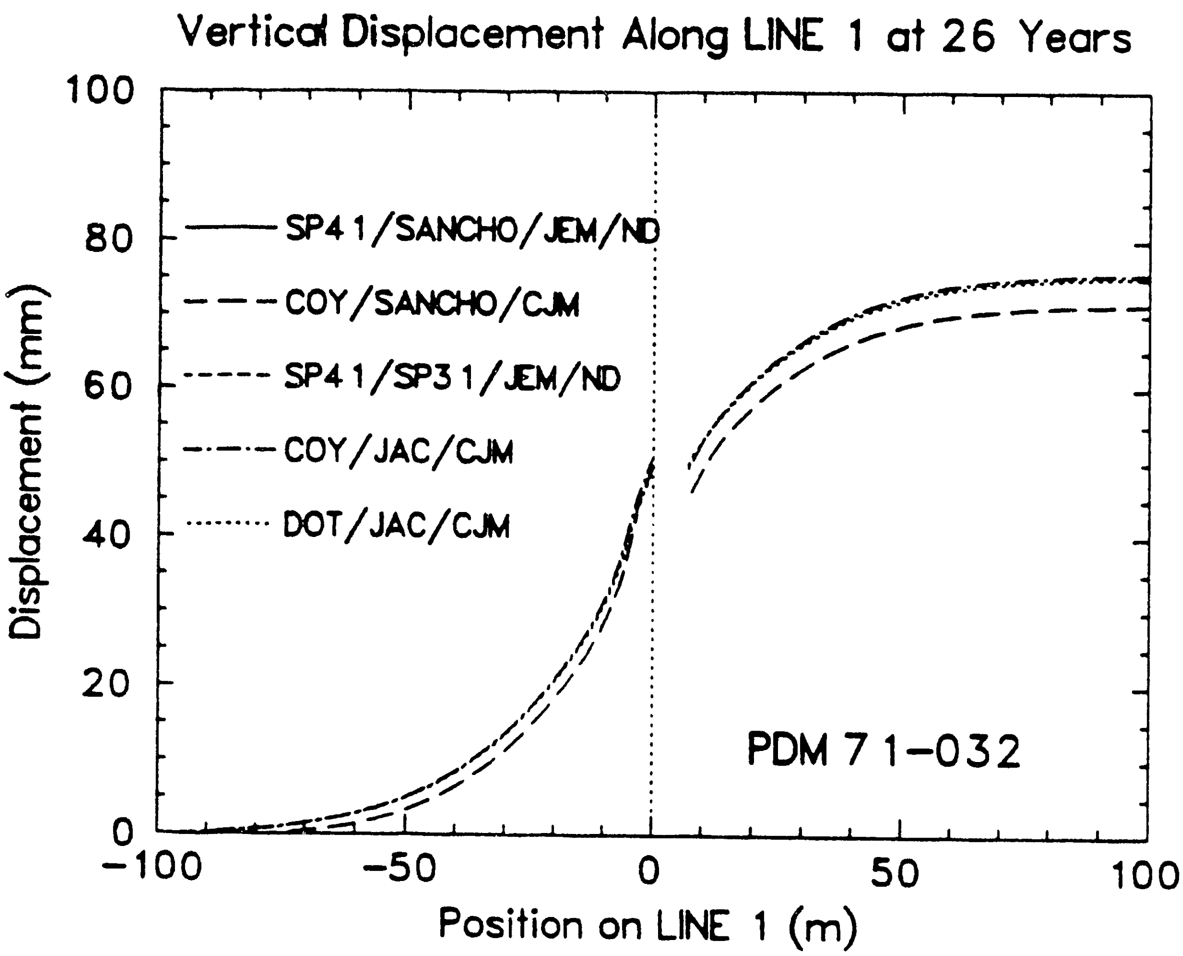

Figure 5-10. Comparison of Results for the Vertical Displacement Along Line 1 (Figure 2-3) at 26 Yr, Initial Analysis

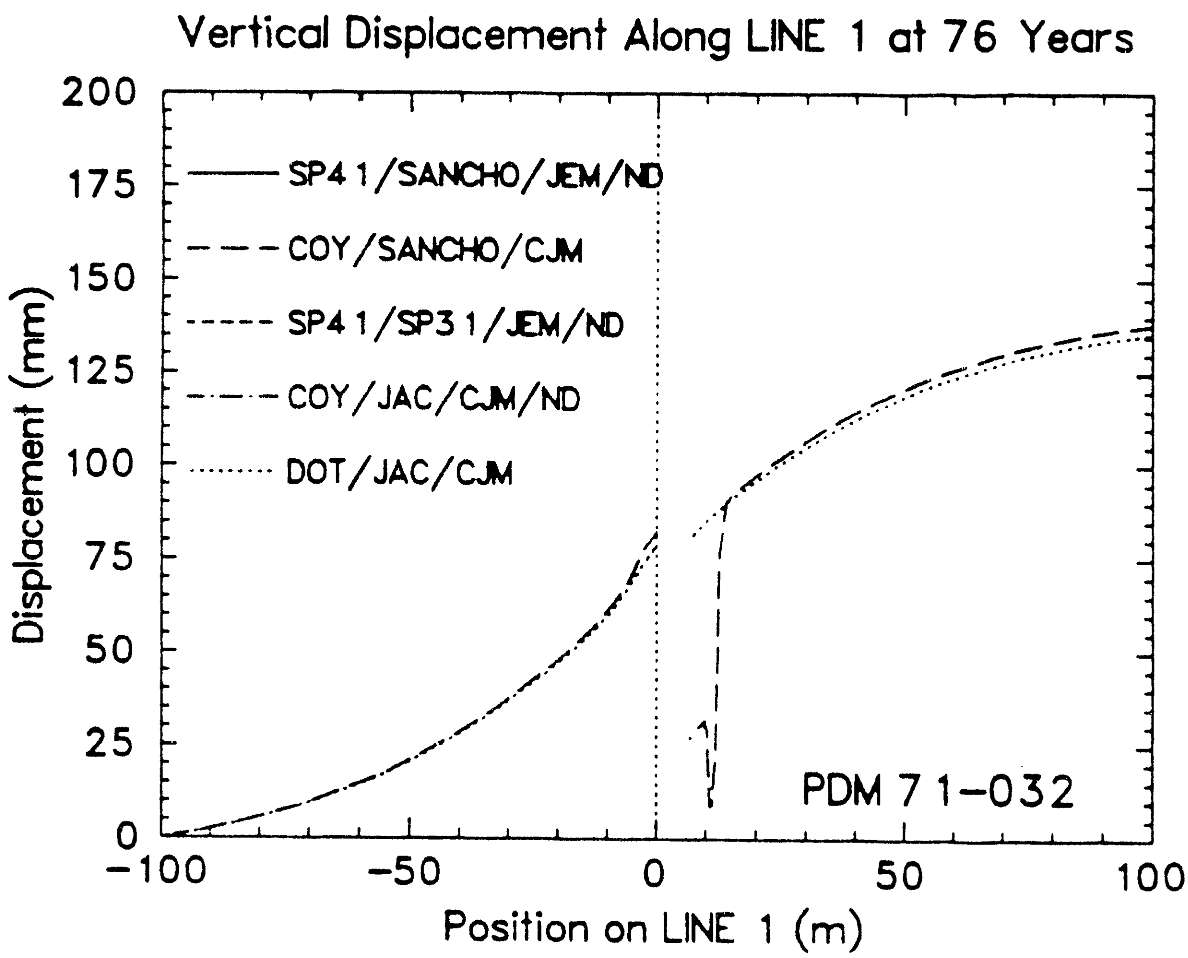

Figure 5-11. Comparison of Results for the Vertical Displacement Along Line 1 (Figure 2-3) at 76 Yr, Initial Analysis

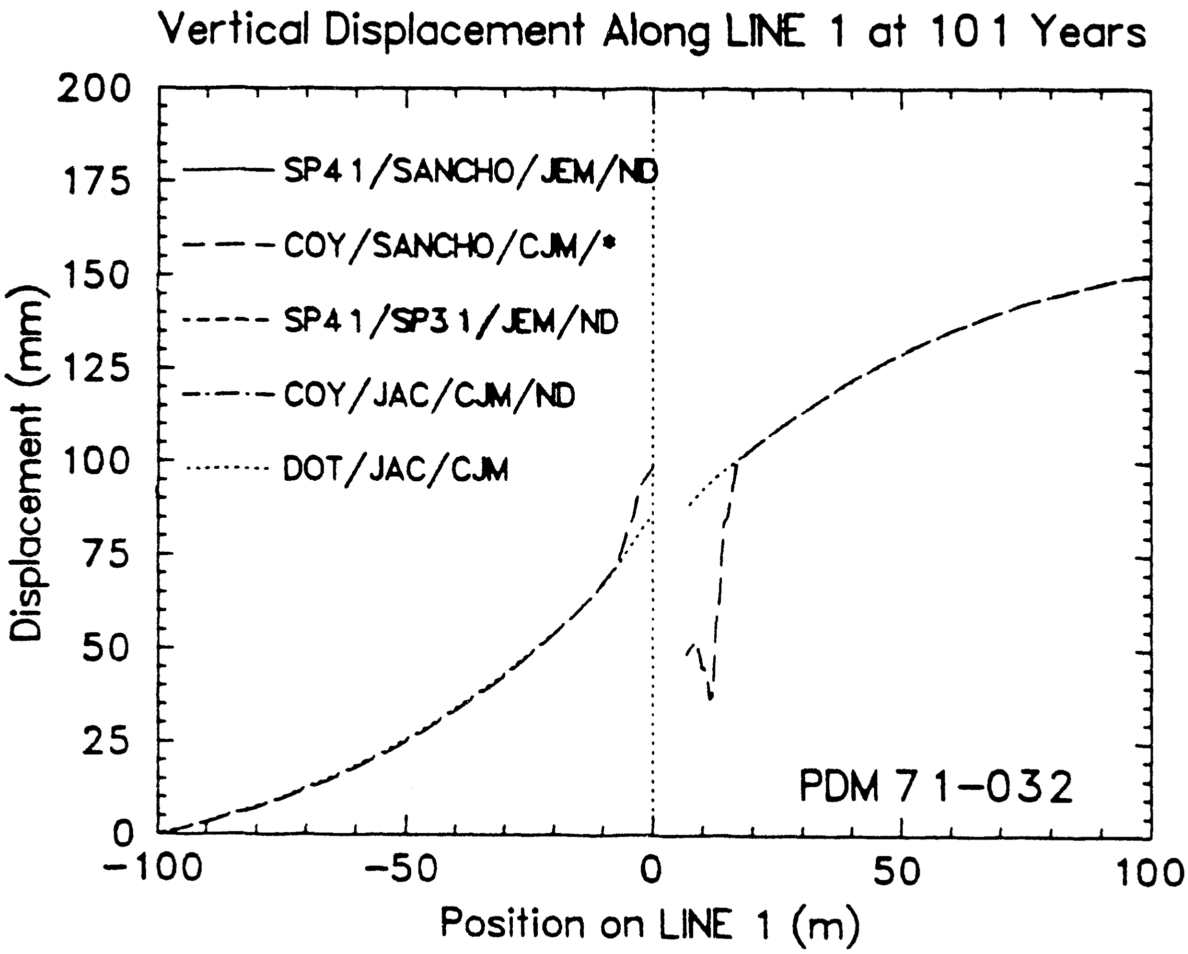

Figure 5-12. Comparison of Results for the Vertical Displacement Along Line 1 (Figure 2-3) at 101 Yr, Initial Analysis

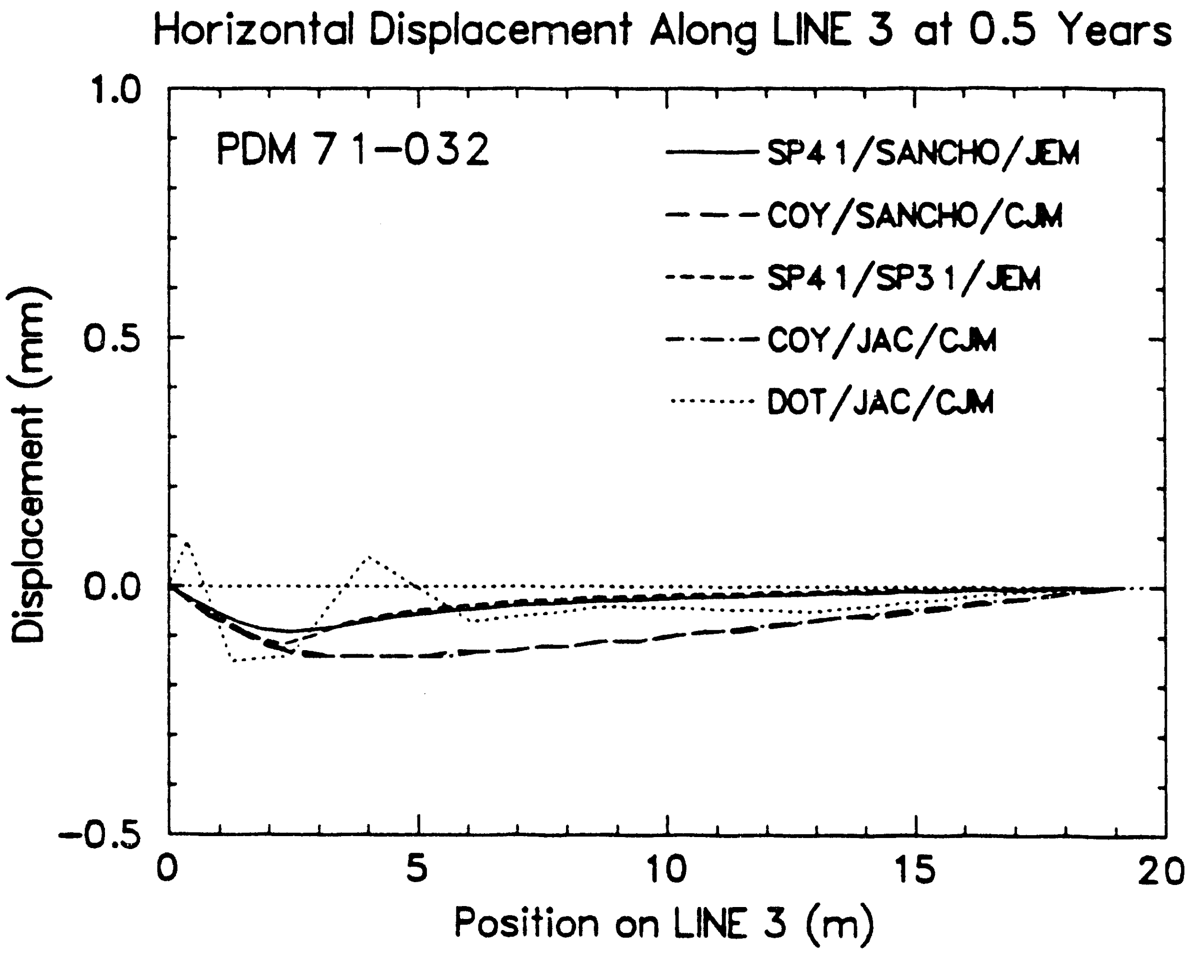

Figure 5-13. Comparison of Results for the Horizontal Displacement Along Line 3 (Figure 2-3) at 0.5 Yr, Initial Analysis

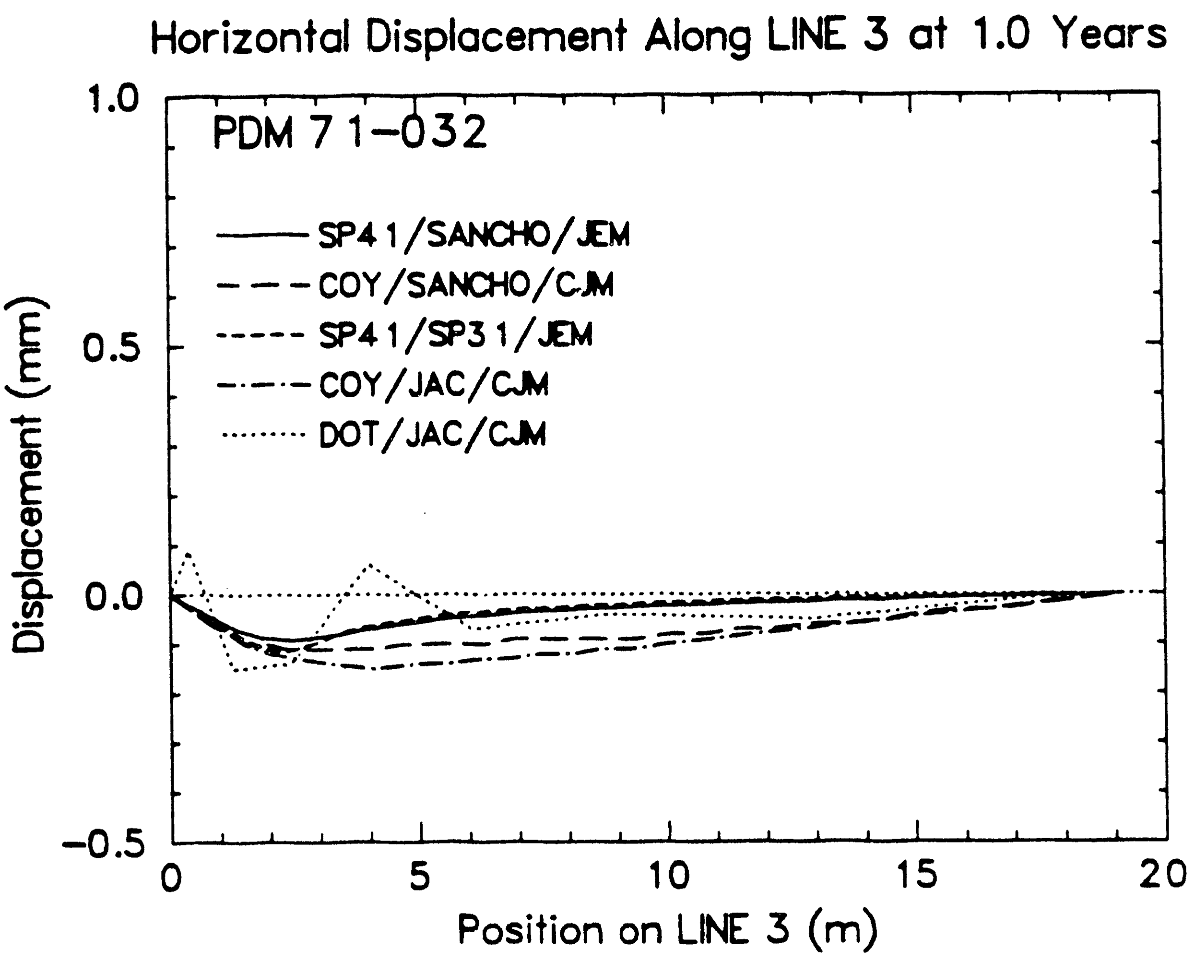

Figure 5-14. Comparison of Results for the Horizontal Displacement Along Line 3 (Figure 2-3) at 1 Yr, Initial Analysis

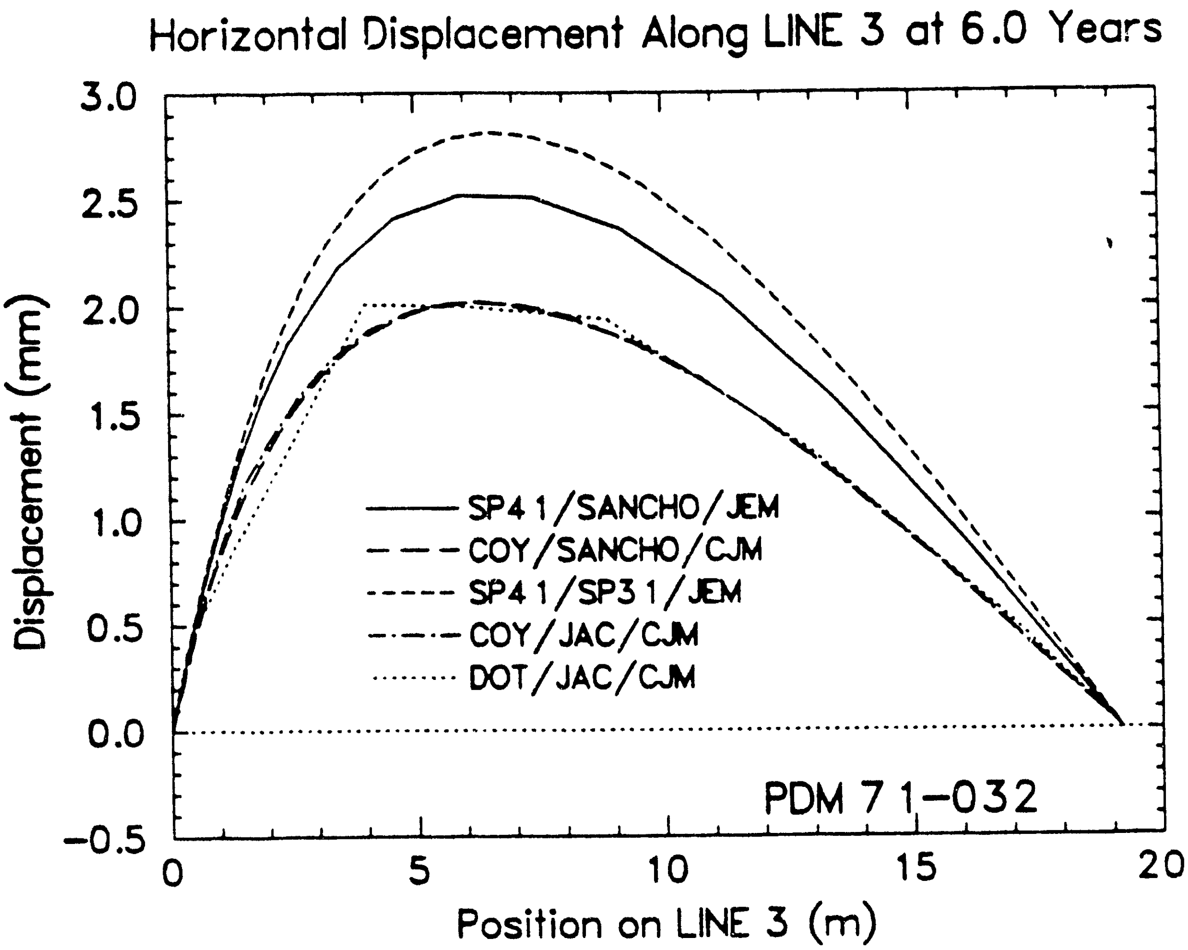

Figure 5-15. Comparison of Results for the Horizontal Displacement Along Line 3 (Figure 2-3) at 6 Yr, Initial Analysis

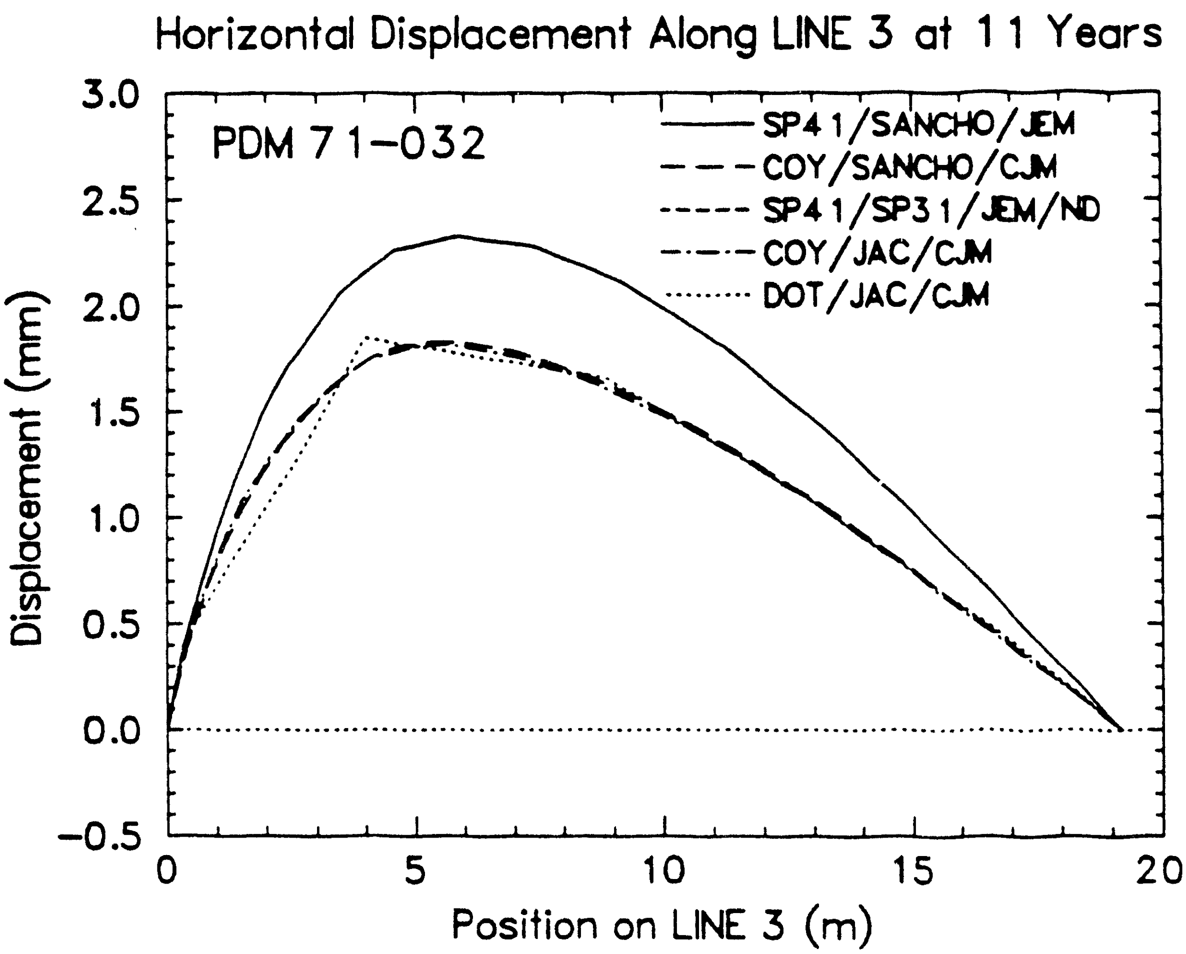

Figure 5-16. Comparison of Results for the Horizontal Displacement Along Line 3 (Figure 2-3) at 11 Yr, Initial Analysis

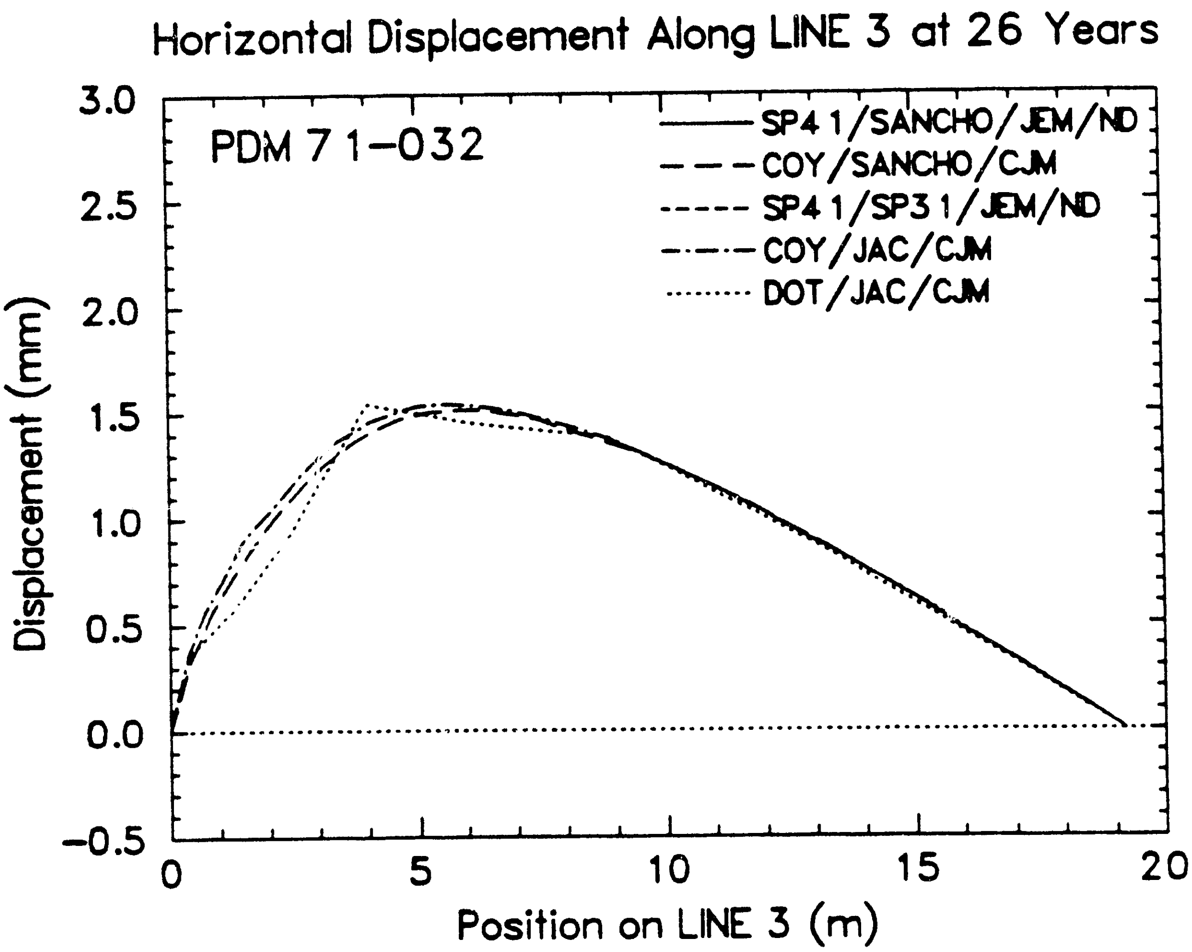

Figure 5-17. Comparison of Results for the Horizontal Displacement Along Line 3 (Figure 2-3) at 26 Yr, Initial Analysis

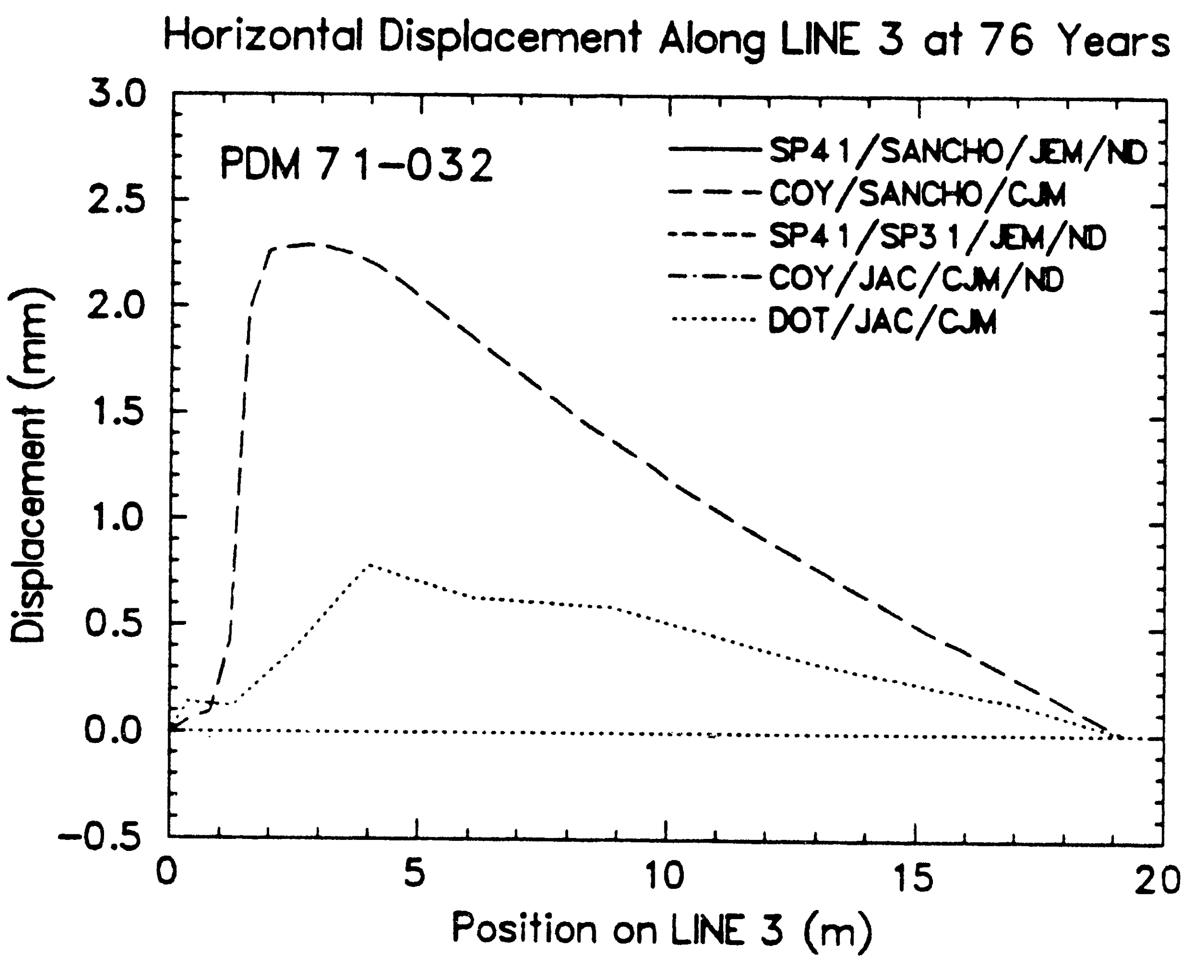

Figure 5-18. Comparison of Results for the Horizontal Displacement Along Line 3 (Figure 2-3) at 76 Yr, Initial Analysis

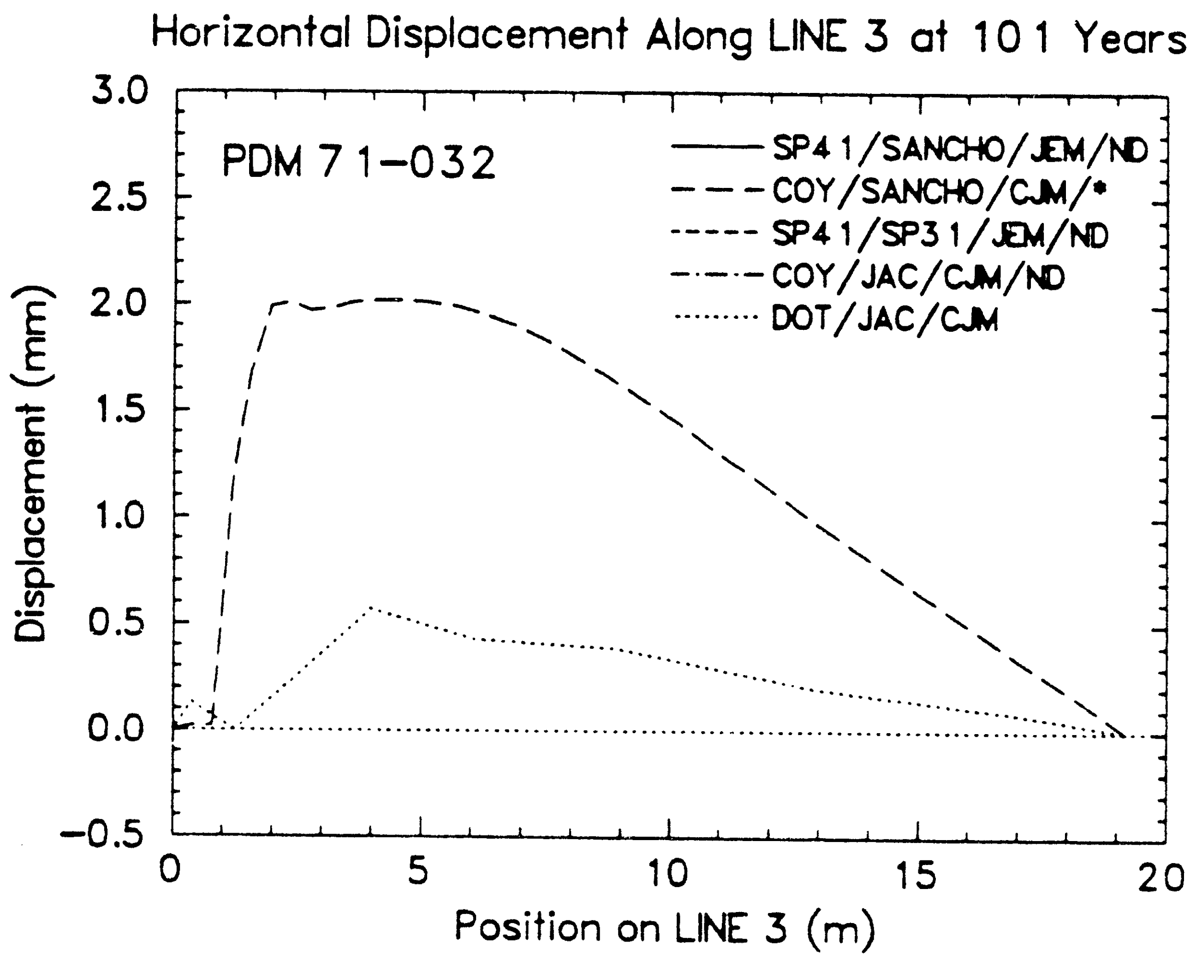

Figure 5-19. Comparison of Results for the Horizontal Displacement Along Line 3 (Figure 2-3) at 101 Yr, Initial Analysis

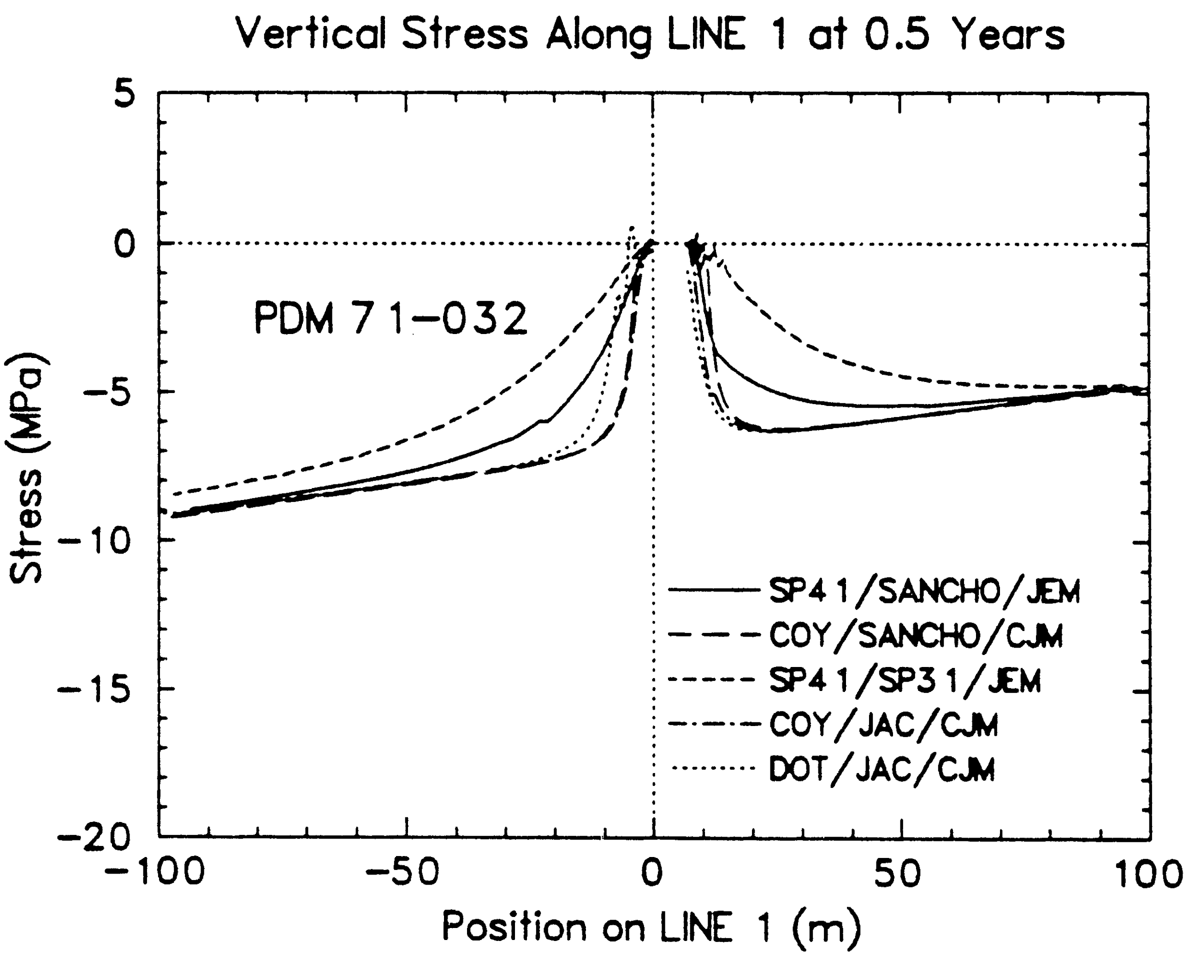

Figure 5-20. Comparison of Results for the Vertical Stress Along Line 1 (Figure 2-3) at 0.5 Yr, Initial Analysis

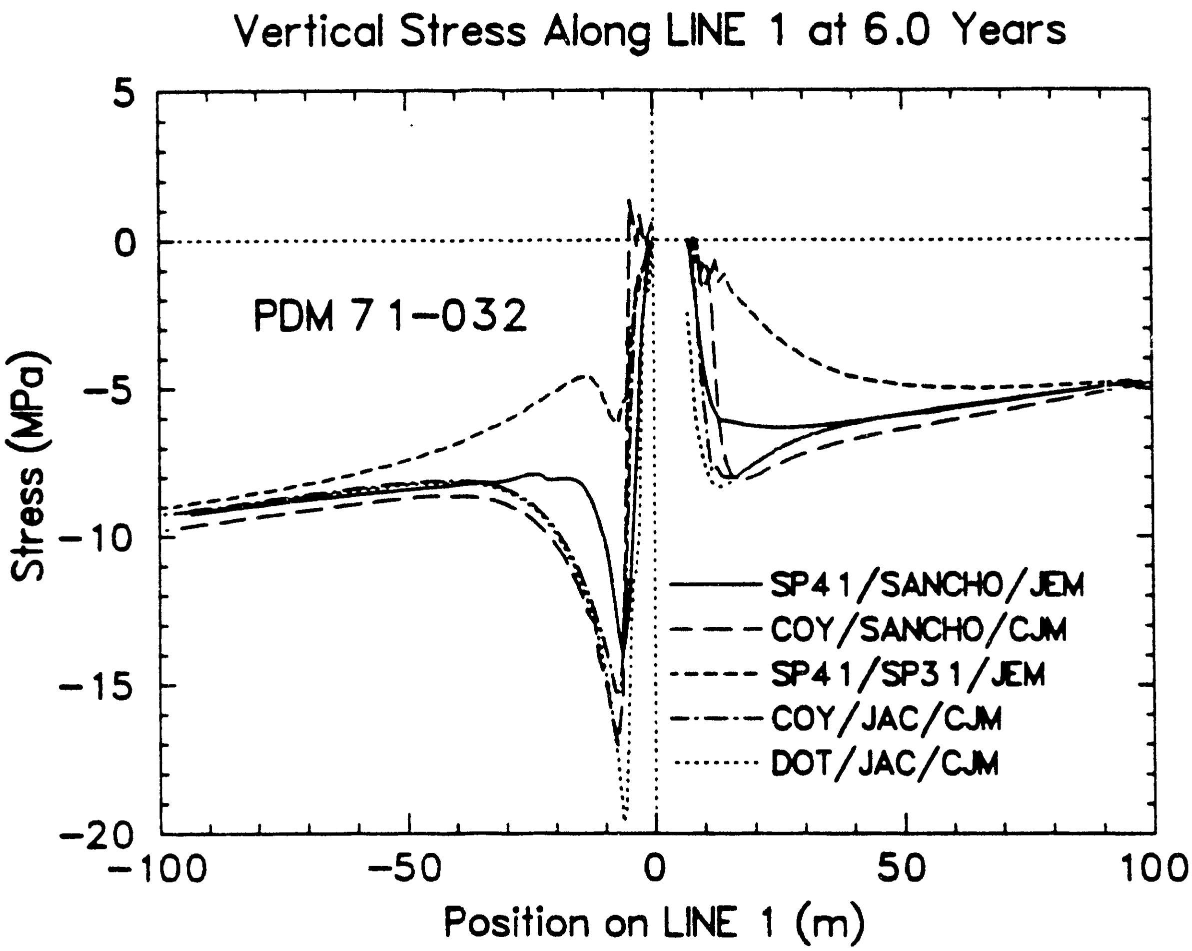

Figure 5-21. Comparison of Results for the Vertical Stress Along Line 1 (Figure 2-3) at 6 Yr, Initial Analysis

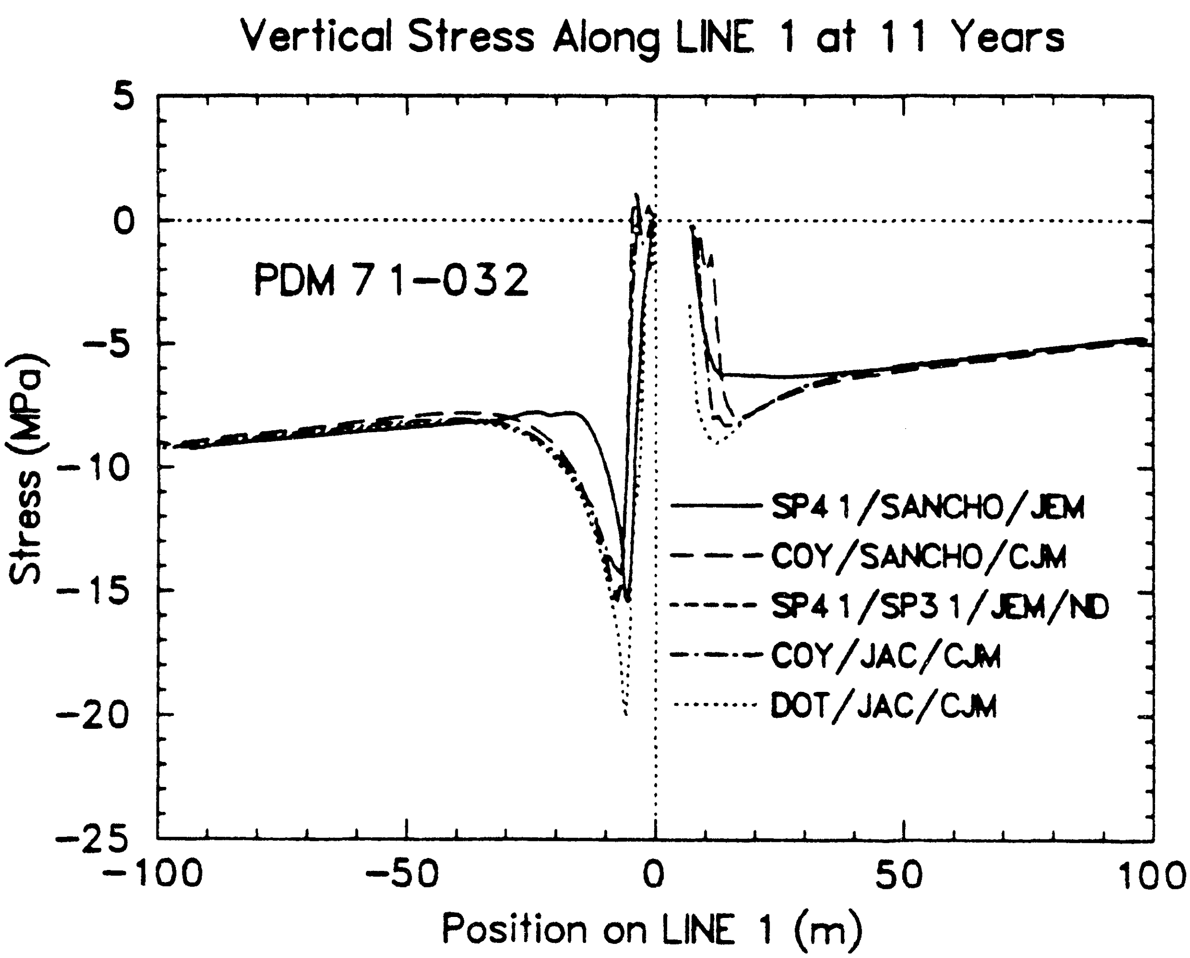

Figure 5-22. Comparison of Results for the Vertical Stress Along Line 1 (Figure 2-3) at 11 Yr, Initial Analysis

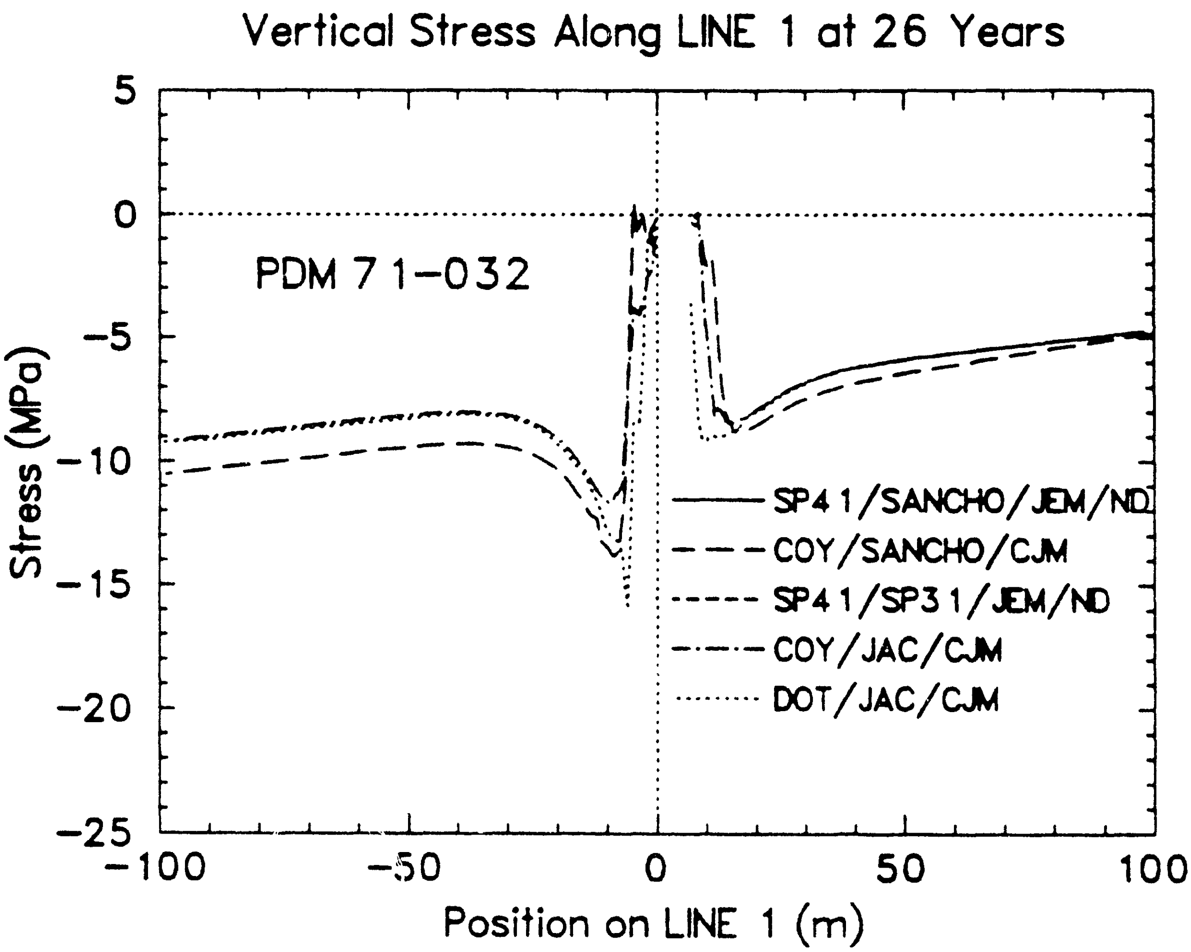

Figure 5-23. Comparison of Results for the Vertical Stress Along Line 1 (Figure 2-3) at 26 Yr, Initial Analysis

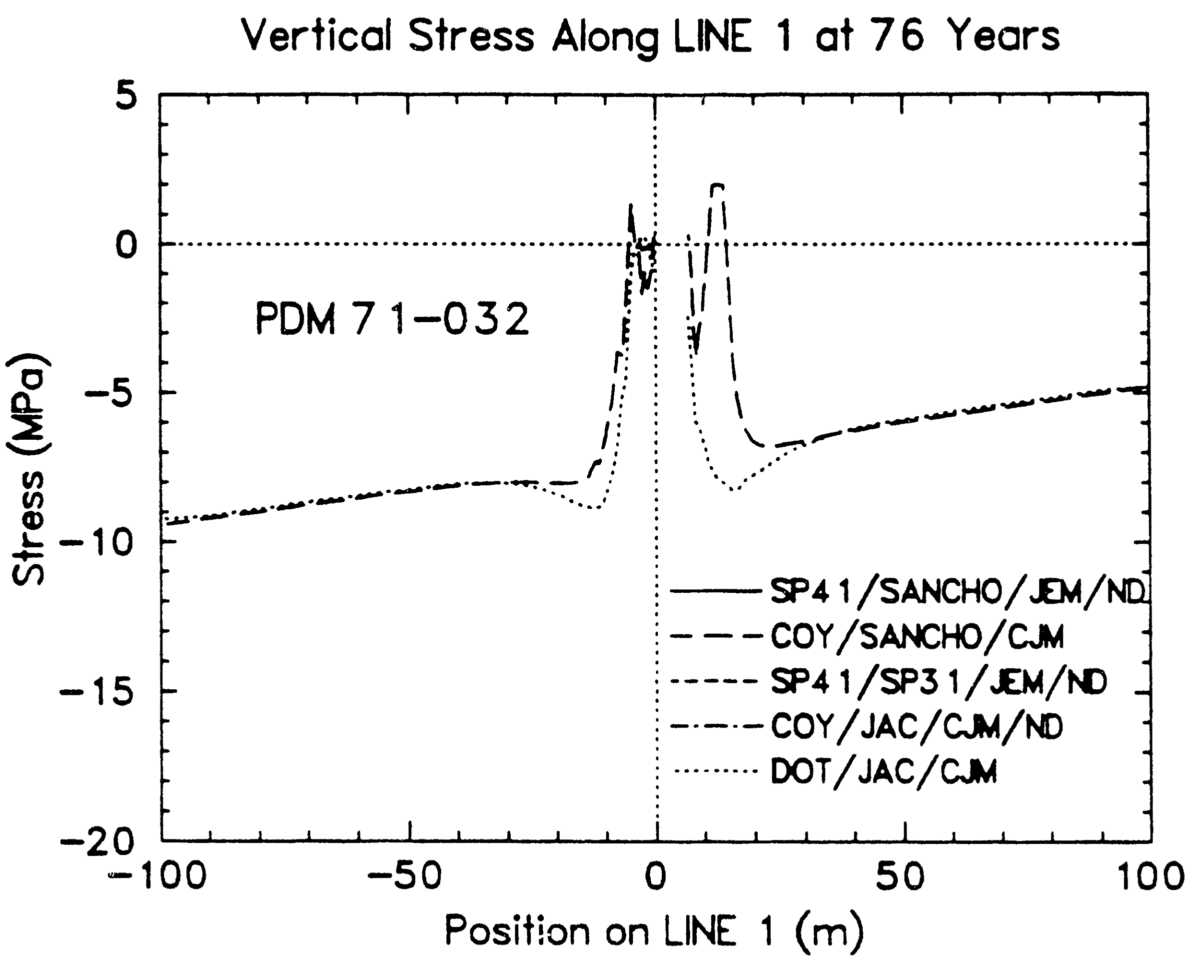

Figure 5-24. Comparison of Results for the Vertical Stress Along Line 1 (Figure 2-3) at 76 Yr, Initial Analysis

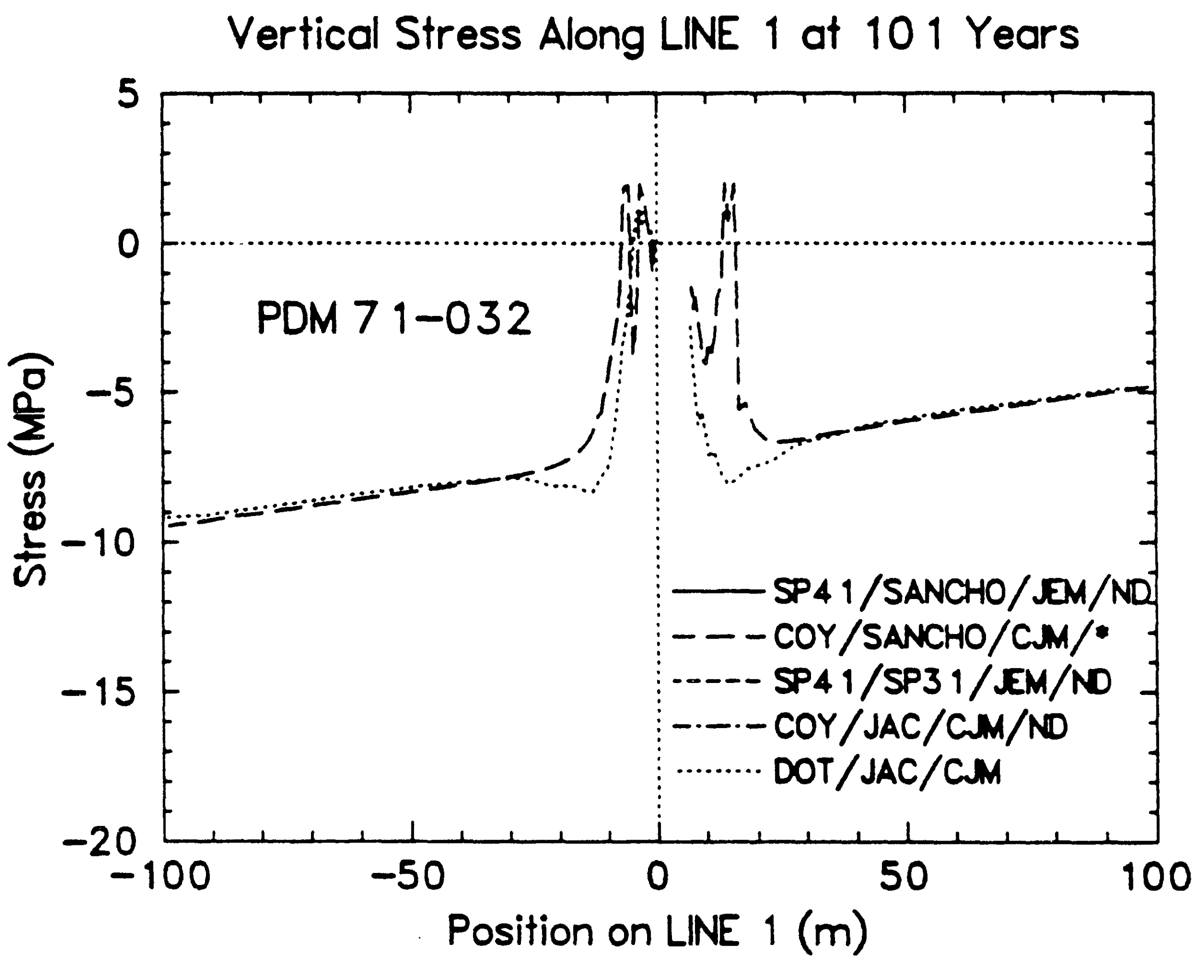

Figure 5-25. Comparison of Results for the Vertical Stress Along Line 1 (Figure 2-3) at 101 Yr, Initial Analysis

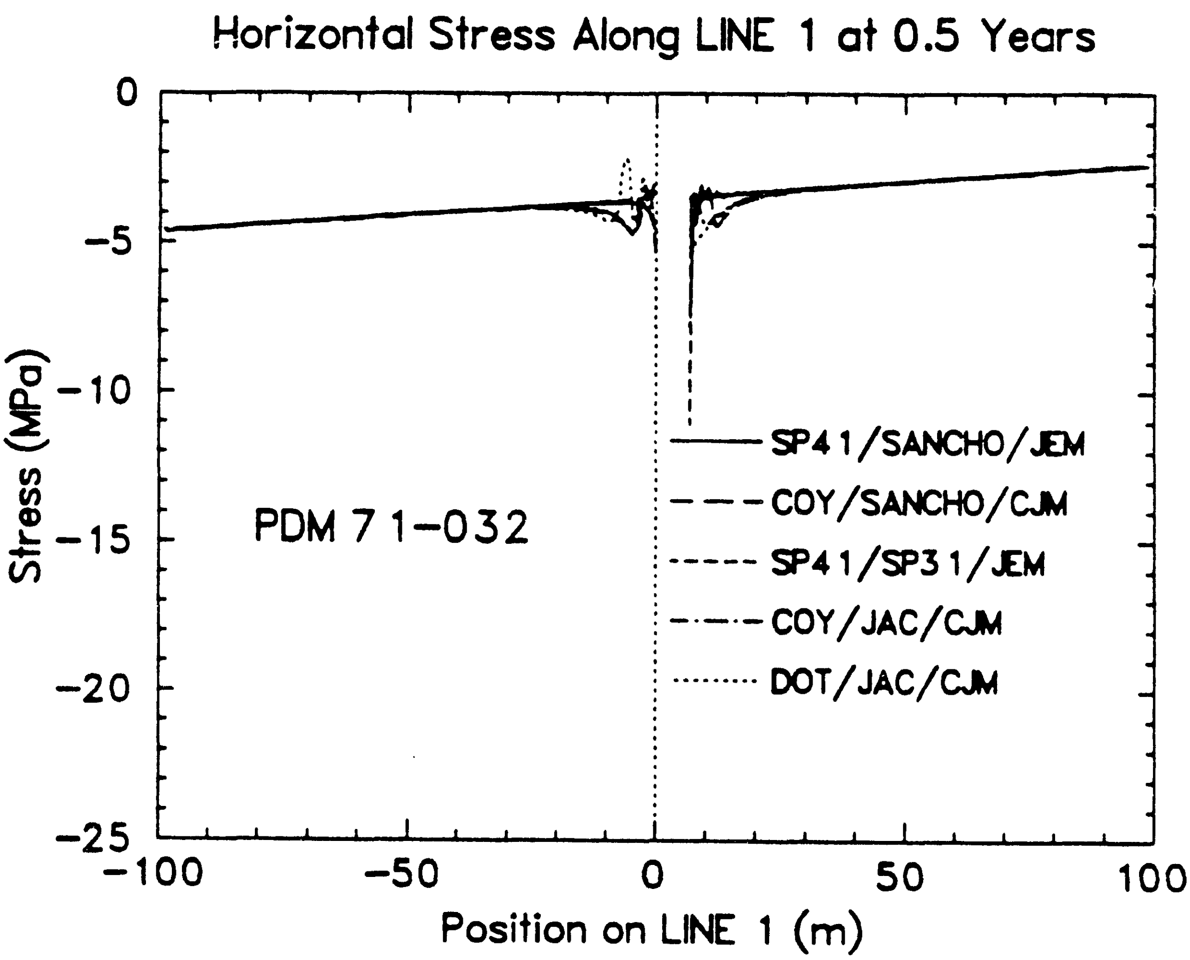

Figure 5-26. Comparison of Results for the Horizontal Stress Along Line 1 (Figure 2-3) at 0.5 Yr, Initial Analysis

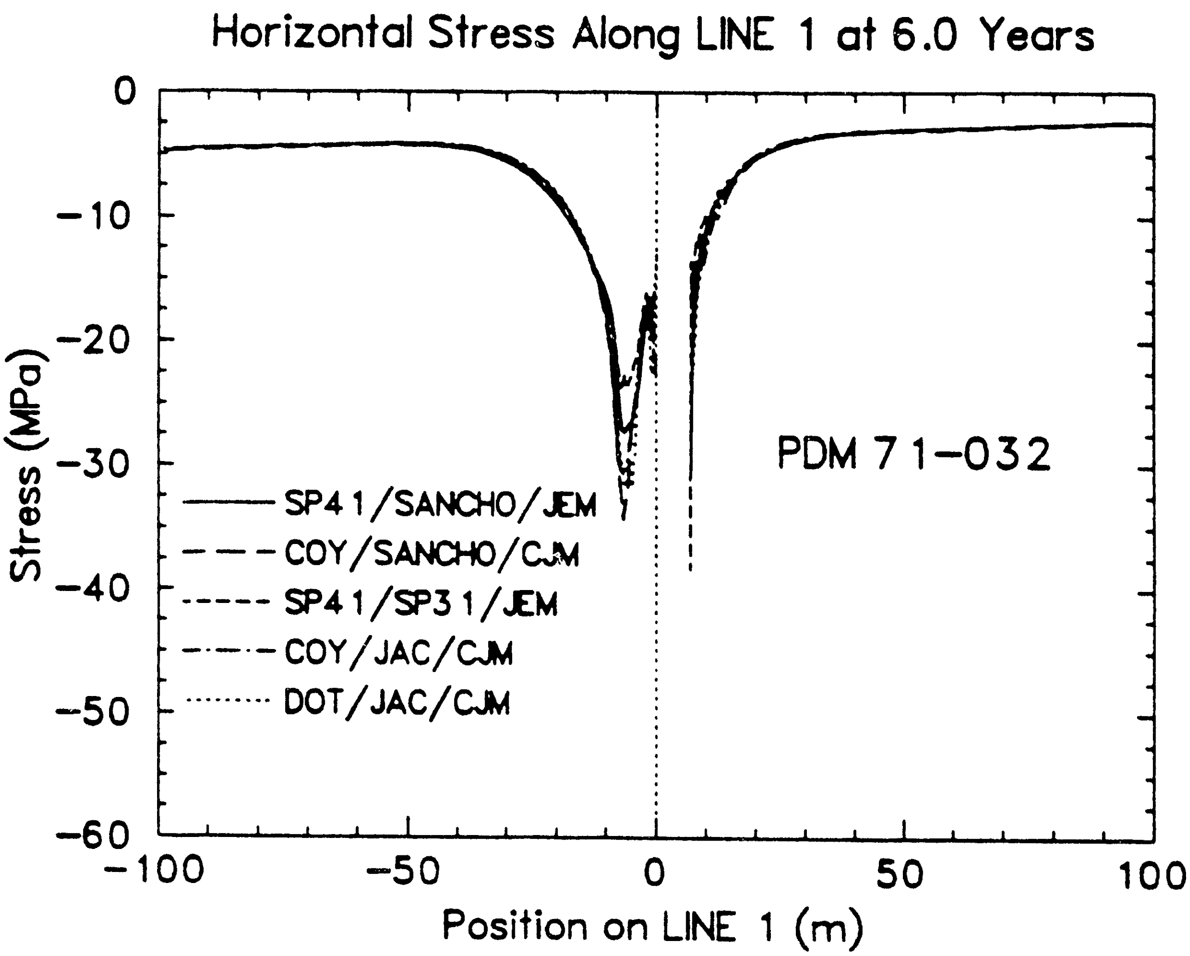

Figure 5-27. Comparison of Results for the Horizontal Stress Along Line 1 (Figure 2-3) at 6 Yr, Initial Analysis

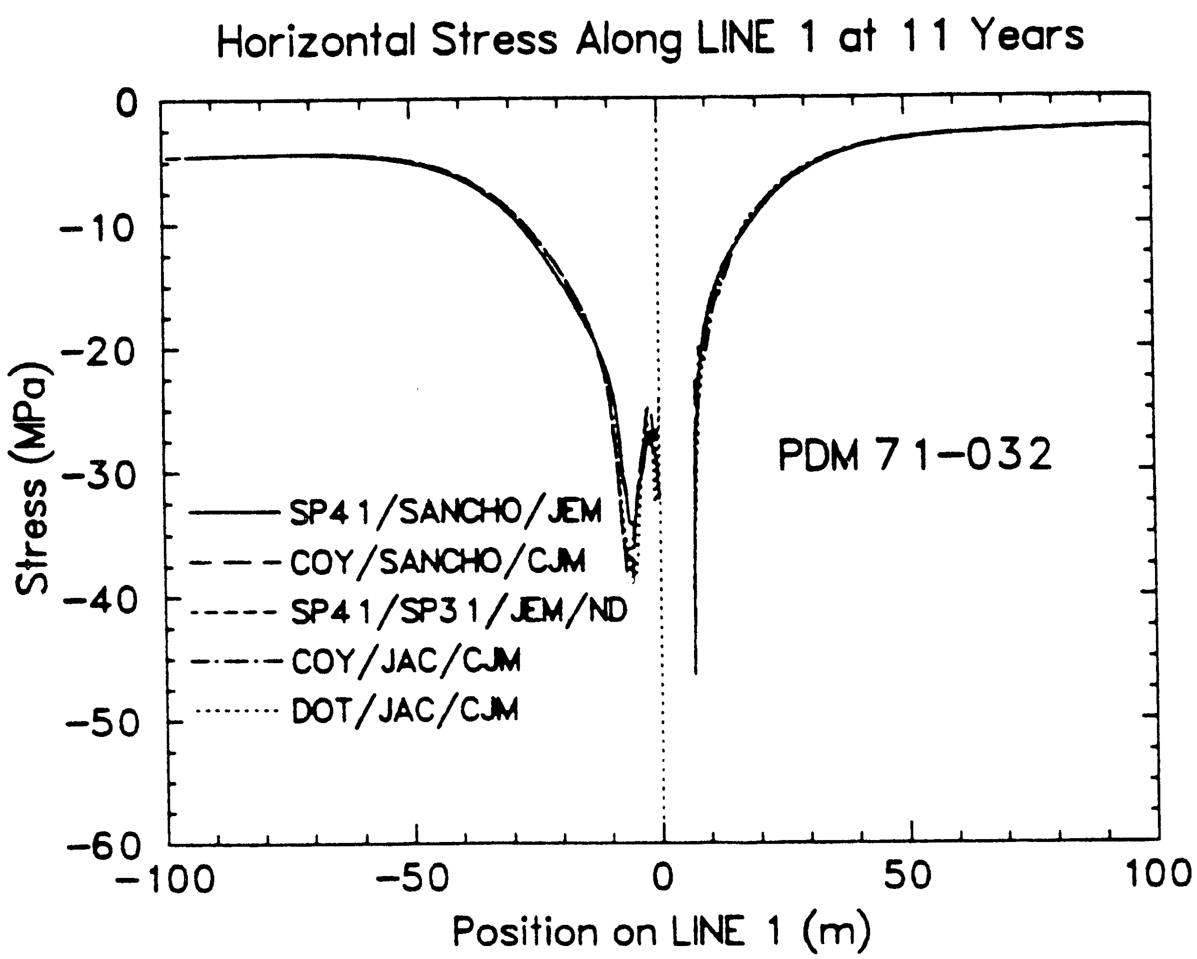

Figure 5-28. Comparison of Results for the Horizontal Stress Along Line 1 (Figure 2-3) at 11 Yr, Initial Analysis

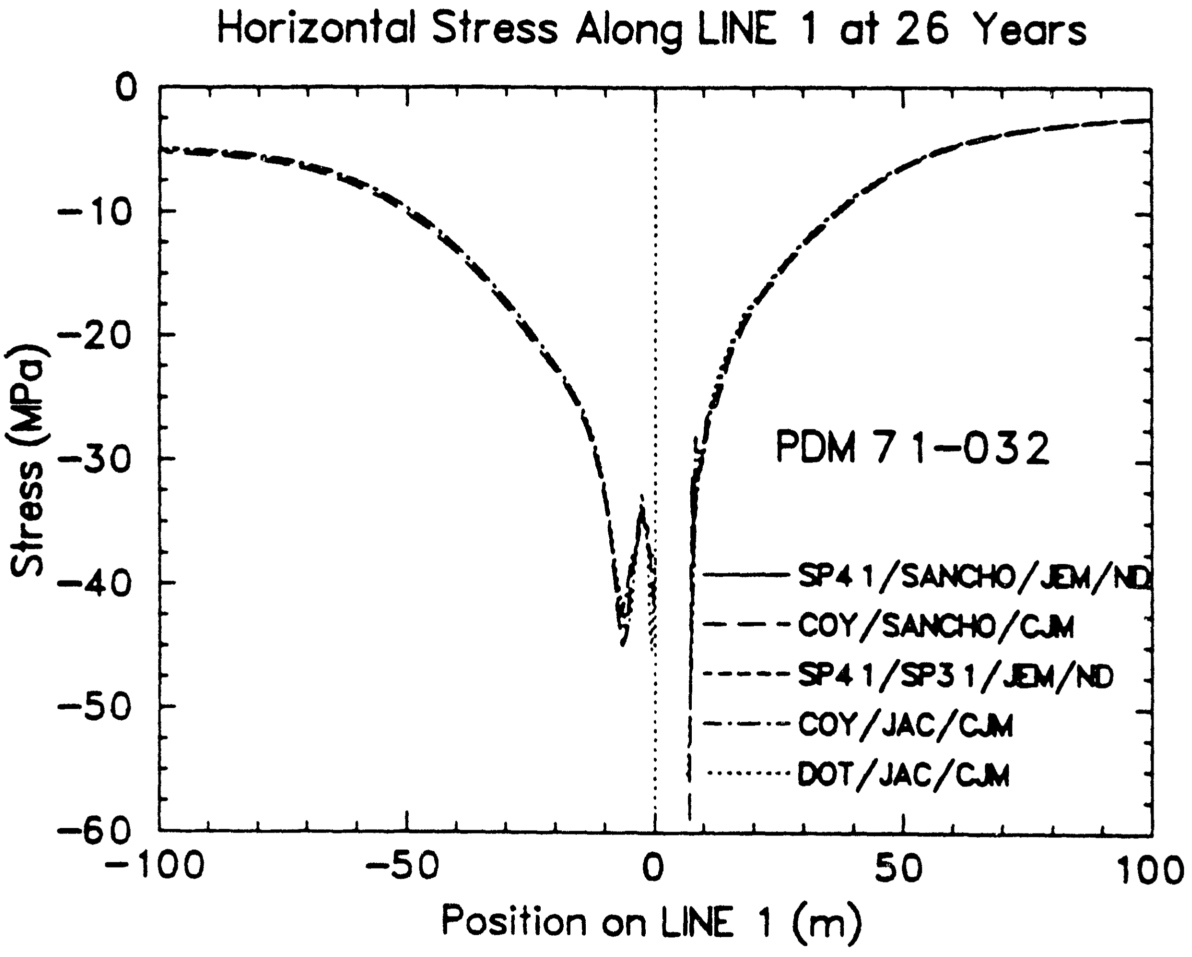

Figure 5-29. Comparison of Results for the Horizontal Stress Along Line 1 (Figure 2-3) at 26 Yr, Initial Analysis

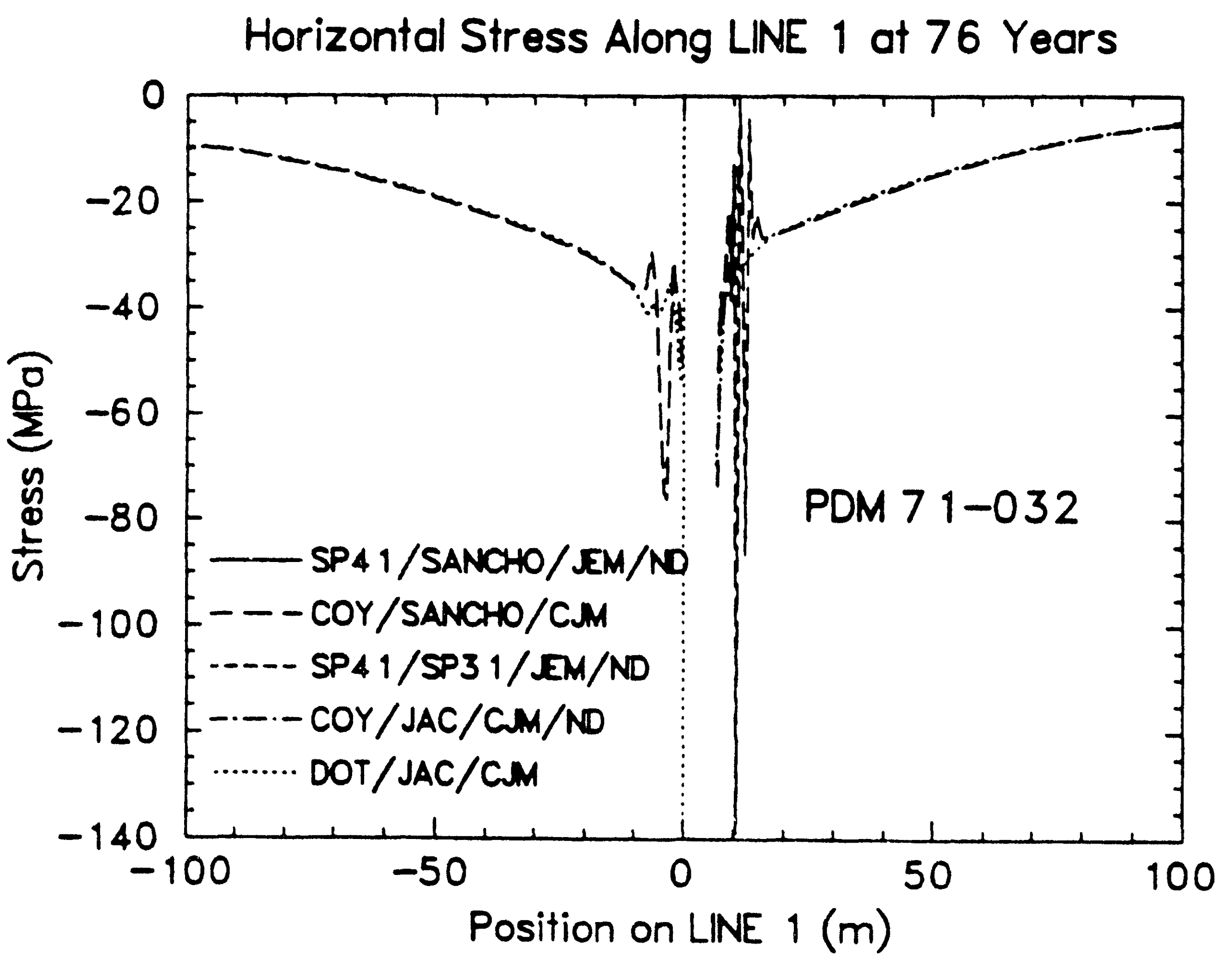

Figure 5-30. Comparison of Results for the Horizontal Stress Along Line 1 (Figure 2-3) at 76 Yr, Initial Analysis

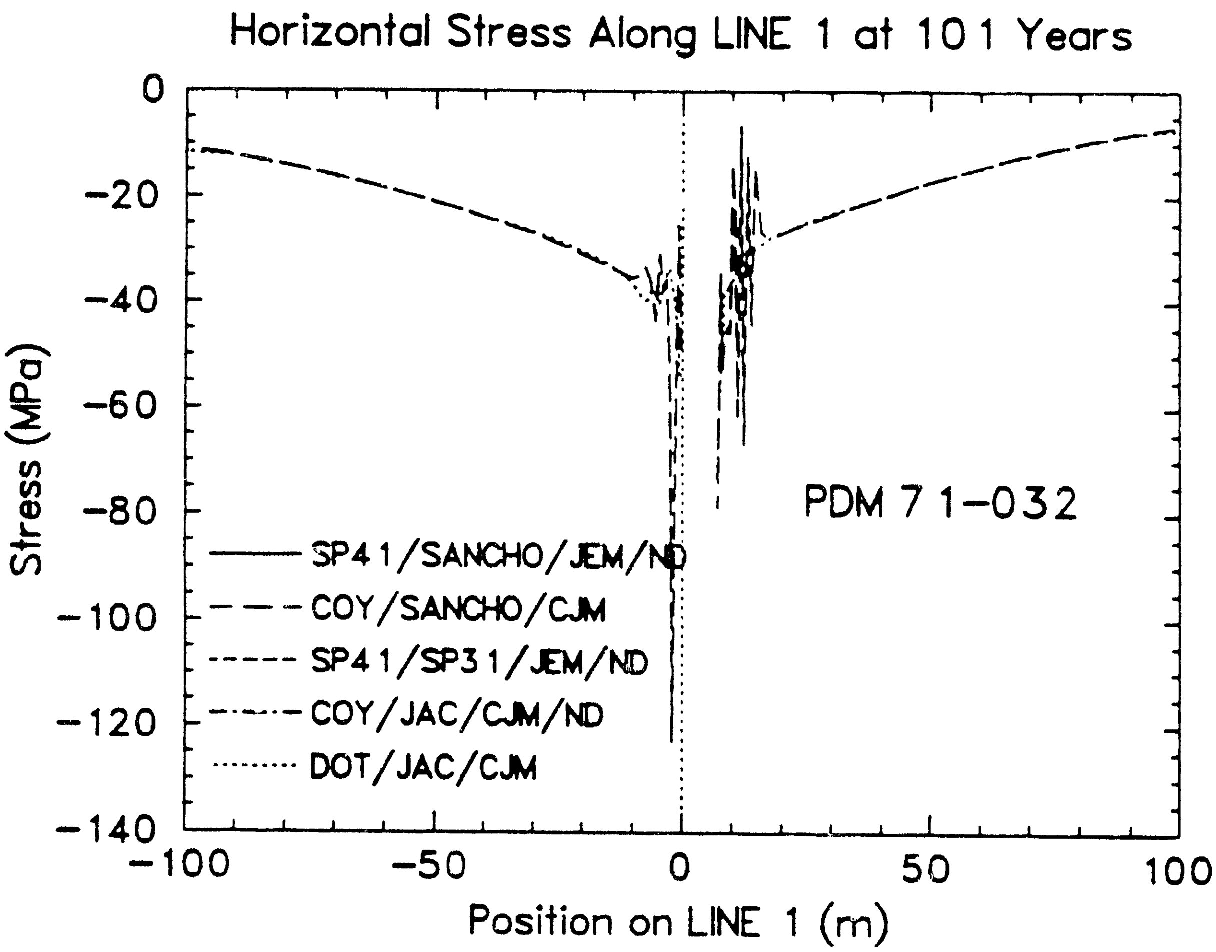

Figure 5-31. Comparison of Results for the Horizontal Str ss Along Line 1 (Figure 2-3) at 101 Yr, Initial Analysis

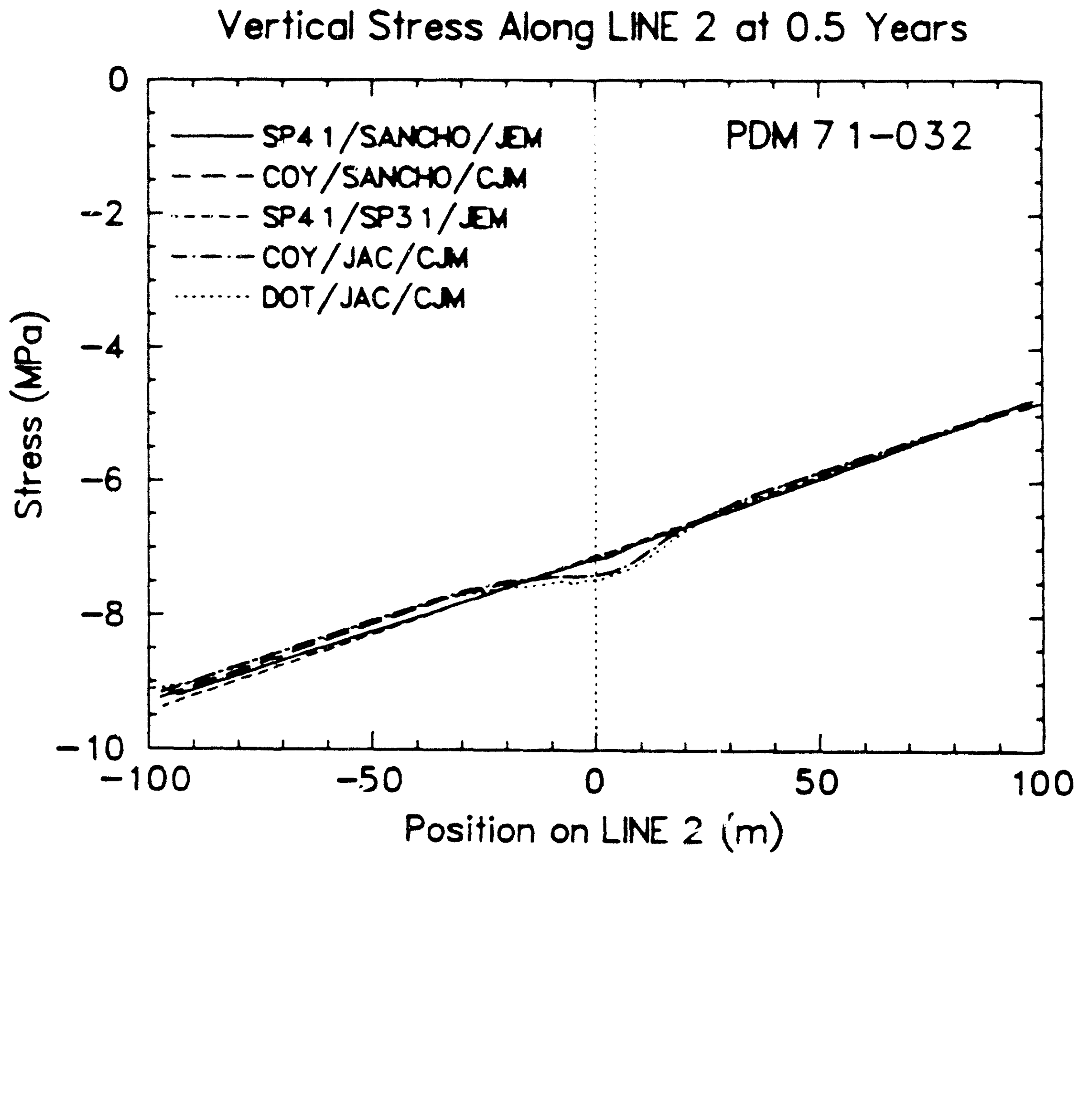

Figure 5-32. Comparison of Results for the Vertical Stress Along Line 2 (Figure 2-3) at 0.5 Yr, Initial Analysis

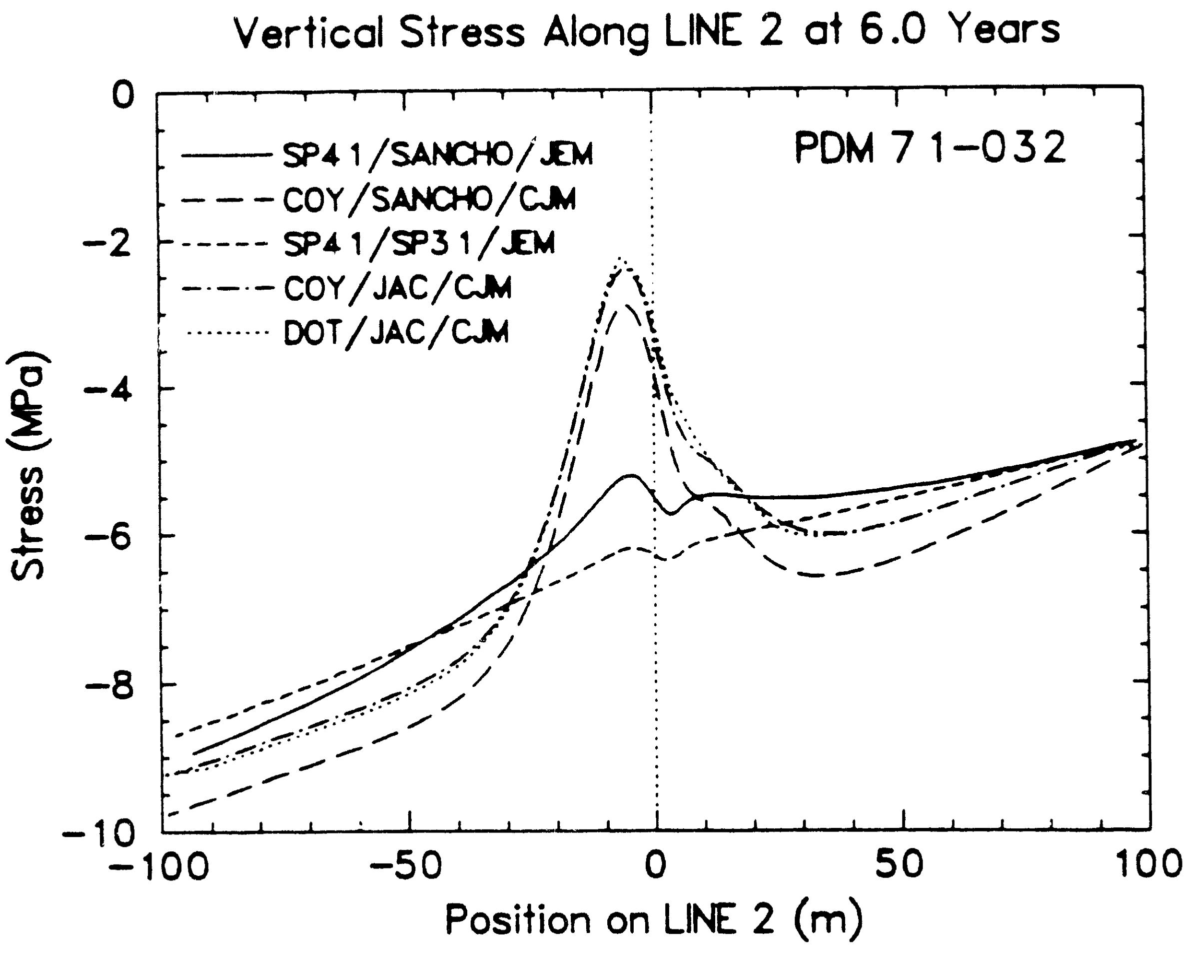

Figure 5-33. Comparison of Results for the Vertical Stress Along Line 2 (Figure 2-3) at 6 Yr, Initial Analysis

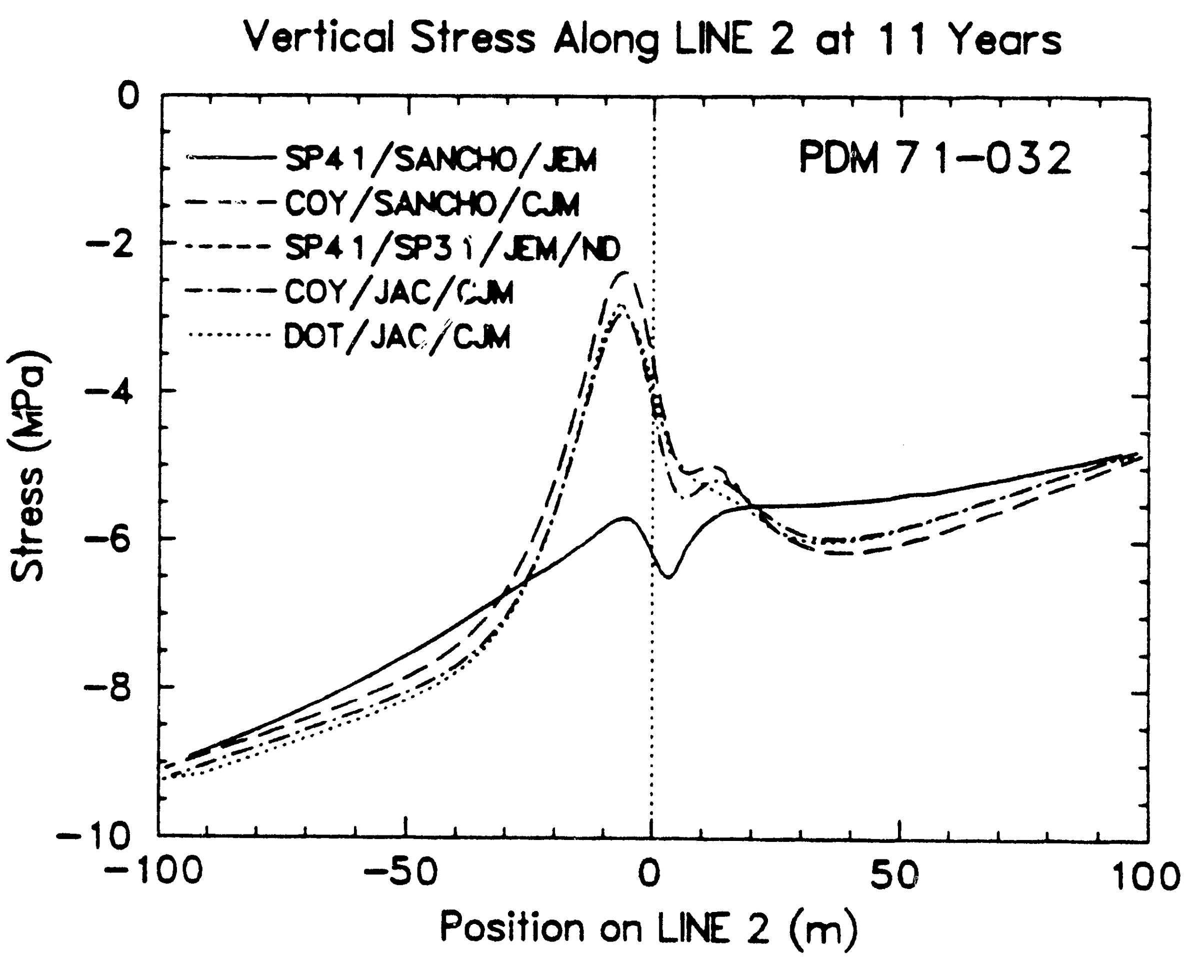

Figure 5-34. Comparison of Results for the Vertical Stress Along Line 2 (Figure 2-3) at 11 Yr, Initial Analysis

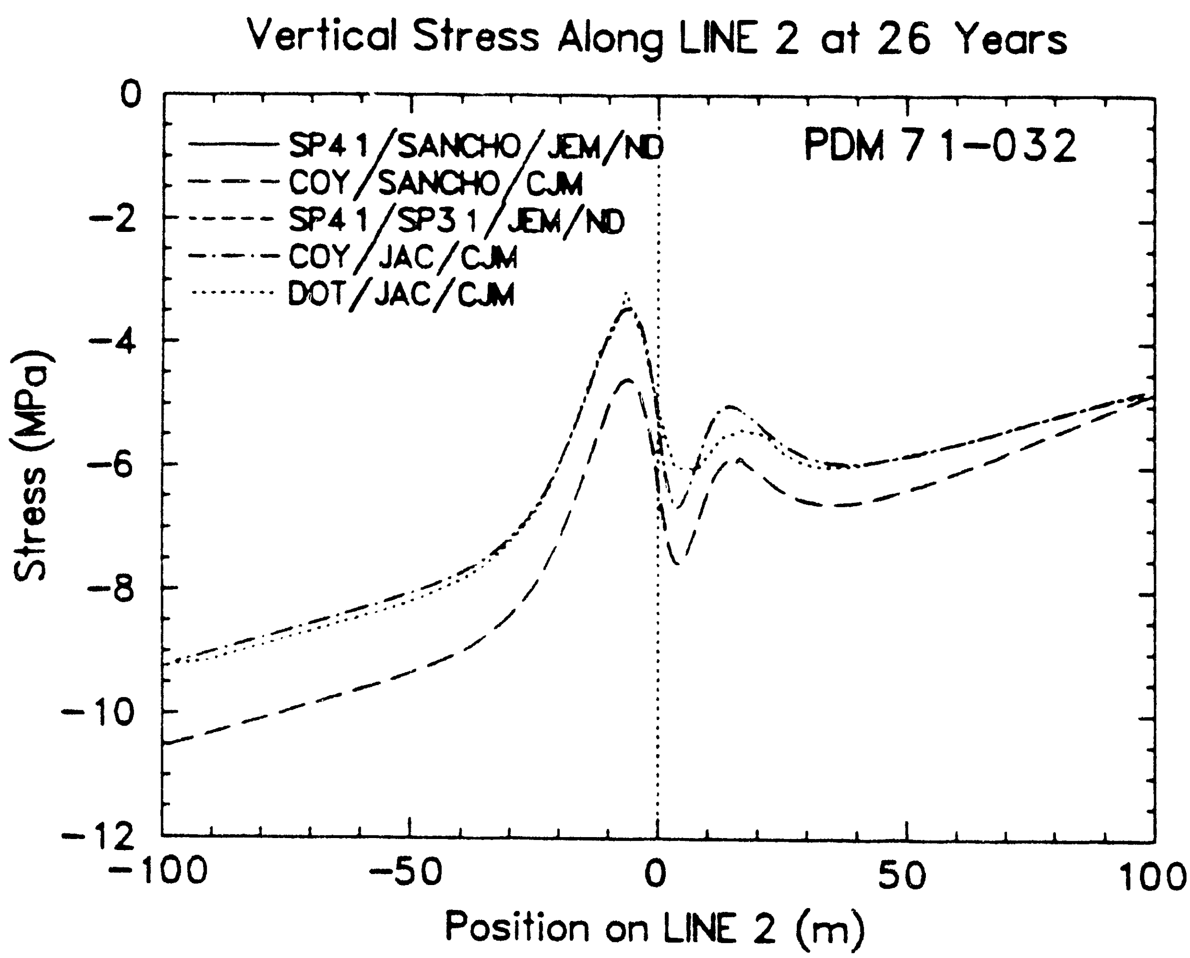

Figure 5-35. Comparison of Results for the Vertical Stress Along Line 2 (Figure 2-3) at 26 Yr, Initial Analysis

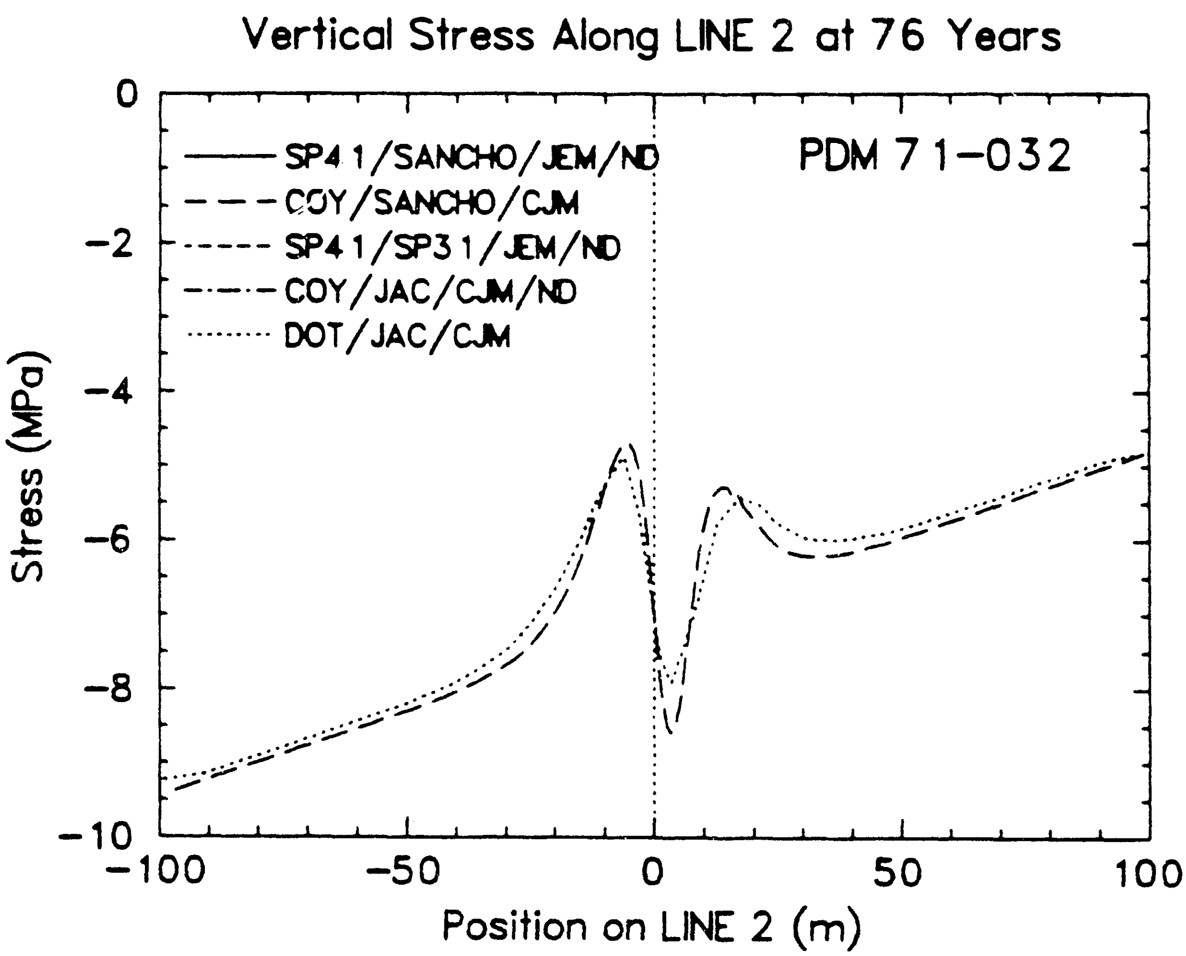

Figure 5-36. Comparison of Results for the Vertical Stress Along Line 2 (Figure 2-3) at 76 Yr, Initial Analysis

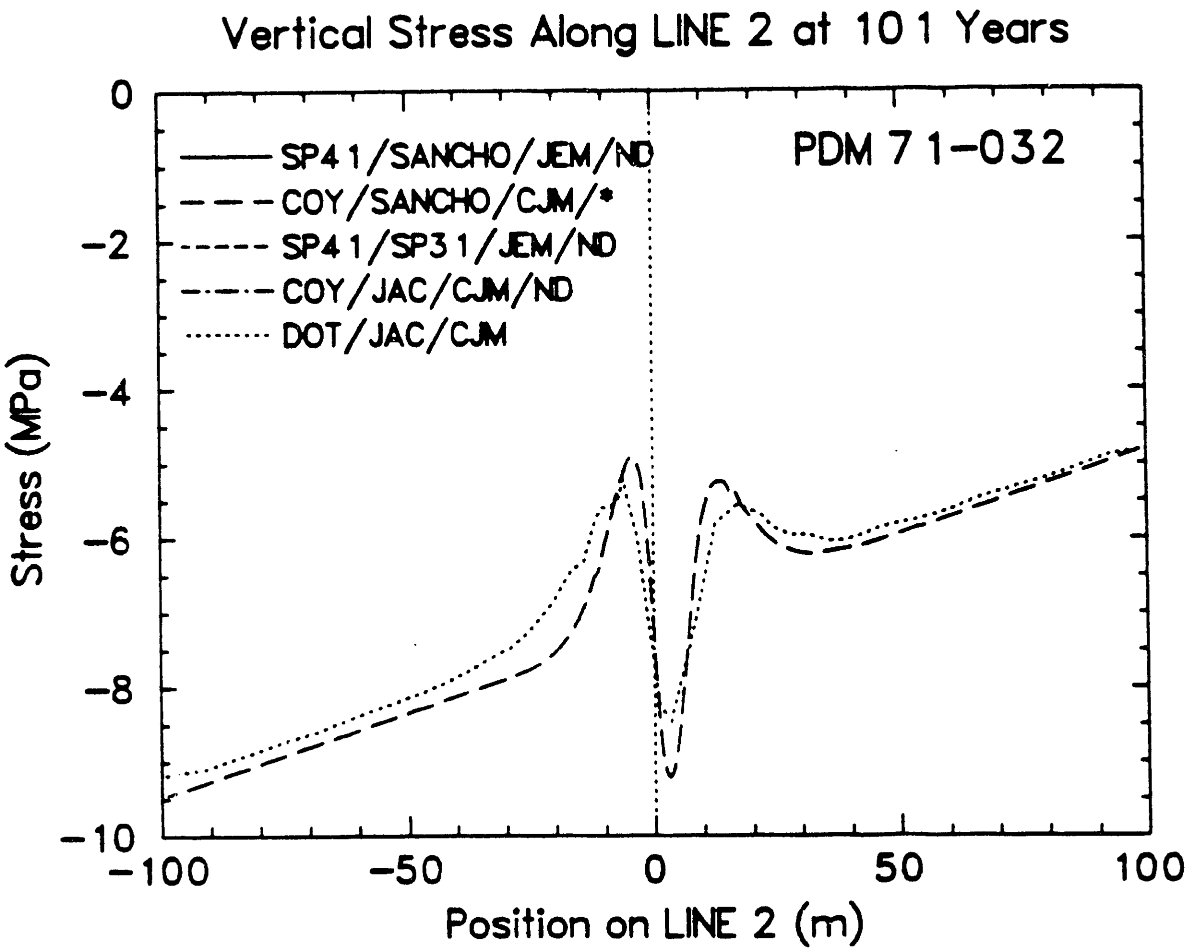

Figure 5-37. Comparison of Results for the Vertical Stress Along Line 2 (Figure 2-3) at 101 Yr, Initial Analysis

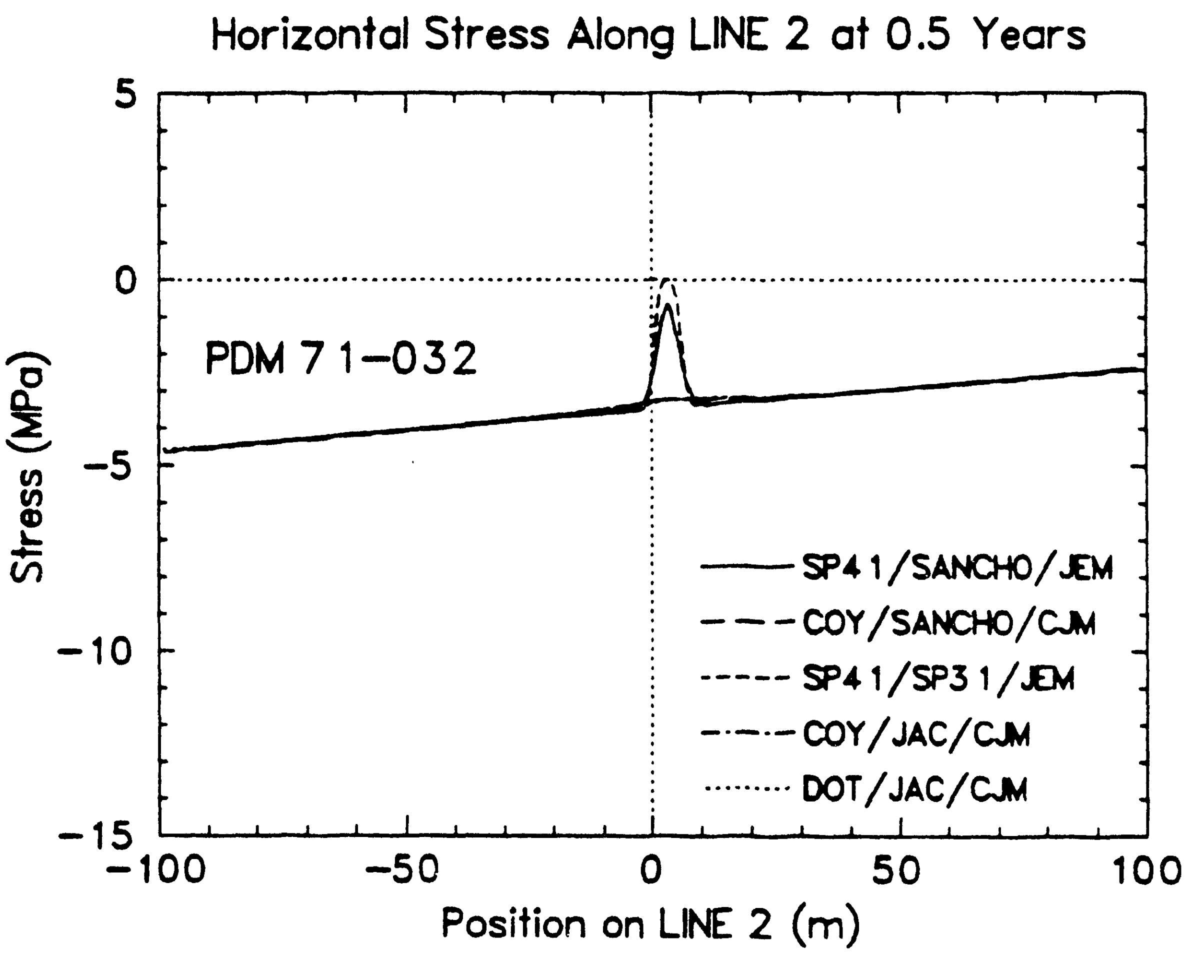

Figure 5-38. Comparison of Results for the Horizontal Stress Along Line 2 (Figure 2-3) at 0.5 Yr, Initial Analysis

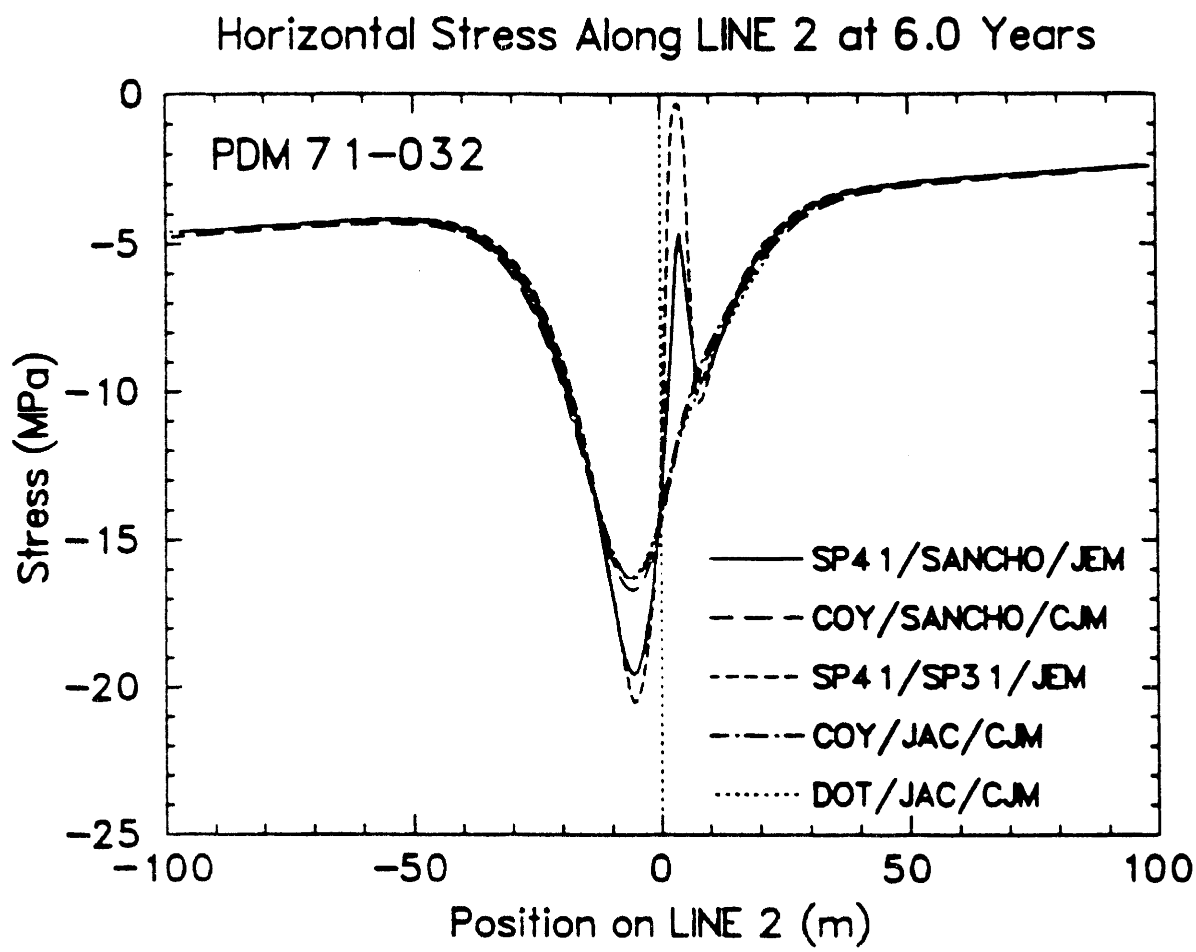

Figure 5-39. Comparison of Results for the Horizontal Stress Along Line 2 (Figure 2-3) at 6 Yr, Initial Analysis

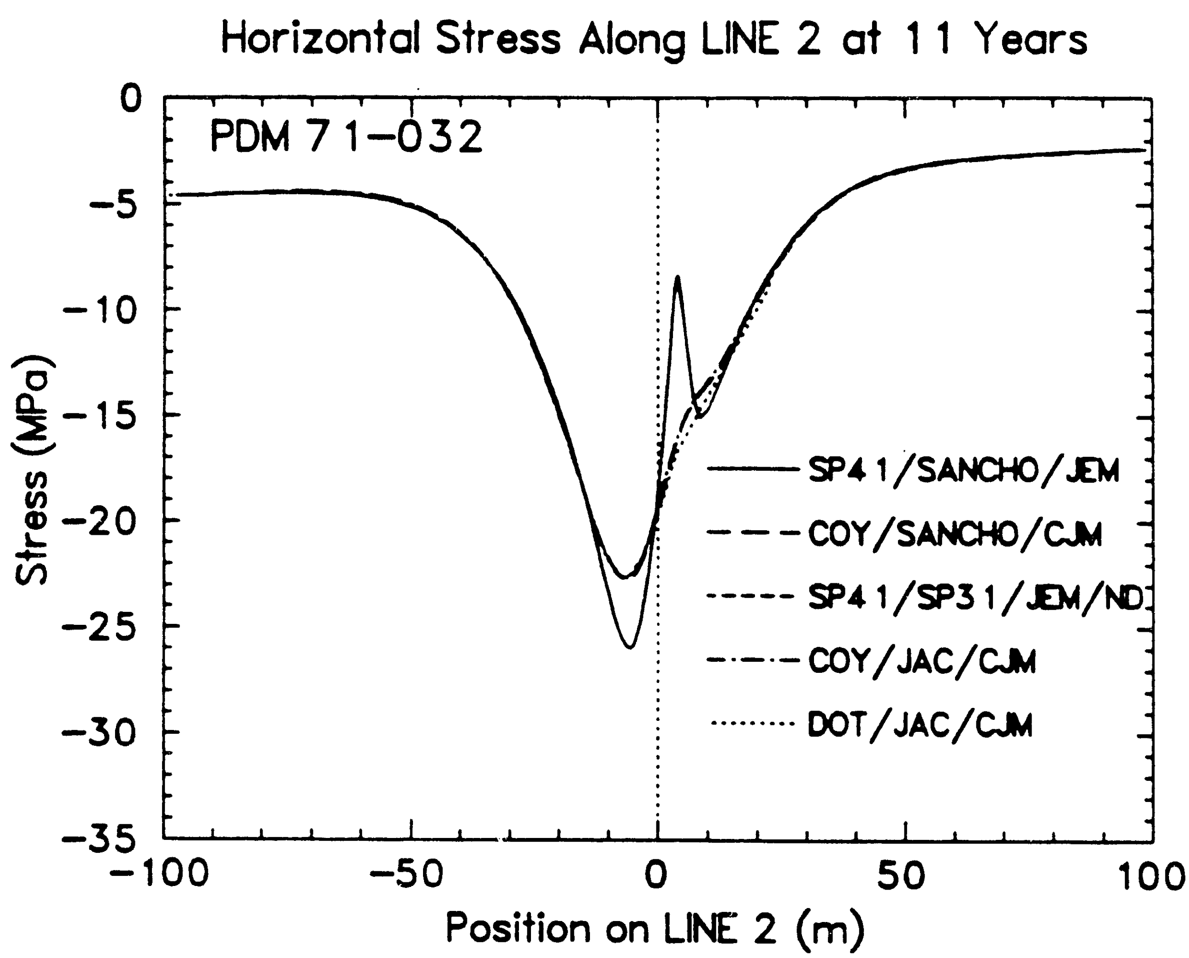

Figure 5-40. Comparison of Results for the Horizontal Stress Along Line 2 (Figure 2-3) at 11 Yr, Initial Analysis

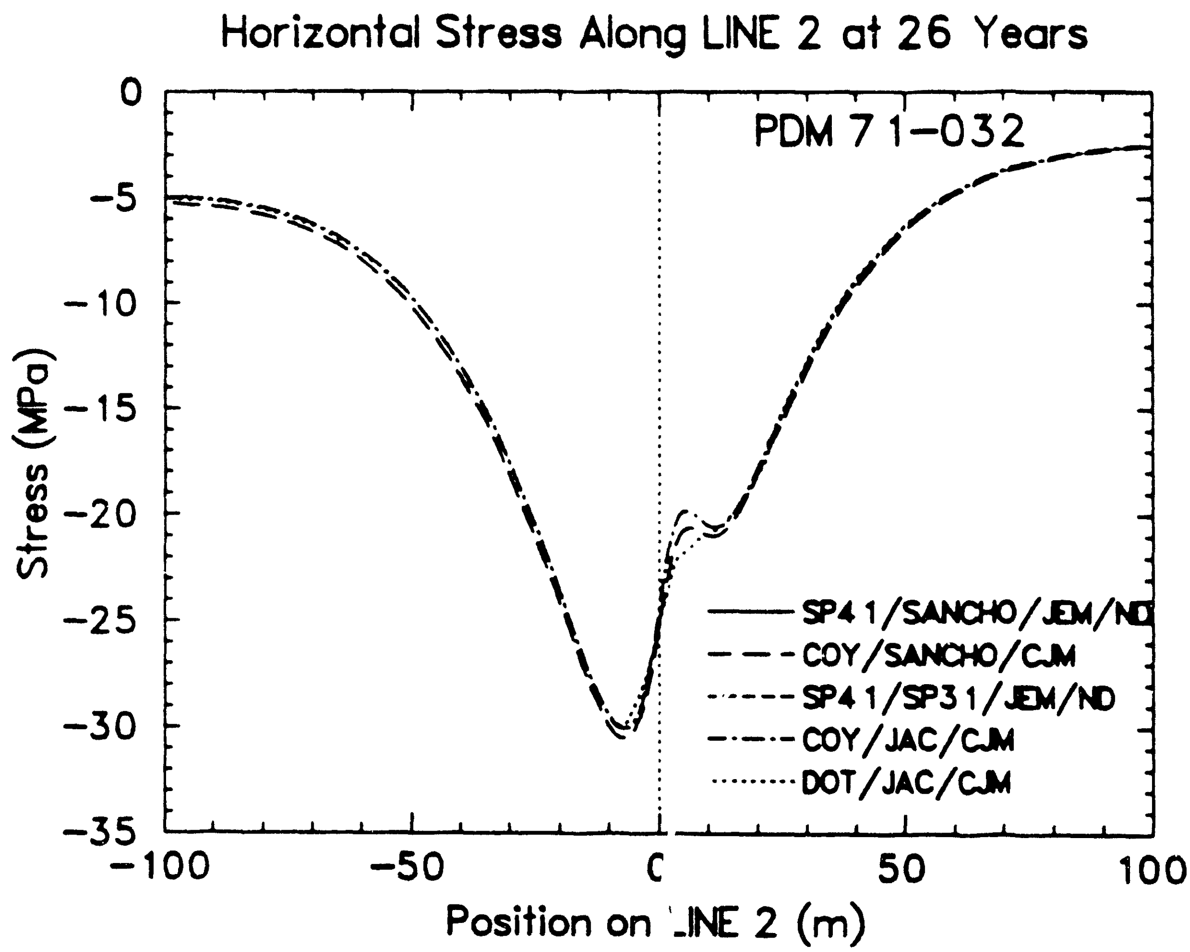

Figure 5-41. Comparison of Results for the Horizontal Stress Along Line 2 (Figure 2-3) at 26 Yr, Initial Analysis

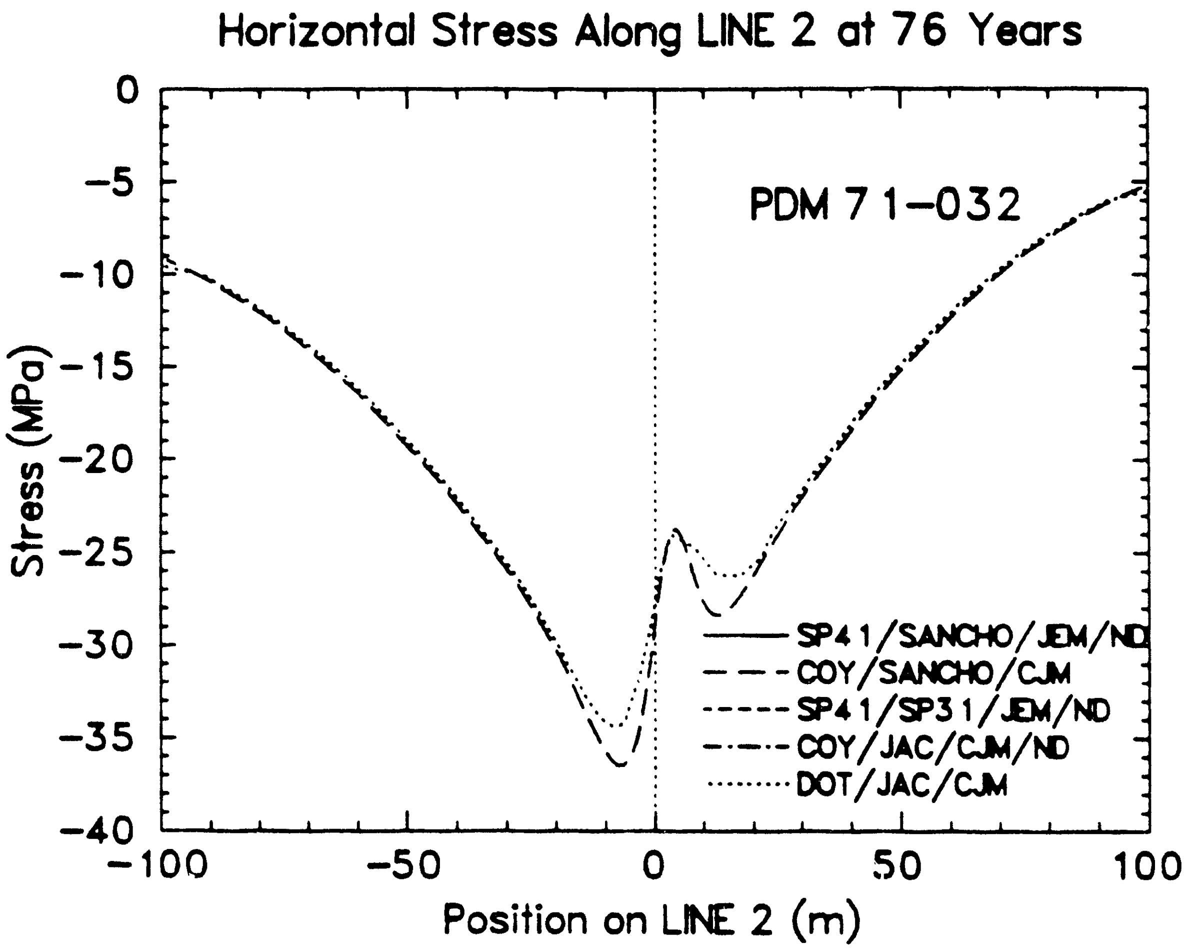

Figure 5-42. Comparison of Results for the Horizontal Stress Along Line 2 (Figure 2-3) at 76 Yr, Initial Analysis

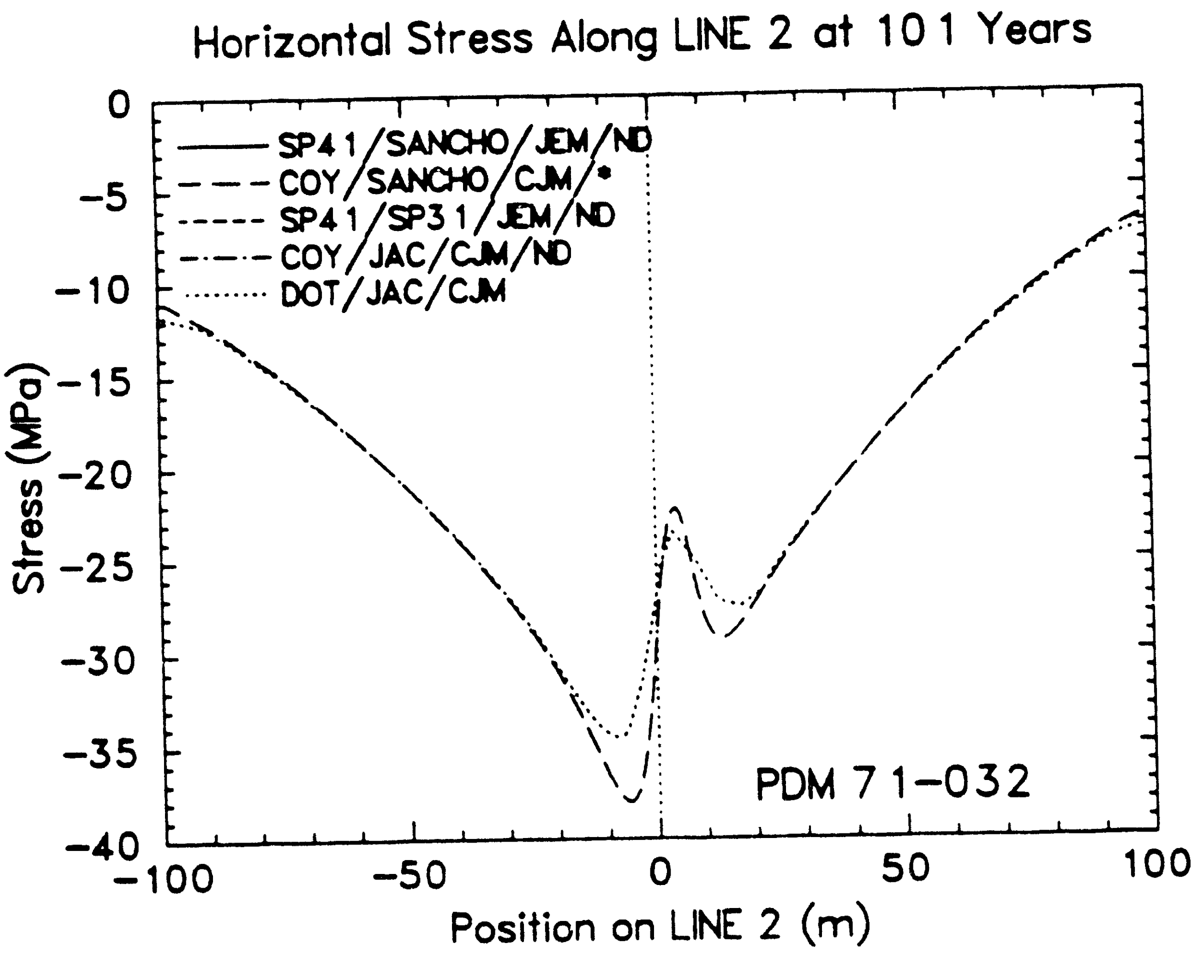

Figure 5-43. Comparison of Results for the Horizontal Stress Along Line 2 (Figure 2-3) at 101 Yr, Initial Analysis

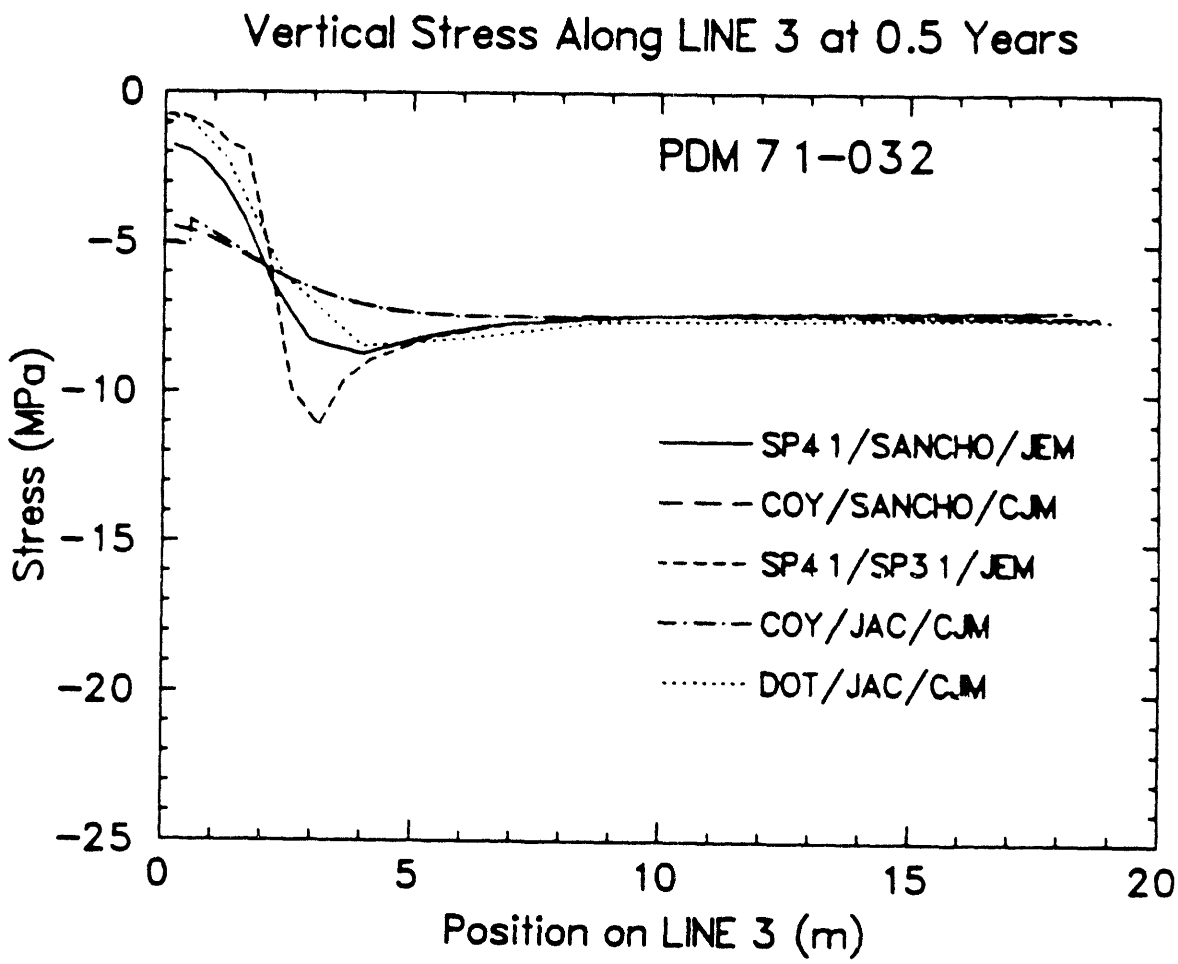

Figure 5-44. Comparison of Results for the Vertical Stress Along Line 3 (Figure 2-3) at 0.5 Yr, Initial Analysis

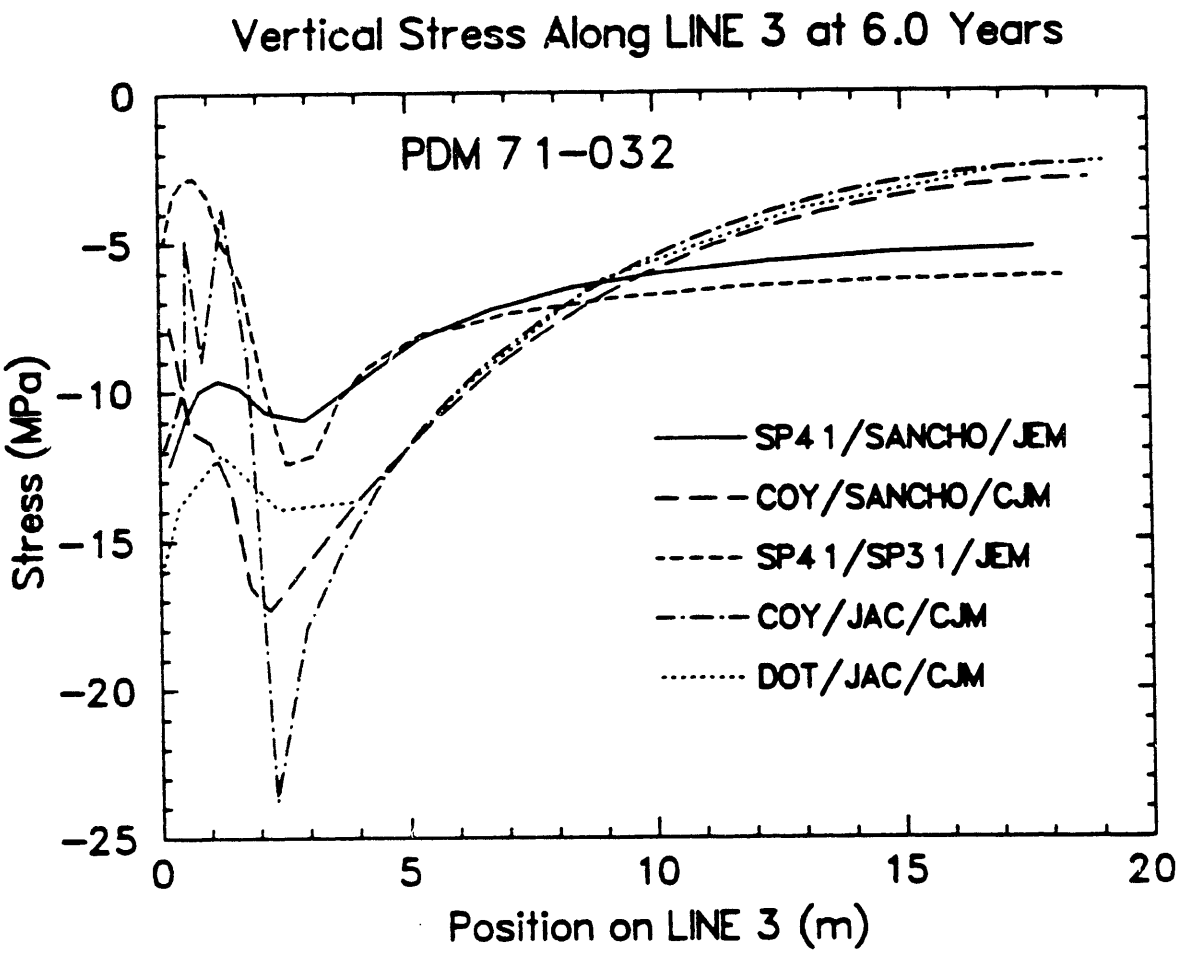

Figure 5-45. Comparison of Results for the Vertical Stress Along Line 3 (Figure 2-3) at 6 Yr, Initial Analysis

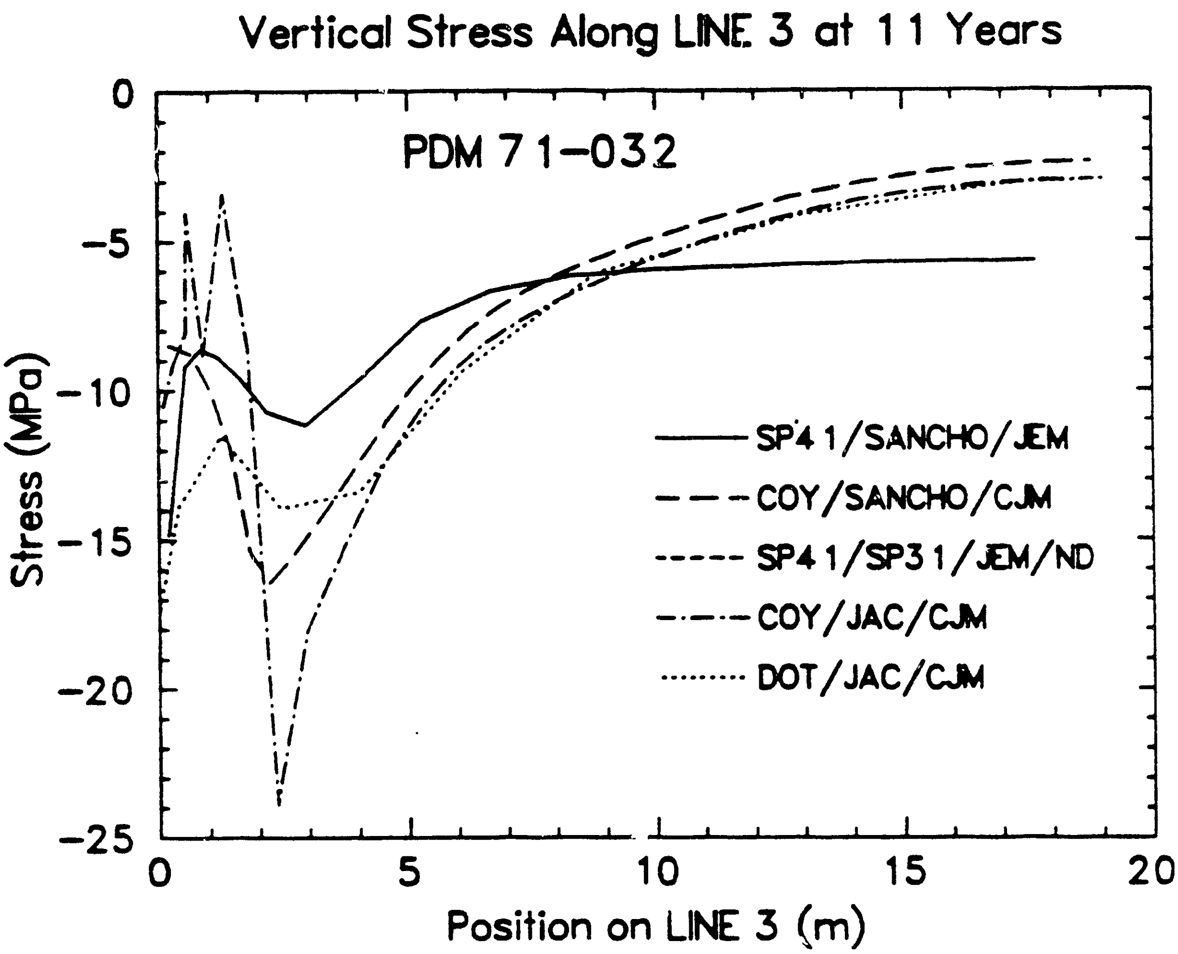

Figure 5-46. Comparison of Results for the Vertical Stress Along Line 3 (Figure 2-3) at 11 Yr, Initial Analysis

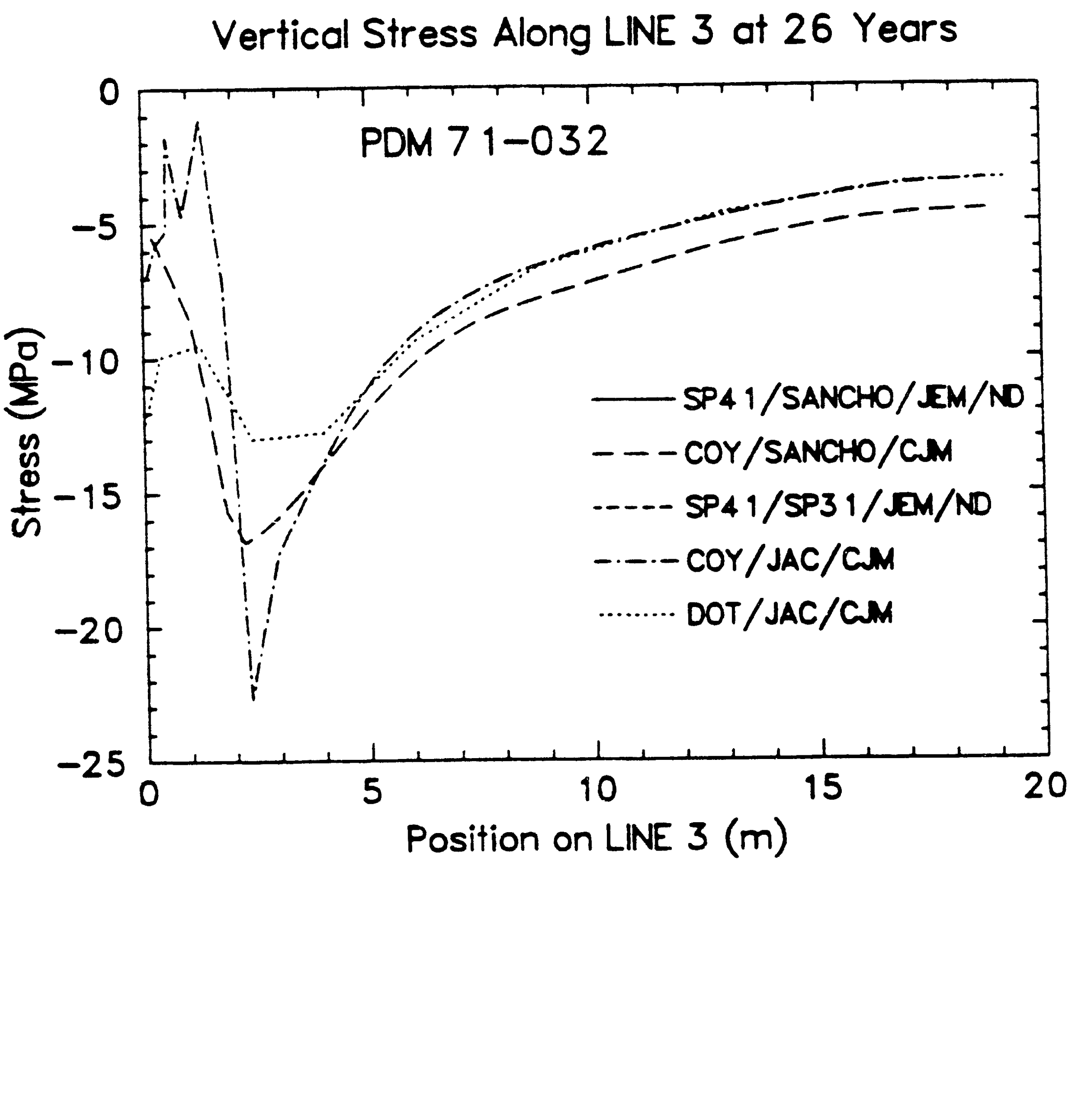

Figure 5-47. Comparison of Results for the Vertical Stress Along Line 3 (Figure 2-3) at 26 Yr, Initial Analysis

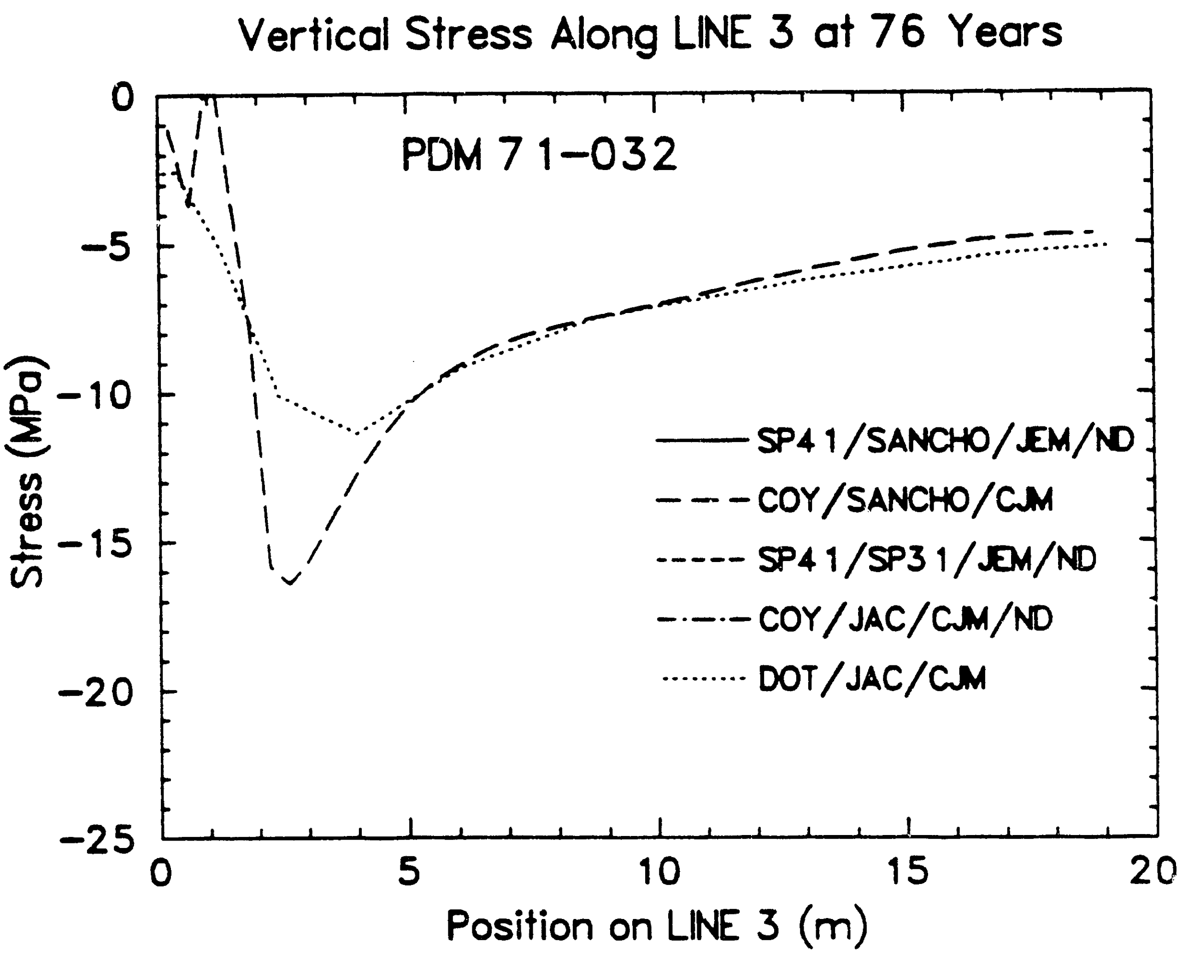

Figure 5-48. Comparison of Results for the Vertical Stress Along Line 3 (Figure 2-3) at 76 Yr, Initial Analysis

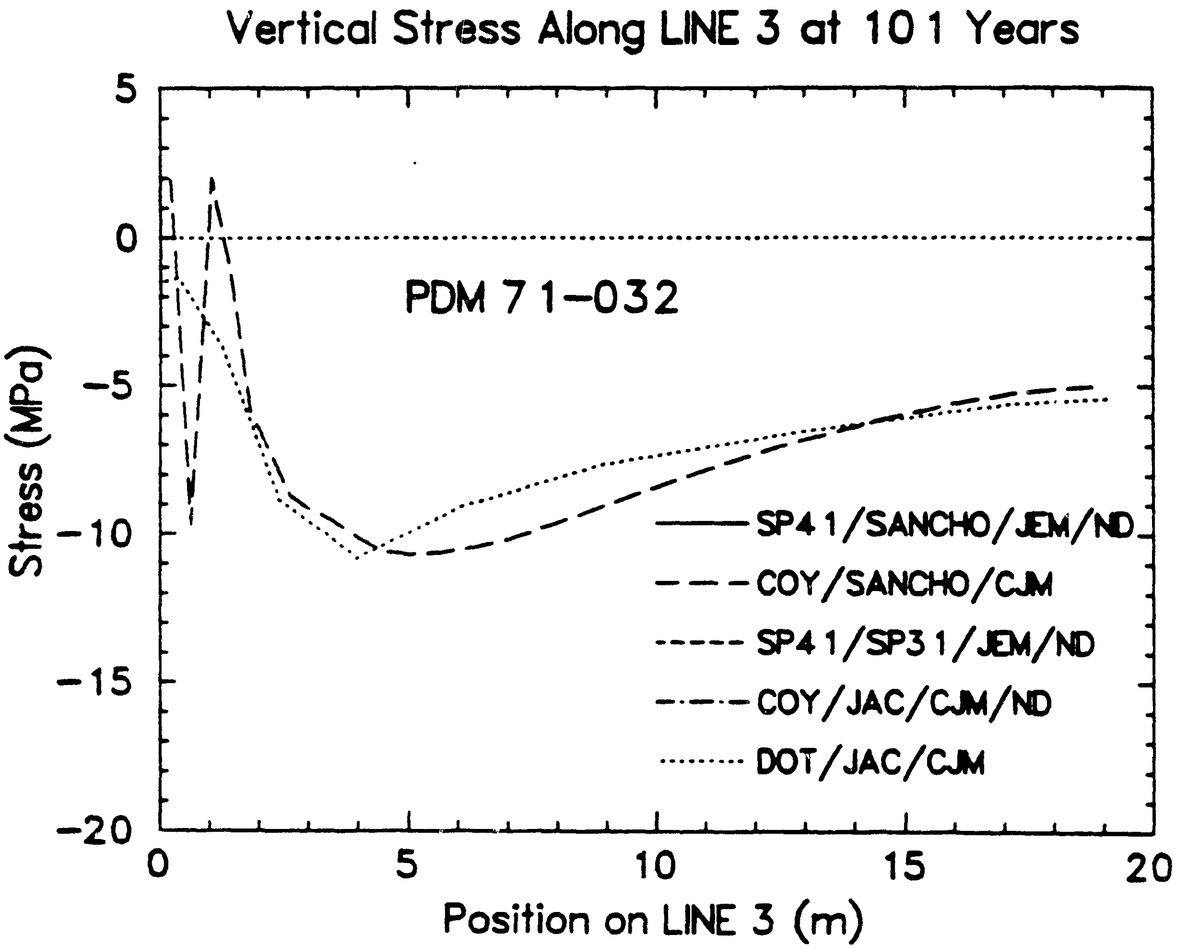

Figure 5-49. Comparison of Results for the Vertical Stress Along Line 3 (Figure 2-3) at 101 Yr, Initial Analysis

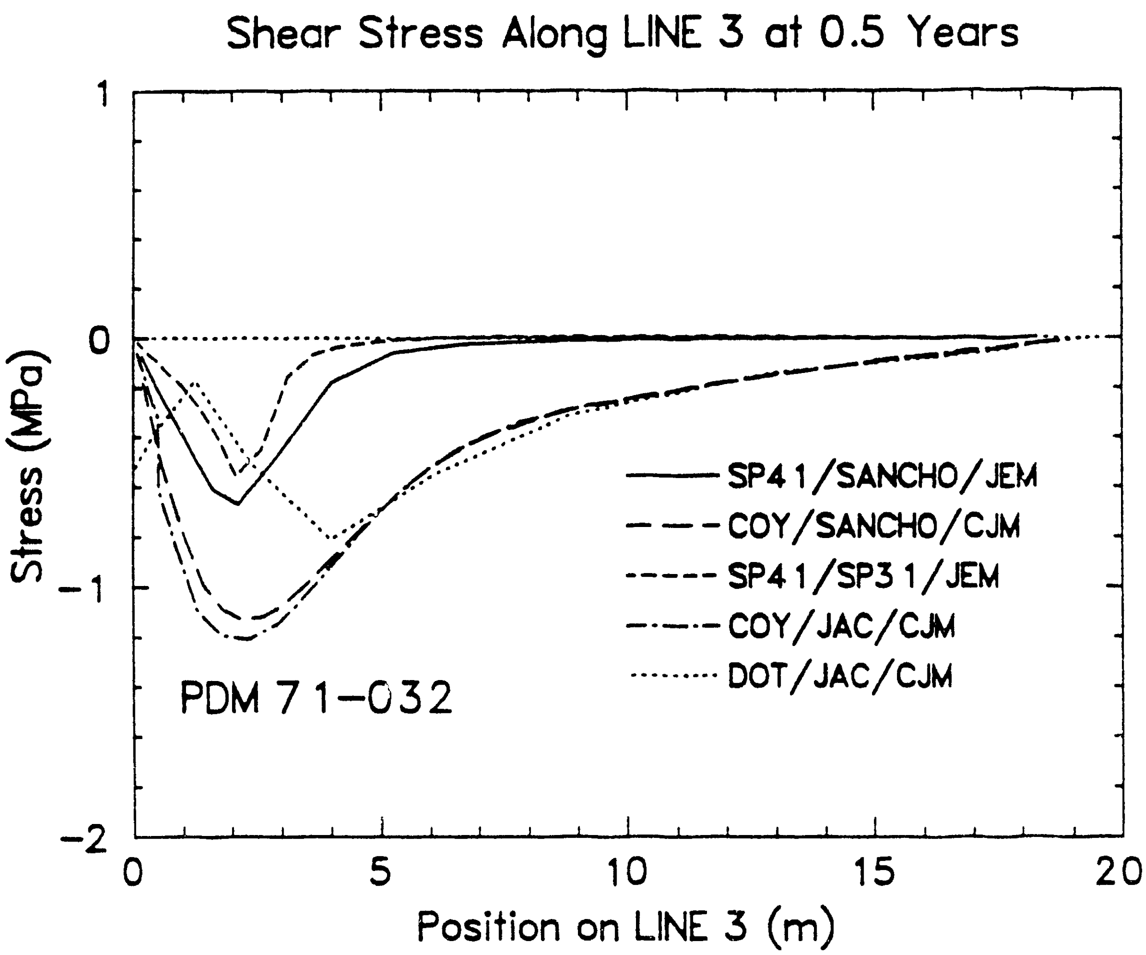

Figure 5-50. Comparison of Results for the Shear Stress Along Line 3 (Figure 2-3) at 0.5 Yr, Initial Analysis

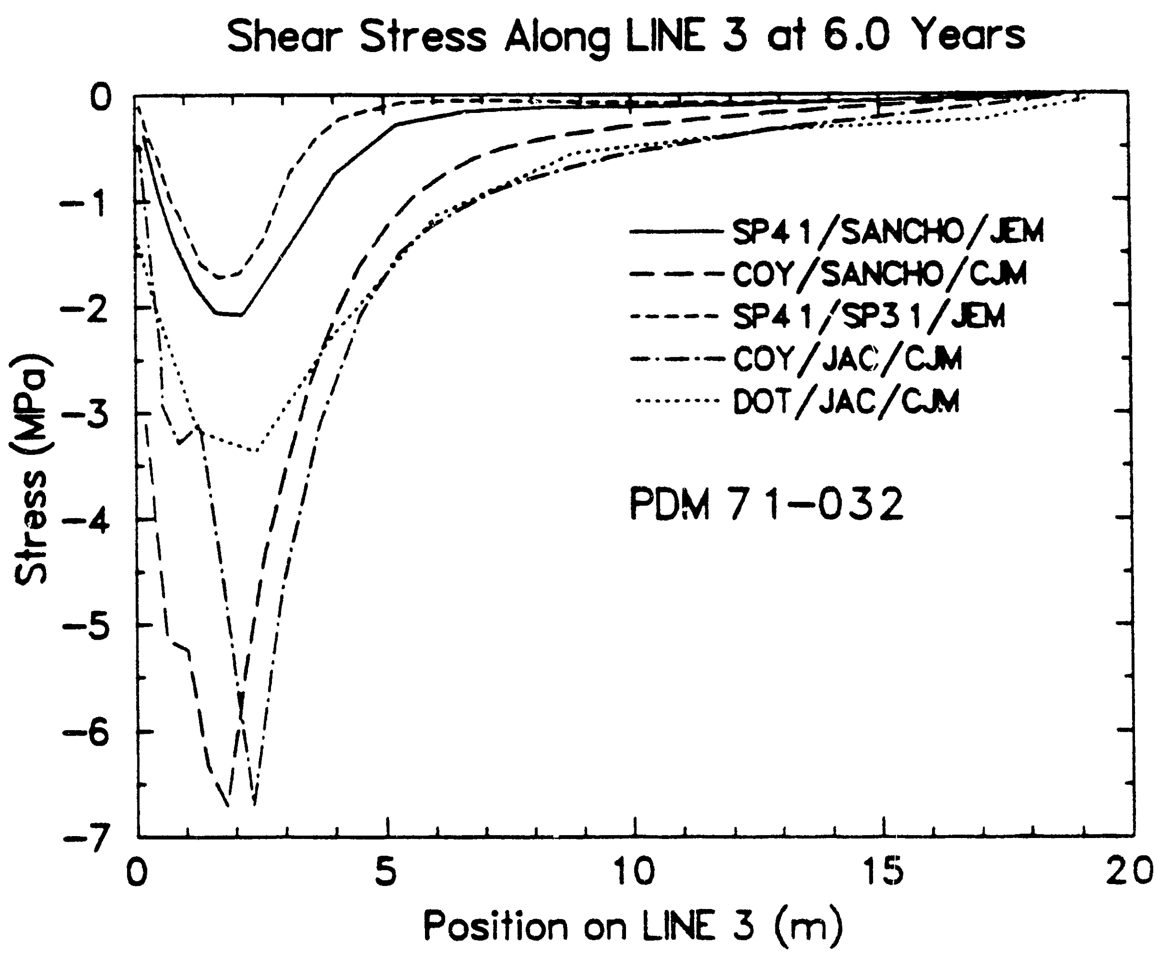

Figure 5-51. Comparison of Results for the Shear Stress Along Line 3 (Figure 2-3) at 6 Yr, Initial Analysis

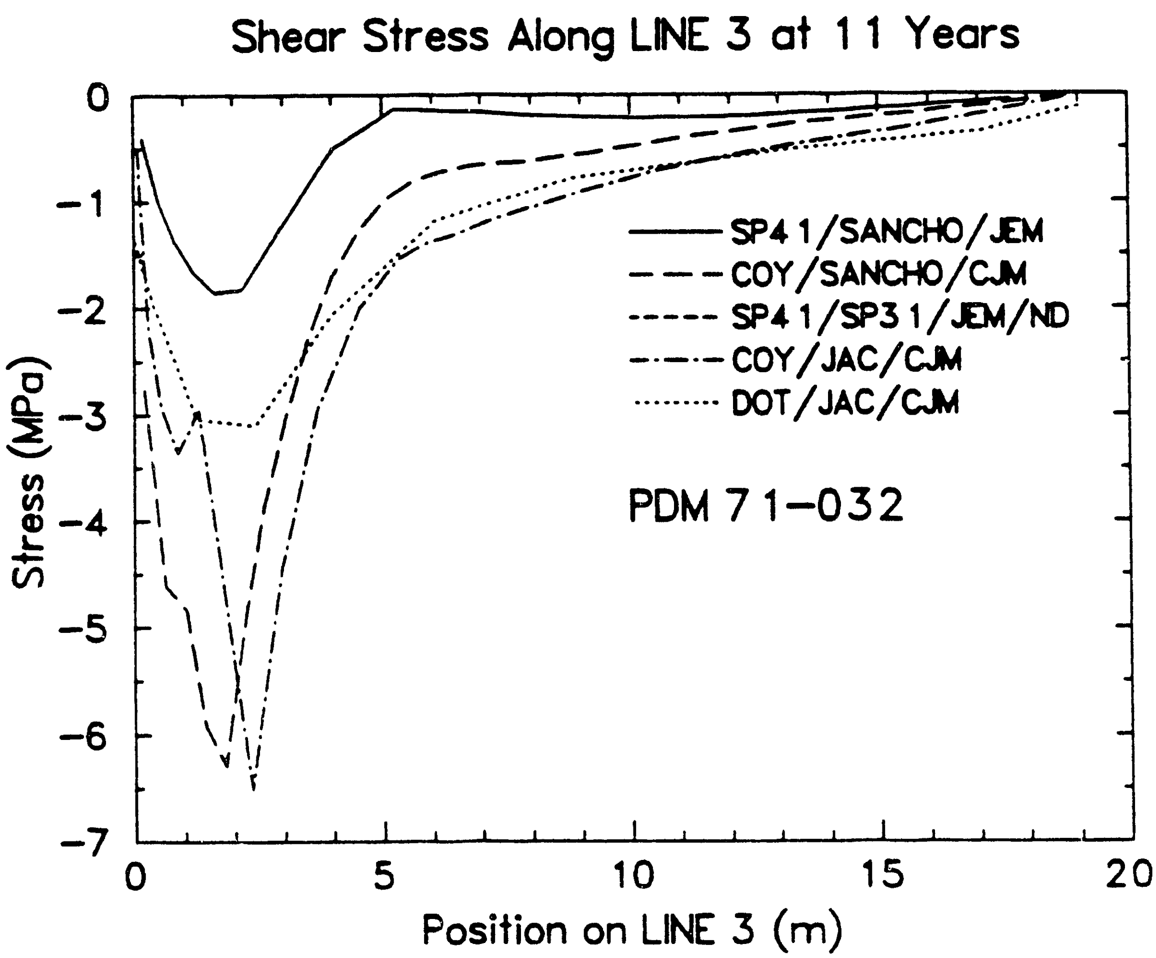

Figure 5-52. Comparison of Results for the Shear Stress Along Line 3 (Figure 2-3) at 11 Yr, Initial Analysis

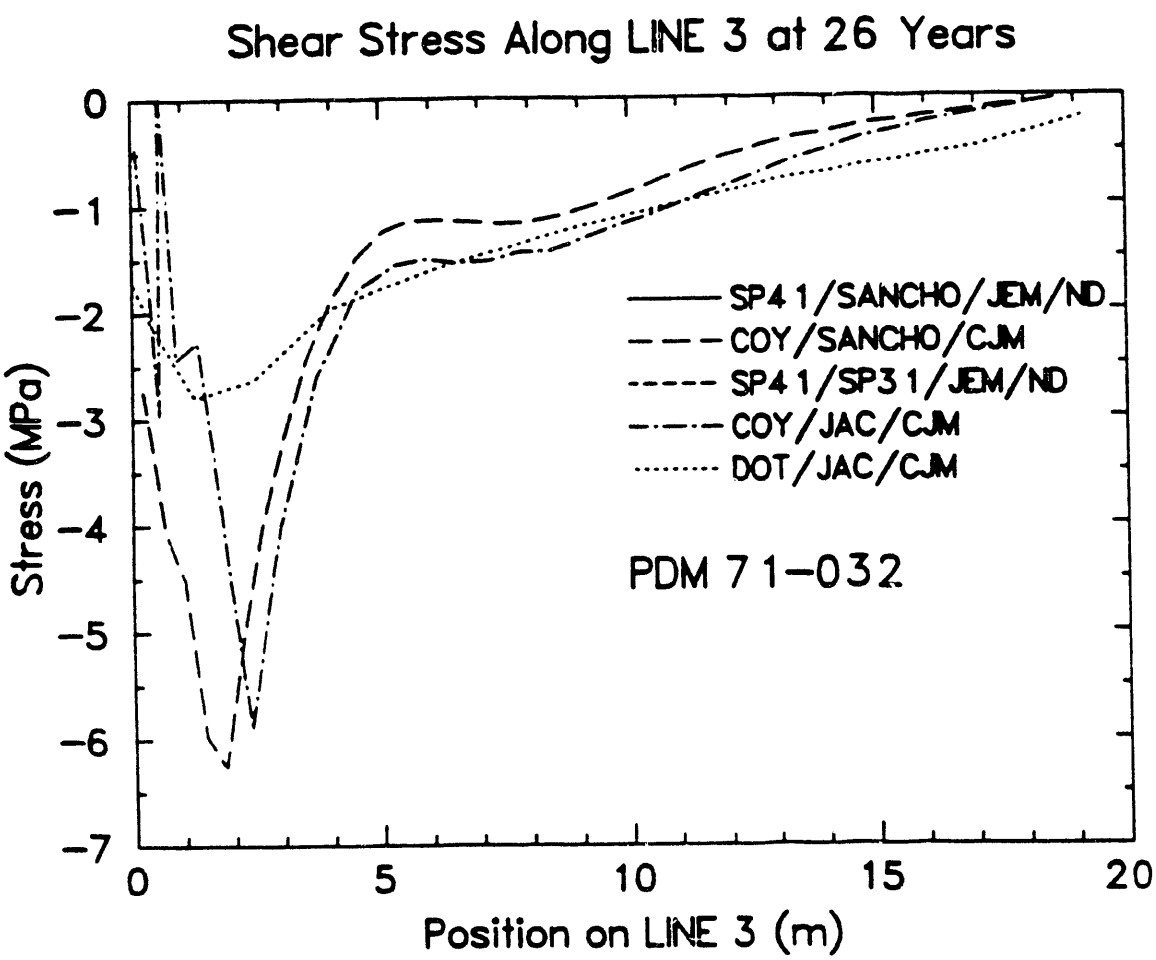

Figure 5-53. Comparison of Results for the Shear Stress Along Line 3 (Figure 2-3) at 26 Yr, Initial Analysis

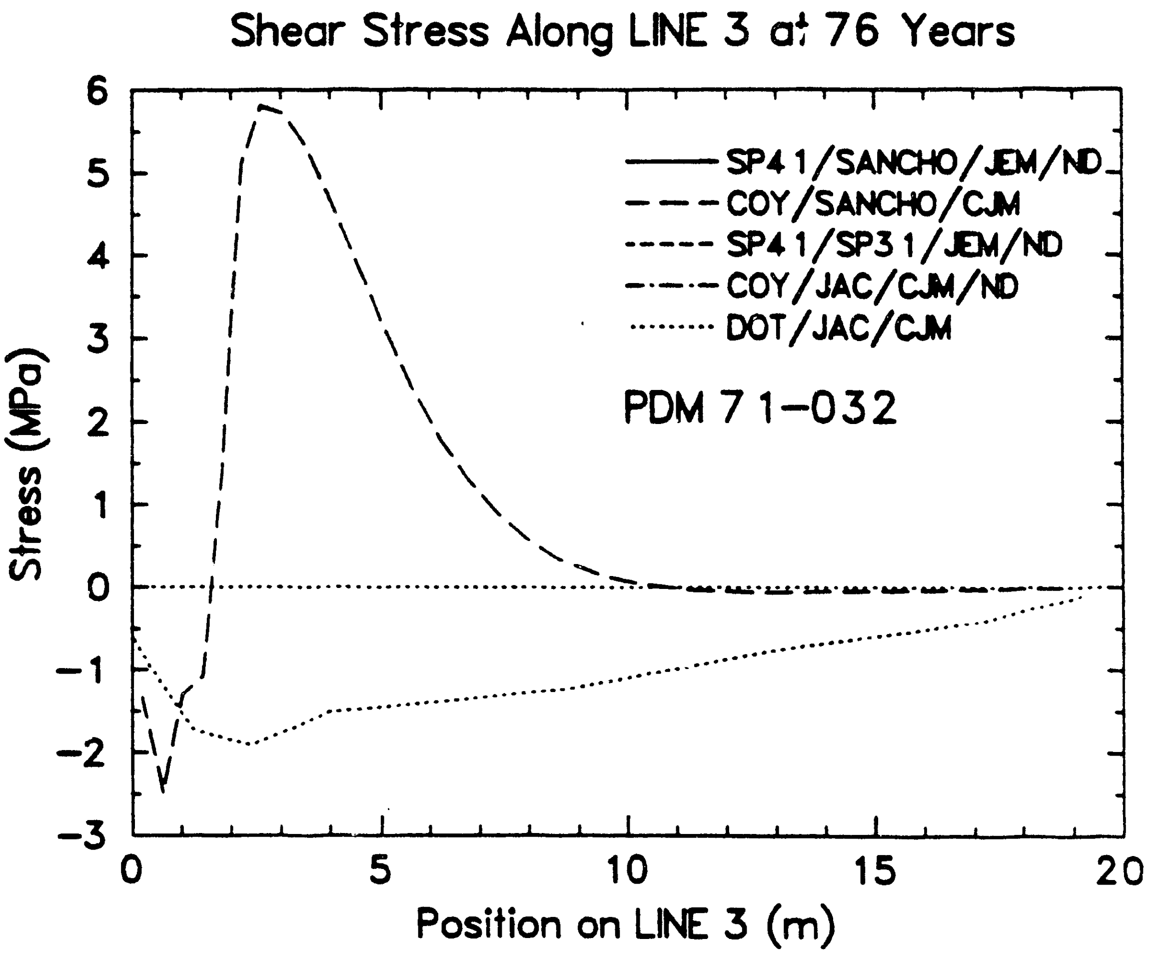

Figure 5-54. Comparison of Results for the Shear Stress Along Line 3 (Figure 2-3) at 76 Yr, Initial Analysis

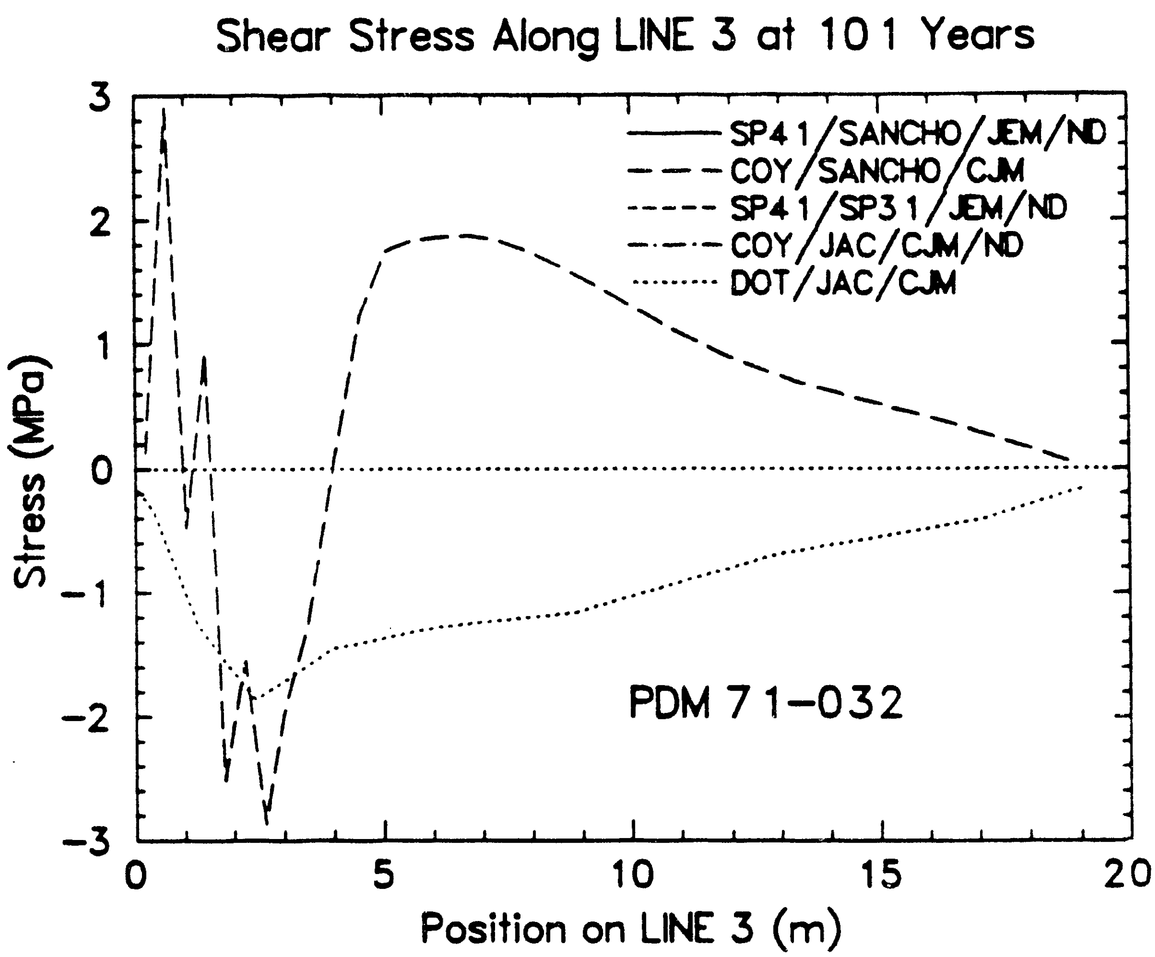

Figure 5-55. Comparison of Results for the Shear Stress Along Line 3 (Figure 2-3) at 101 Yr, Initial Analysis

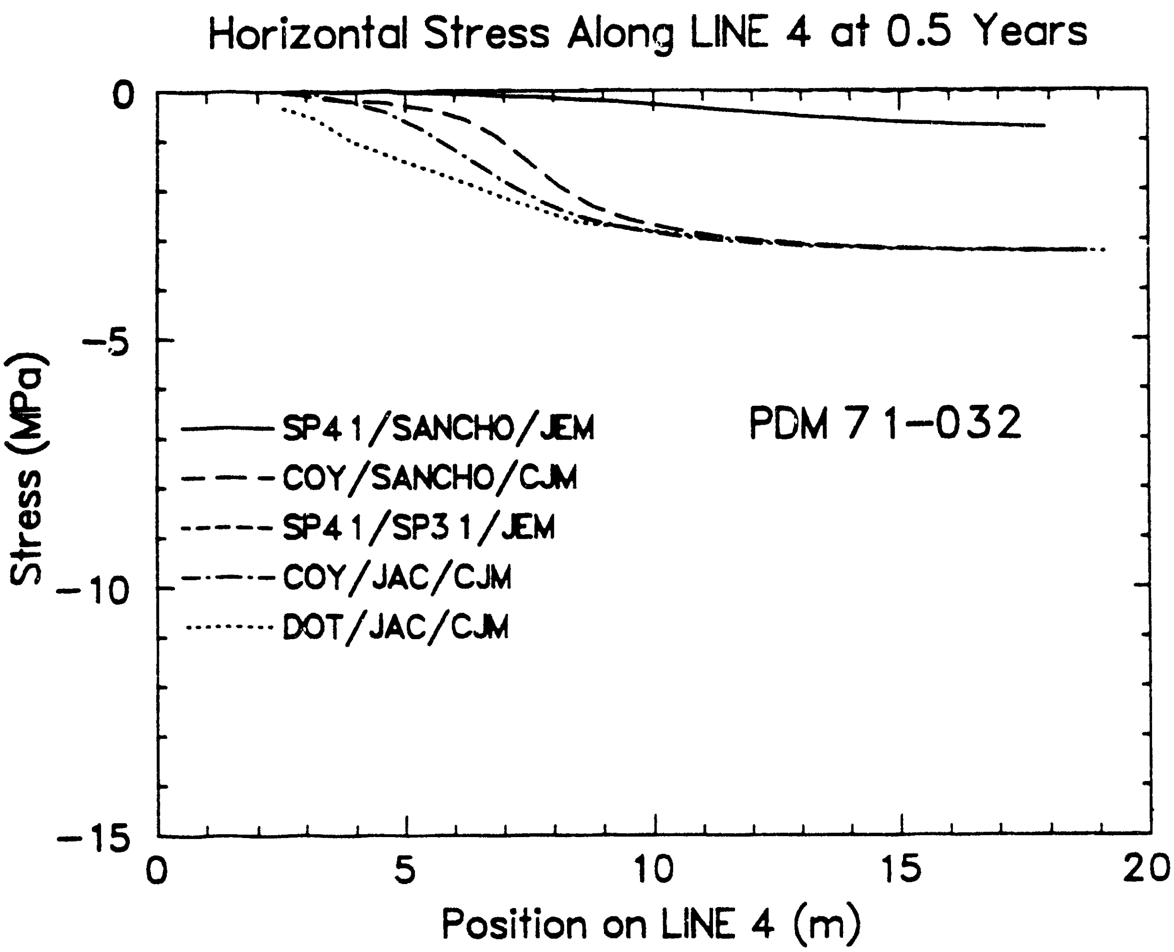

Figure 5-56. Comparison of Results for the Horizontal Stress Along Line 4 (Figure 2-3) at 0.5 Yr, Initial Analysis

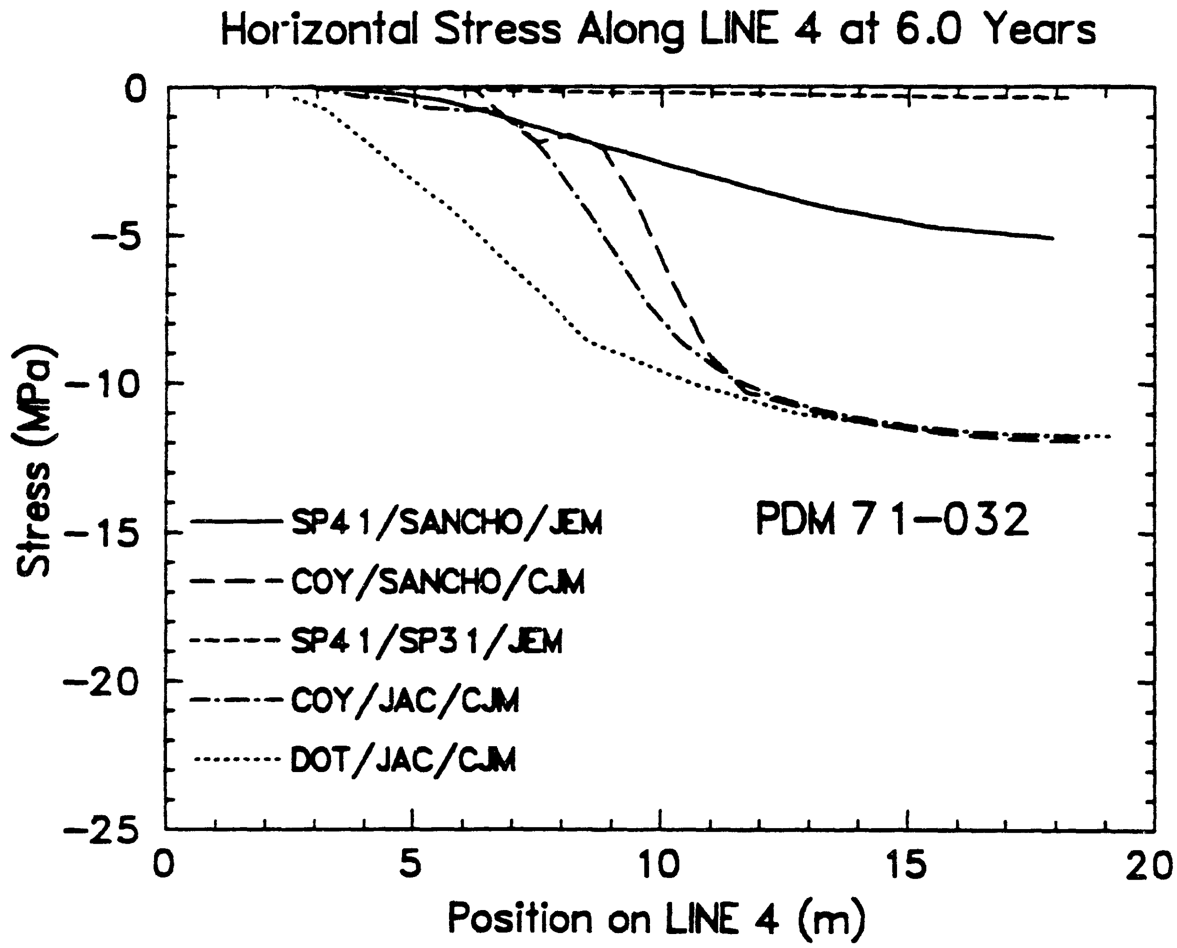

Figure 5-57. Comparison of Results for the Horizontal Stress Along Line 4 (Figure 2-3) at 6 Yr, Initial Analysis

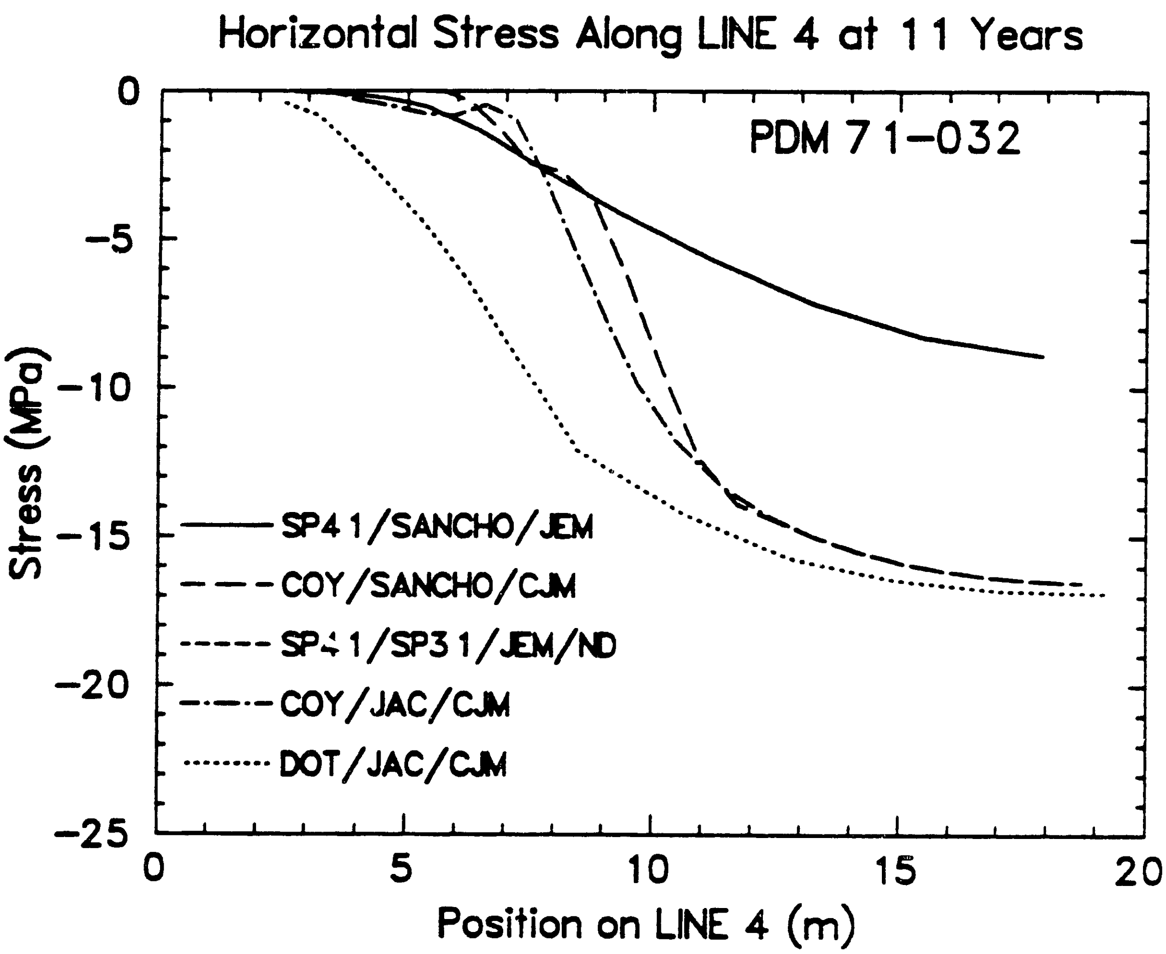

Figure 5-58. Comparison of Results for the Horizontal Stress Along Line 4 (Figure 2-3) at 11 Yr, Initial Analysis

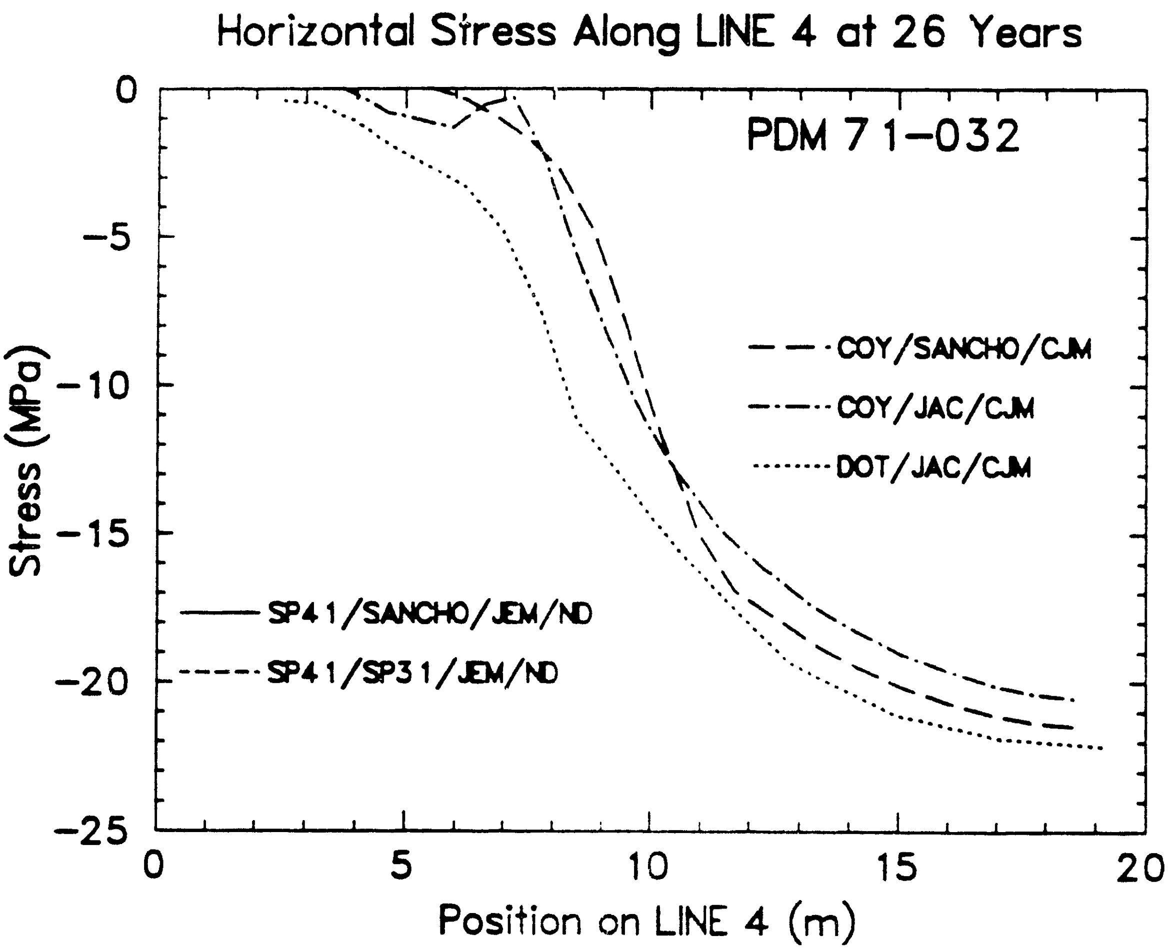

Figure 5-59. Comparison of Results for the Horizontal Stress Along Line 4 (Figure 2-3) at 26 Yr, Initial Analysis

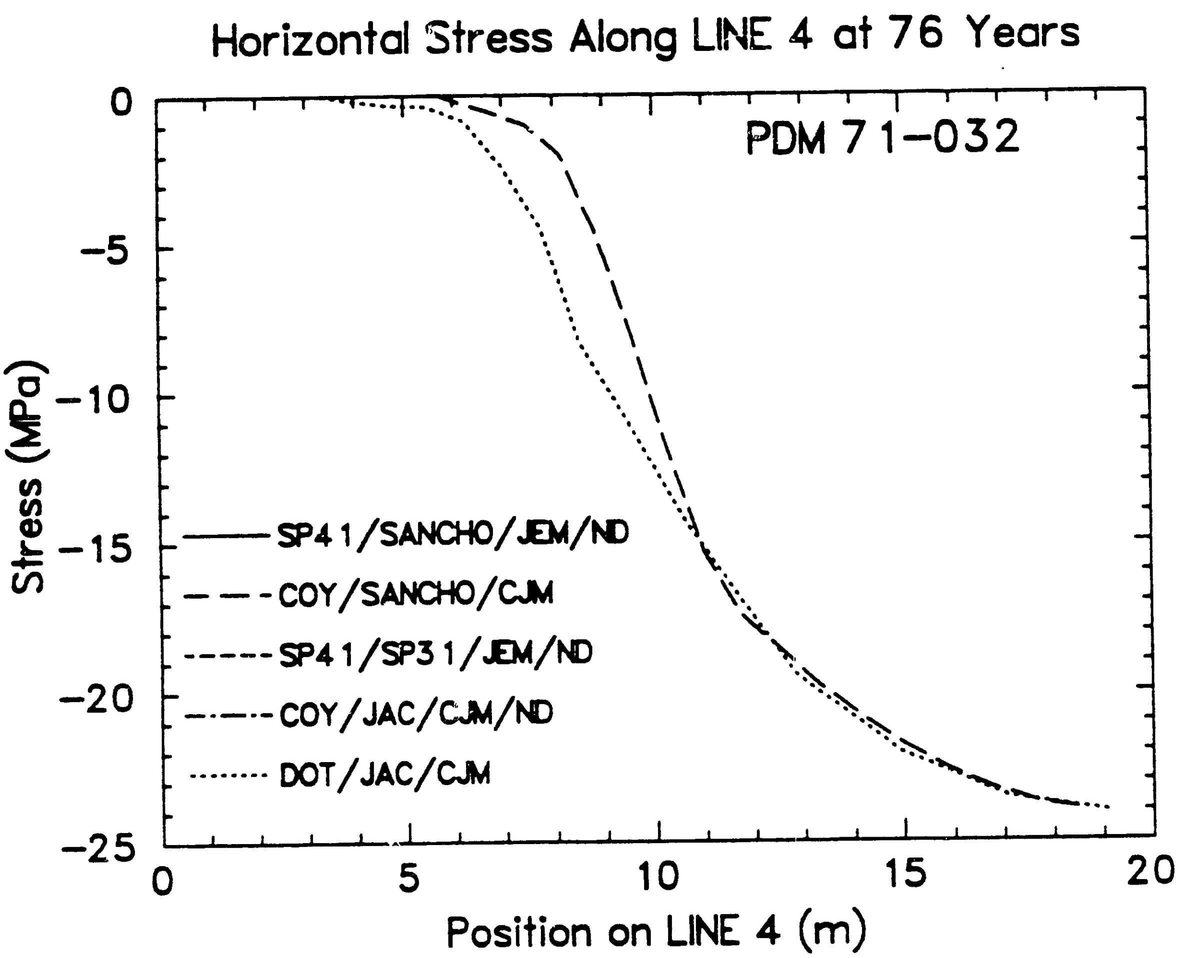

Figure 5-60. Comparison of Results for the Horizontal Stress Along Line 4 (Figure 2-3) at 76 Yr, Initial Analysis

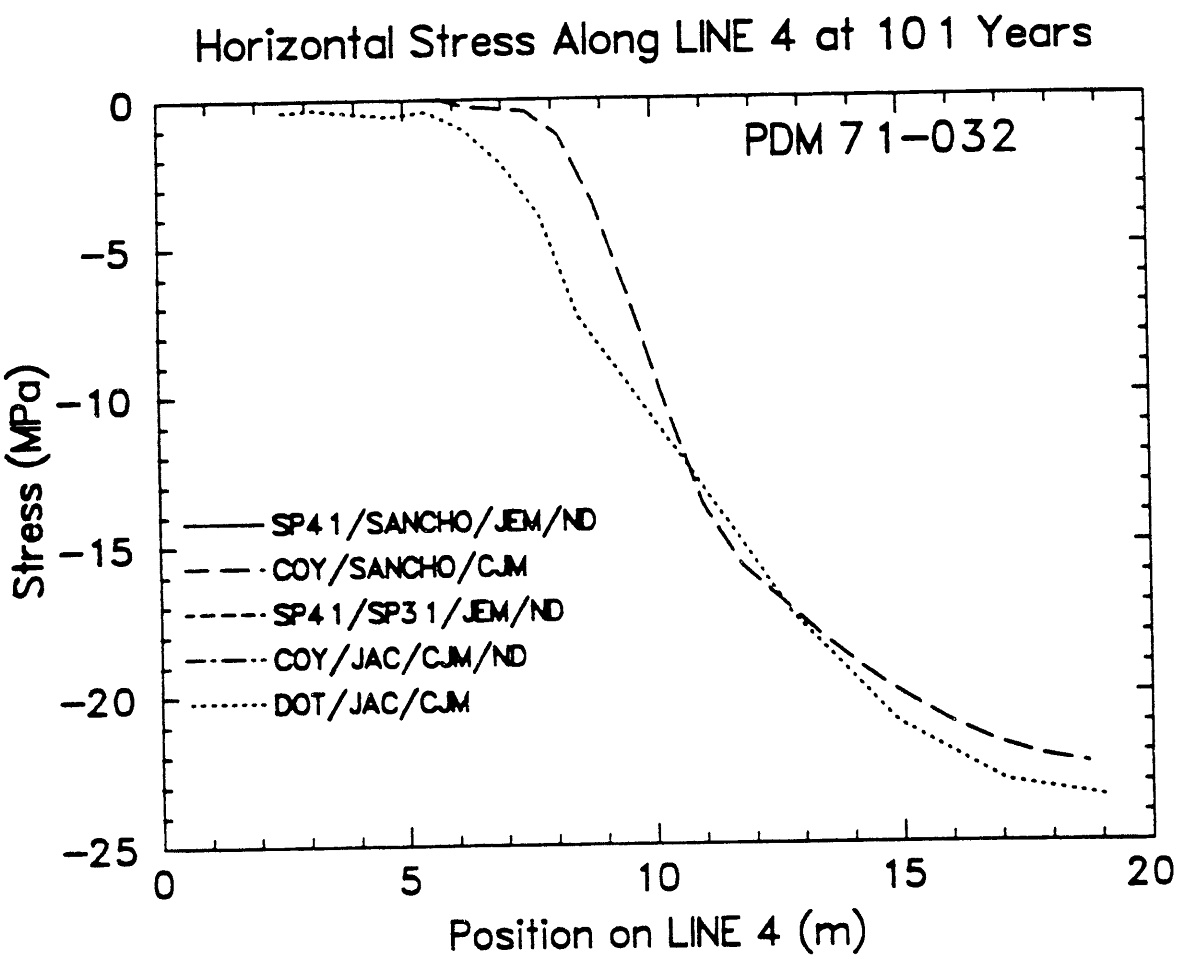

Figure 5-61. Comparison of Results for the Horizontal Stress Along Line 4 (Figure 2-3) at 101 Yr, Initial Analysis

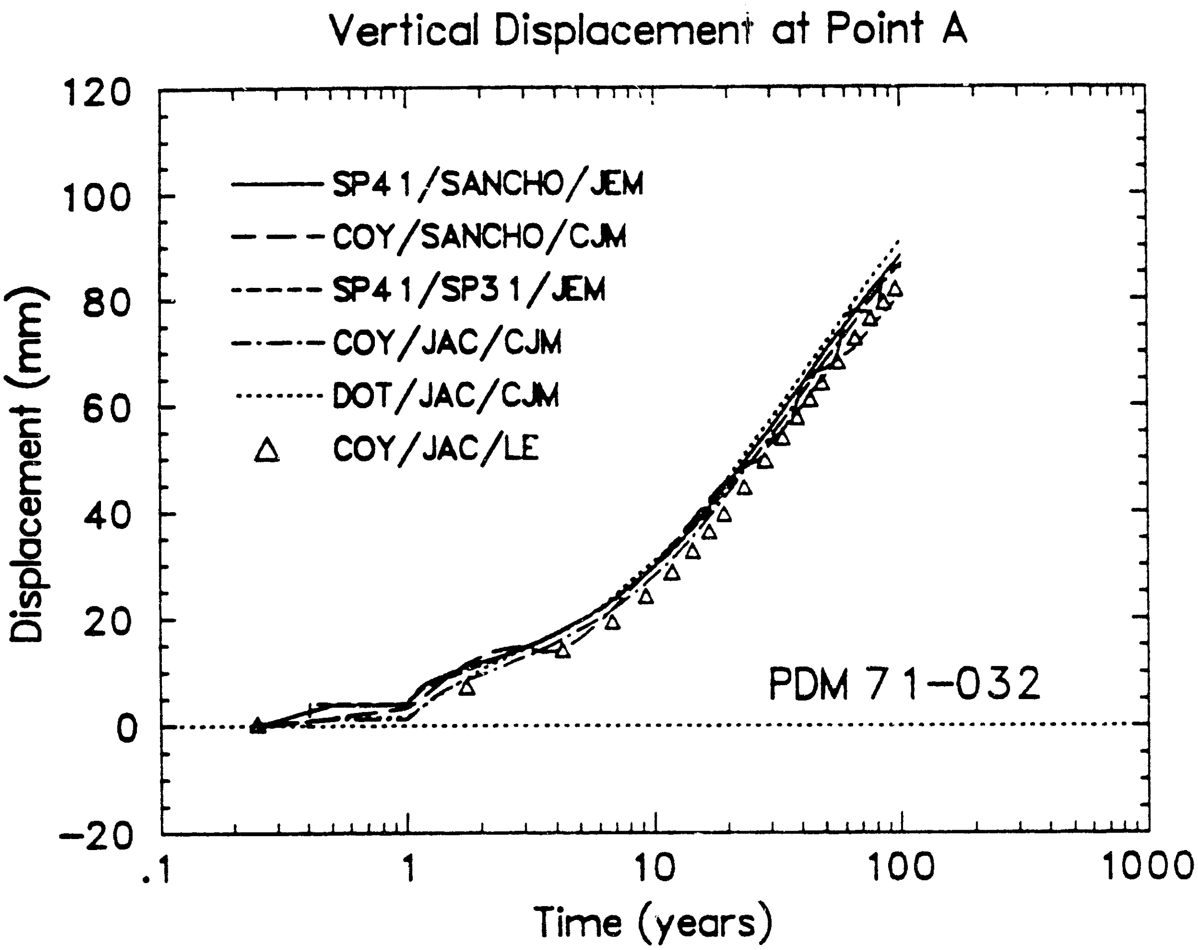

Figure 5-62. Comparison of Results for the Vertical Displacement History at Point A (Figure 2-3), Second Analysis

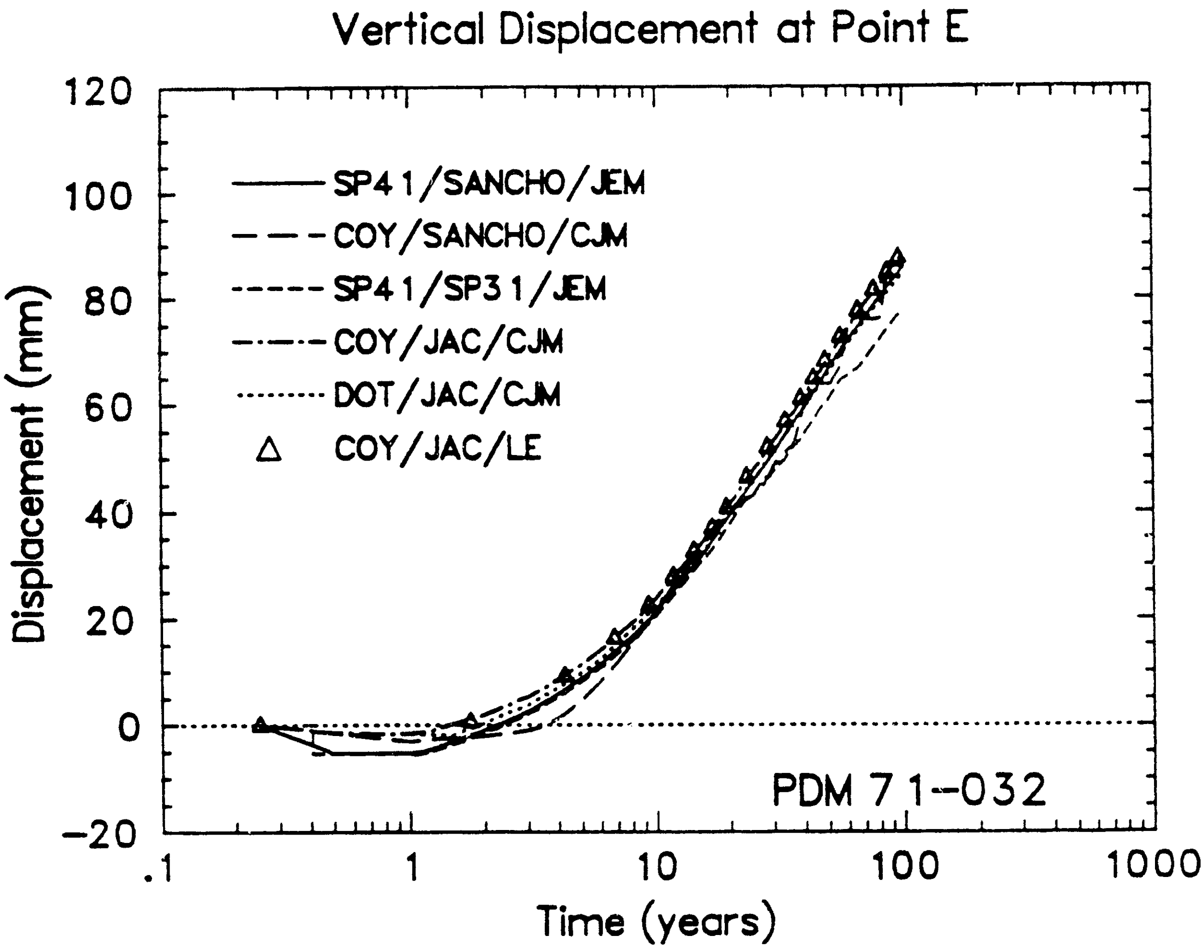

Figure 5-63. Comparison of Results for the Vertical Displacement History at Point E (Figure 2-3), Second Analysis

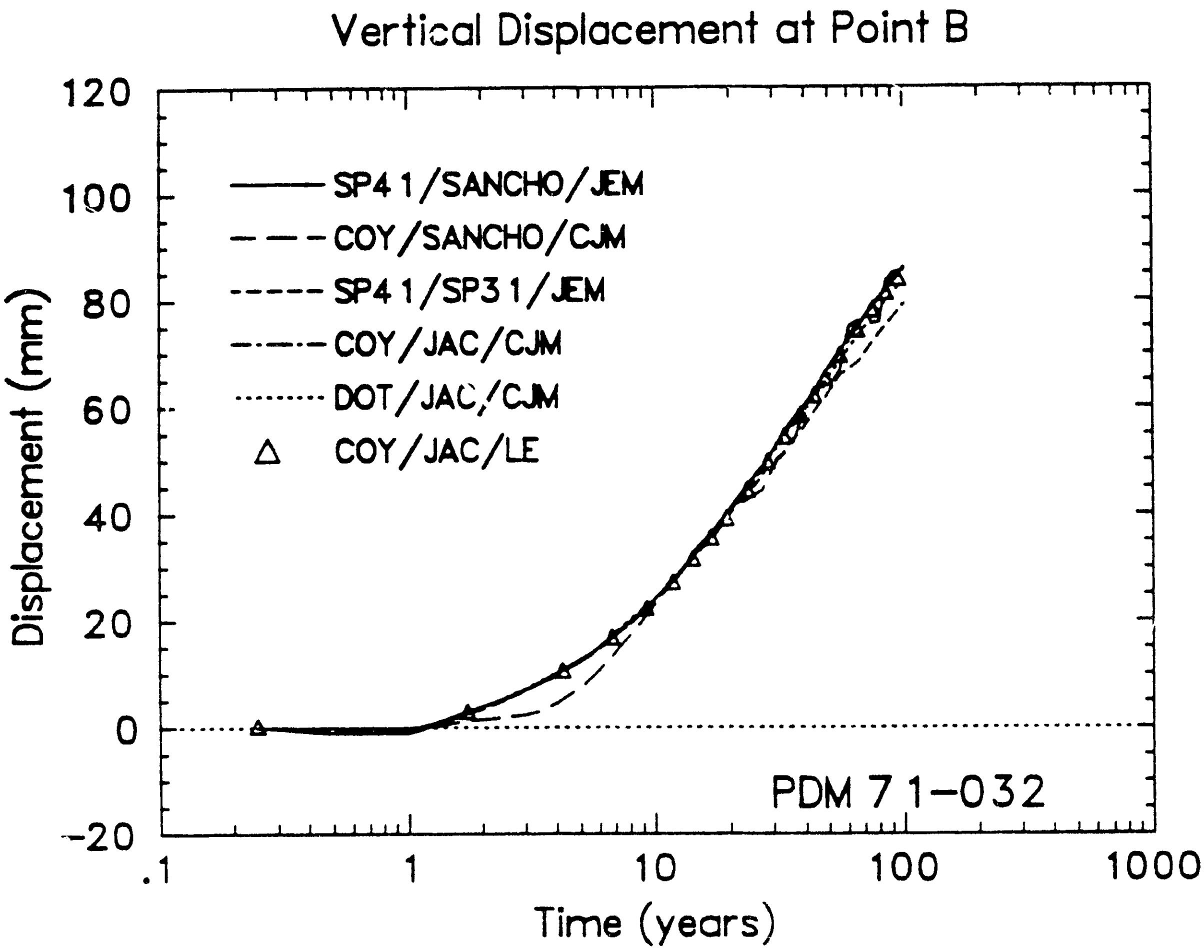

Figure 5-64. Comparison of Results for the Vertical Displacement History at Point B (Figure 2-3), Second Analysis

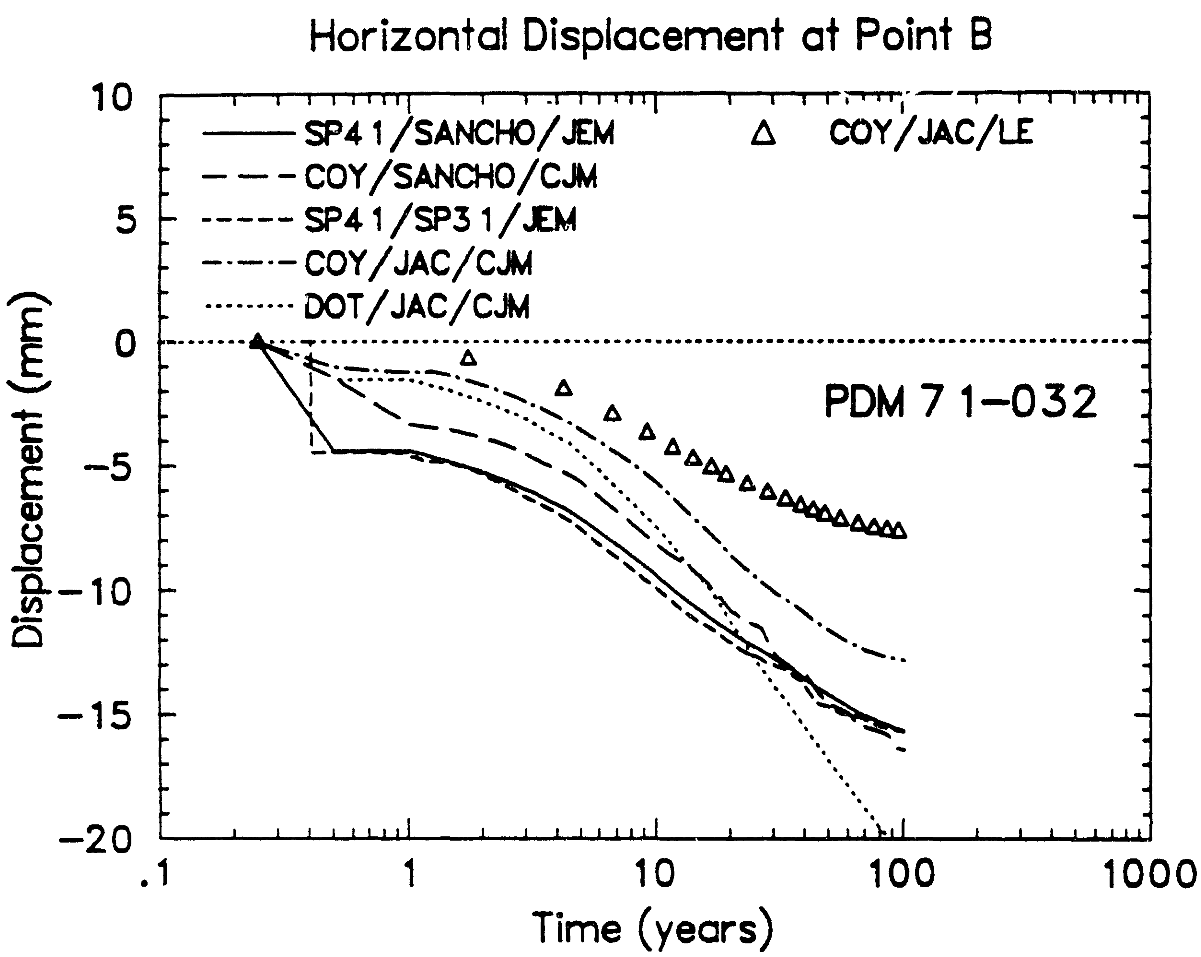

Figure 5-65. Comparison of Results for the Horizontal Displacement History at Point B (Figure 2-3), Second Analysis

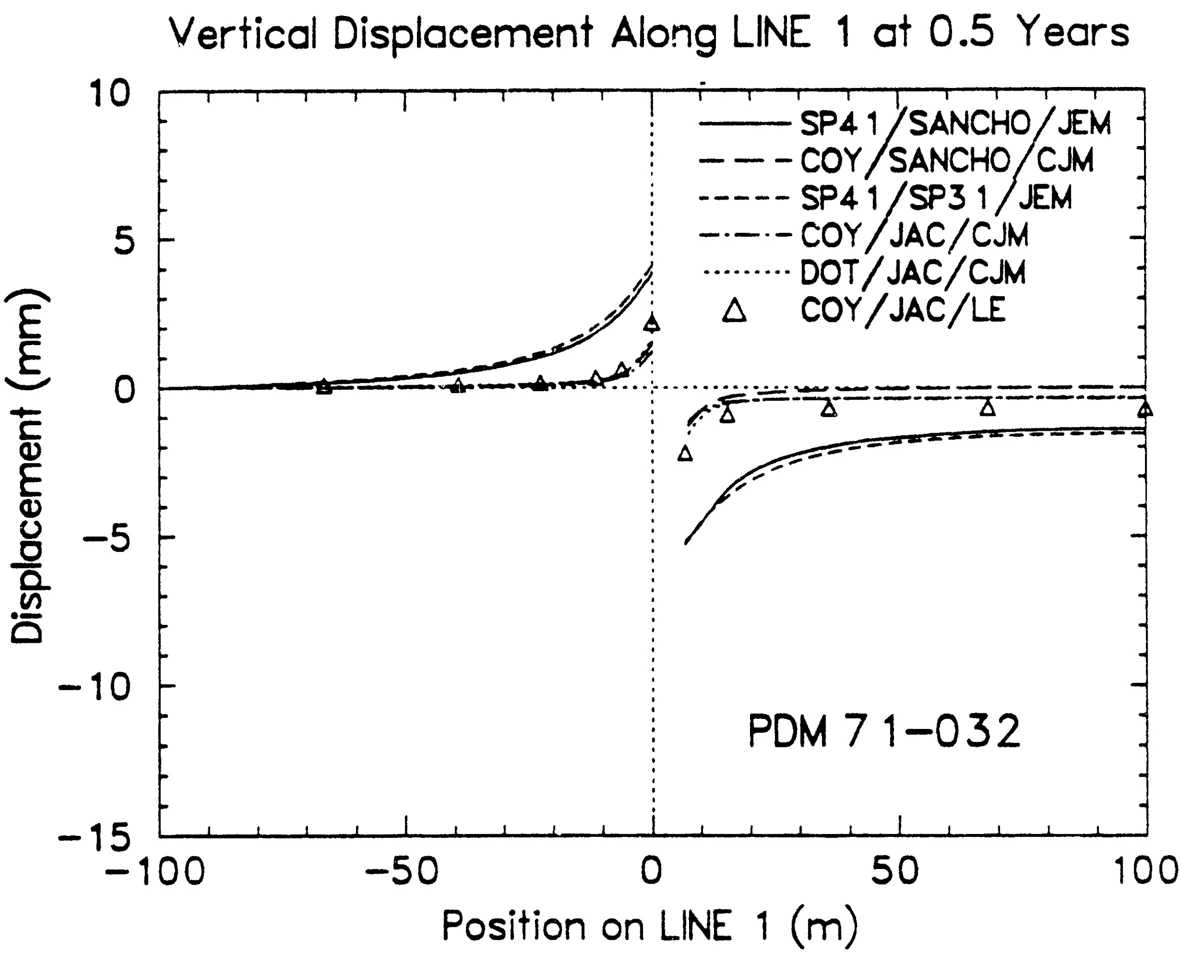

Figure 5-66. Comparison of Results for the Vertical Displacement Along Line 1 (Figure 2-3) at 0.5 Yr, Second Analysis

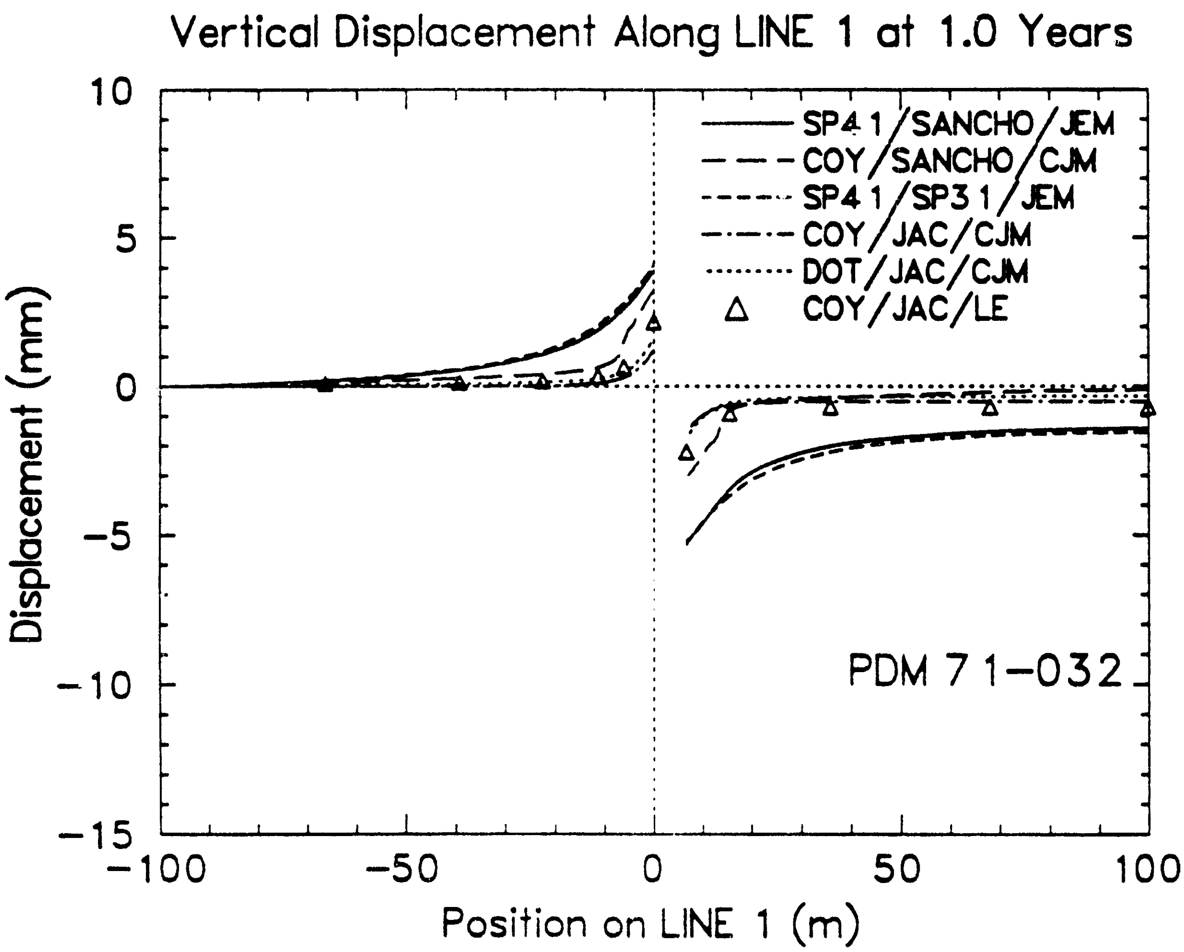

Figure 5-67. Comparison of Results for the Vertical Displacement Along Line 1 (Figure 2-3) at 1 Yr, Second Analysis

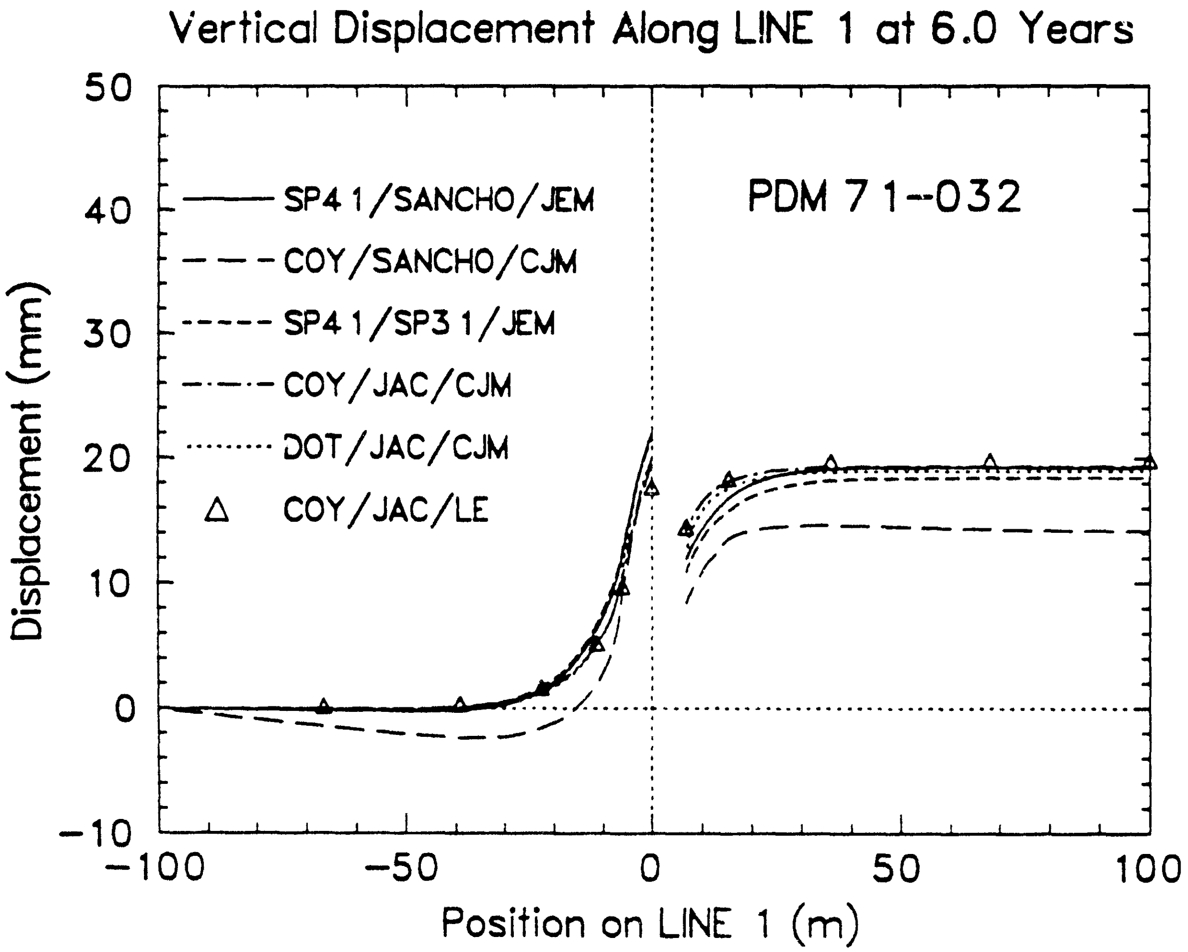

Figure 5-68. Comparison of Results for the Vertical Displacement Along Line 1 (Figure 2-3) at 6 Yr, Second Analysis

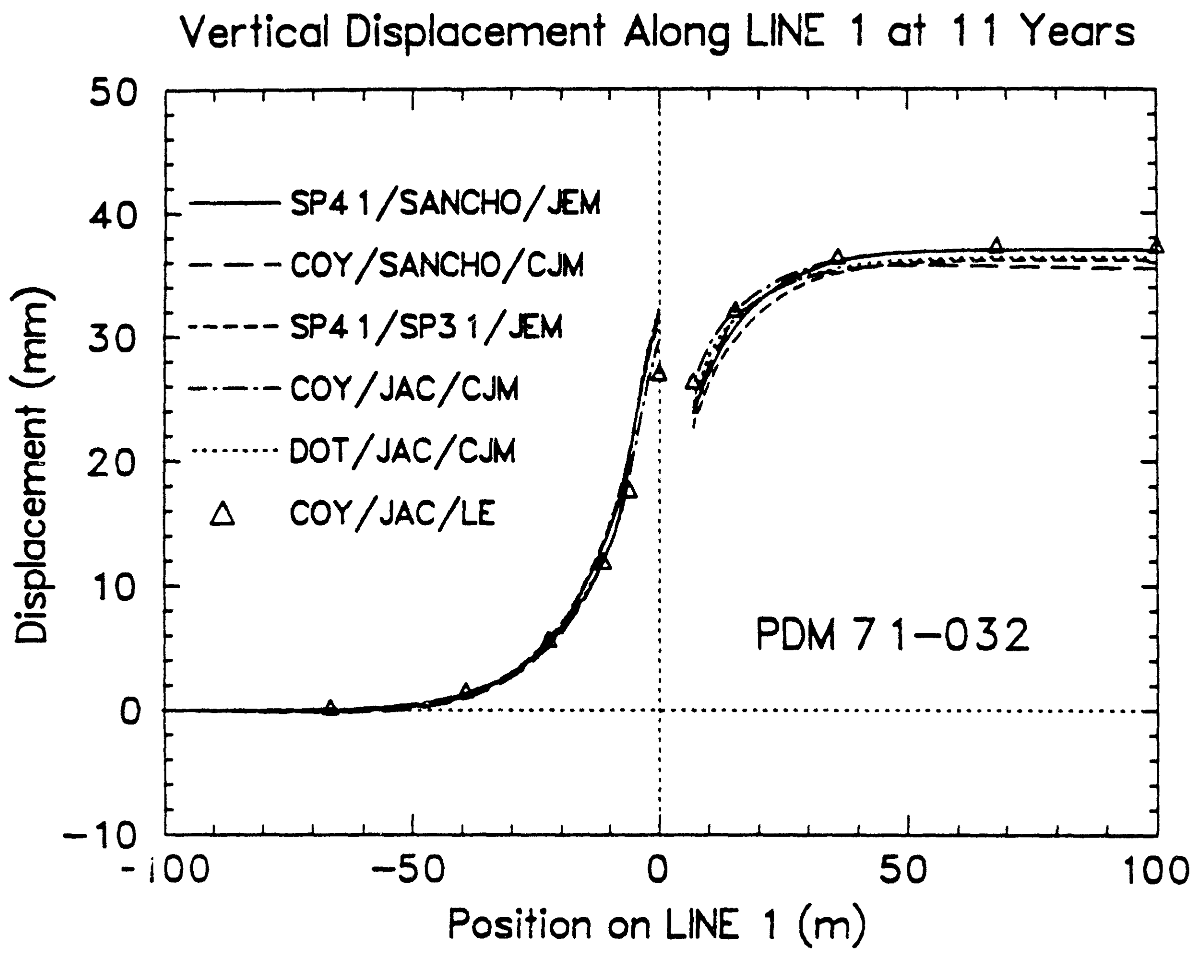

Figure 5-69. Comparison of Results for the Vertical Displacement Along Line 1 (Figure 2-3) at 11 Yr, Second Analysis

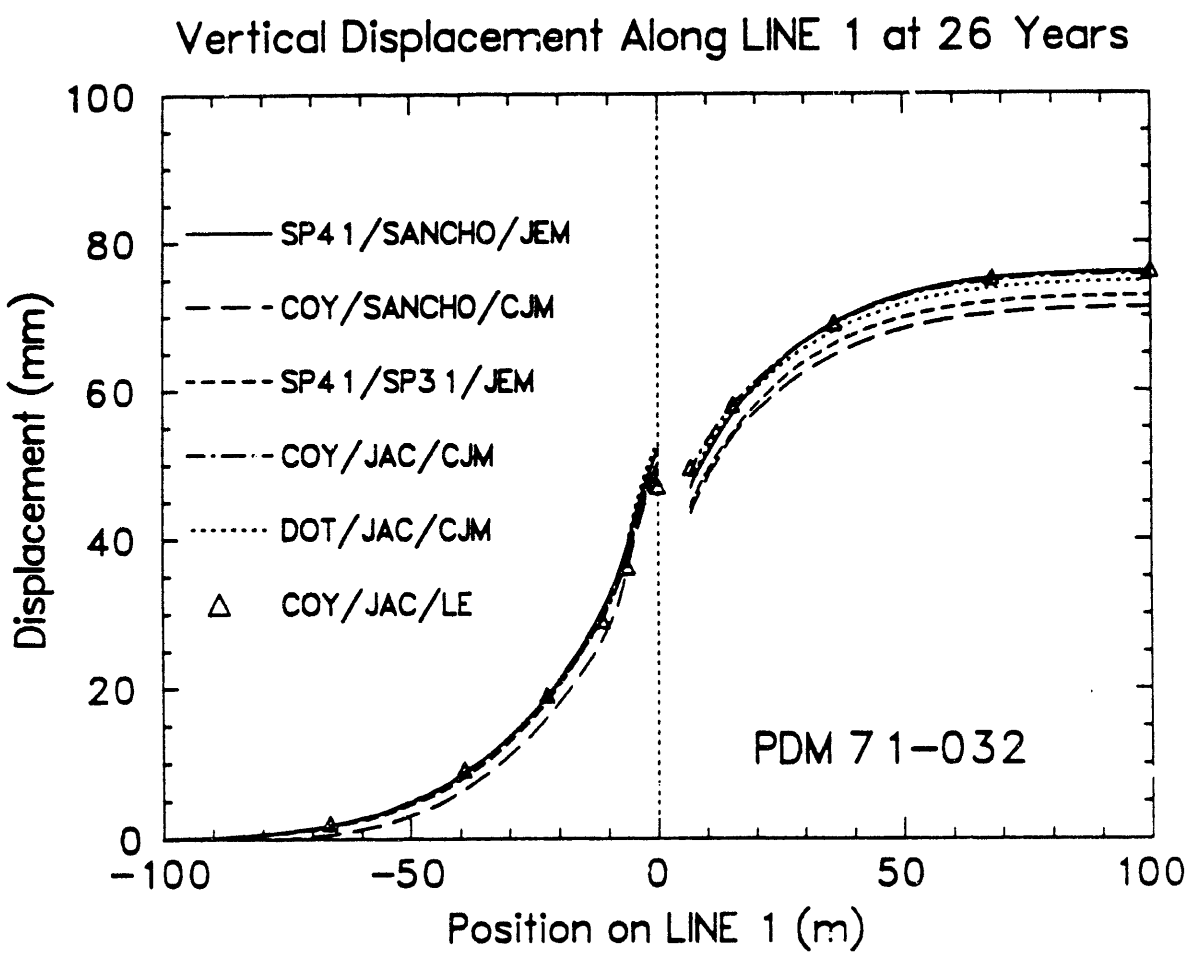

Figure 5-70. Comparison of Results for the Vertical Displacement Along Line 1 (Figure 2-3) at 26 Yr, Second Analysis

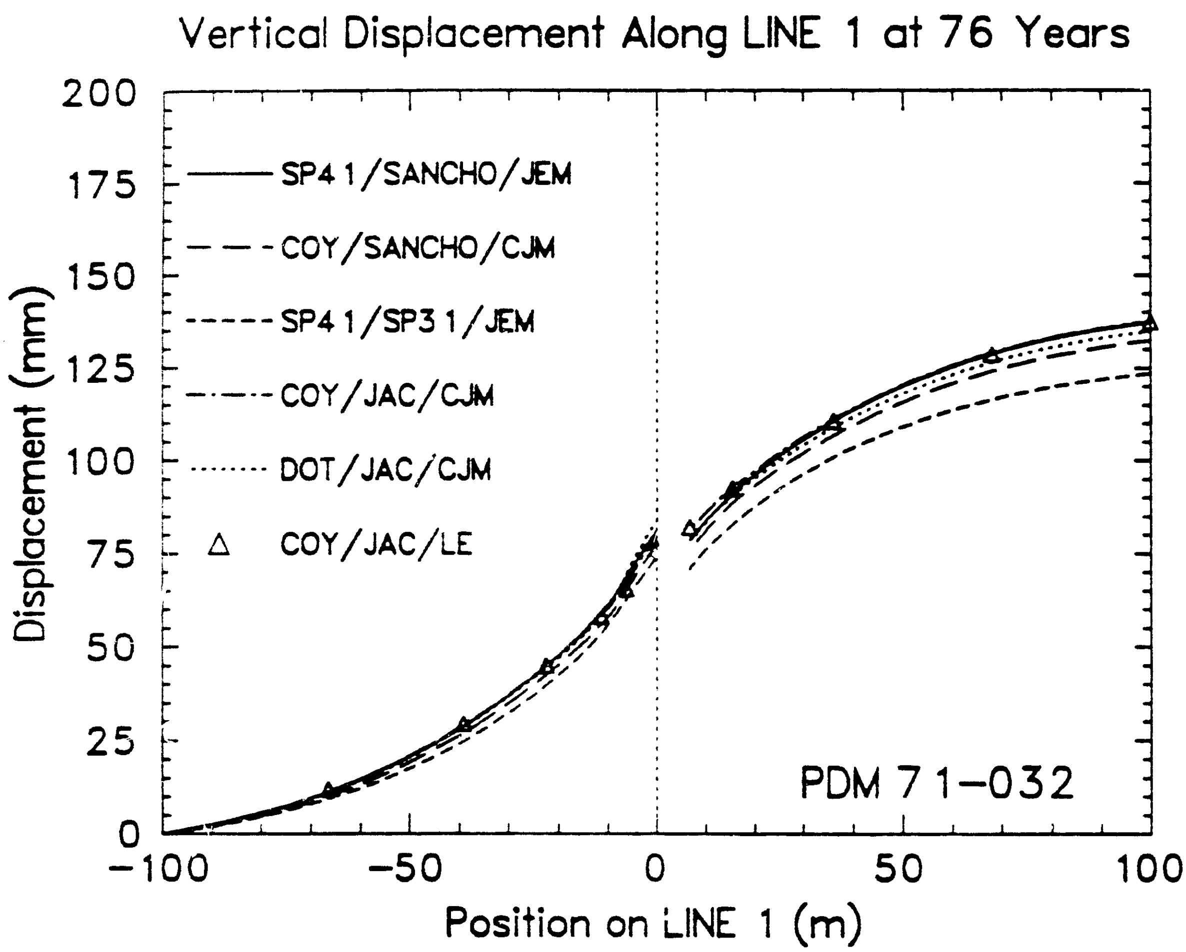

Figure 5-71. Comparison of Results for the Vertical Displacement Along Line 1 (Figure 2-3) at 76 Yr, Second Analysis

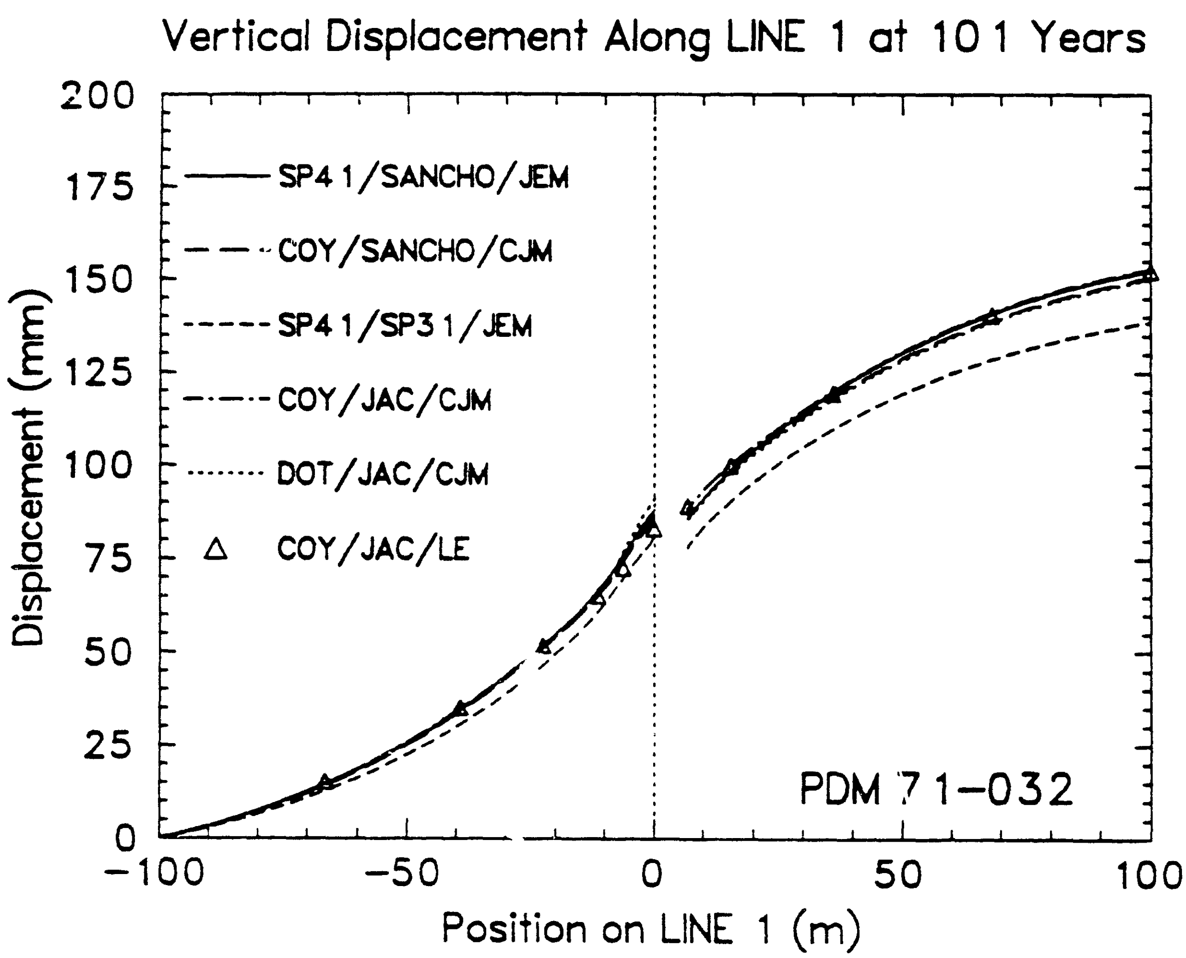

Figure 5-72. Comparison of Results for the Vertical Displacement Along Line 1 (Figure 2-3) at 101 Yr, Second Analysis

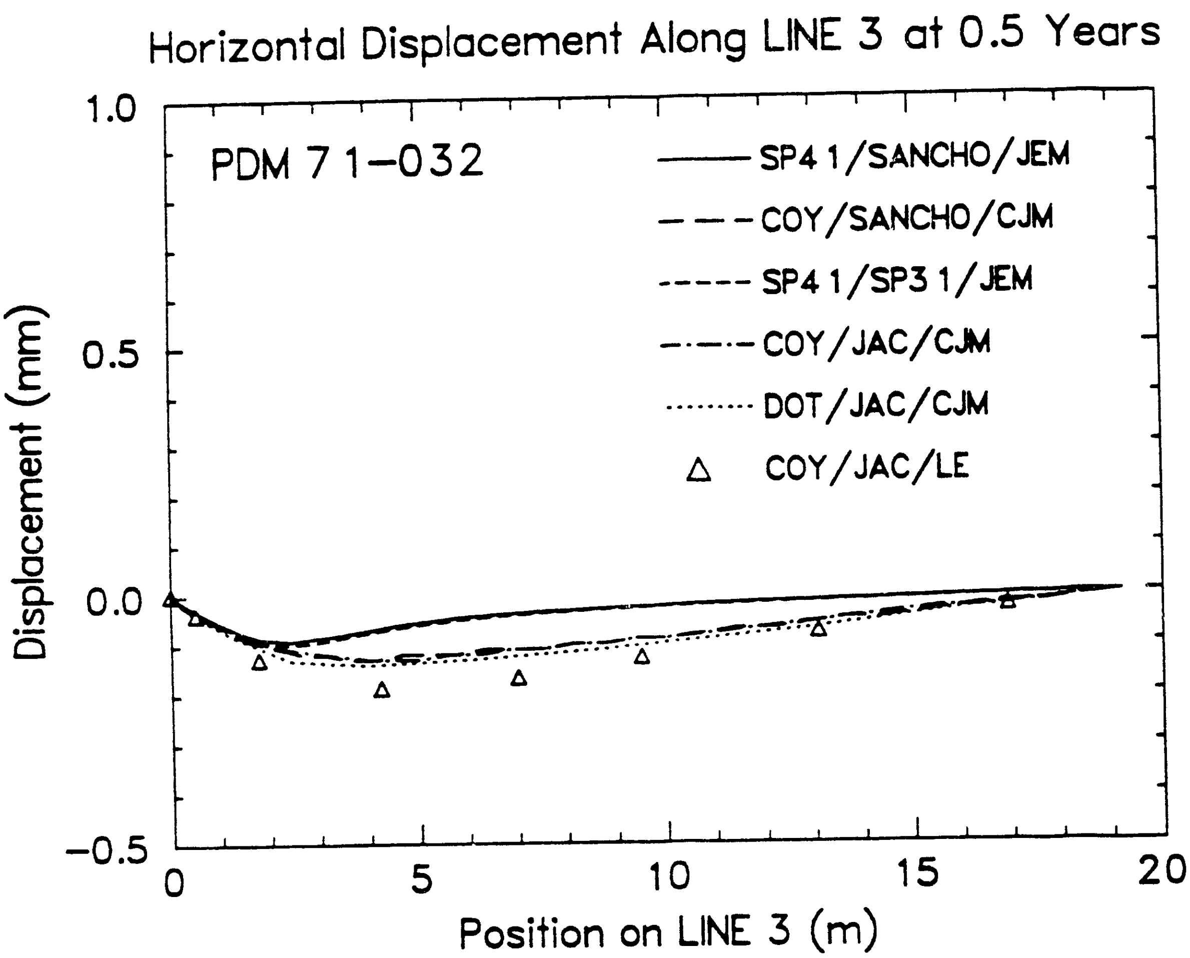

Figure 5-73. Comparison of Results for the Horizontal Displacement Along Line 3 (Figure 2-3) at 0.5 Yr, Second Analysis

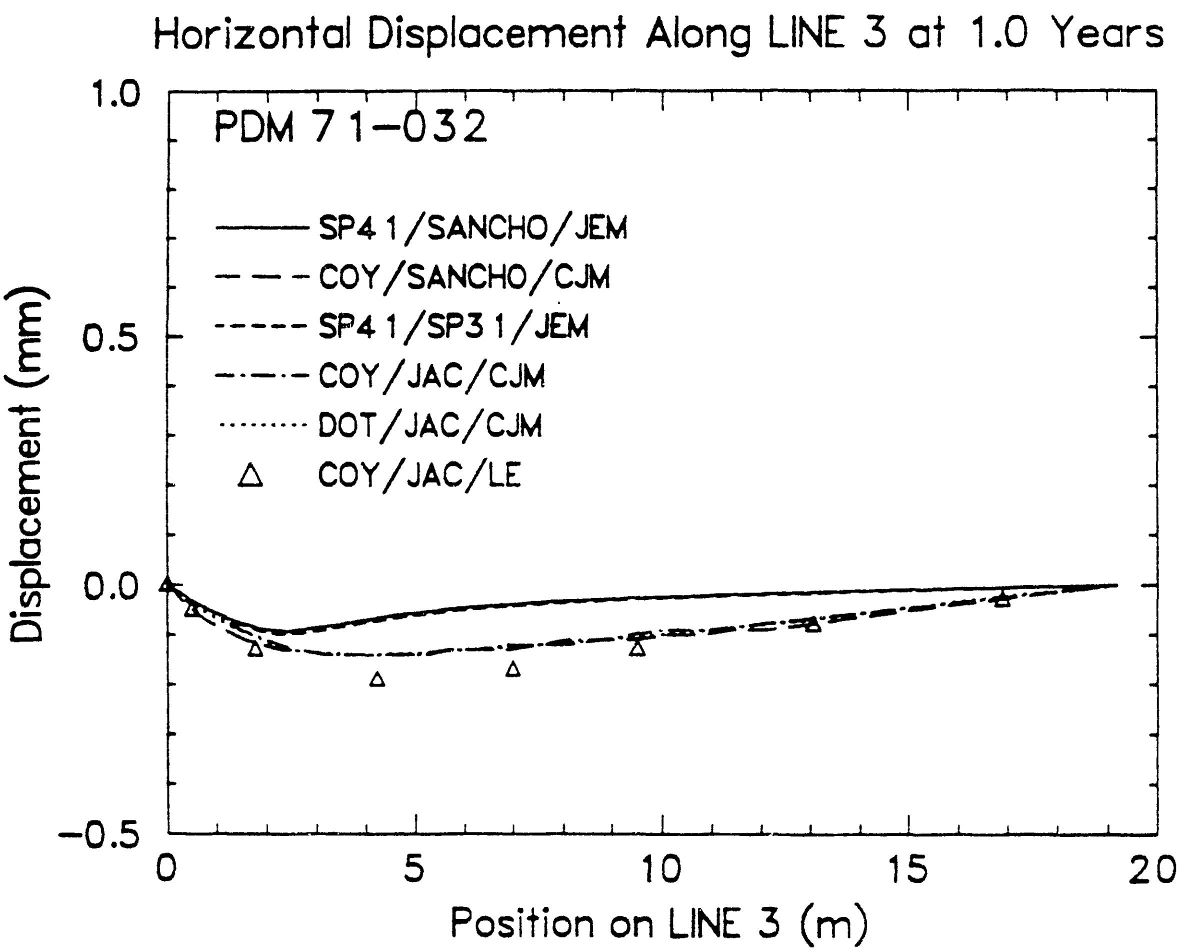

Figure 5-74. Comparison of Results for the Horizontal Displacement Along Line 3 (Figure 2-3) at 1 Yr, Second Analysis

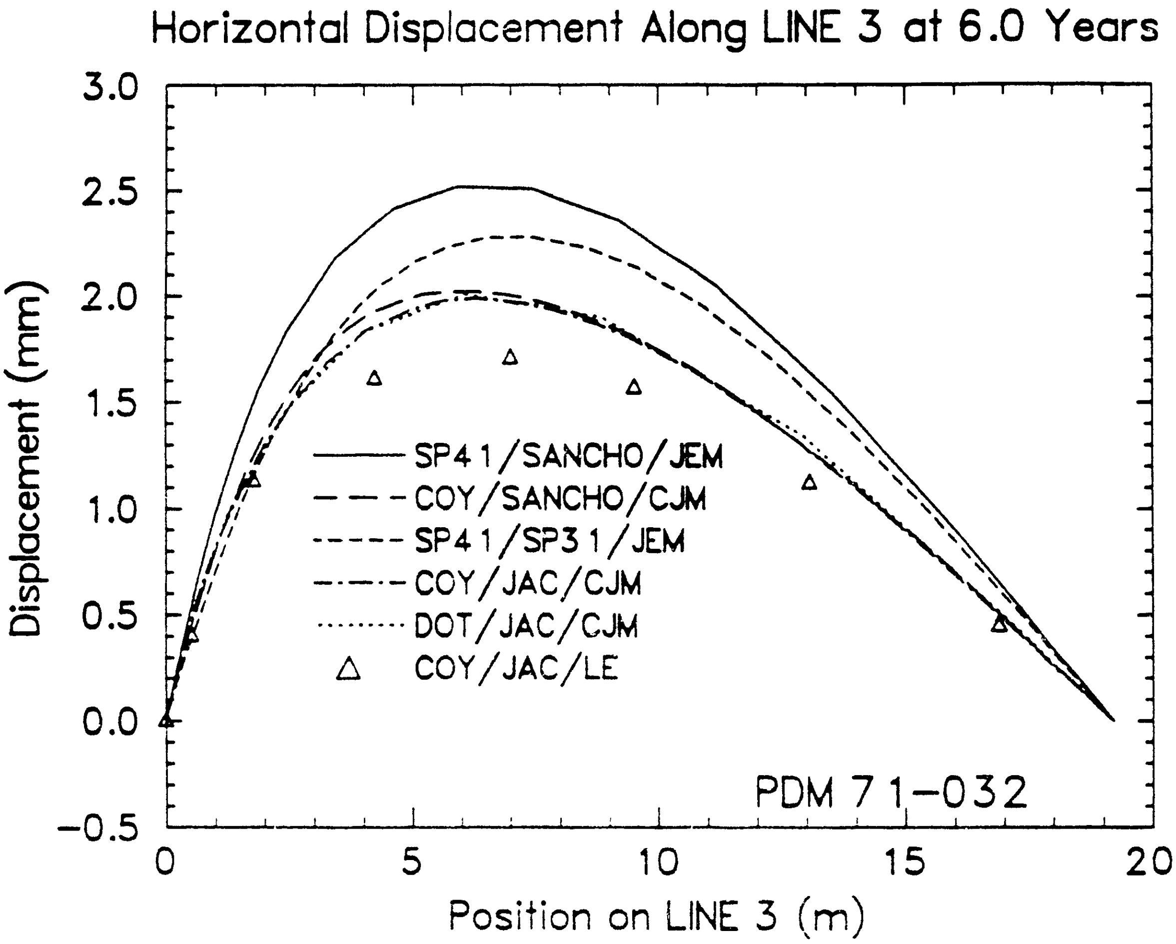

Figure 5-75. Comparison of Results for the Horizontal Displacement Along Line 3 (Figure 2-3) at 6 Yr, Second Analysis

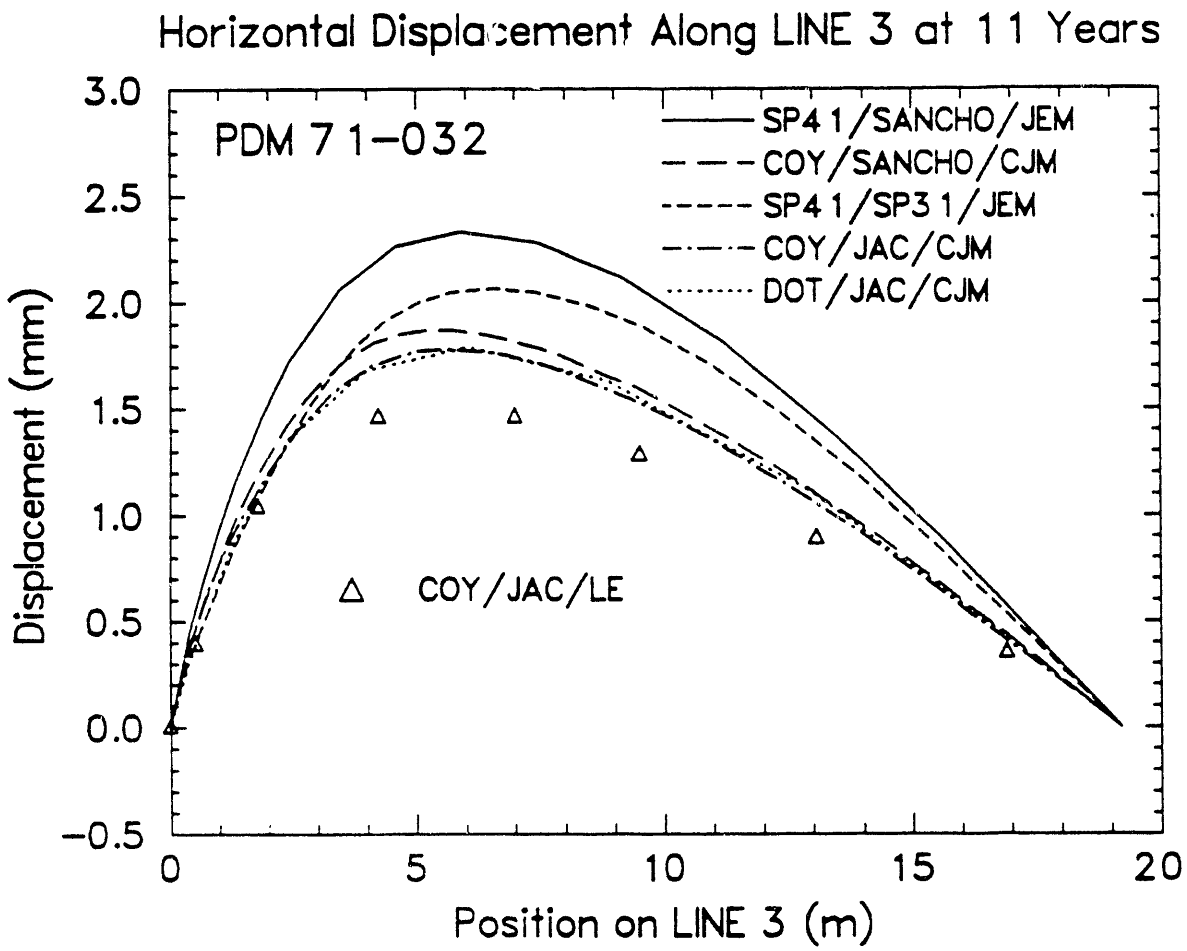

Figure 5-76. Comparison of Results for the Horizontal Displacement Along Line 3 (Figure 2-3) at 11 Yr, Second Analysis

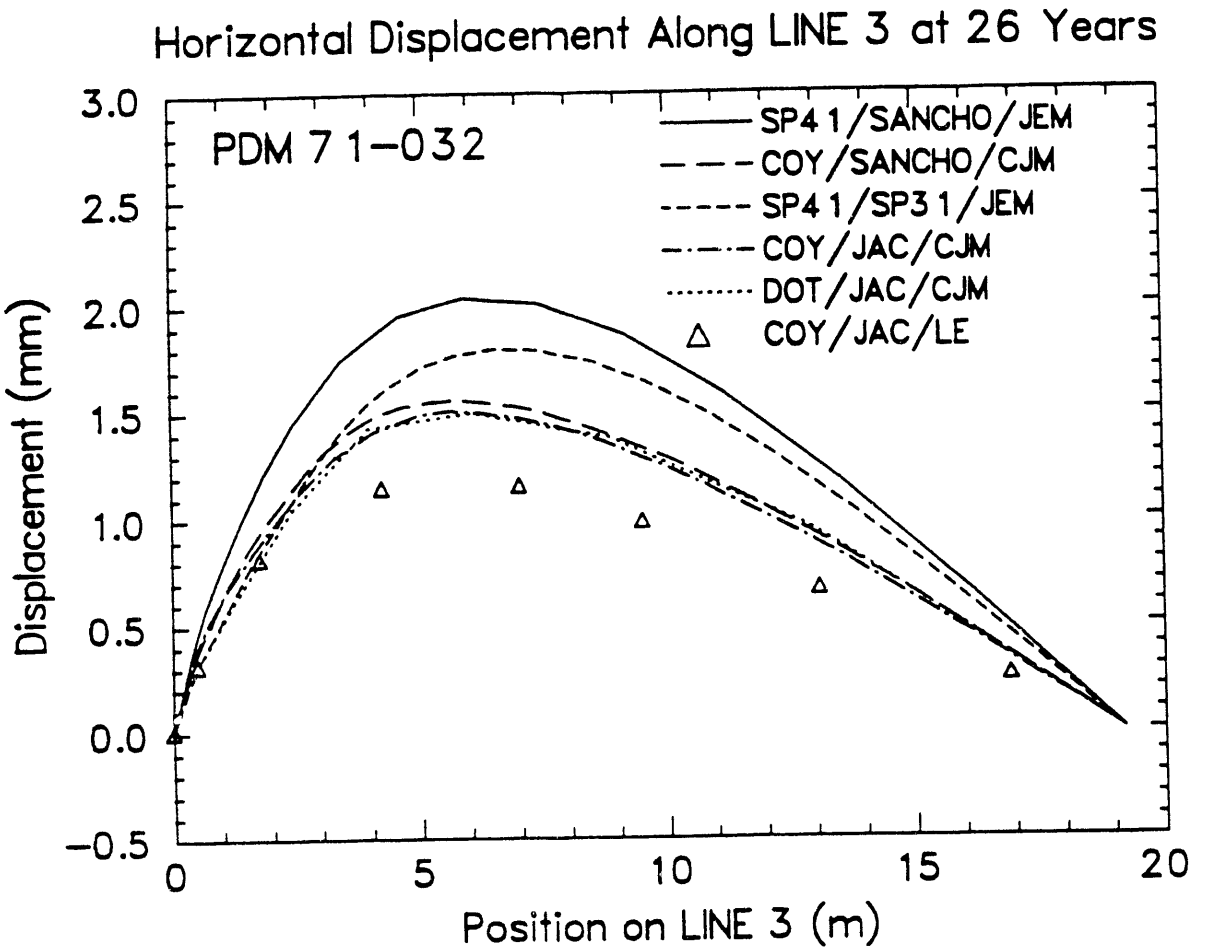

Figure 5-77. Comparison of Results for the Horizontal Displacement Along Line 3 (Figure 2-3) at 26 Yr, Second Analysis

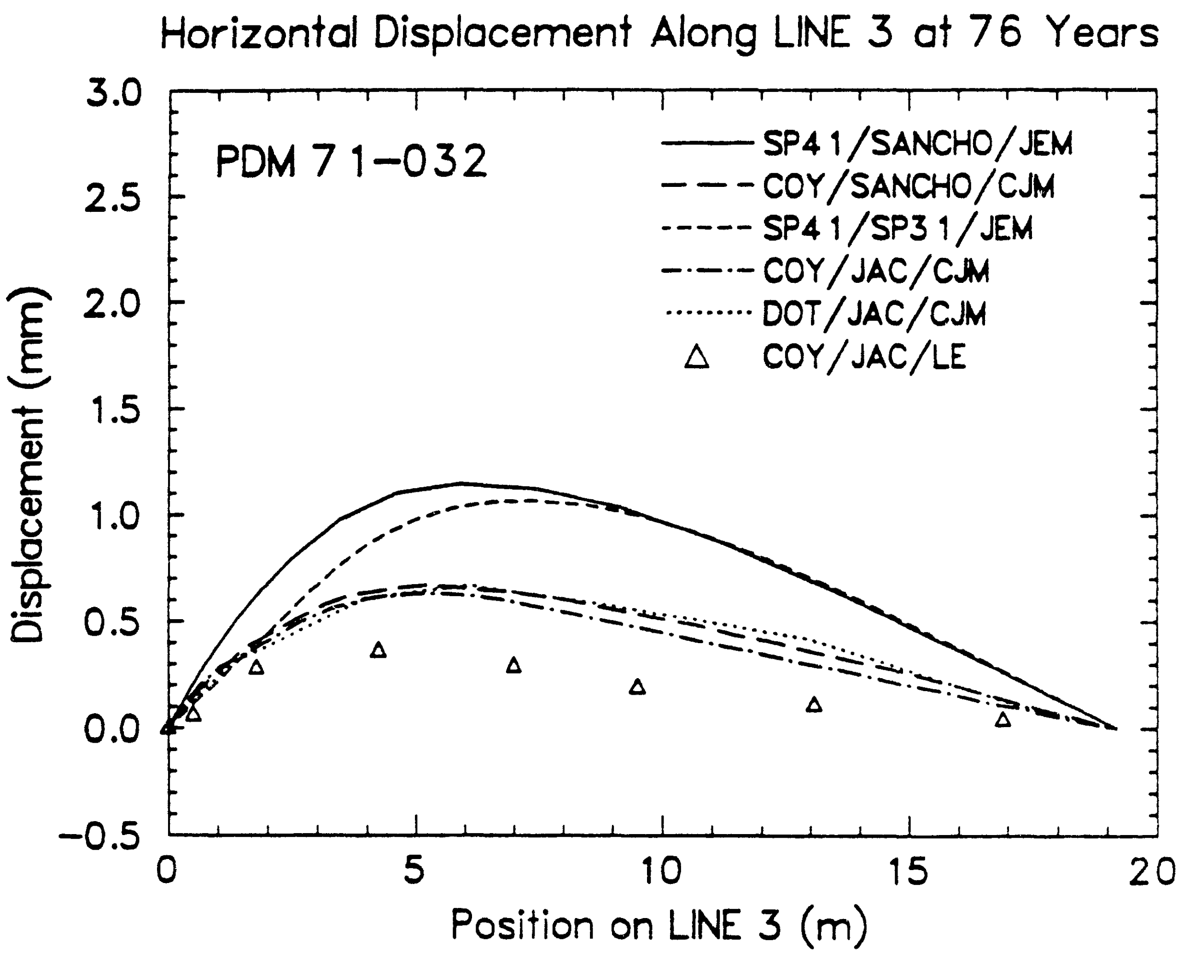

Figure 5-78. Comparison of Results for the Horizontal Displacement Along Line 3 (Figure 2-3) at 76 Yr, Second Analysis

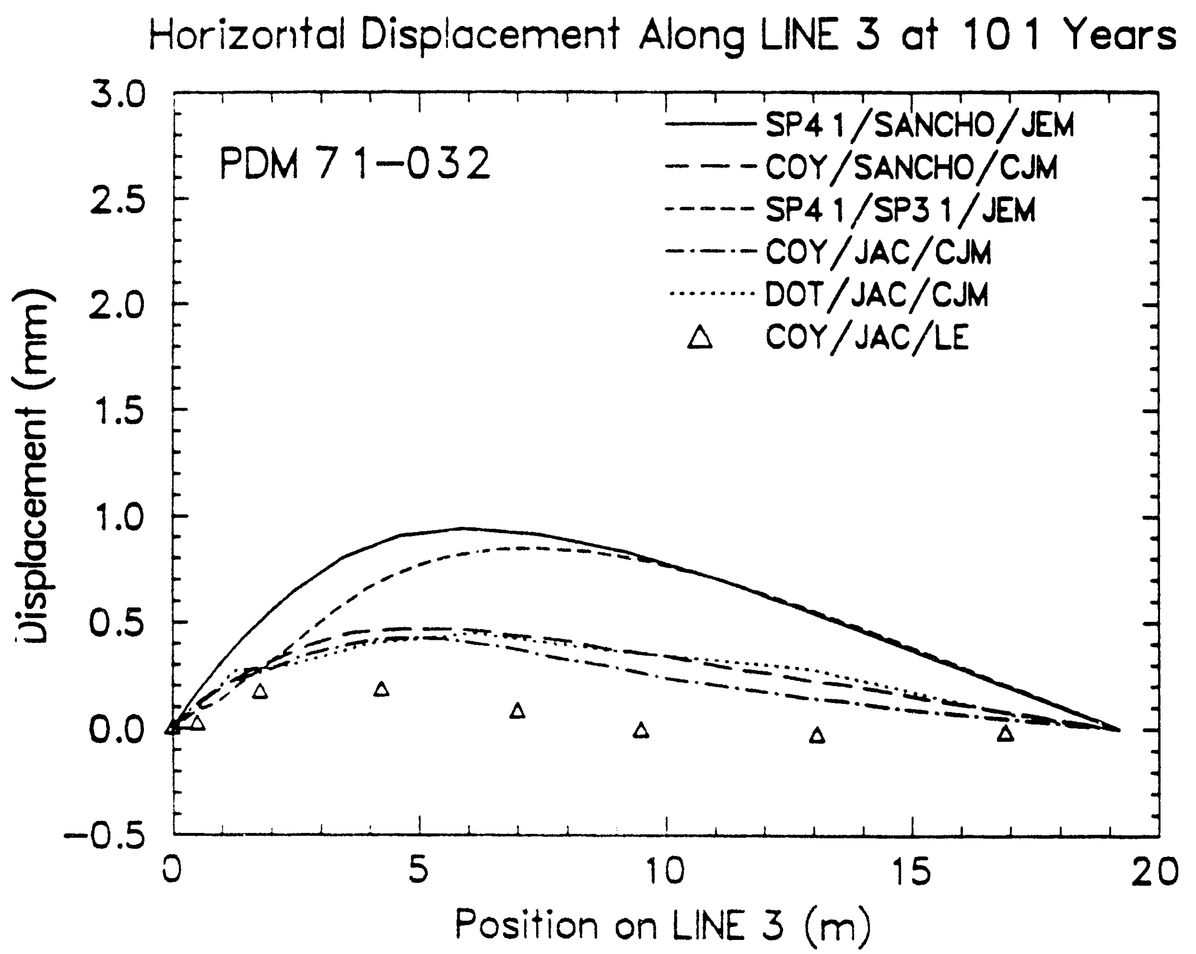

Figure 5-79. Comparison of Results for the Horizontal Displacement Along Line 3 (Figure 2-3) at 101 Yr, Second Analysis

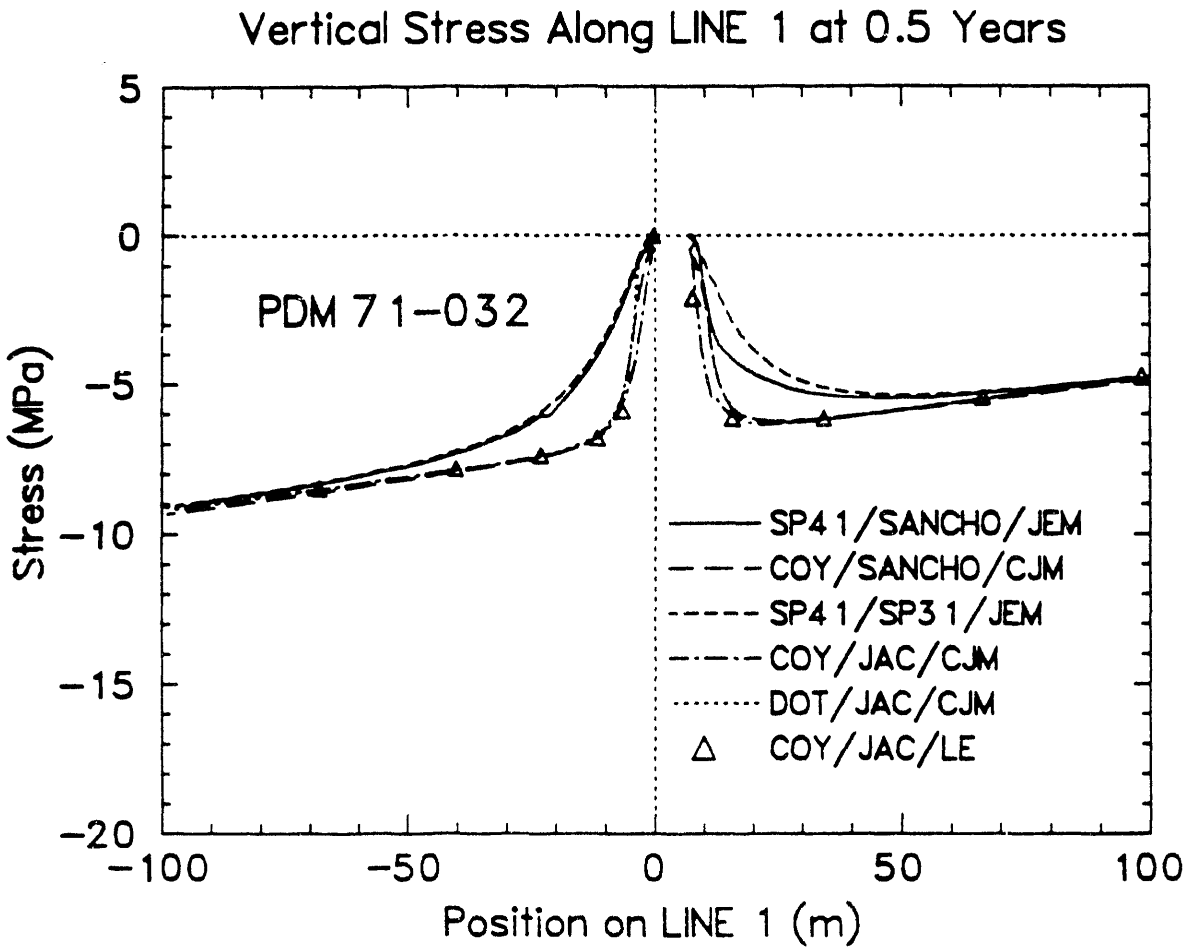

Figure 5-80. Comparison of Results for the Vertical Stress Along Line 1 (Figure 2-3) at 0.5 Yr, Second Analysis

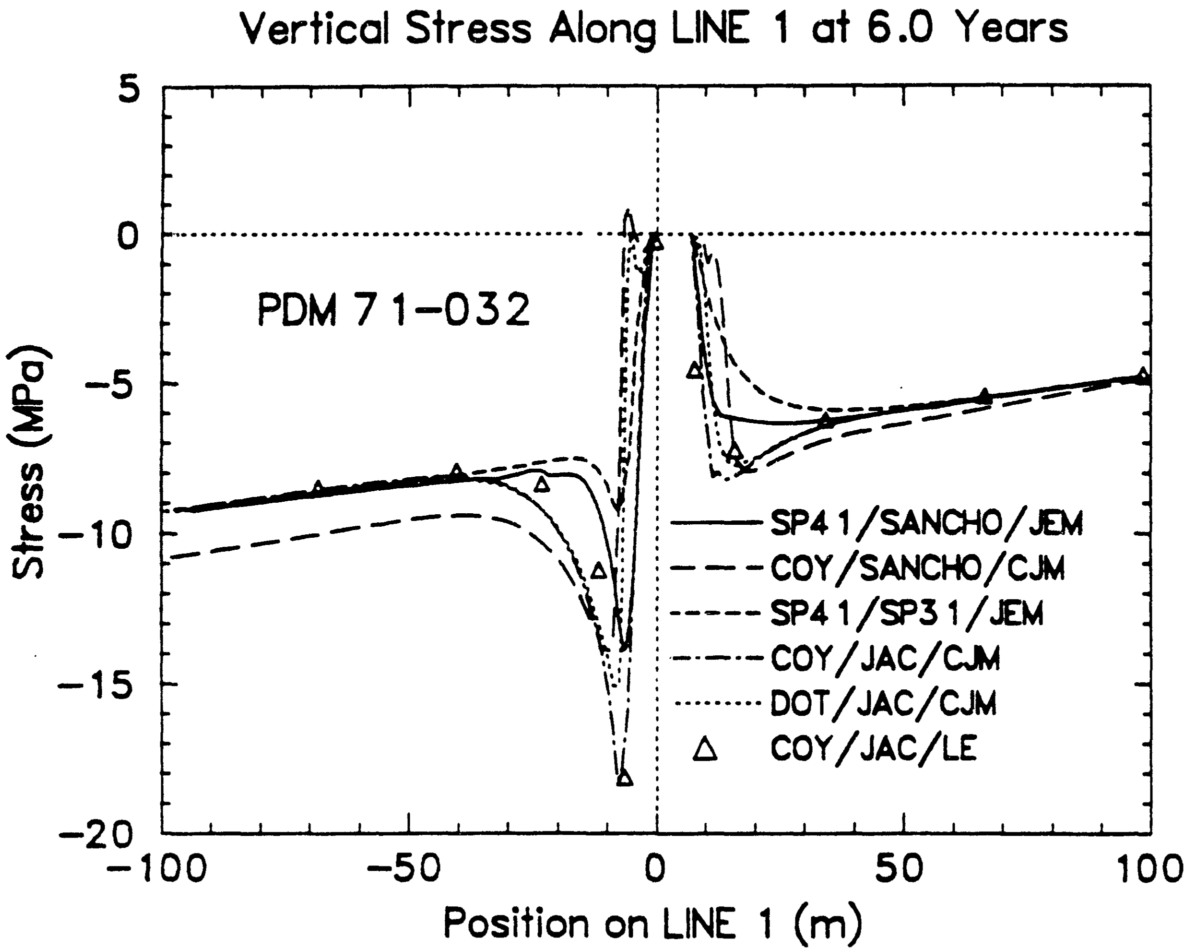

Figure 5-81. Comparison of Results for the Vertical Stress Along Line 1 (Figure 2-3) at 6 Yr, Second Analysis

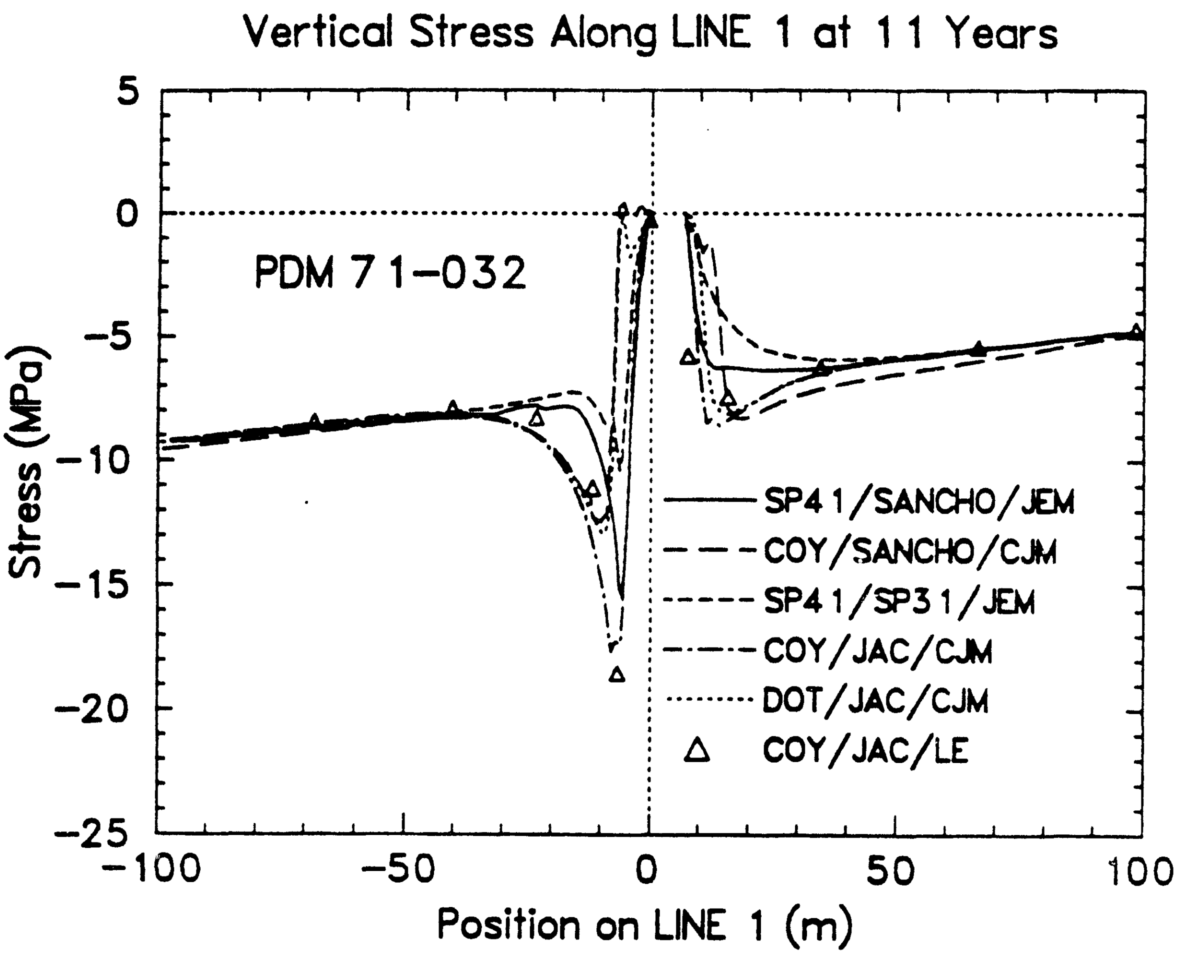

Figure 5-82. Comparison of Results for the Vertical Stress Along Line 1 (Figure 2-3) at 11 Yr, Second Analysis

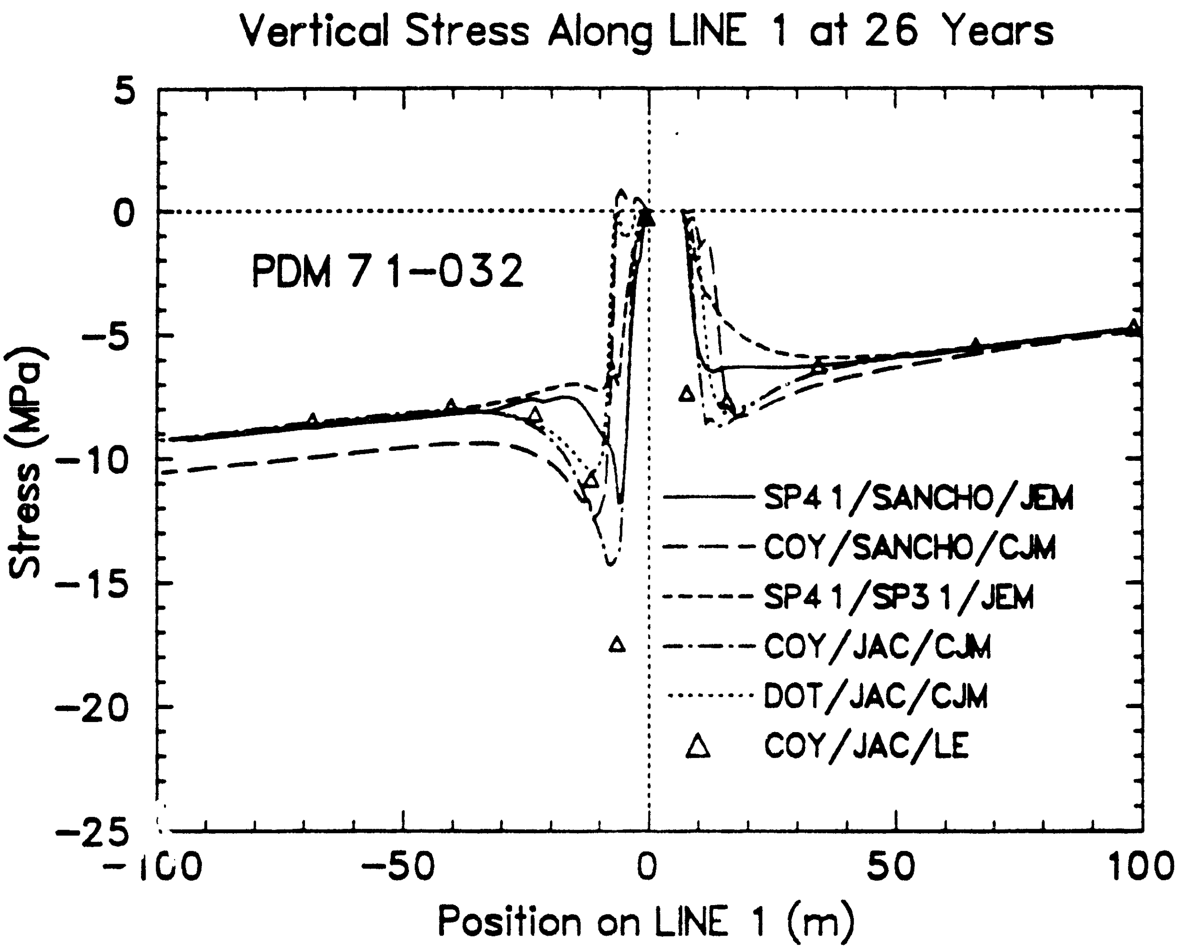

Figure 5-83. Comparison of Results for the Vertical Stress Along Line 1 (Figure 2-3) at 26 Yr, Second Analysis

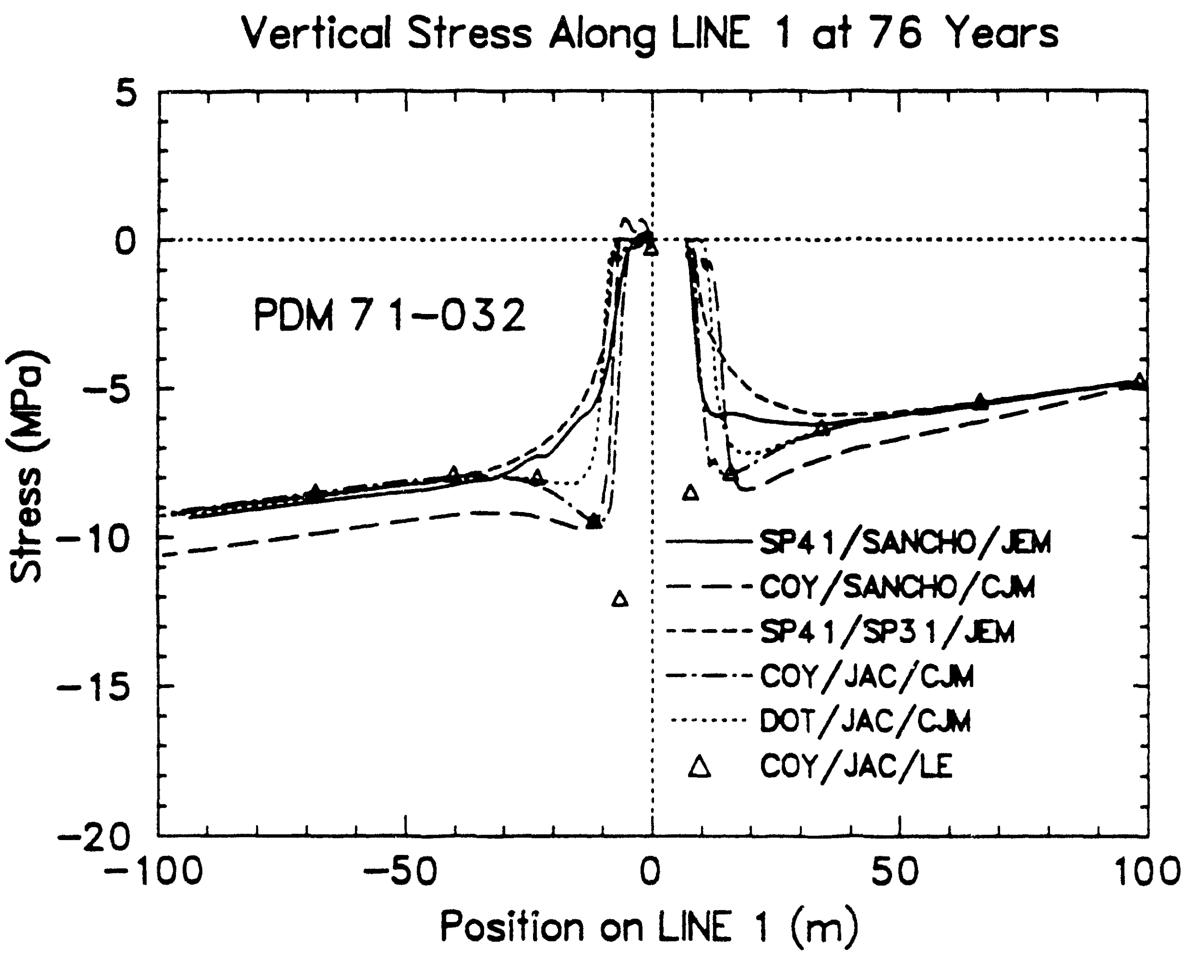

Figure 5-84. Comparison of Results for the Vertical Stress Along Line 1 (Figure 2-3) at 76 Yr, Second Analysis

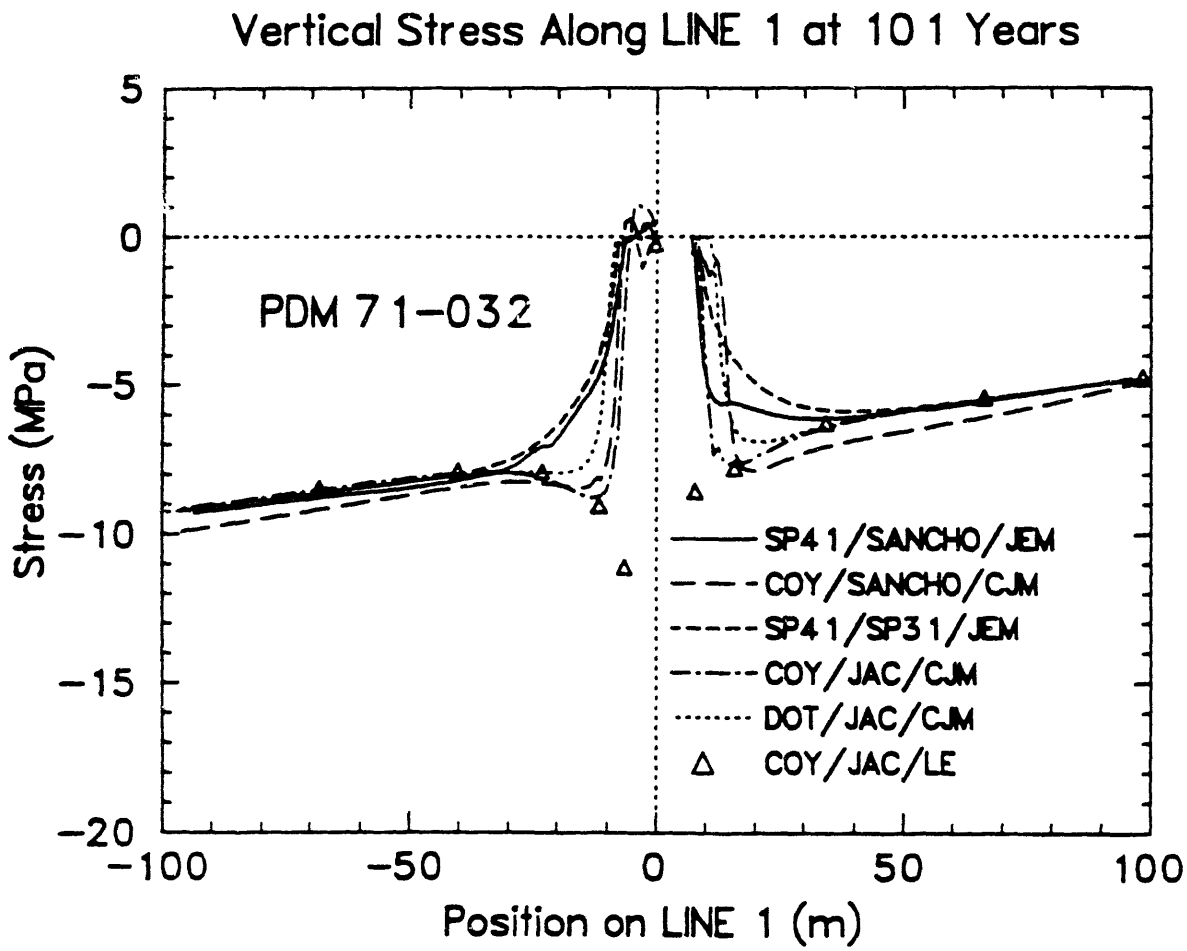

Figure 5-85. Comparison of Results for the Vertical Stress Along Line 1 (Figure 2-3) at 101 Yr, Second Analysis

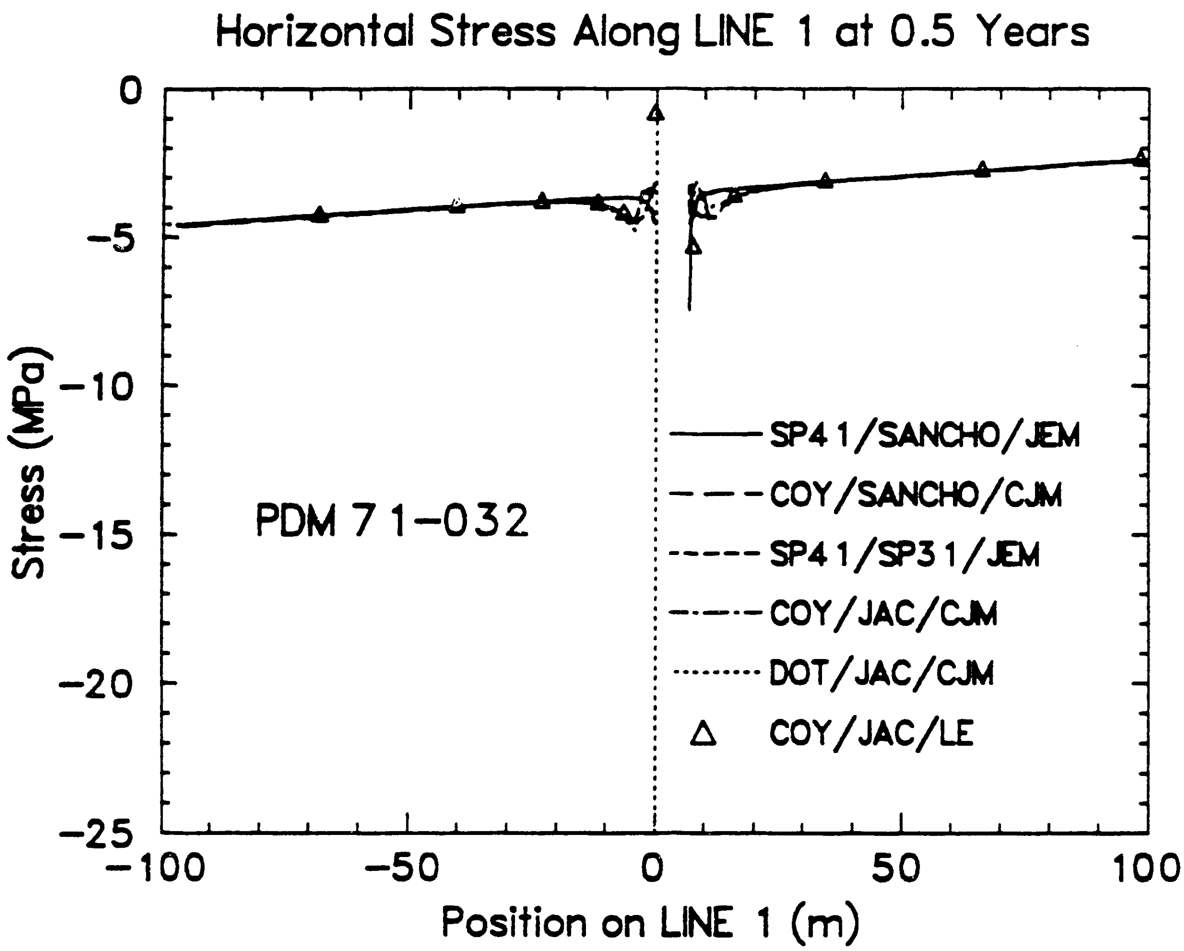

Figure 5-86. Comparison of Results for the Horizontal Stress Along Line 1 (Figure 2-3) at 0.5 Yr, Second Analysis

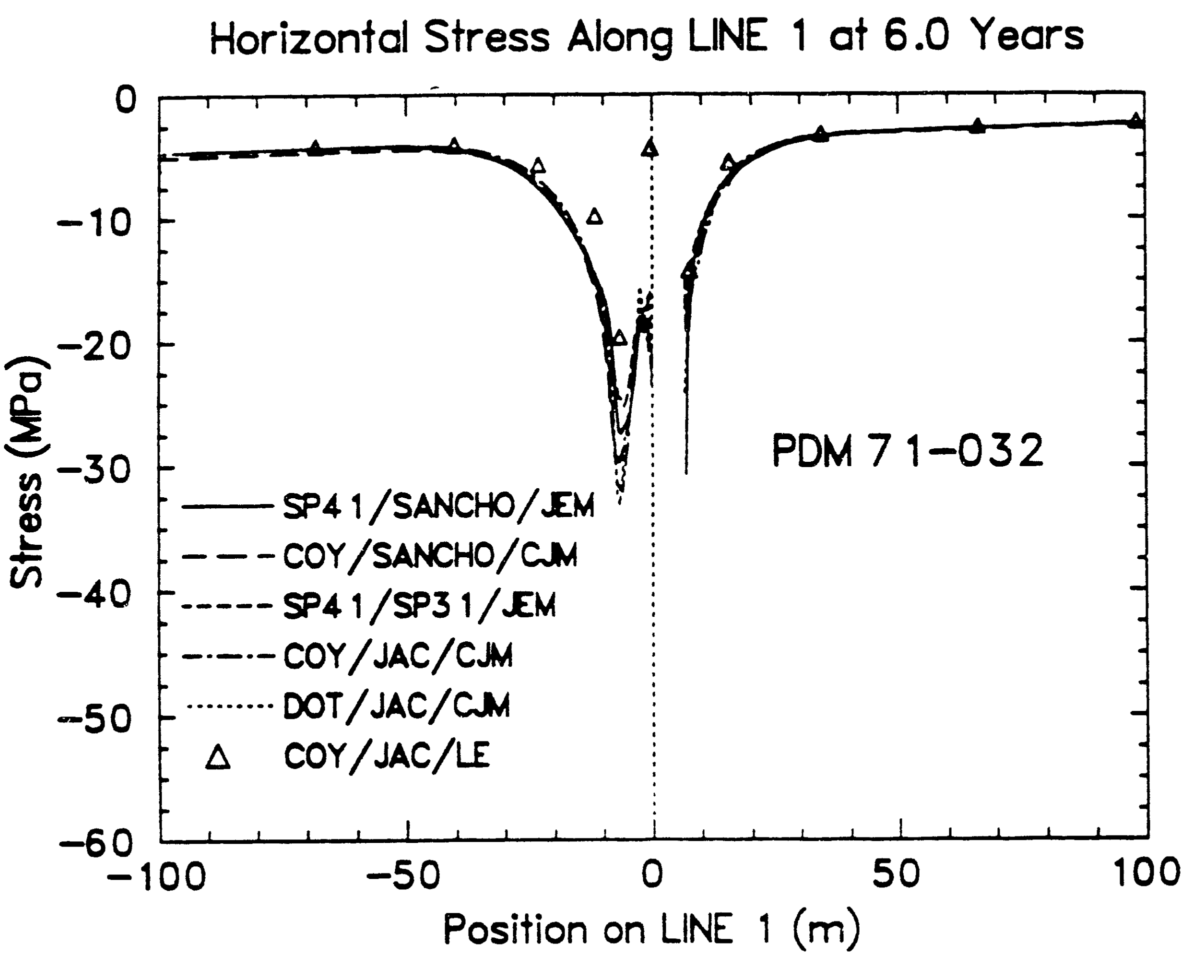

Figure 5-87. Comparison of Results for the Horizontal Stress Along Line 1 (Figure 2-3) at 6 Yr, Second Analysis

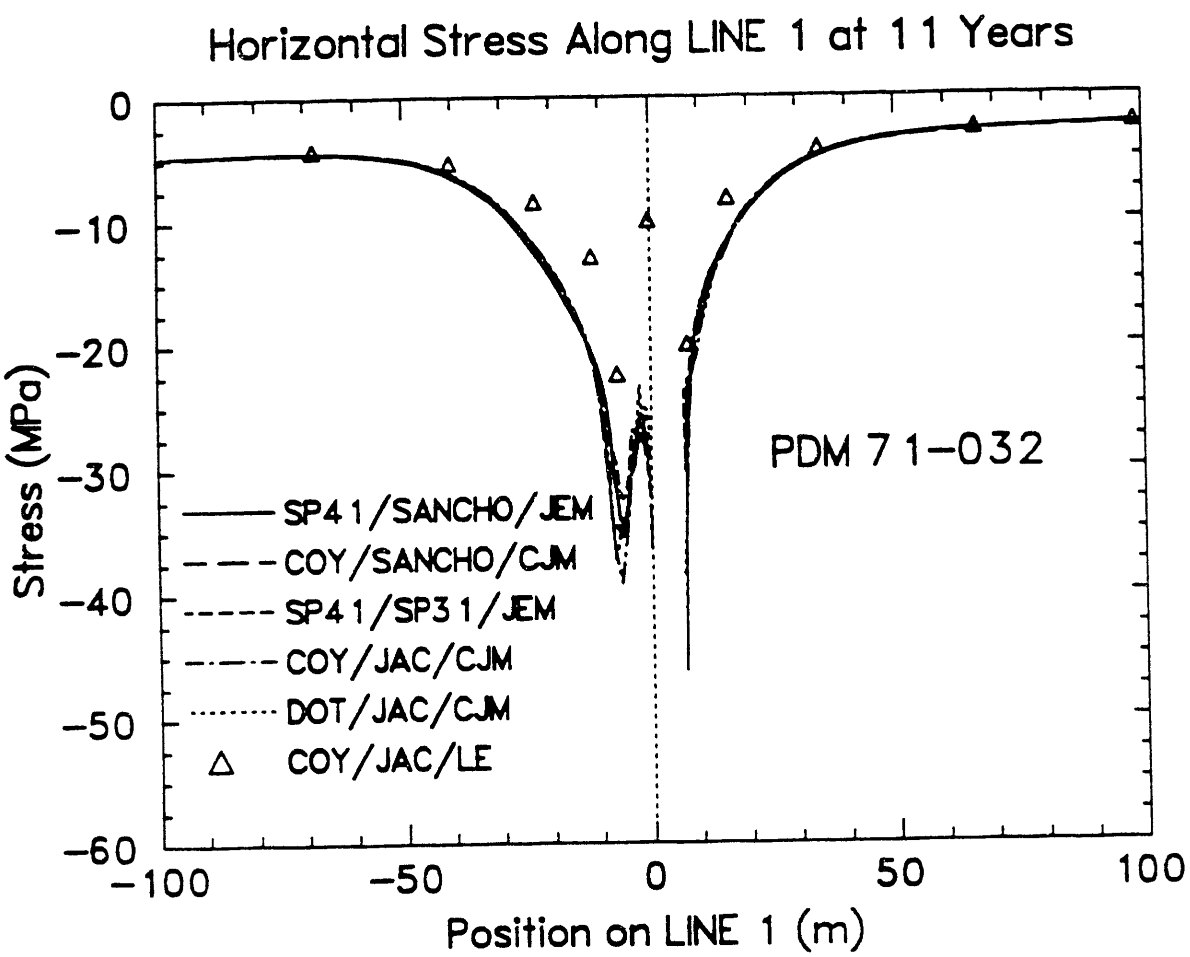

Figure 5-88. Comparison of Results for the Horizontal Stress Along Line 1 (Figure 2-3) at 11 Yr, Second Analysis

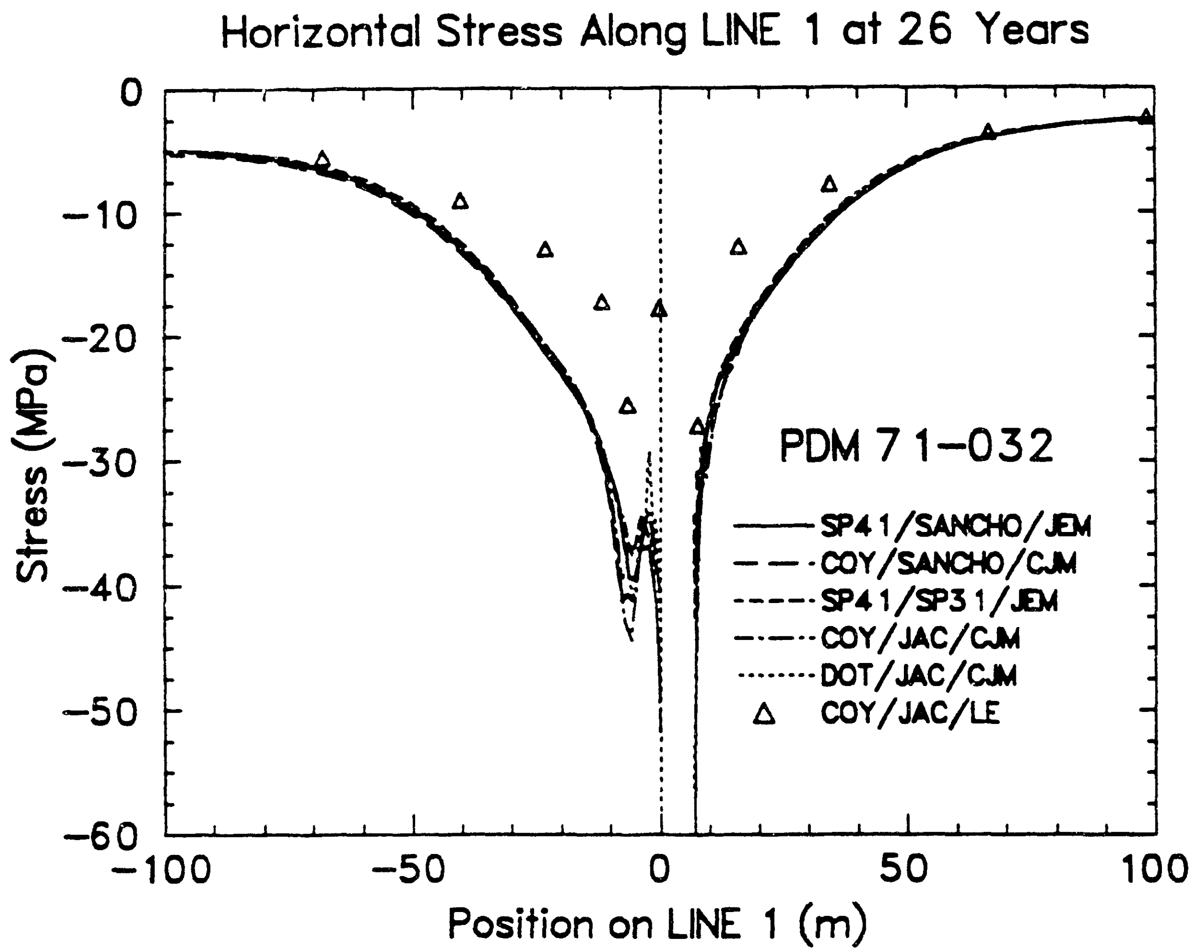

Figure 5-89. Comparison of Results for the Horizontal Stress Along Line 1 (Figure 2-3) at 26 Yr, Second Analysis

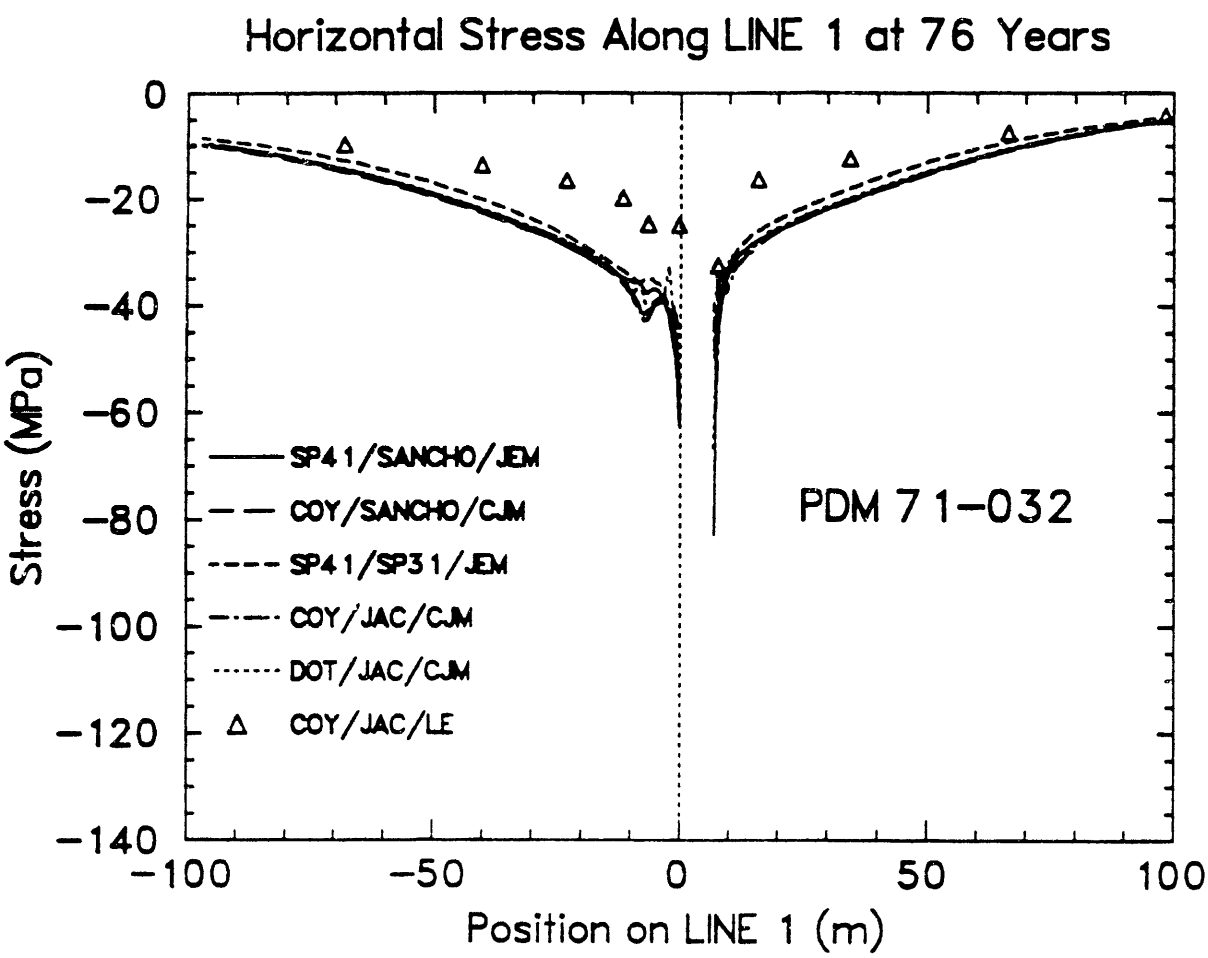

Figure 5-90. Comparison of Results for the Horizontal Stress Along Line 1 (Figure 2-3) at 76 Yr, Second Analysis

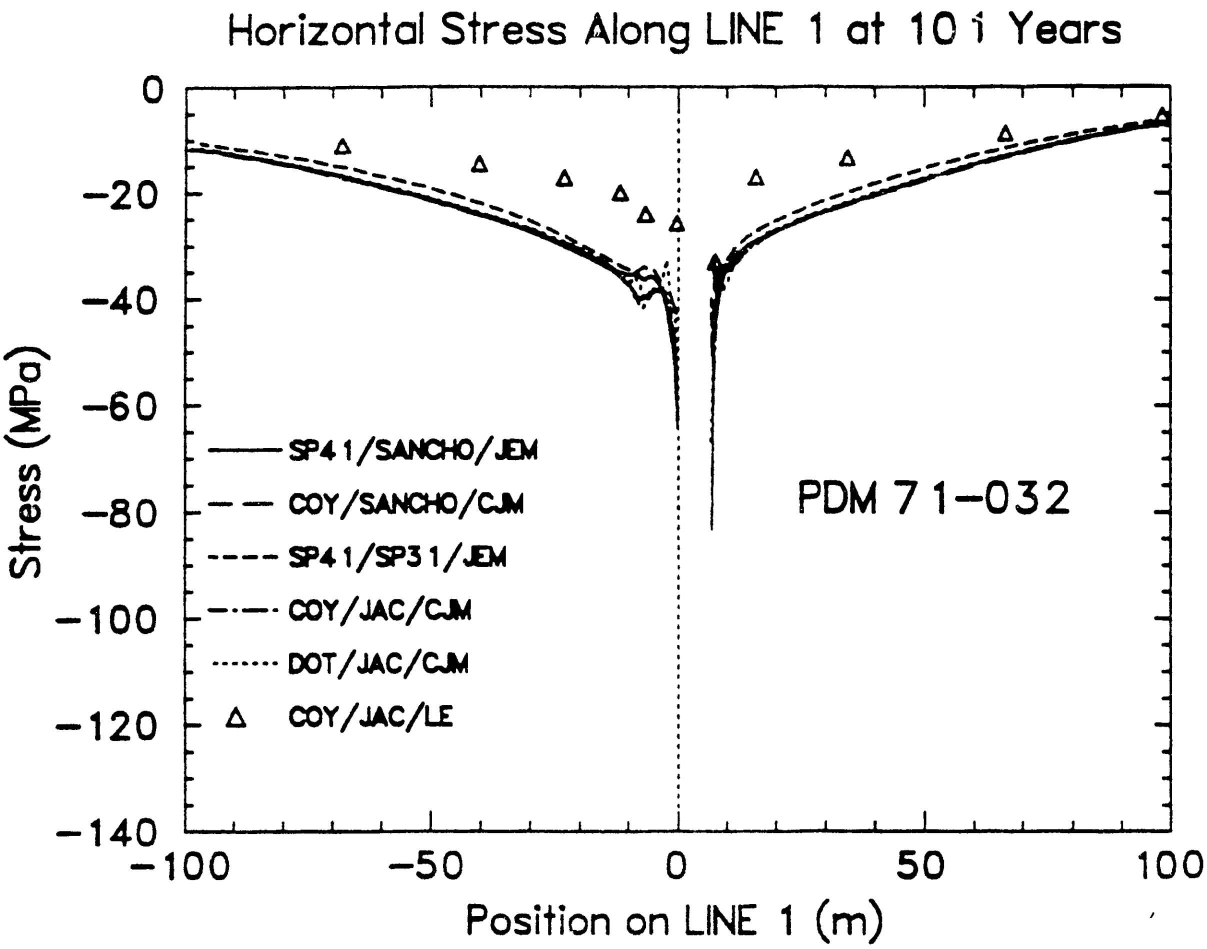

Figure 5-91. Comparison of Results for the Horizontal Stress Along Line 1 (Figure 2-3) at 101 Yr, Second Analysis

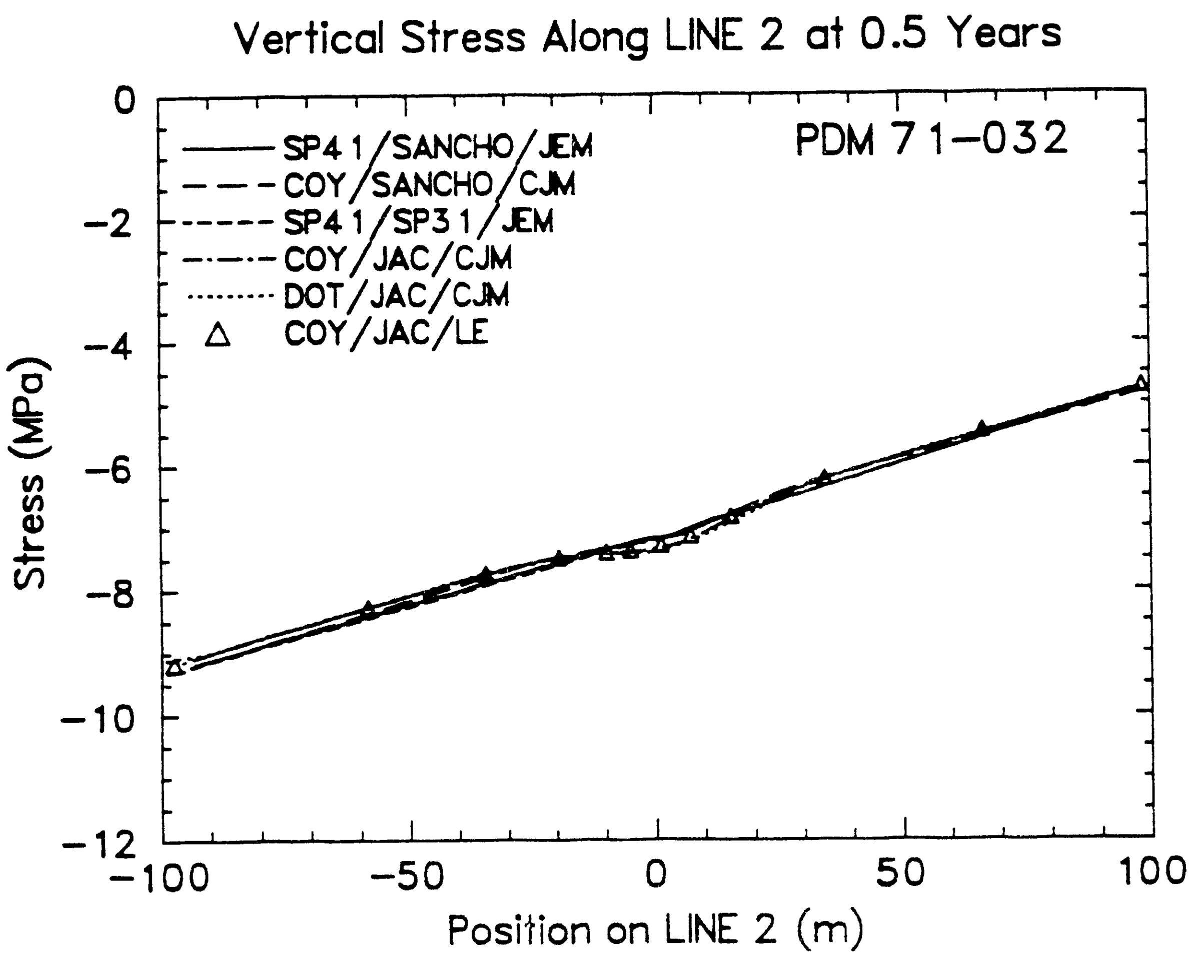

Figure 5-92. Comparison of Results for the Vertical Stress Along Line 2 (Figure 2-3) at 0.5 Yr, Second Analysis

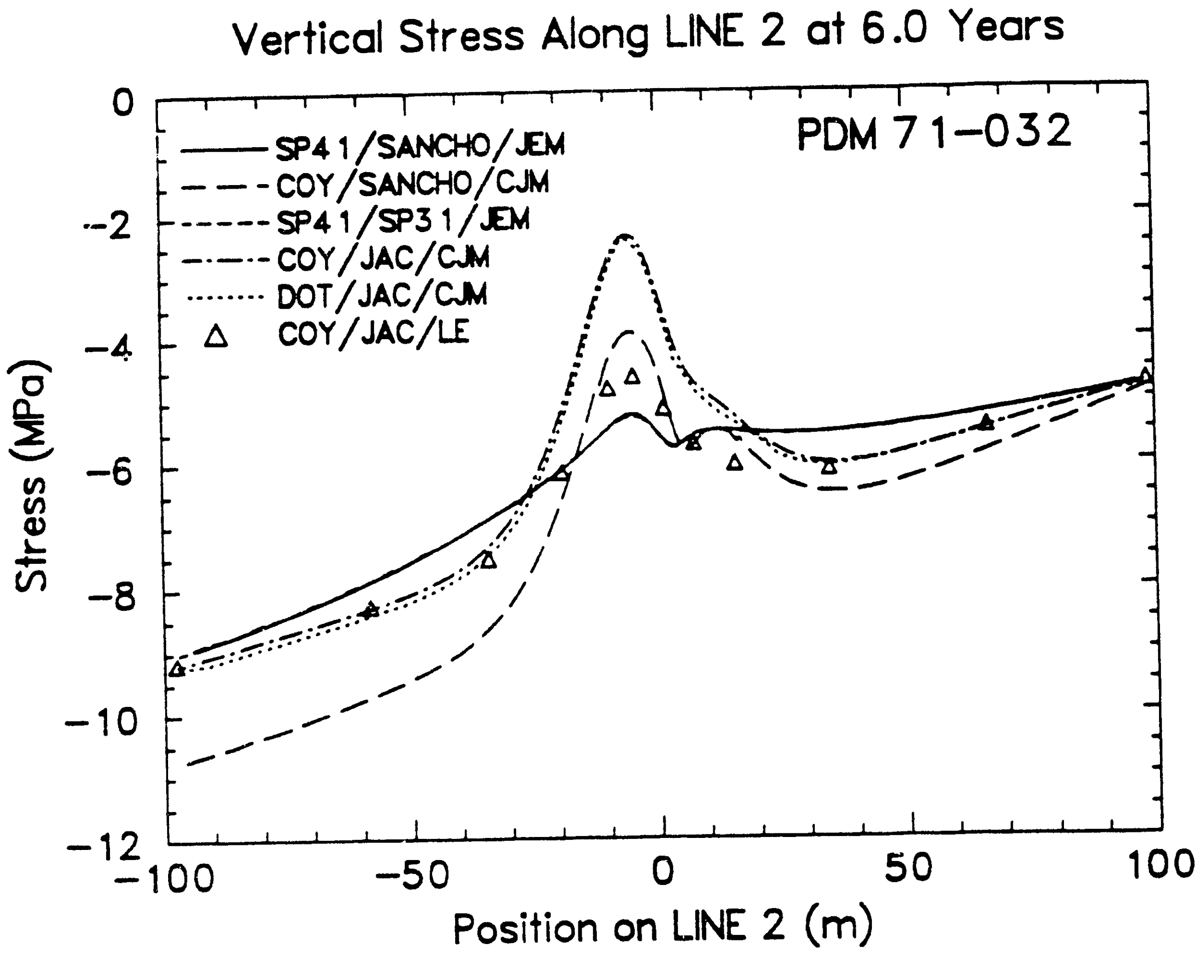

Figure 5-93. Comparison of Results for the Vertical Stress Along Line 2 (Figure 2-3) at 6 Yr, Second Analysis

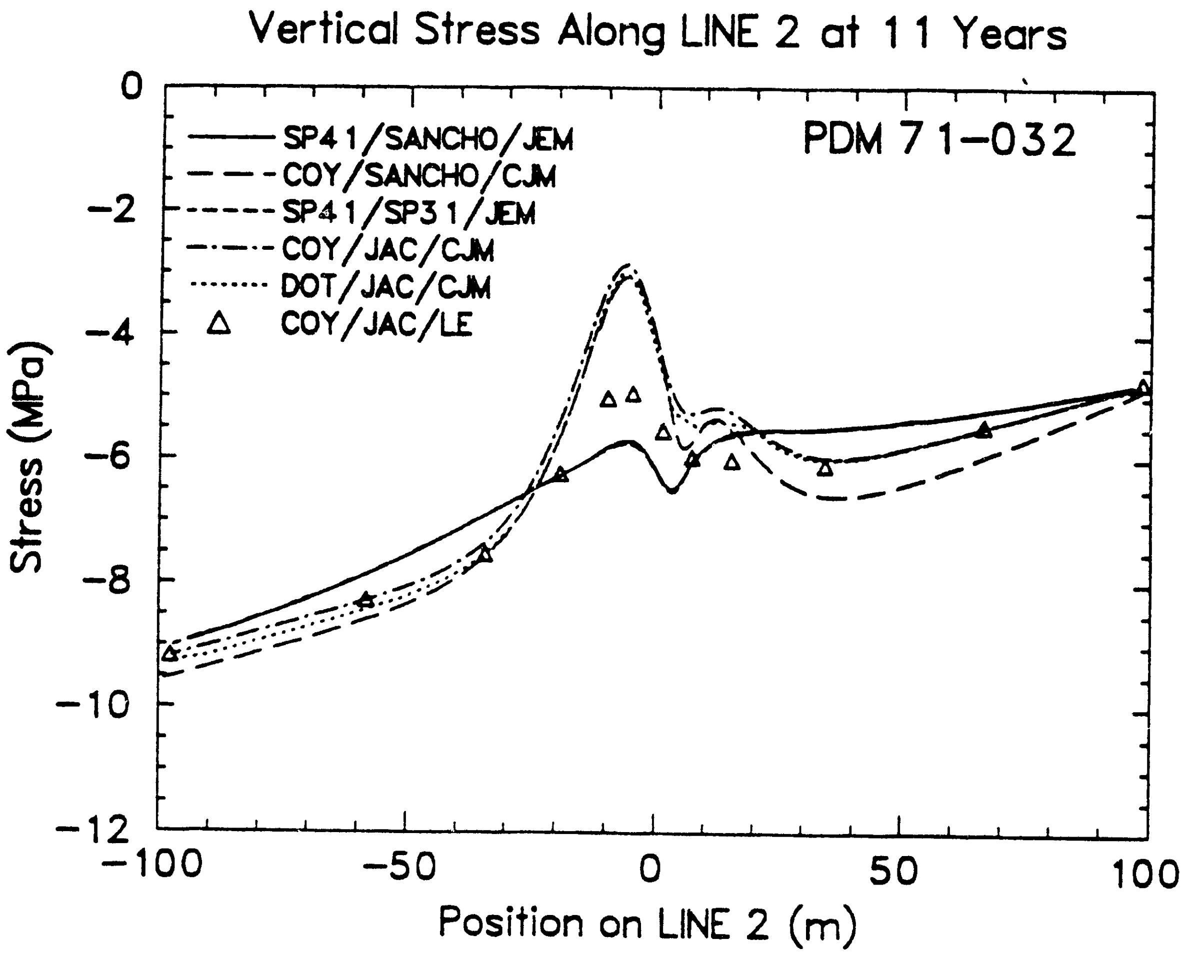

Figure 5-94. Comparison of Results for the Vertical Stress Along Line 2 (Figure 2-3) at 11 Yr, Second Analysis

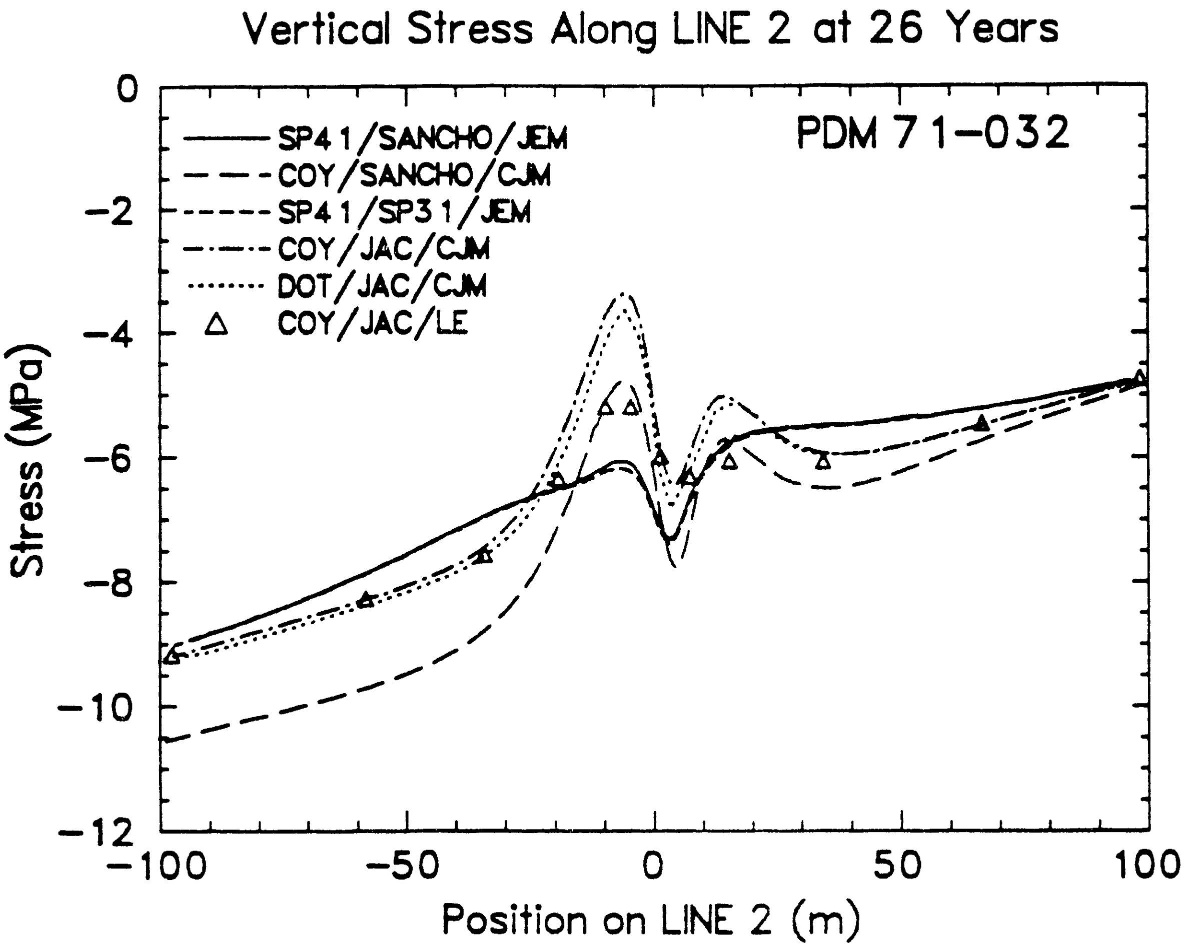

Figure 5-95. Comparison of Results for the Vertical Stress Along Line 2 (Figure 2-3) at 26 Yr, Second Analysis

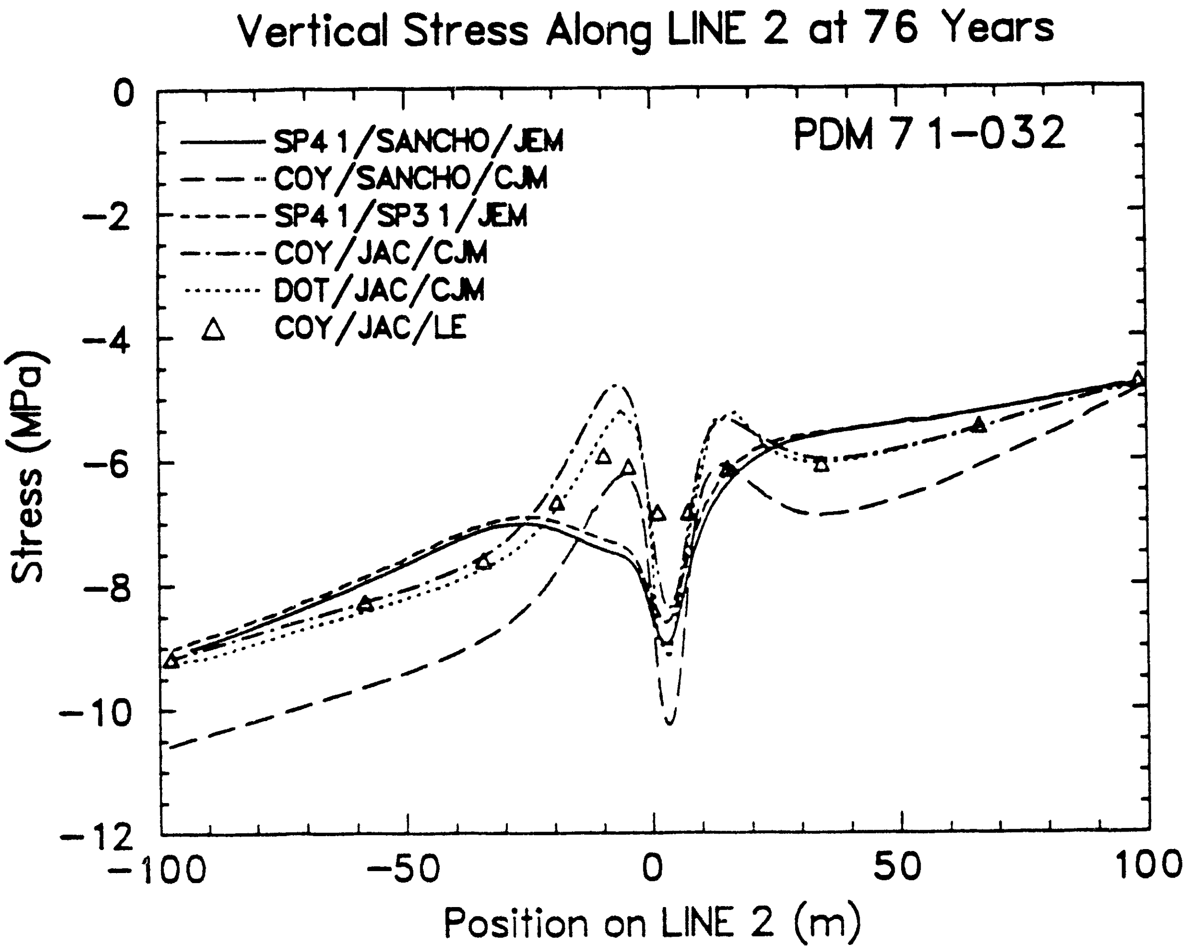

Figure 5-96. Comparison of Results for the Vertical Stress Along Line 2 (Figure 2-3) at 76 Yr, Second Analysis

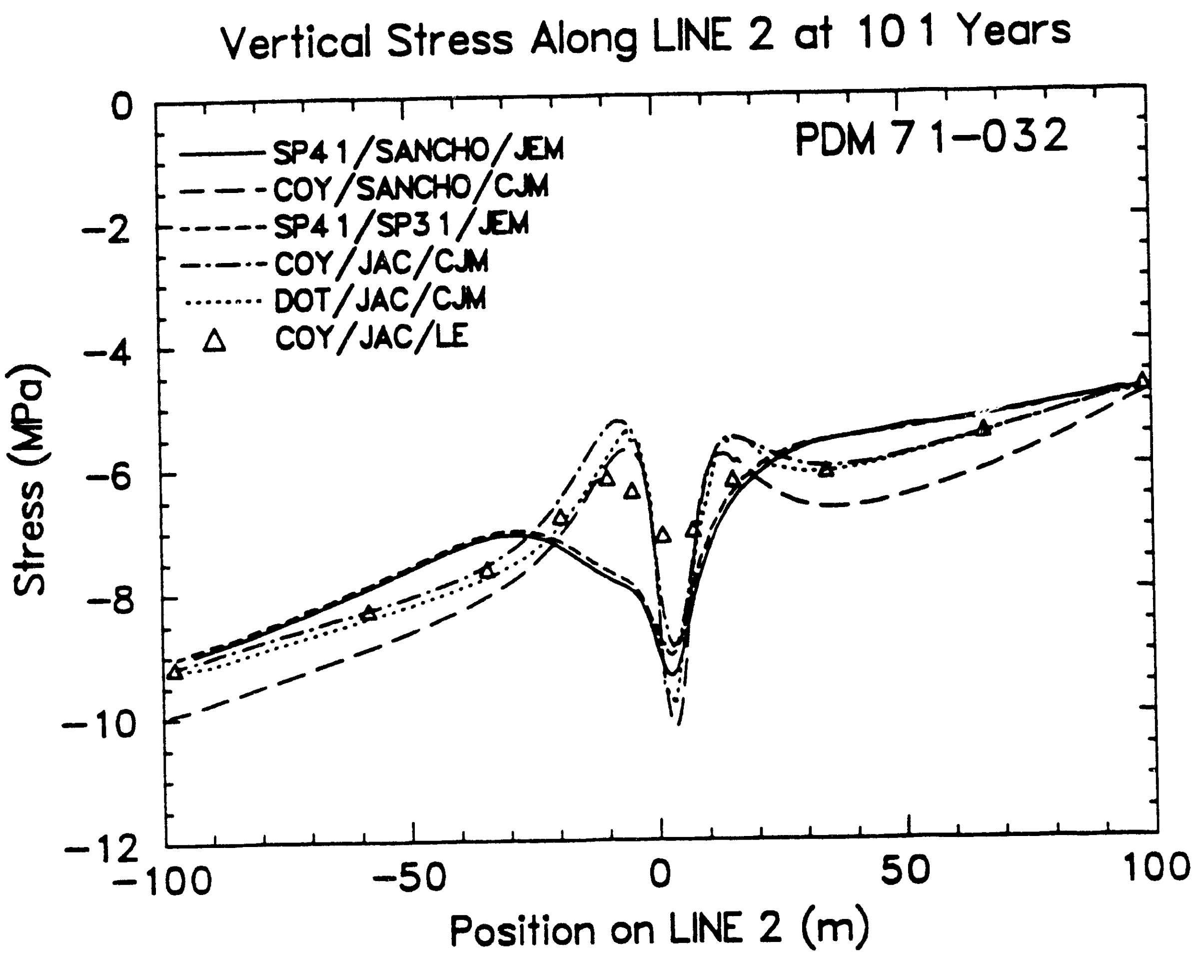

Figure 5-97. Comparison of Results for the Vertical Stress Along Line 2 (Figure 2-3) at 101 Yr, Second Analysis

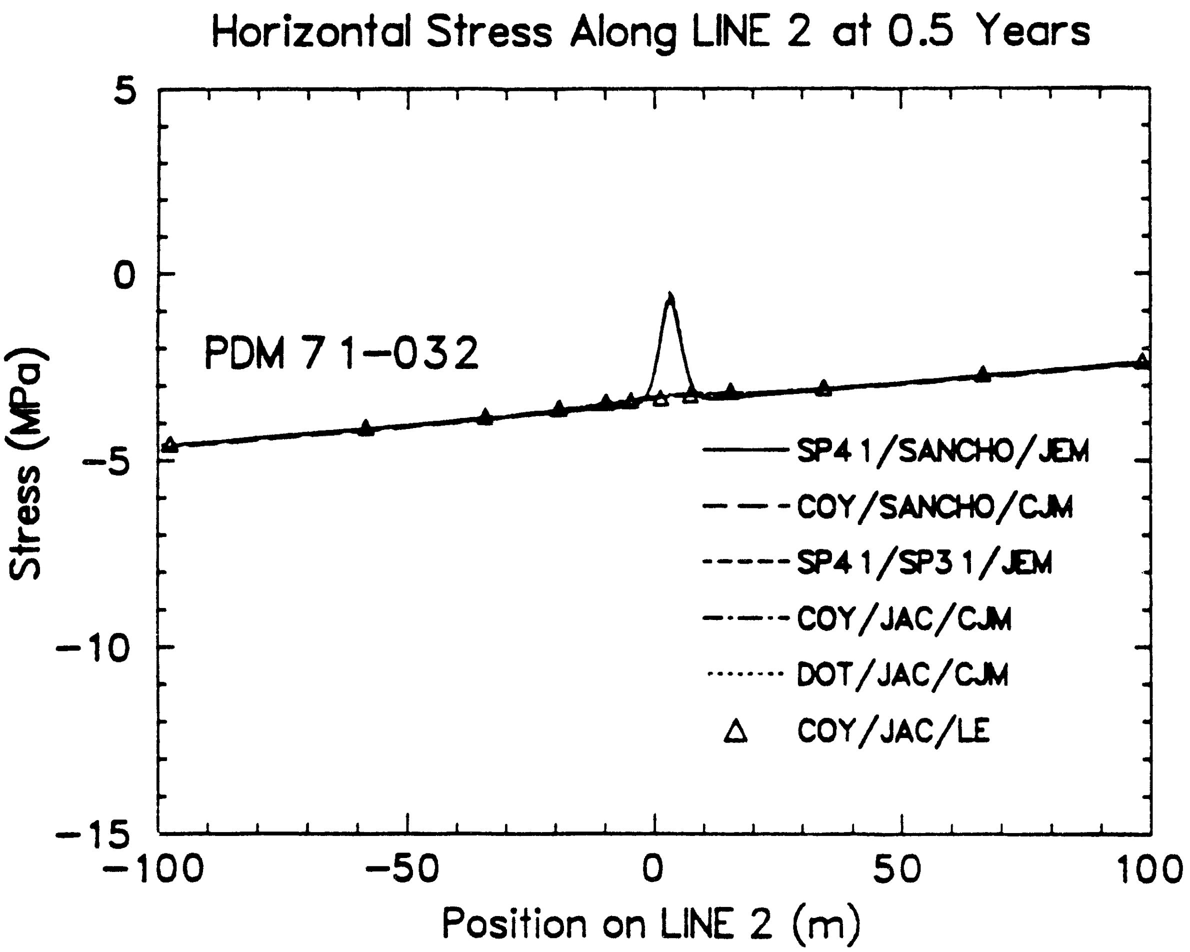

Figure 5-98. Comparison of Results for the Horizontal Stress Along Line 2 (Figure 2-3) at 0.5 Yr, Second Analysis

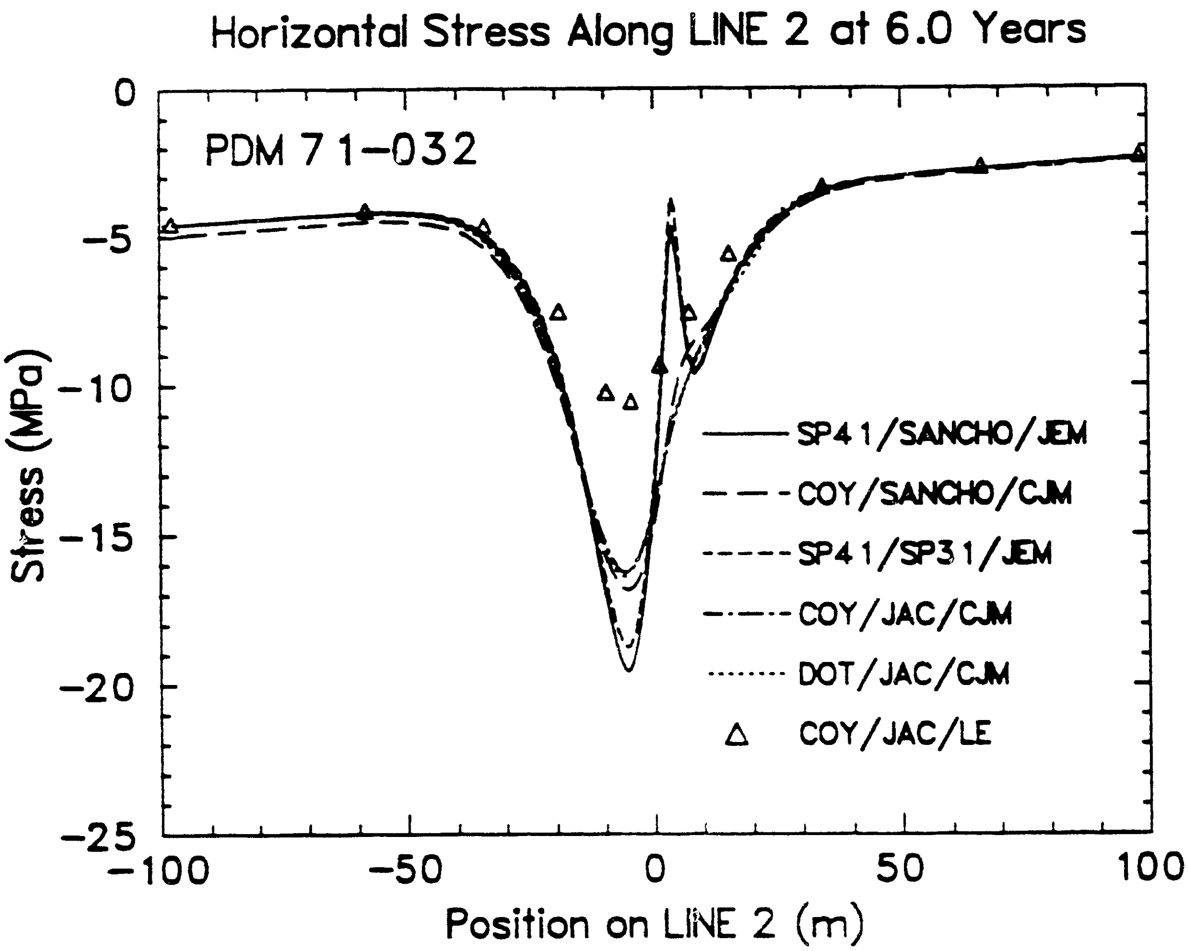

Figure 5-99. Comparison of Results for the Horizontal Stress Along Line 2 (Figure 2-3) at 6 Yr, Second Analysis

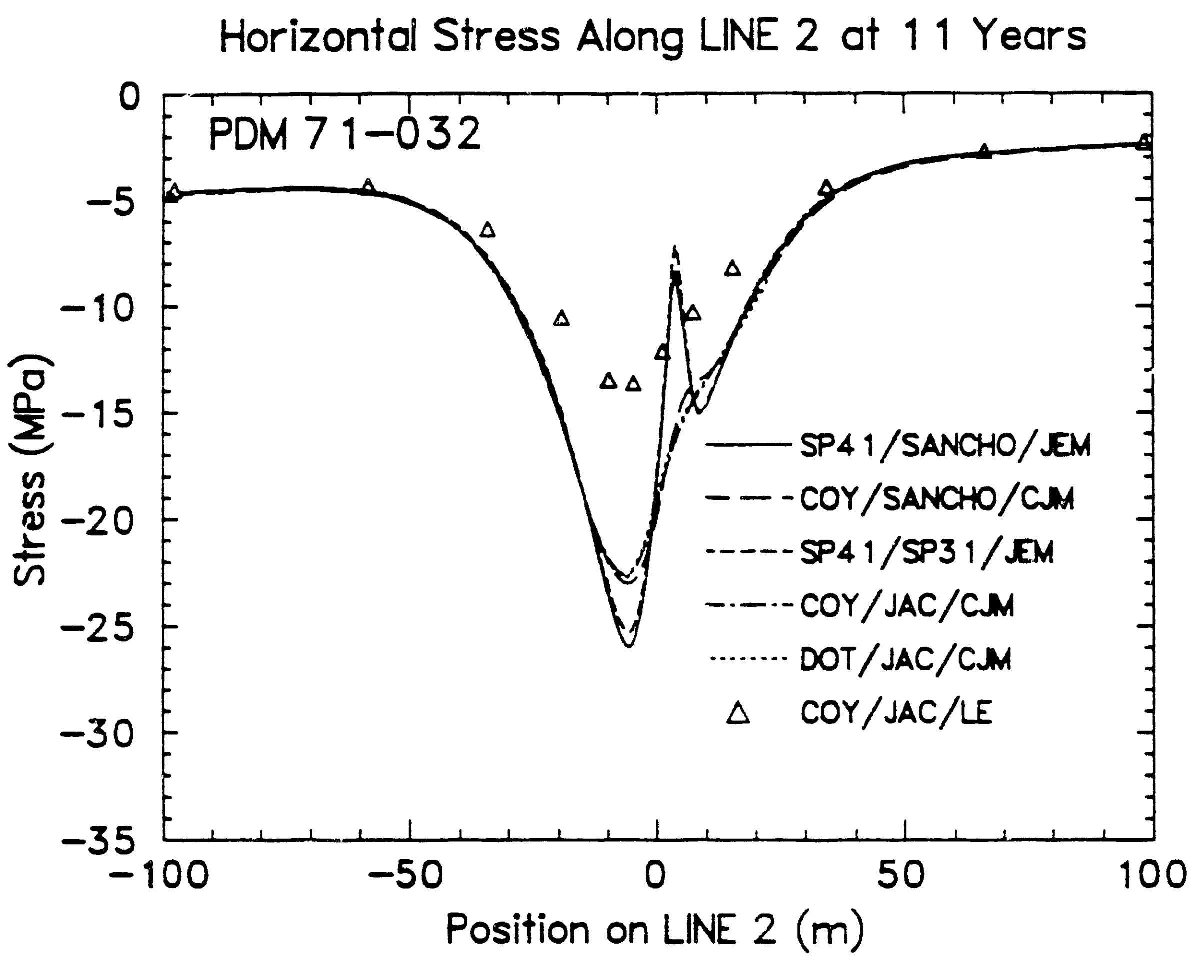

Figure 5-100. Comparison of Results for the Horizontal Stress Along Line 2 (Figure 2-3) at 11 Yr, Second Analysis

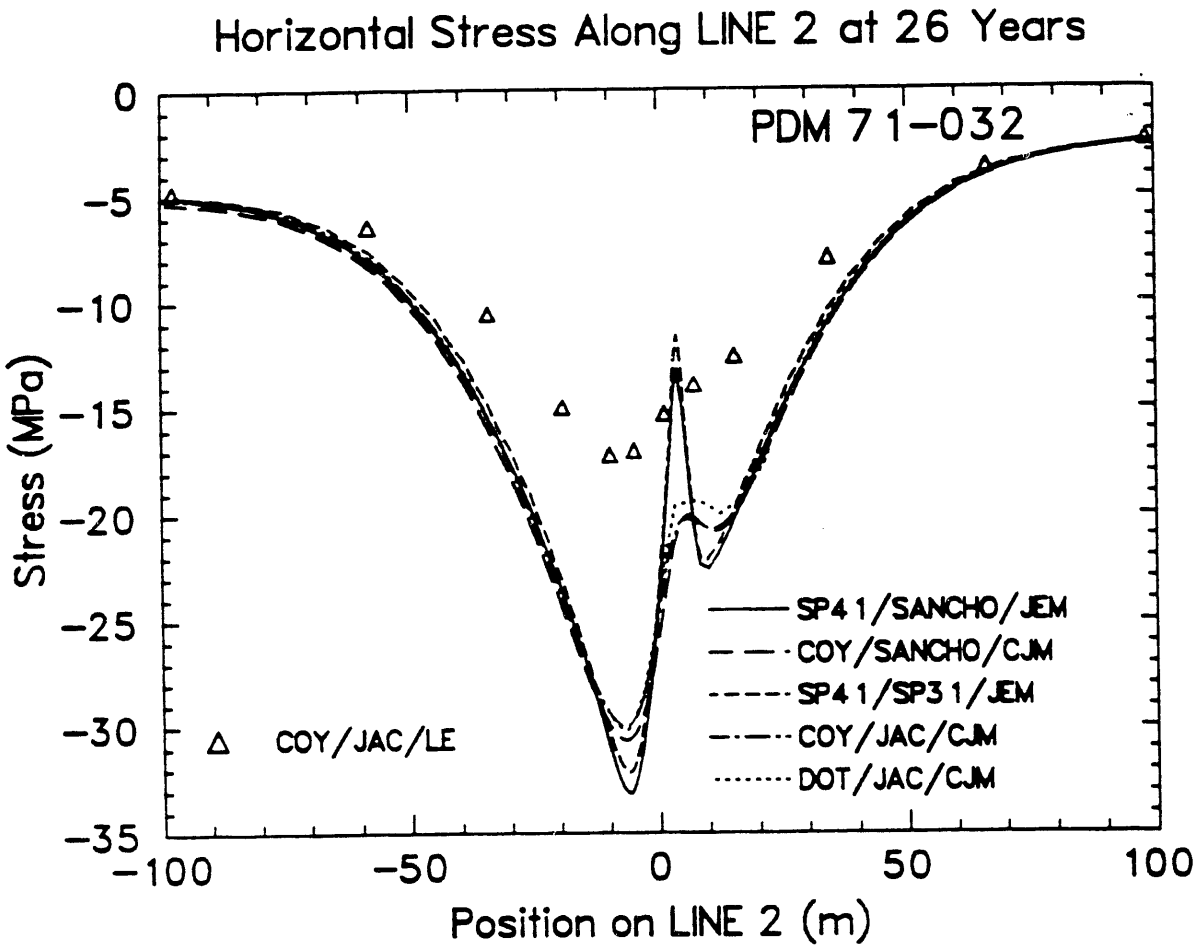

Figure 5-101. Comparison of Results for the Horizontal Stress Along Line 2 (Figure 2-3) at 26 Yr, Second Analysis

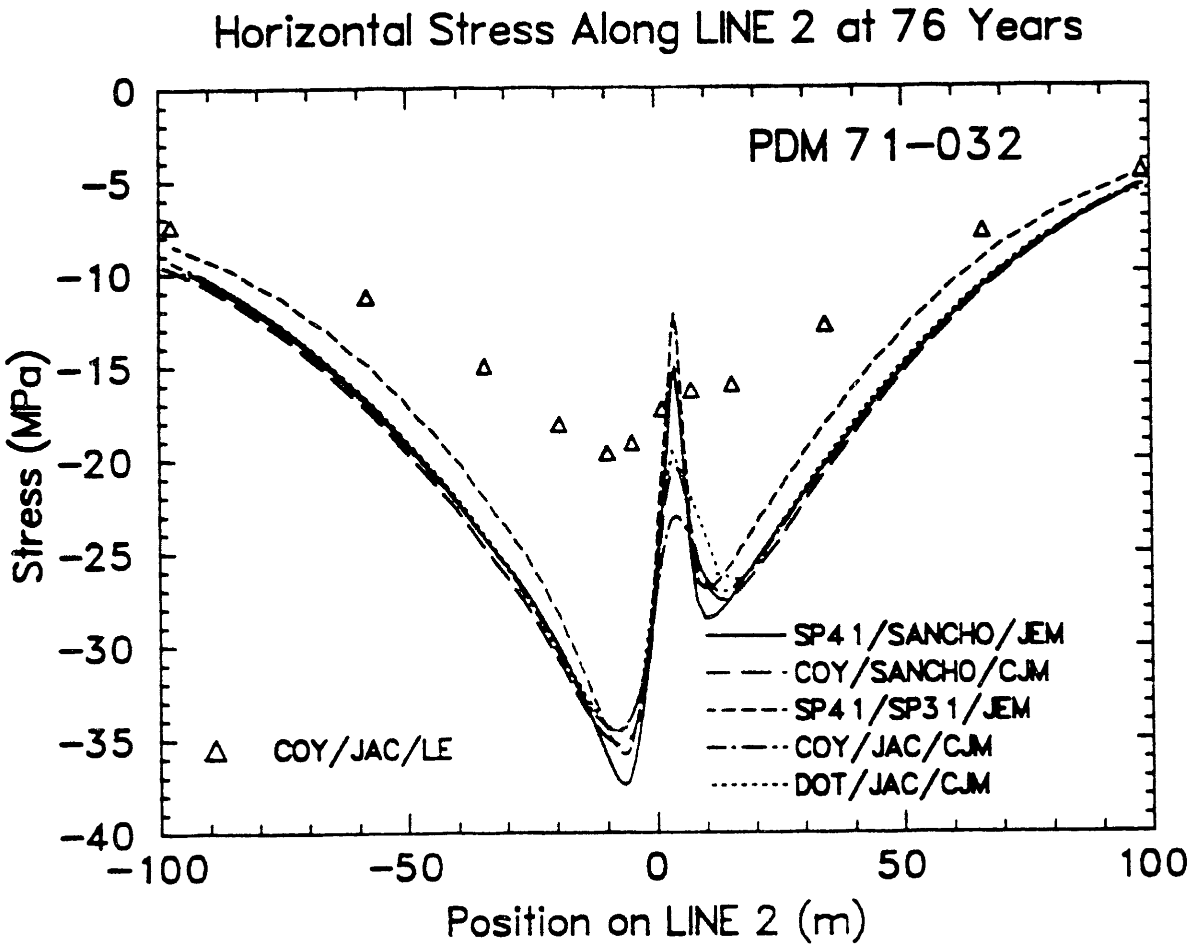

Figure 5-102. Comparison of Results for the Horizontal Stress Along Line 2 (Figure 2-3) at 76 Yr, Second Analysis

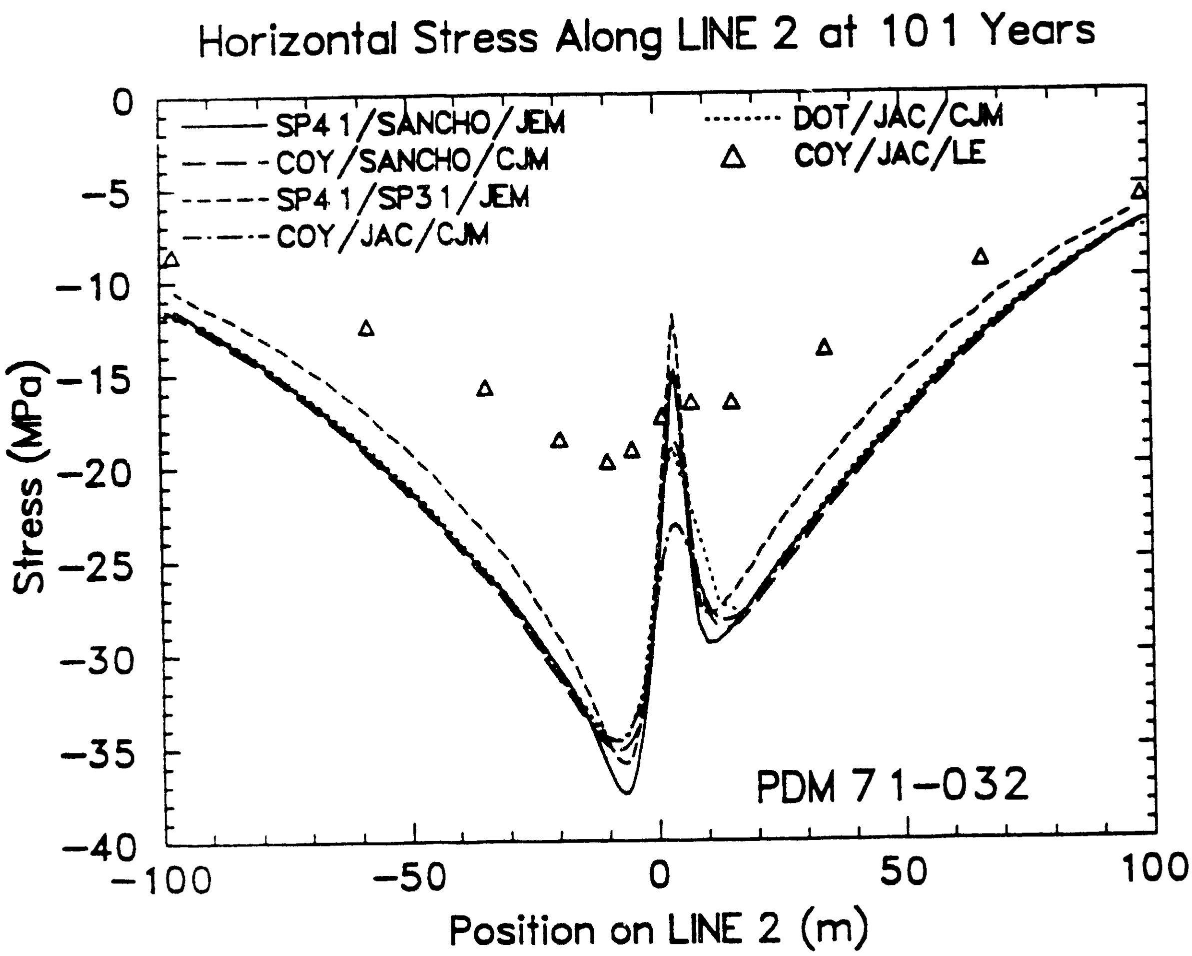

Figure 5-103. Comparison of Results for the Horizontal Stress Along Line 2 (Figure 2-3) at 101 Yr, Second Analysis

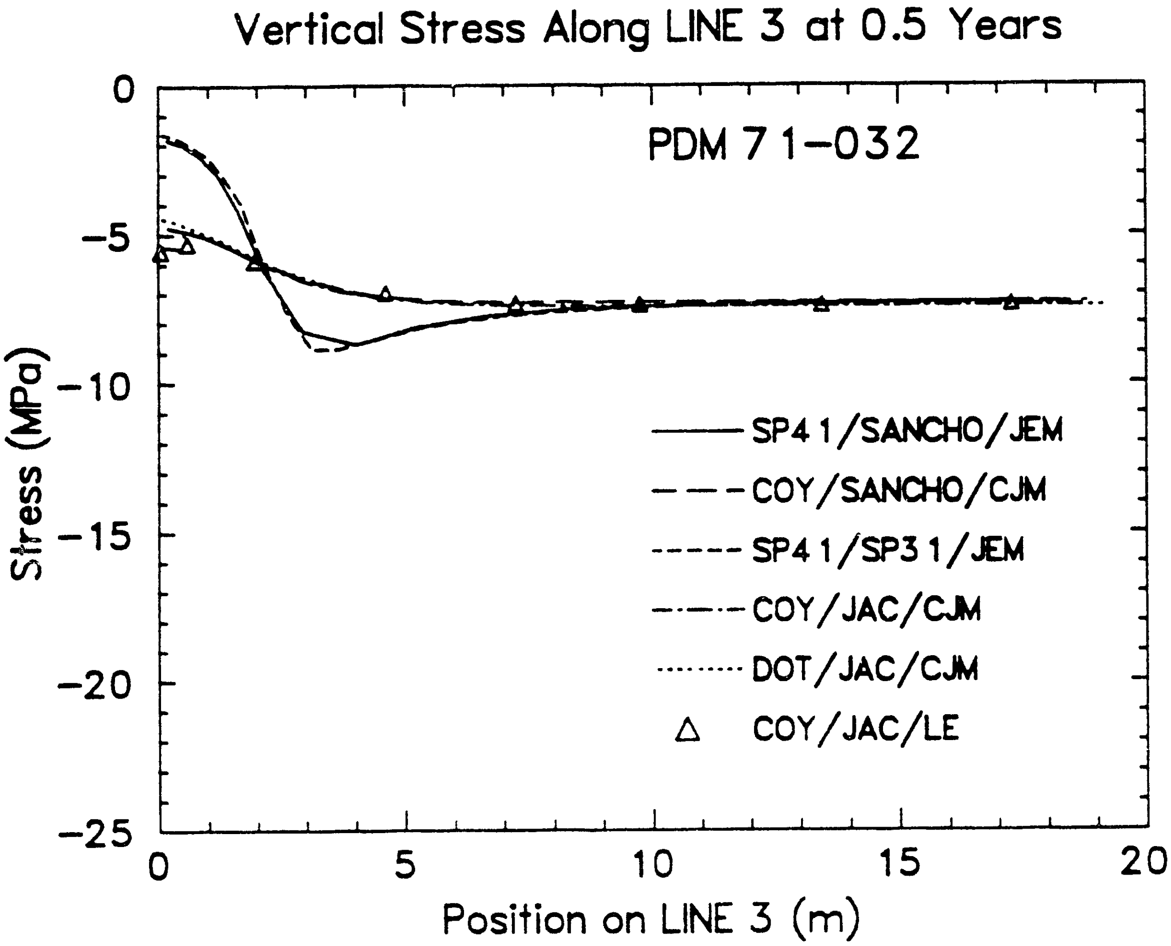

Figure 5-104. Comparison of Results for the Vertical Stress Along Line 3 (Figure 2-3) at 0.5 Yr, Second Analysis

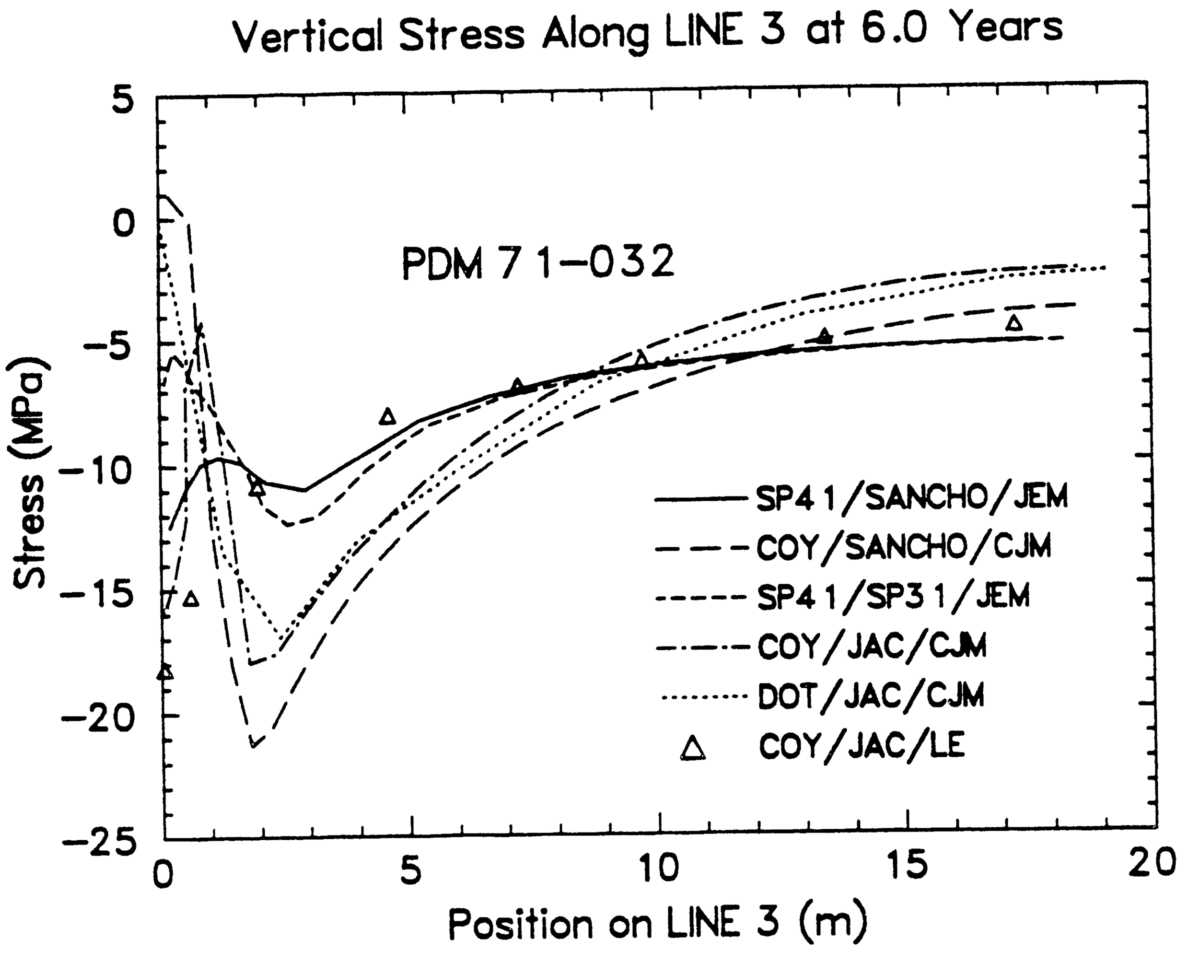

Figure 5-105. Comparison of Results for the Vertical Stress Along Line 3 (Figure 2-3) at 6 Yr, Second Analysis

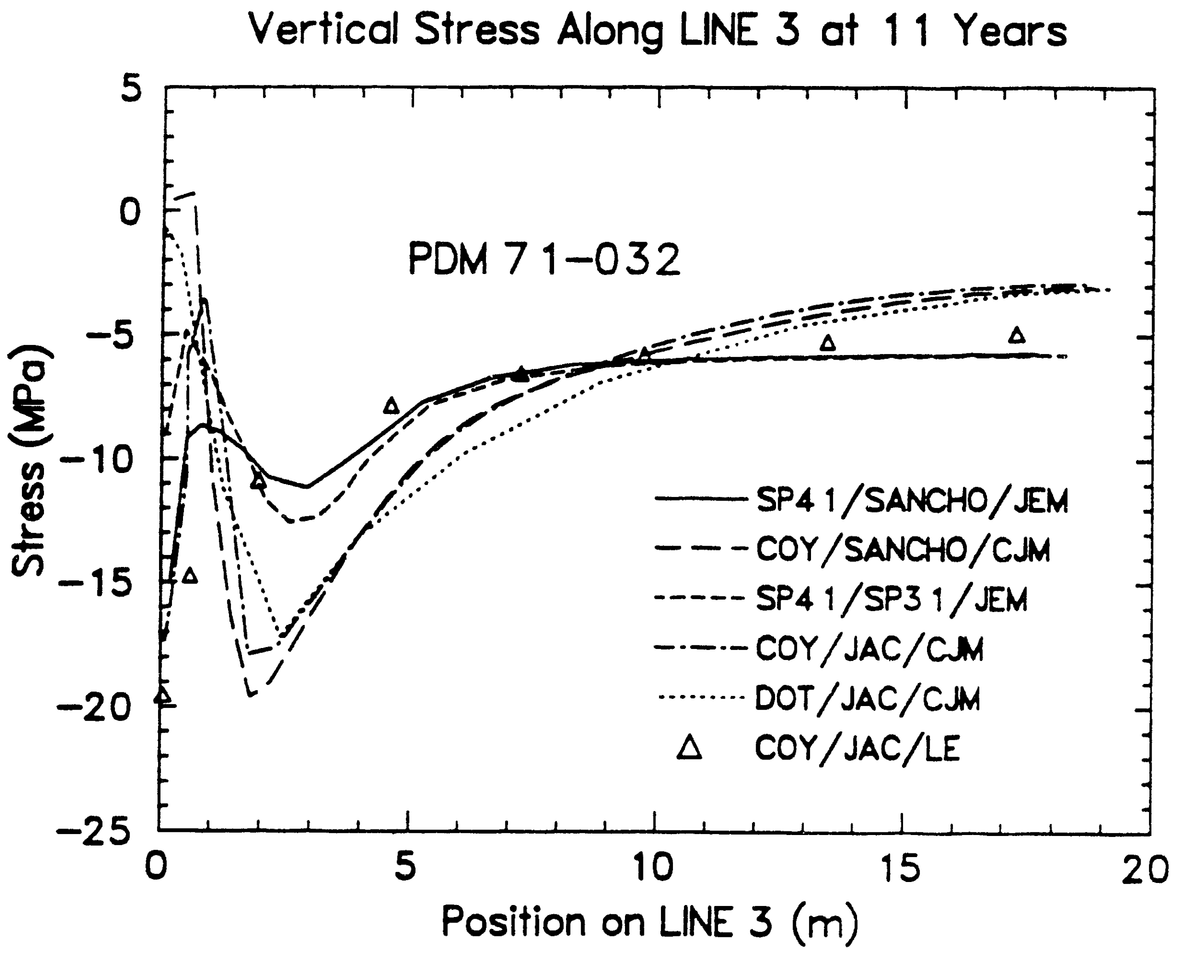

Figure 5-106. Comparison of Results for the Vertical Stress Along Line 3 (Figure 2-3) at 11 Yr, Second Analysis

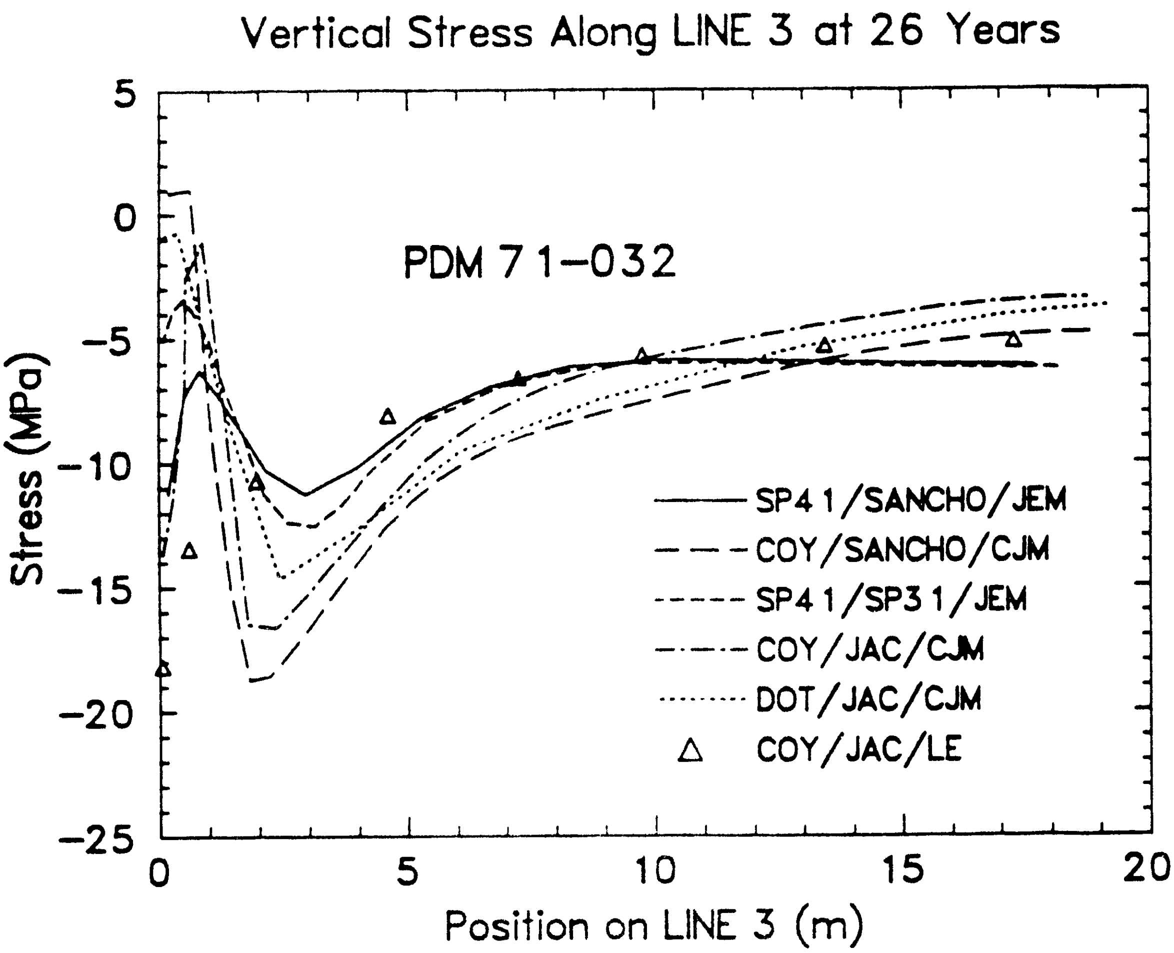

Figure 5-107. Comparison of Results for the Vertical Stress Along Line 3 (Figure 2-3) at 26 Yr, Second Analysis

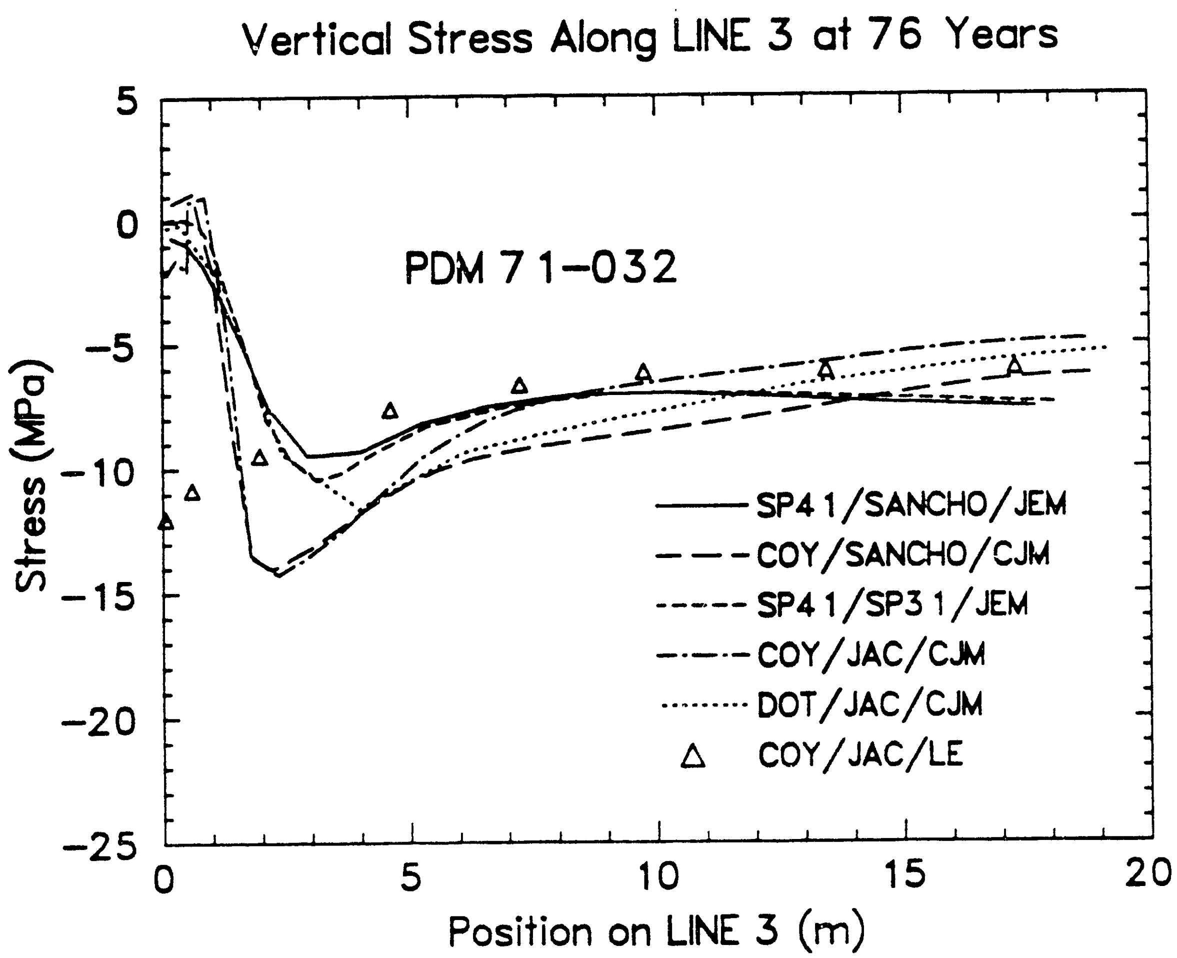

Figure 5-108. Comparison of Results for the Vertical Stress Along Line 3 (Figure 2-3) at 76 Yr, Second Analysis

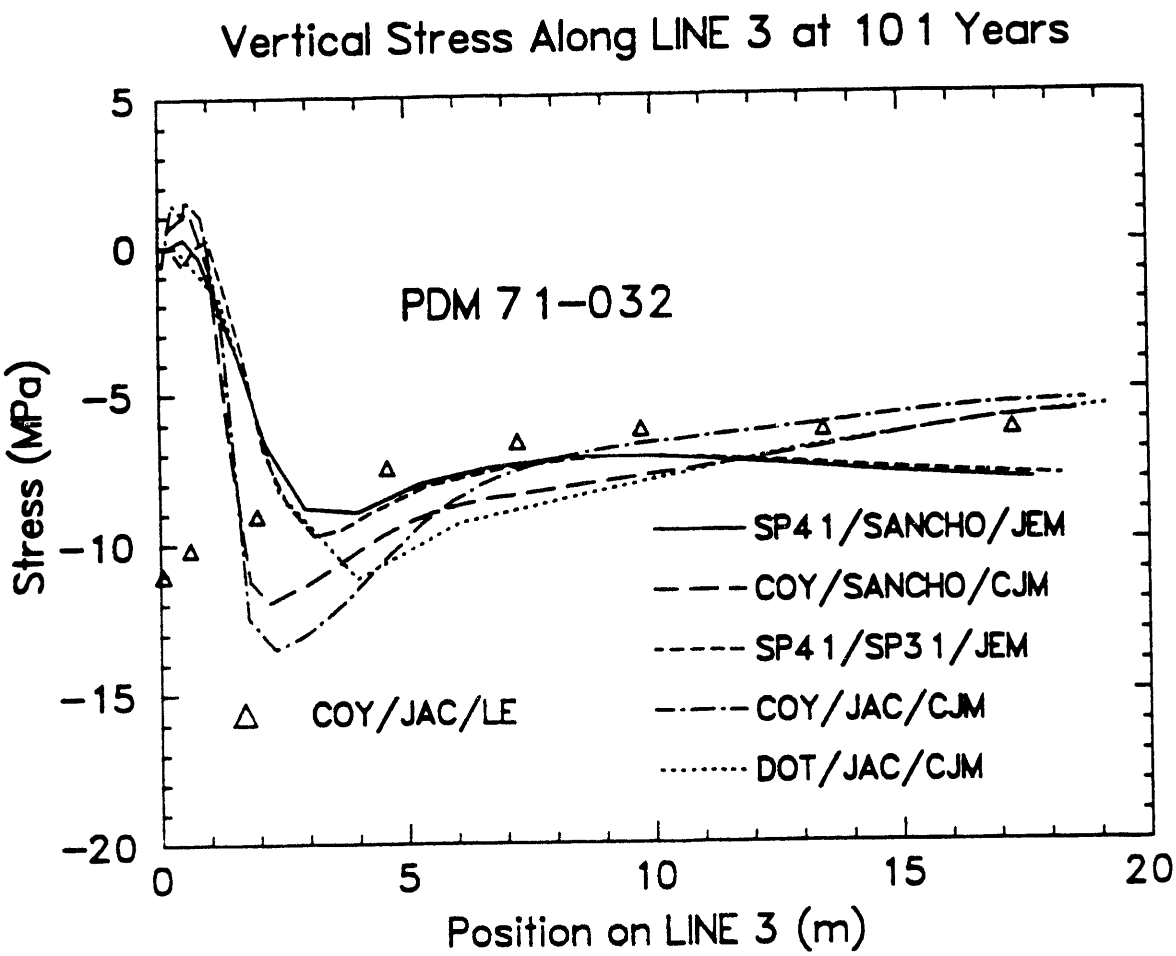

Figure 5-109. Comparison of Results for the Vertical Stress Along Line 3 (Figure 2-3) at 101 Yr, Second Analysis

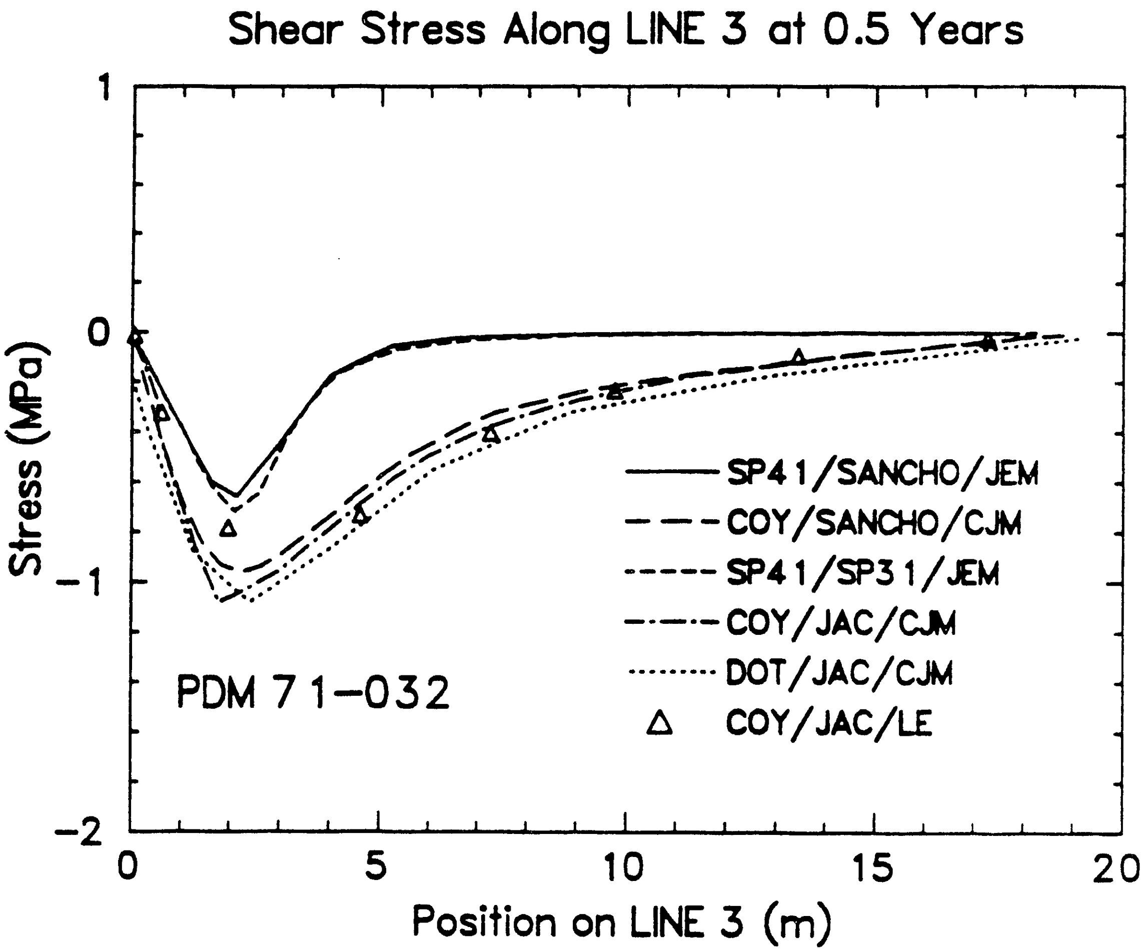

Figure 5-110. Comparison of Results for the Shear Stress Along Line 3 (Figure 2-3) at 0.5 Yr, Second Analysis

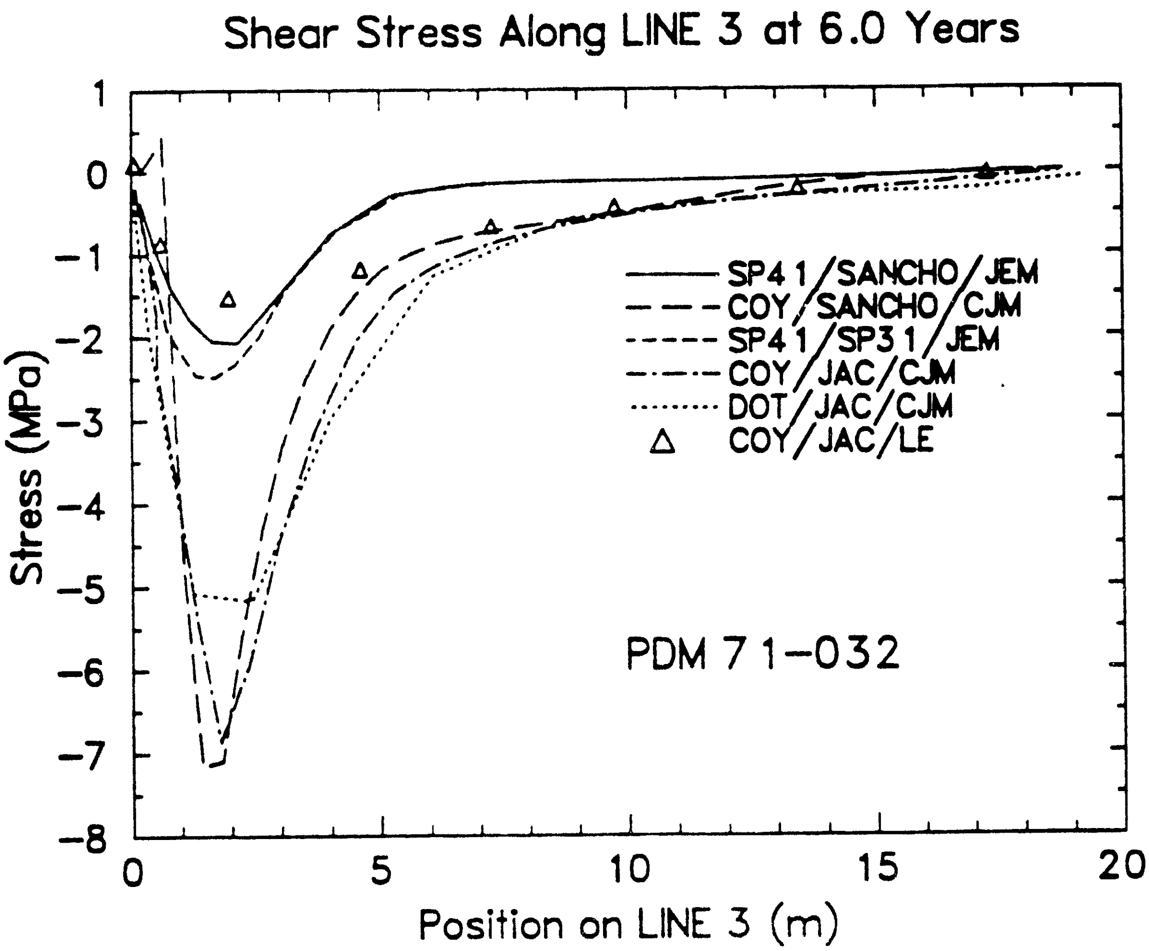

Figure 5-111. Comparison of Results for the Shear Stress Along Line 3 (Figure 2-3) at 6 Yr, Second Analysis

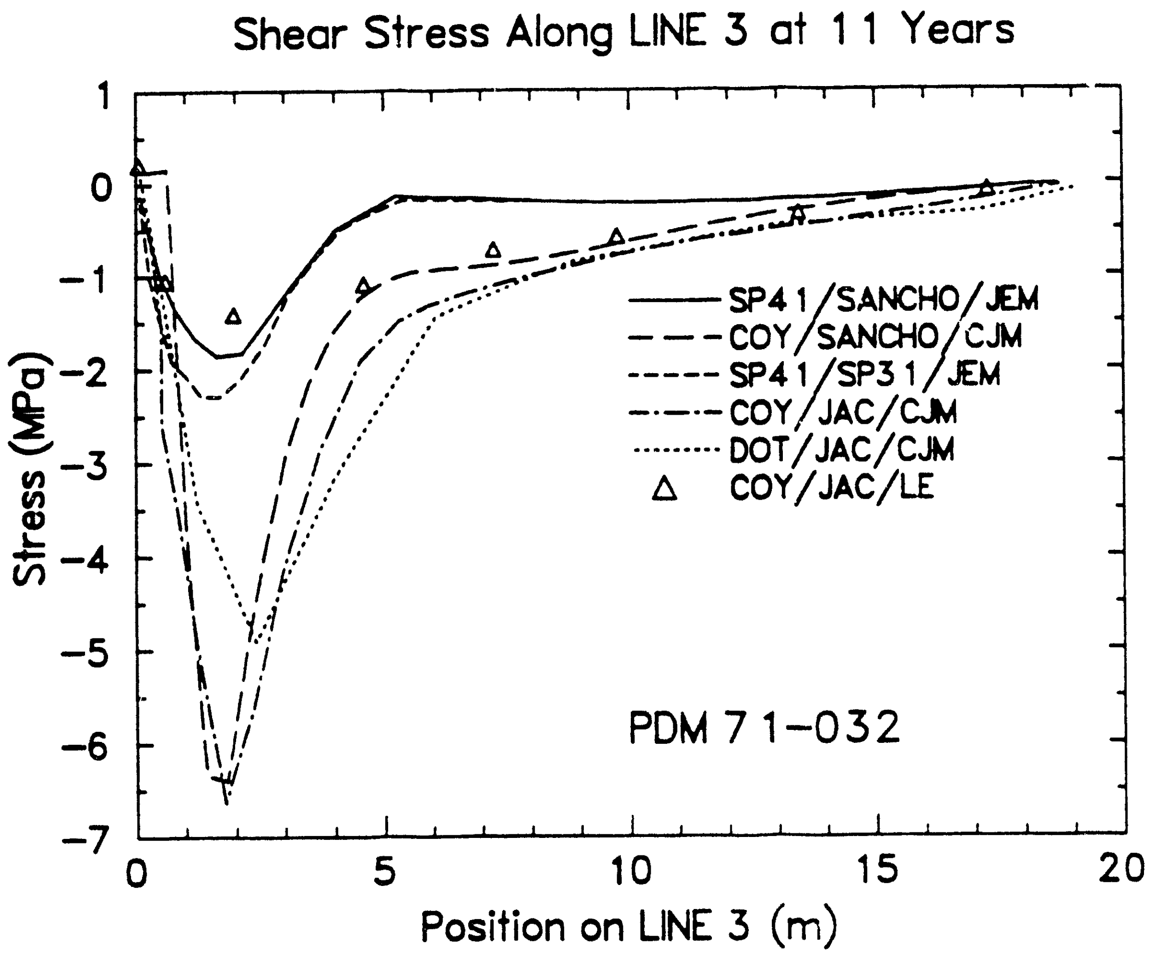

Figure 5-112. Comparison of Results for the Shear Stress Along Line 3 (Figure 2-3) at 11 Yr, Second Analysis

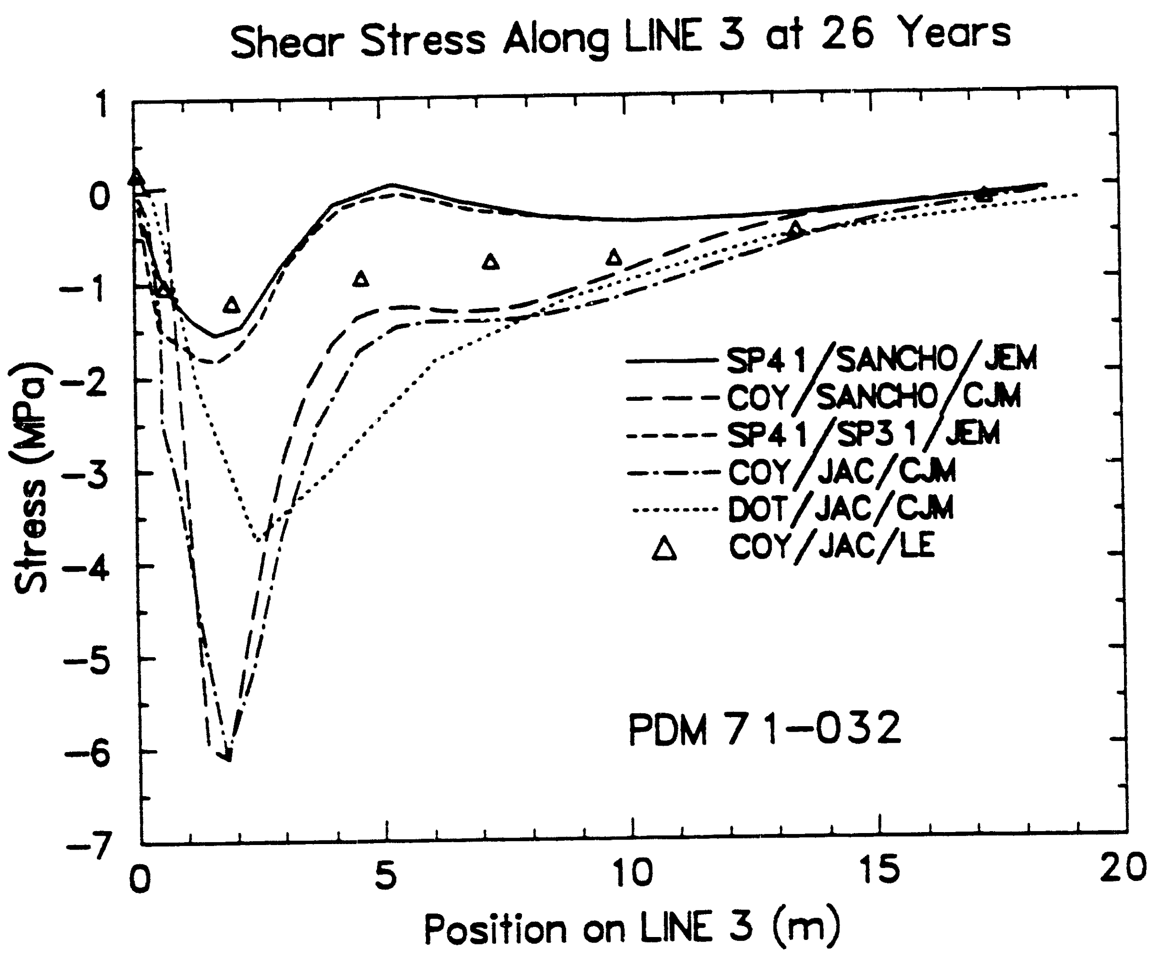

Figure 5-113. Comparison of Results for the Shear Stress Along Line 3 (Figure 2-3) at 26 Yr, Second Analysis

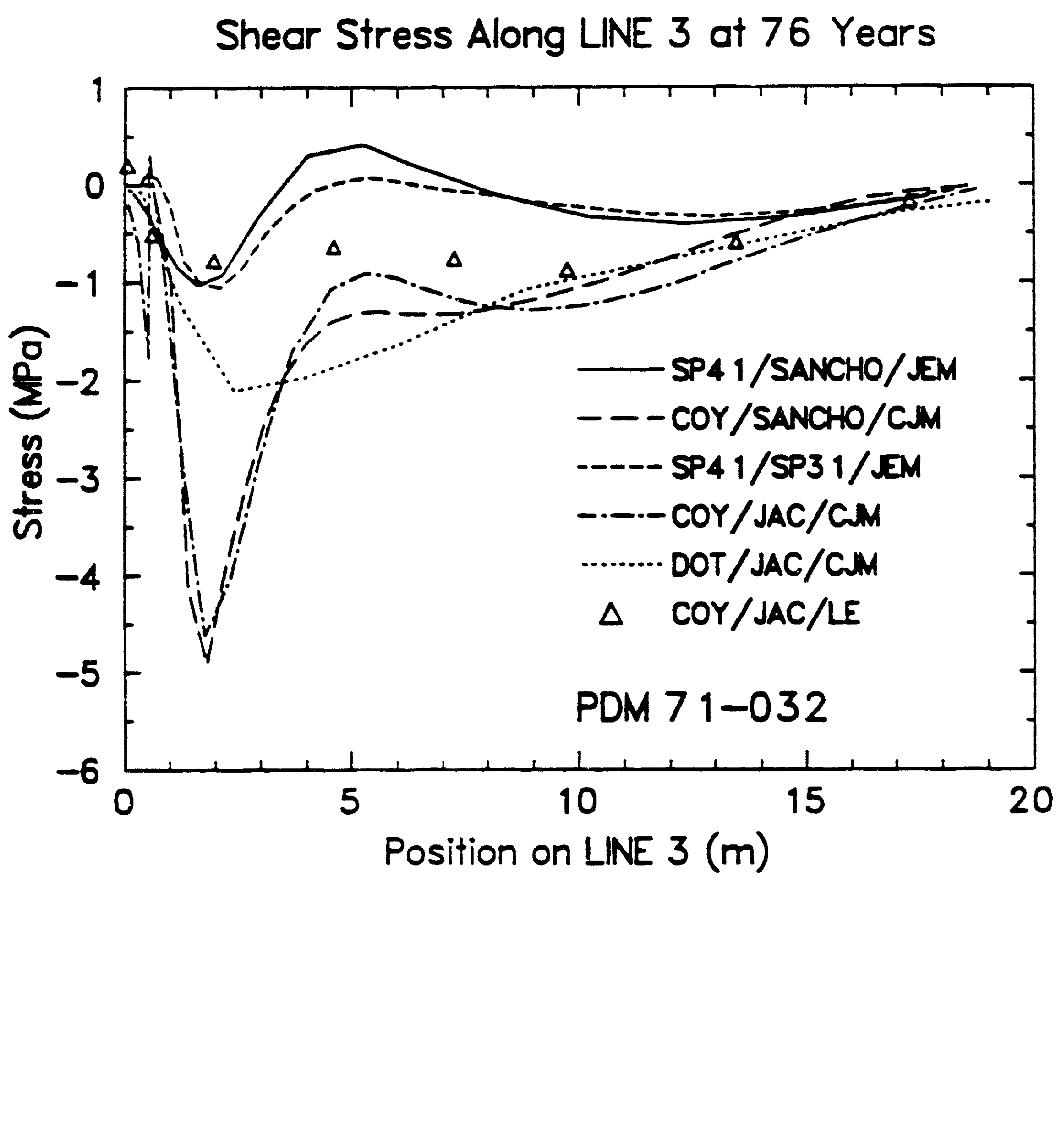

Figure 5-114. Comparison of Results for the Shear Stress Along Line 3 (Figure 2-3) at 76 Yr, Second Analysis

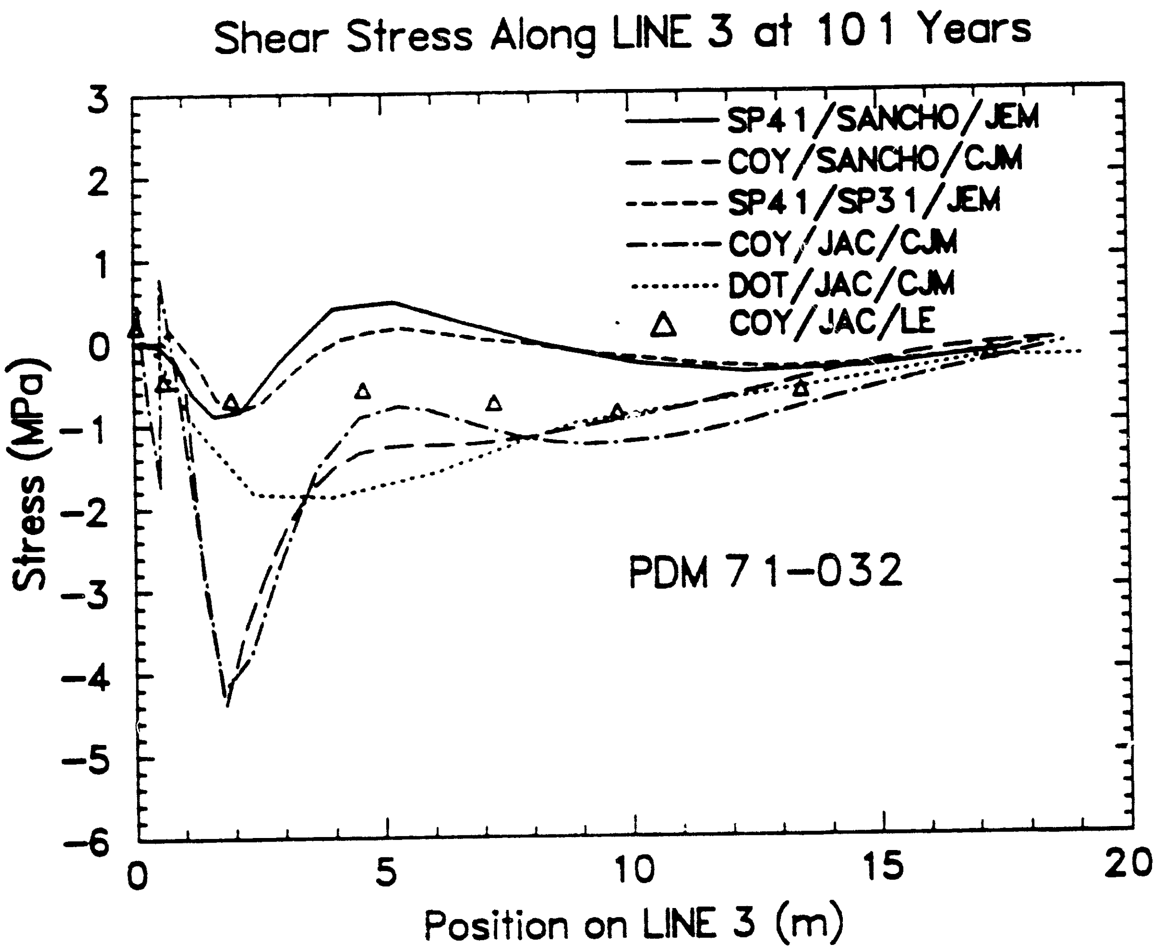

Figure 5-115. Comparison of Results for the Shear Stress Along Line 3 (Figure 2-3) at 101 Yr, Second Analysis

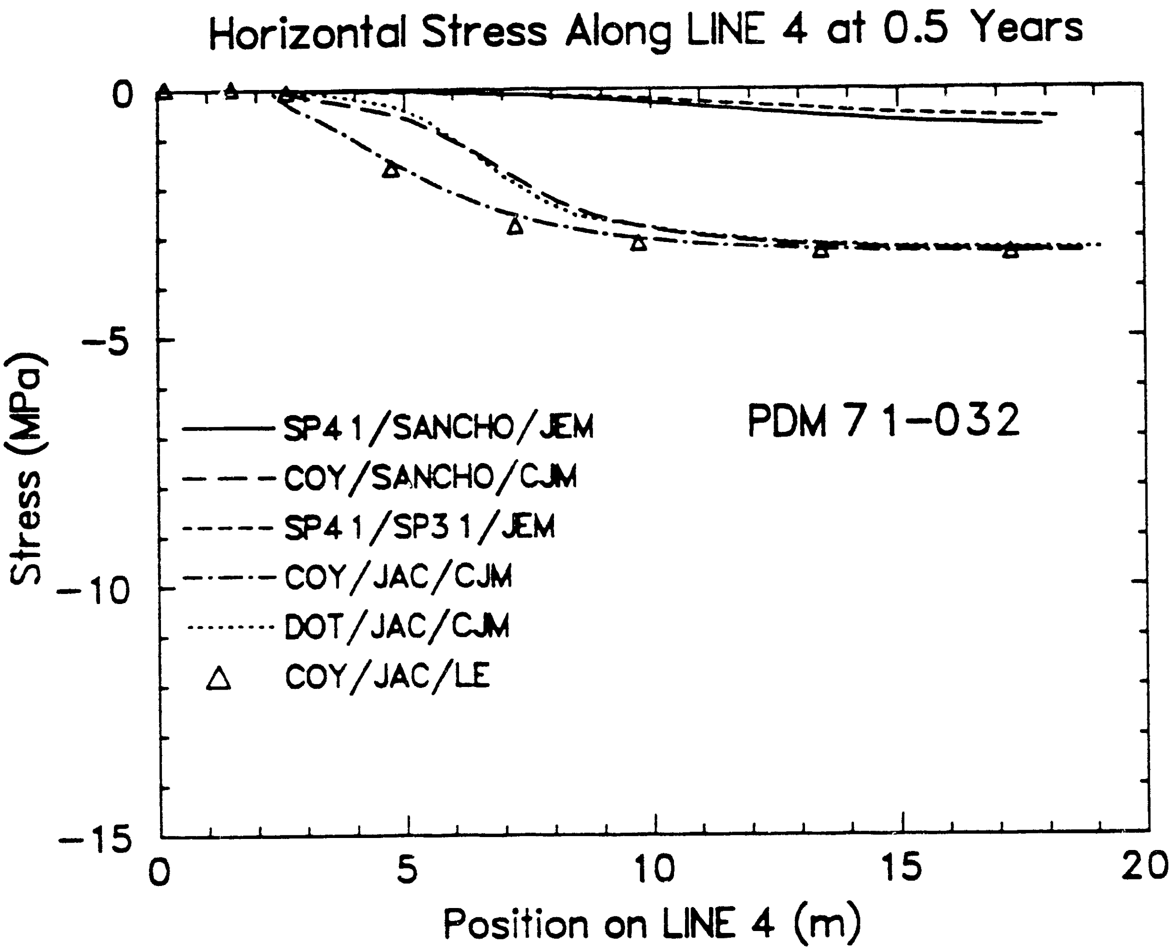

Figure 5-116. Comparison of Results for the Horizontal Stress Along Line 4 (Figure 2-3) at 0.5 Yr, Second Analysis

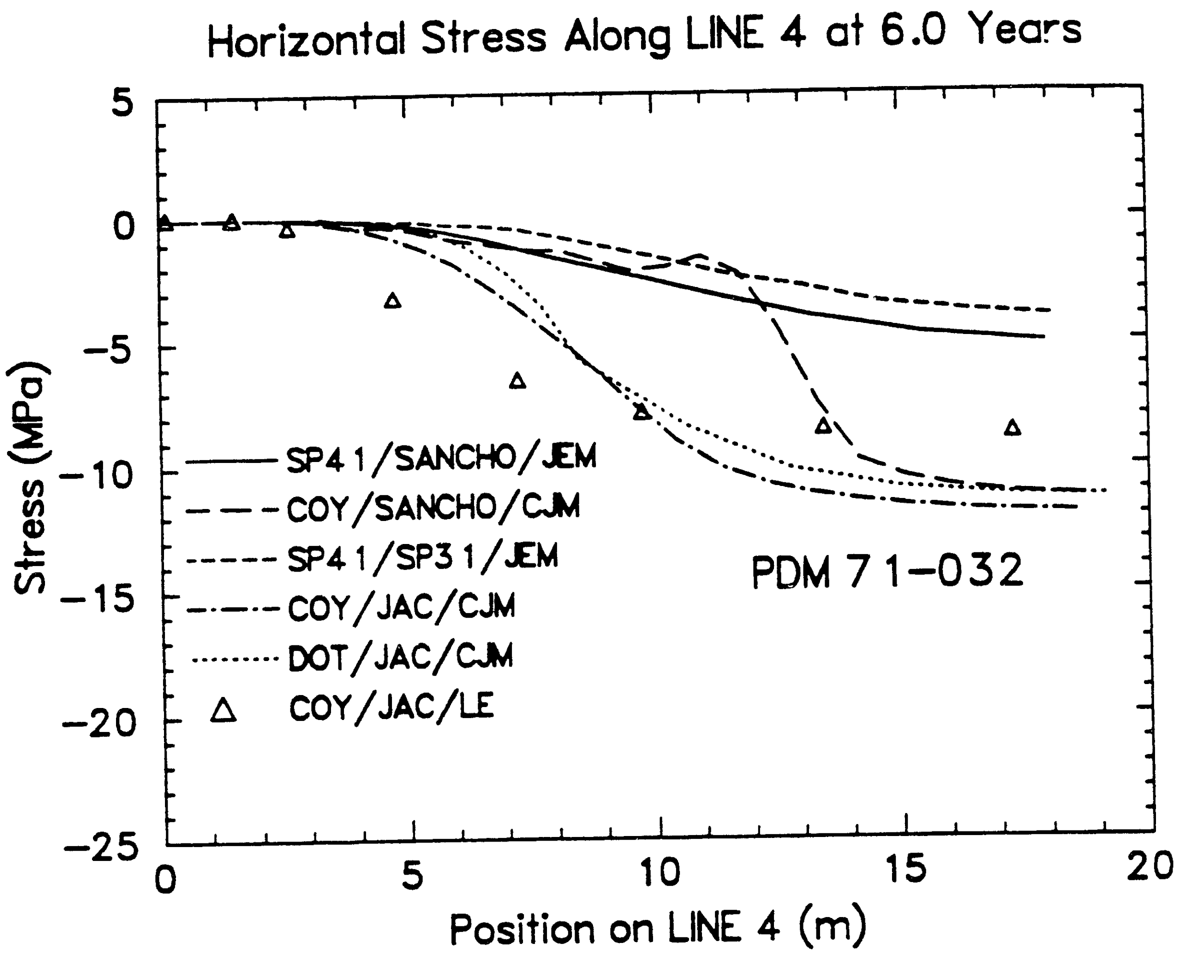

Figure 5-117. Comparison of Results for the Horizontal Stress Along Line 4 (Figure 2-3) at 6 Yr, Second Analysis

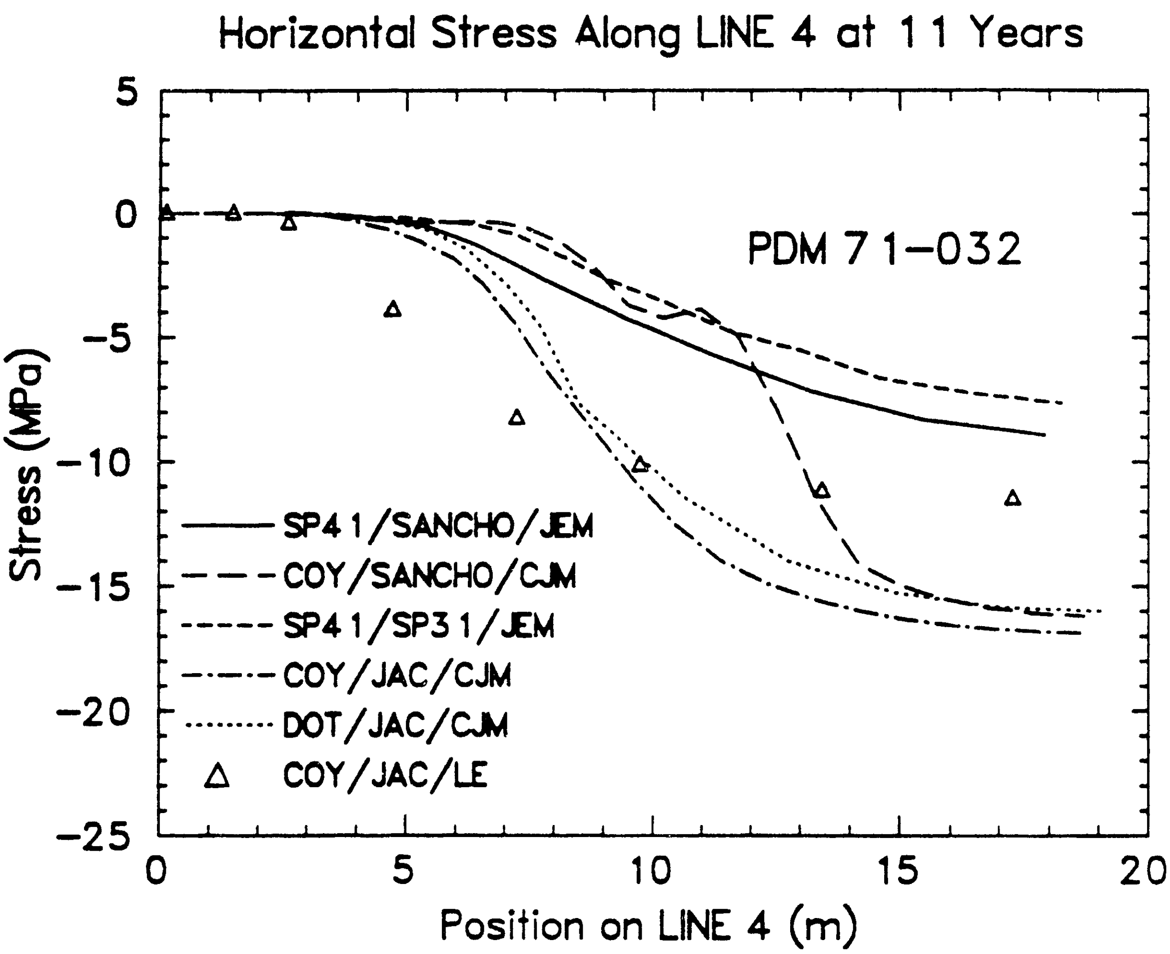

Figure 5-118. Comparison of Results for the Horizontal Stress Along Line 4 (Figure 2-3) at 11 Yr, Second Analysis

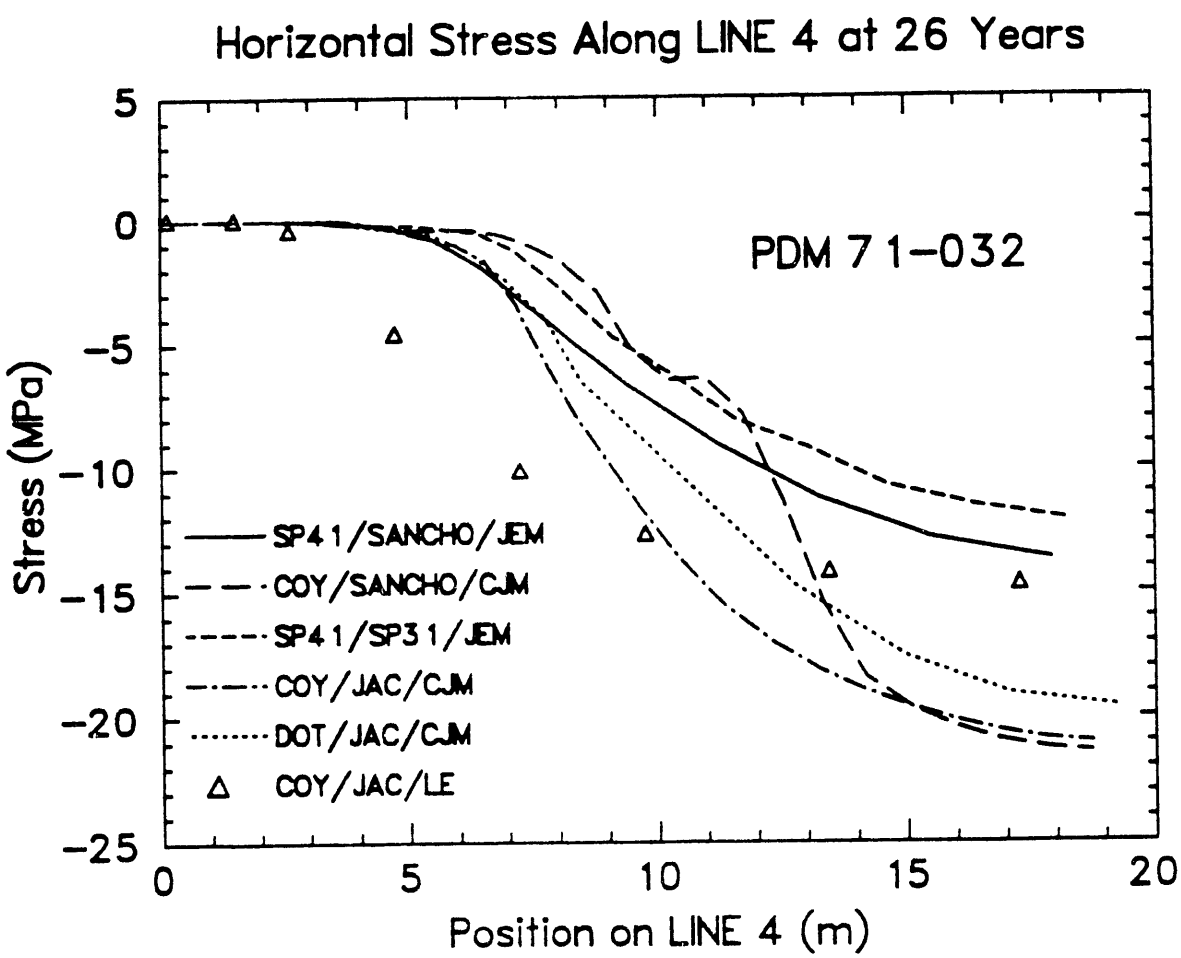

Figure 5-119. Comparison of Results for the Horizontal Stress Along Line 4 (Figure 2-3) at 26 Yr, Second Analysis

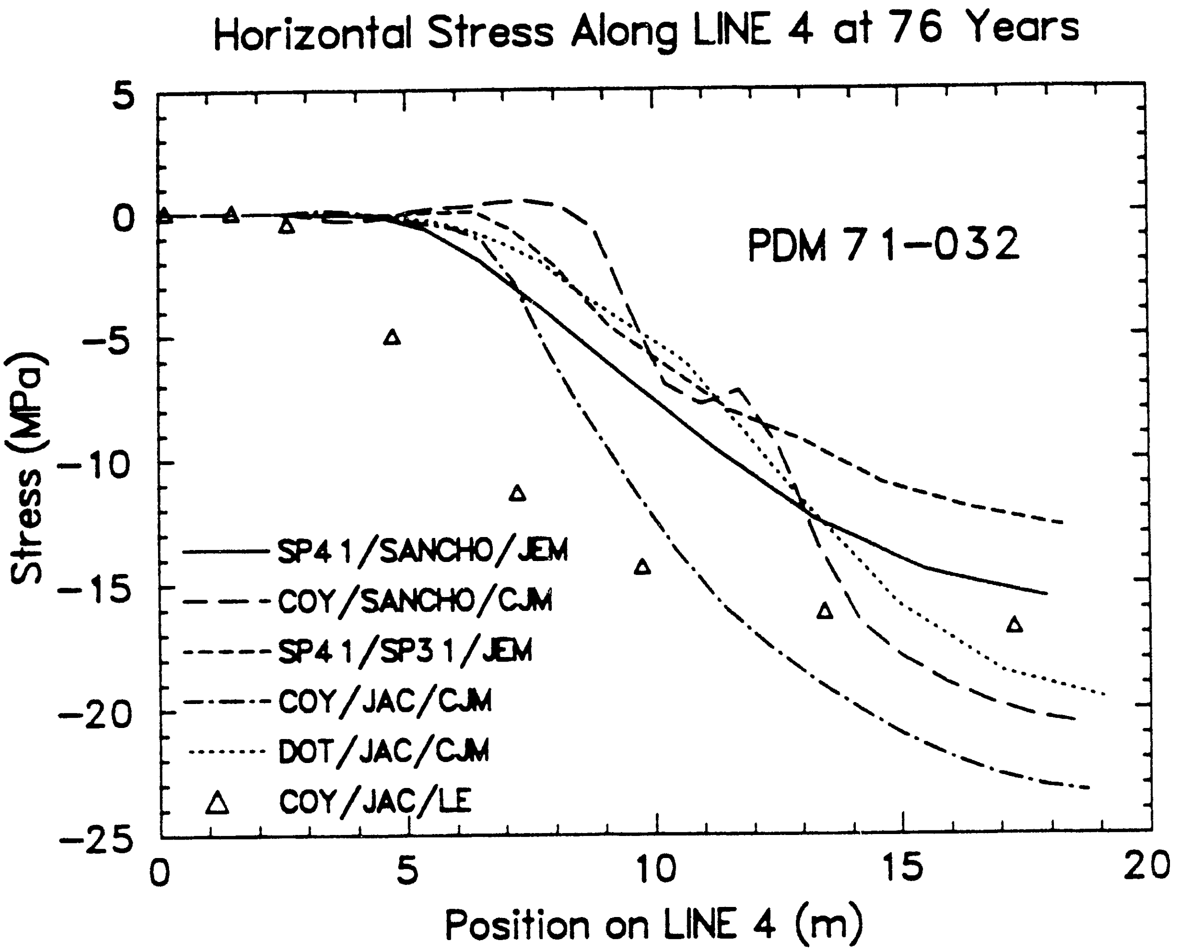

Figure 5-120. Comparison of Results for the Horizontal Stress Along Line 4 (Figure 2-3) at 76 Yr, Second Analysis

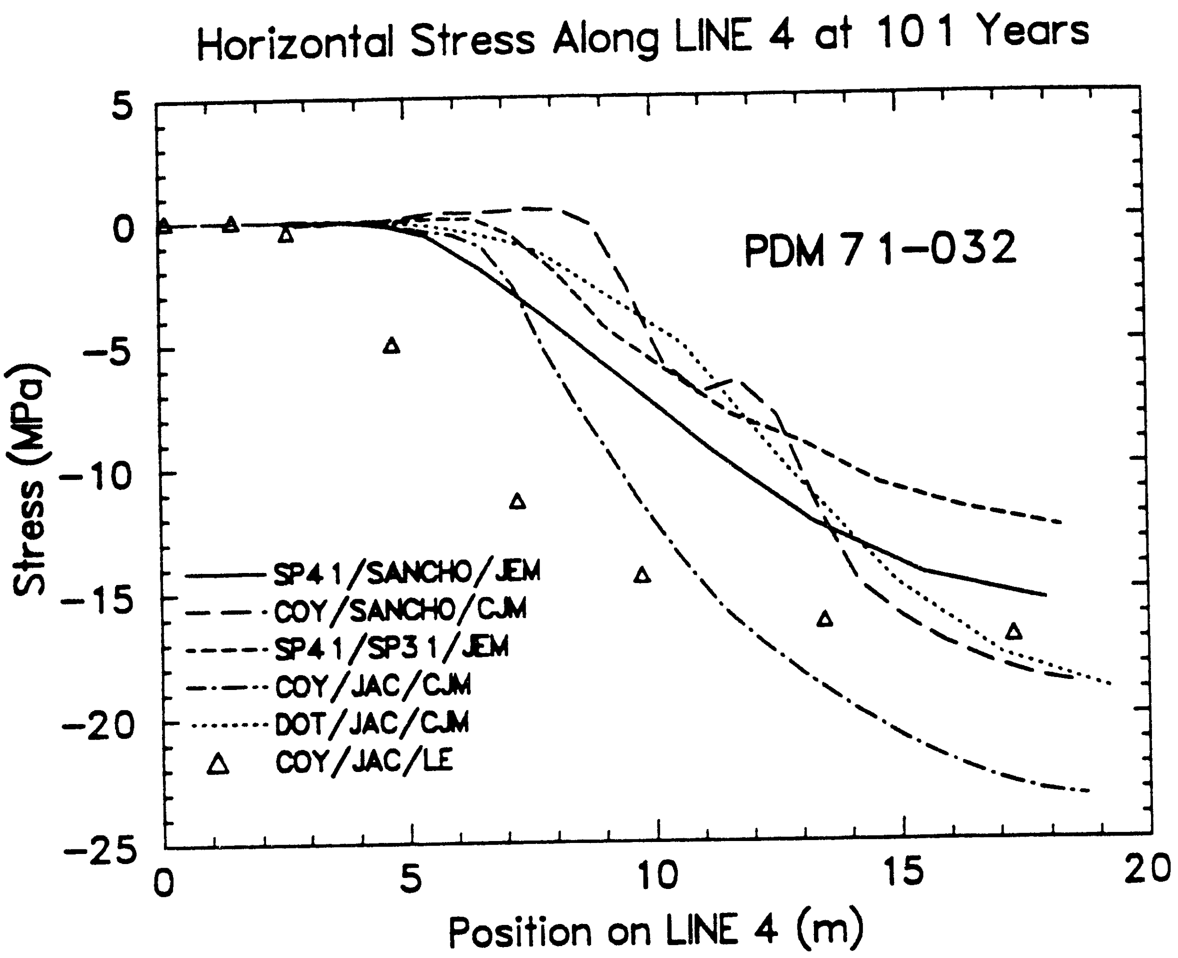

Figure 5-121. Comparison of Results for the Horizontal Stress Along Line 4 (Figure 2-3) at 101 Yr, Second Analysis

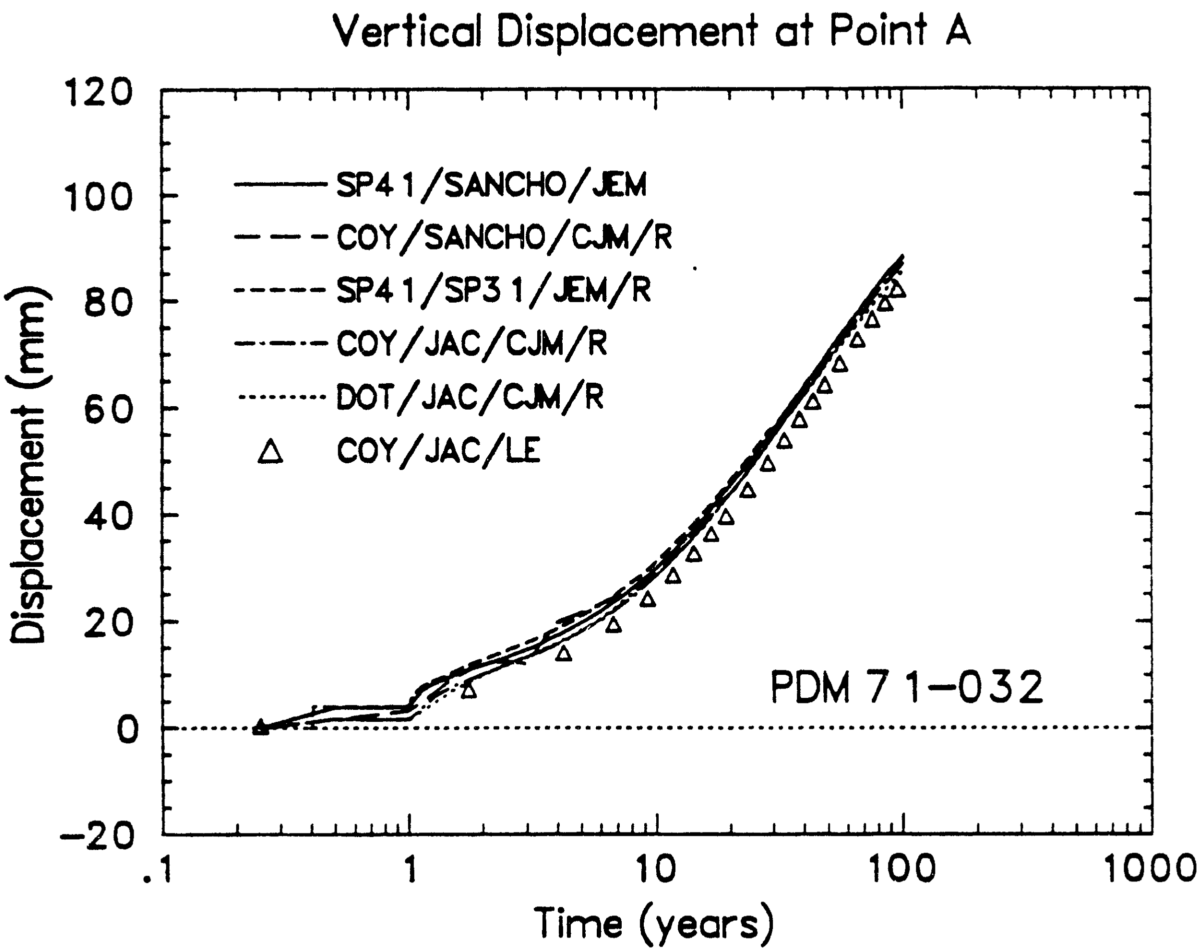

Figure 5-122. Comparison of Results for the Vertical Displacement History (Figure 2-3) at Point A, Third Analysis

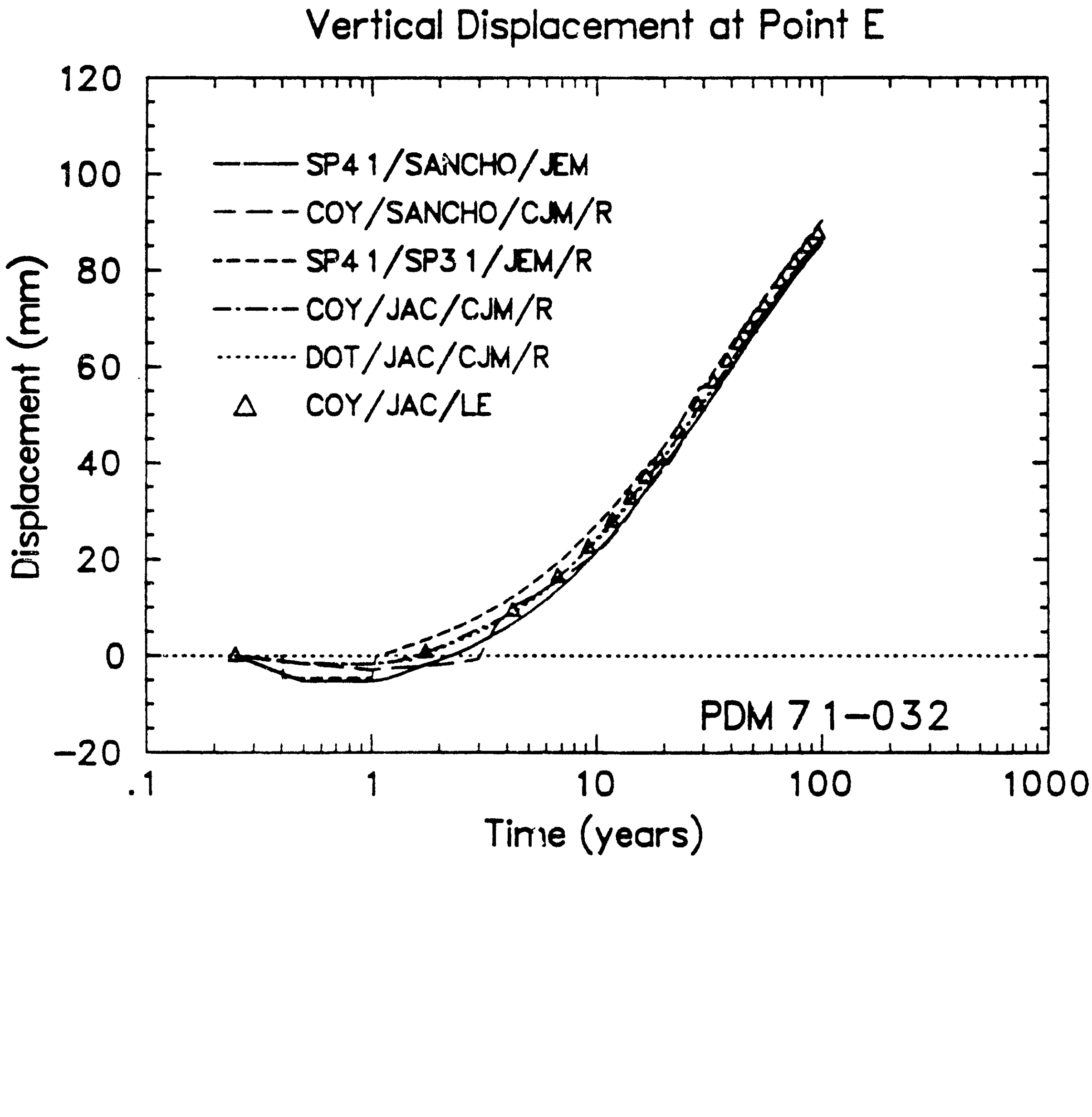

Figure 5-123. Comparison of Results for the Vertical Displacement History (Figure 2-3) at Point E, Third Analysis

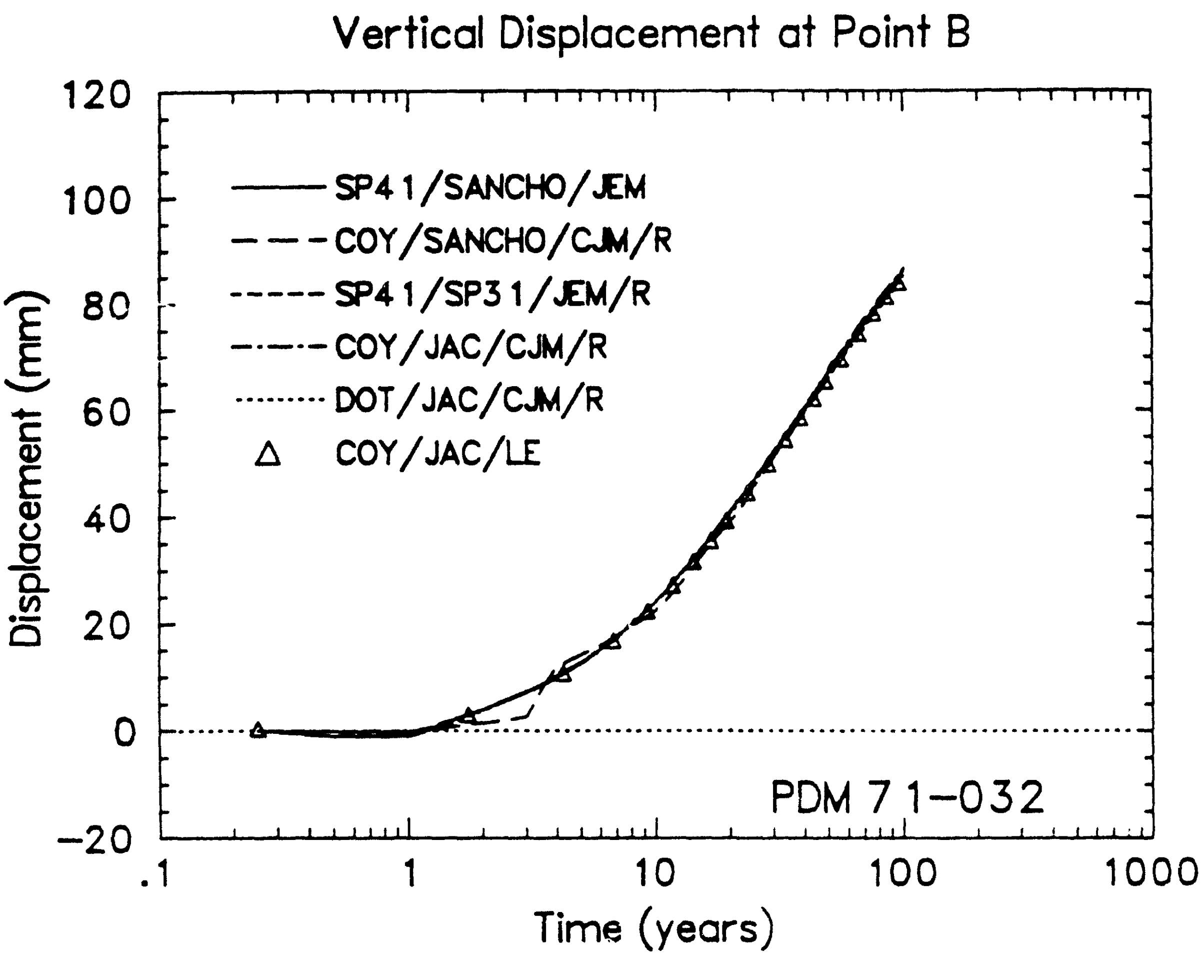

Figure 5-124. Comparison of Results for the Vertical Displacement History (Figure 2-3) at Point B, Third Analysis

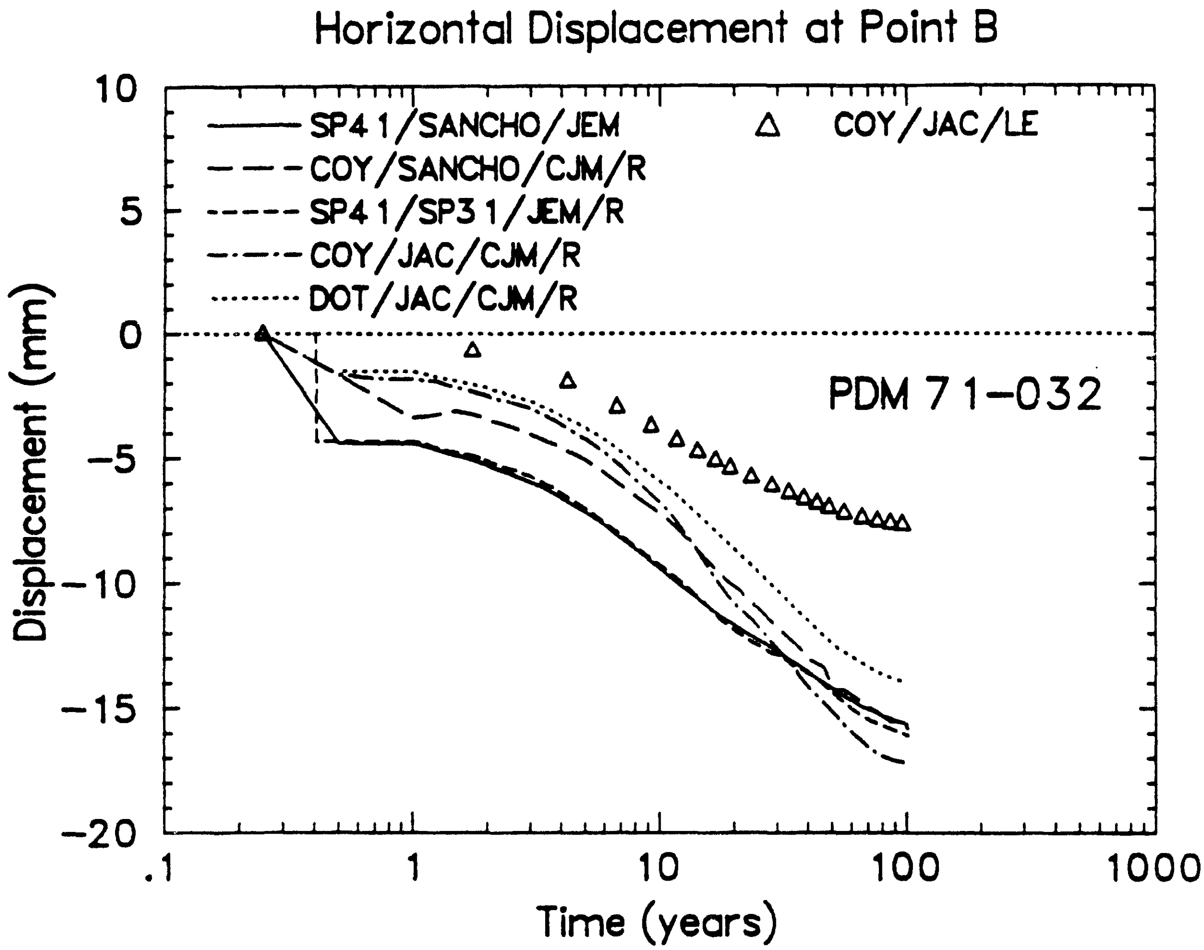

Figure 5-125. Comparison of Results for the Horizontal Displacement History (Figure 2-3) at Point B, Third Analysis

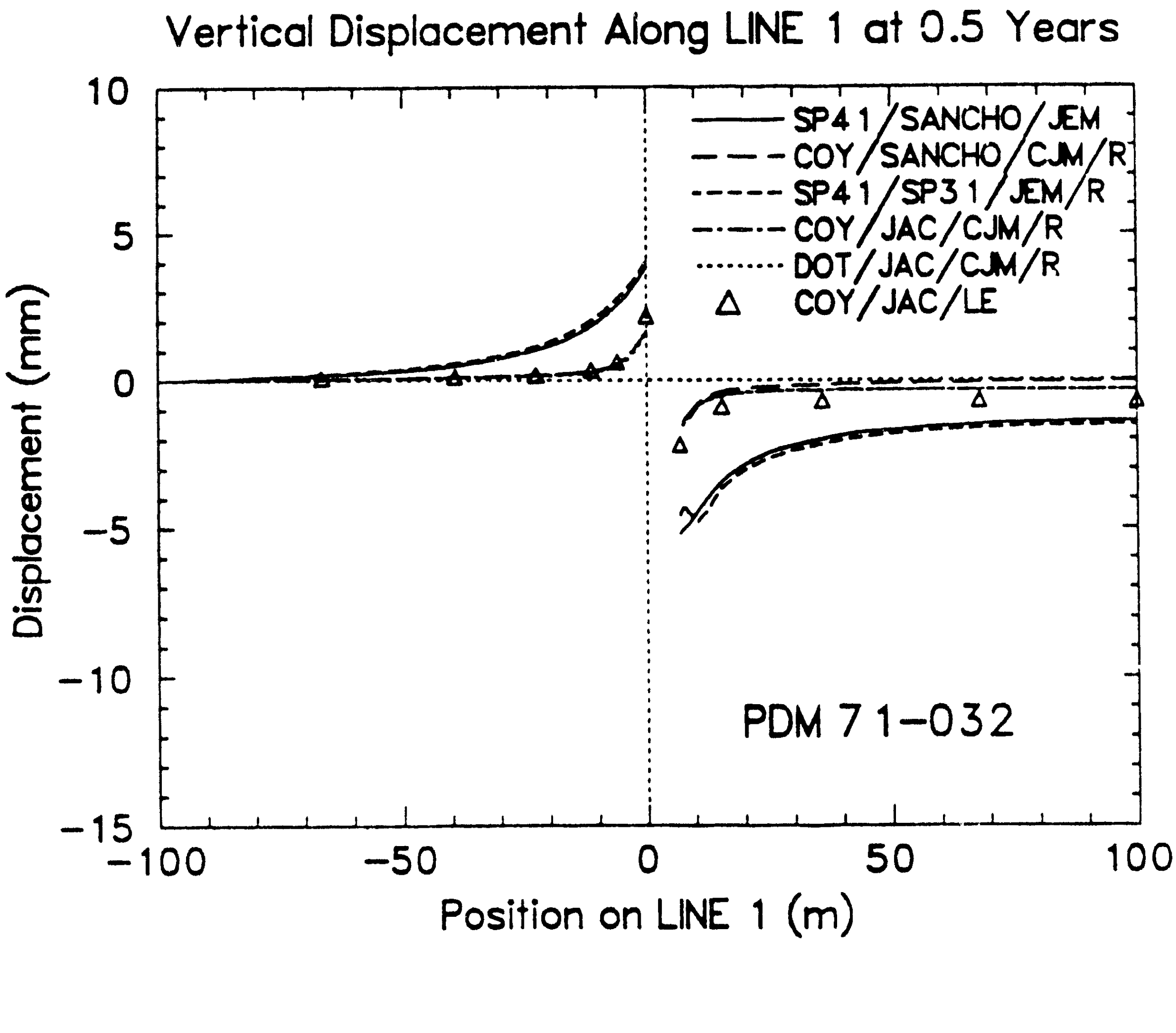

Figure 5-126. Comparison of Results for the Vertical Displacement Along Line 1 (Figure 2-3) at 0.5 Yr, Third Analysis

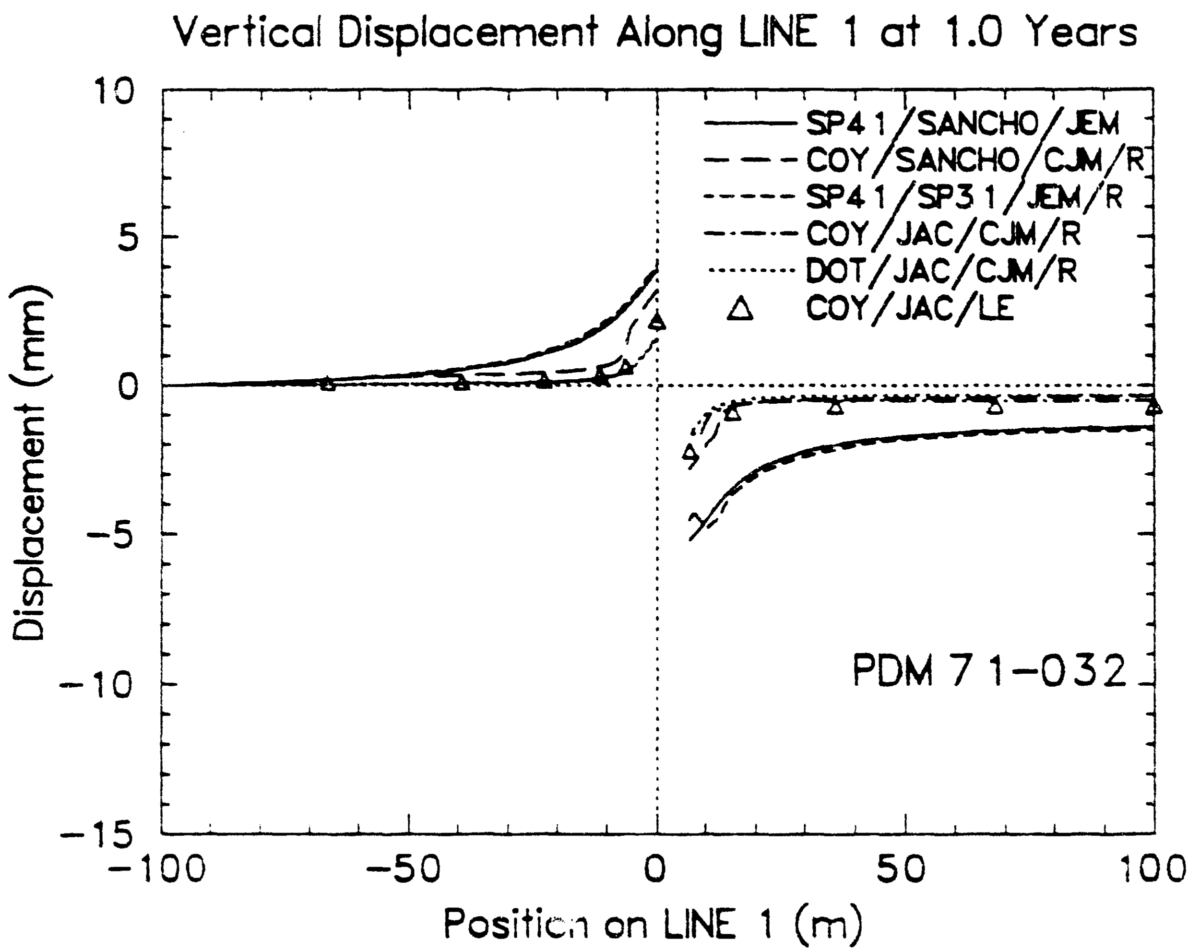

Figure 5-127. Comparison of Results for the Vertical Displacement Along Line 1 (Figure 2-3) at 1 Yr, Third Analysis

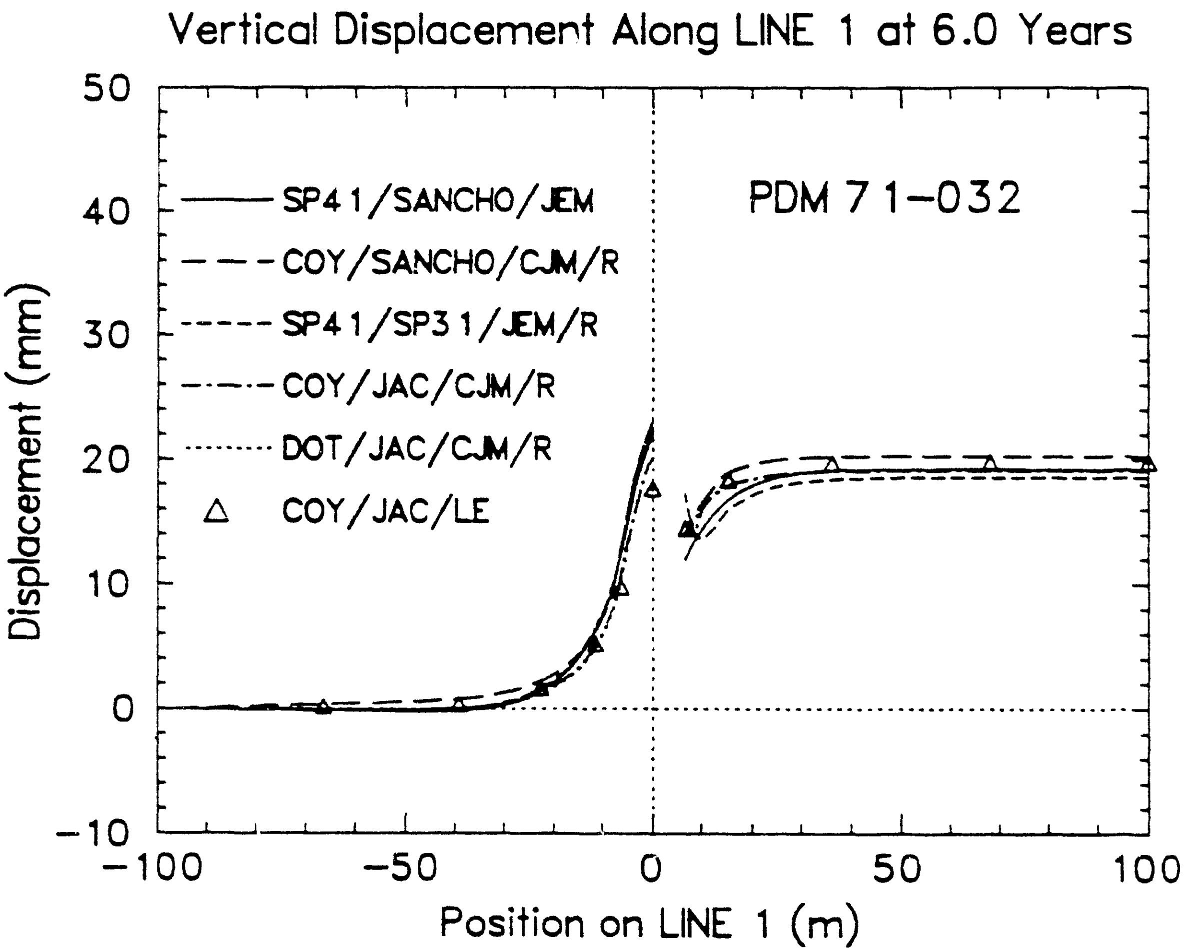

Figure 5-128. Comparison of Results for the Vertical Displacement Along Line 1 (Figure 2-3) at 6 Yr, Third Analysis

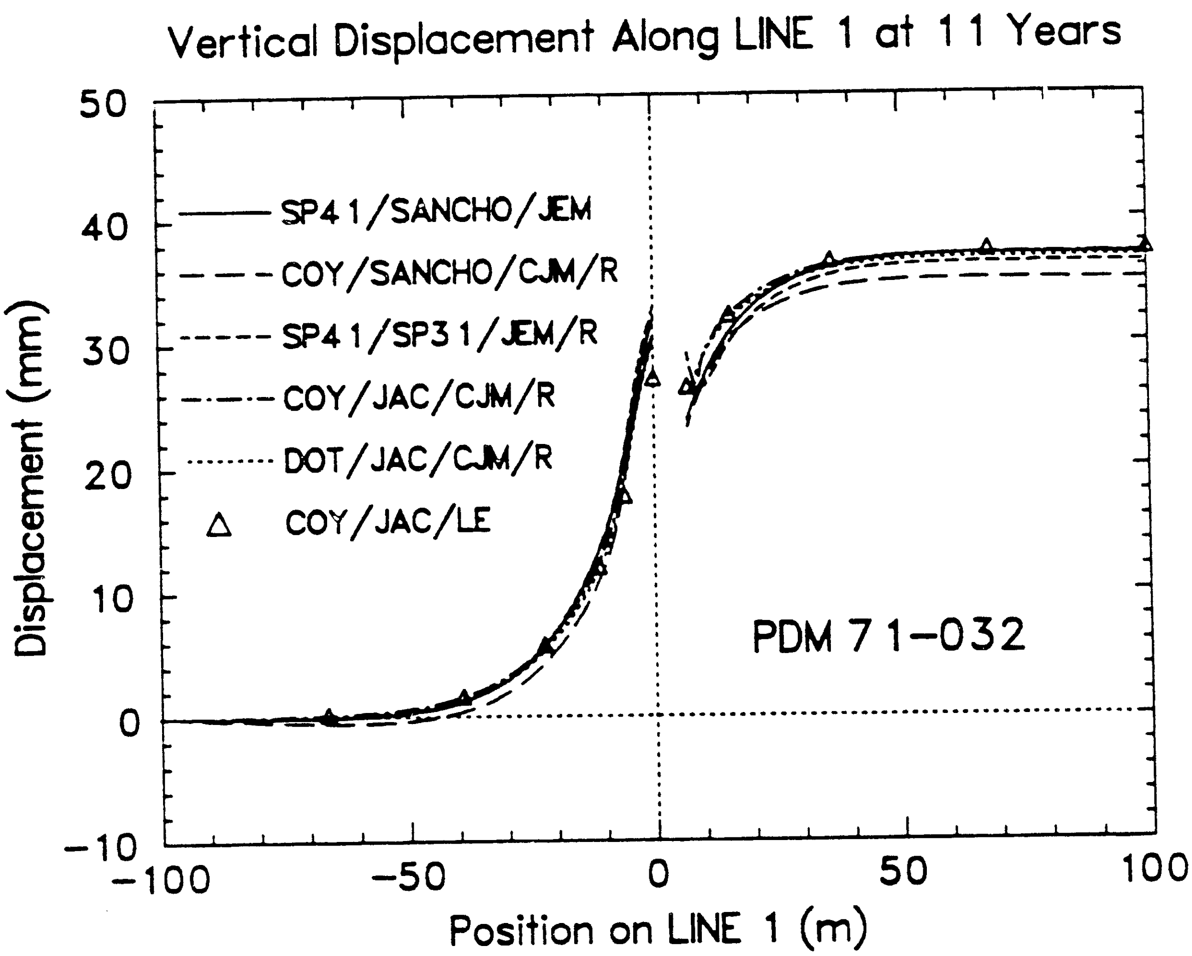

Figure 5-129. Comparison of Results for the Vertical Displacement Along Line 1 (Figure 2-3) at 11 Yr, Third Analysis

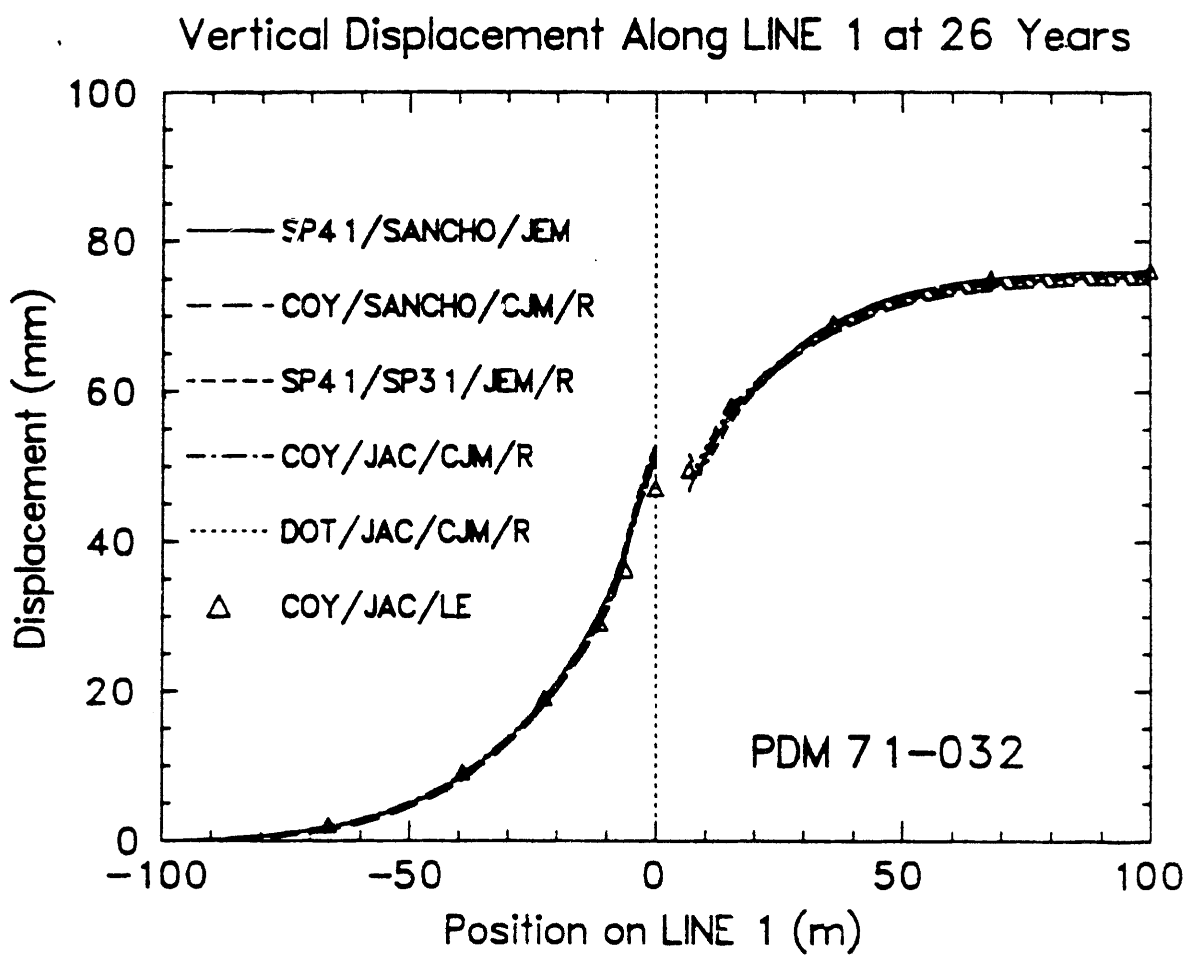

Figure 5-130. Comparison of Results for the Vertical Displacement Along Line 1 (Figure 2-3) at 26 Yr, Third Analysis

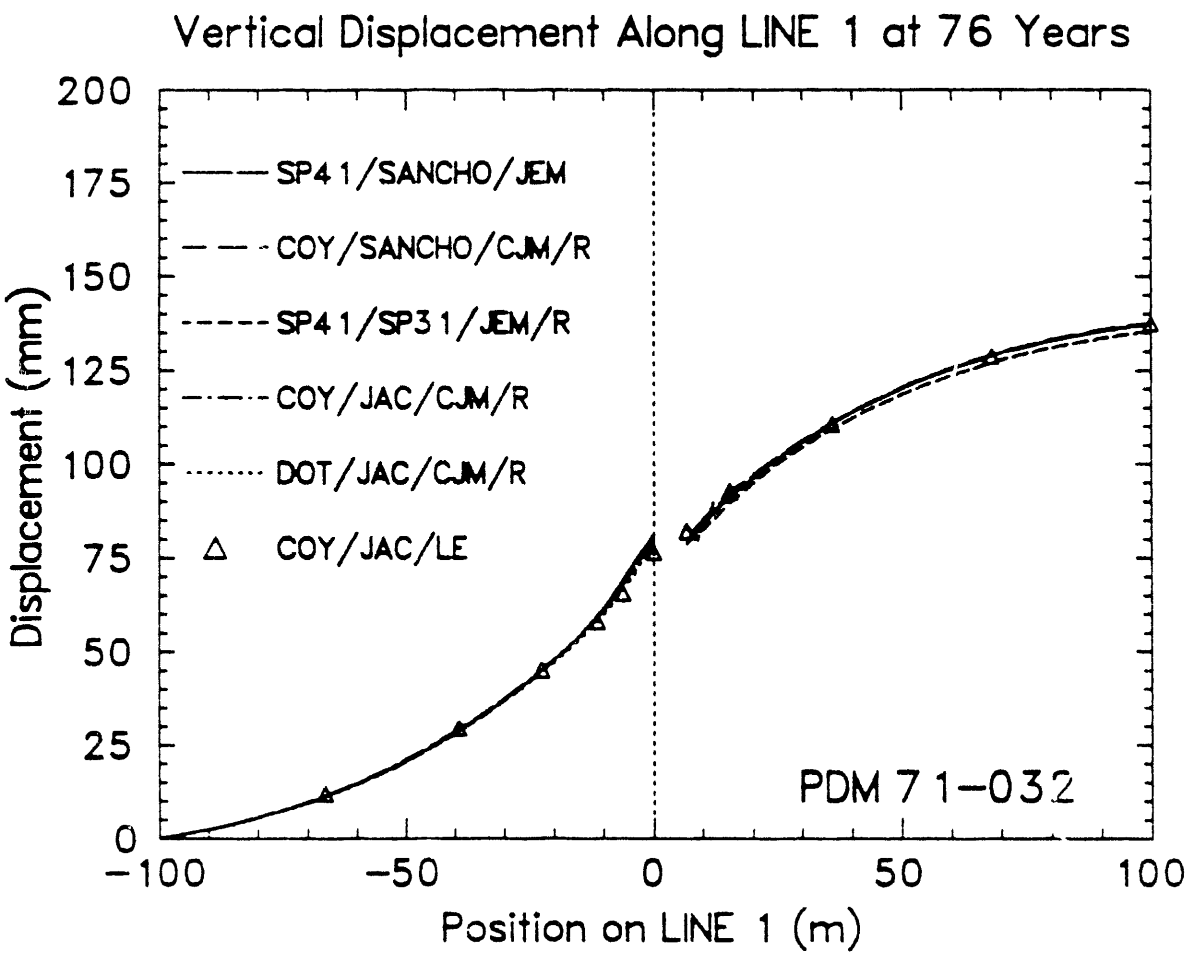

Figure 5-131. Comparison of Results for the Vertical Displacement Along Line 1 (Figure 2-3) at 76 Yr, Third Analysis

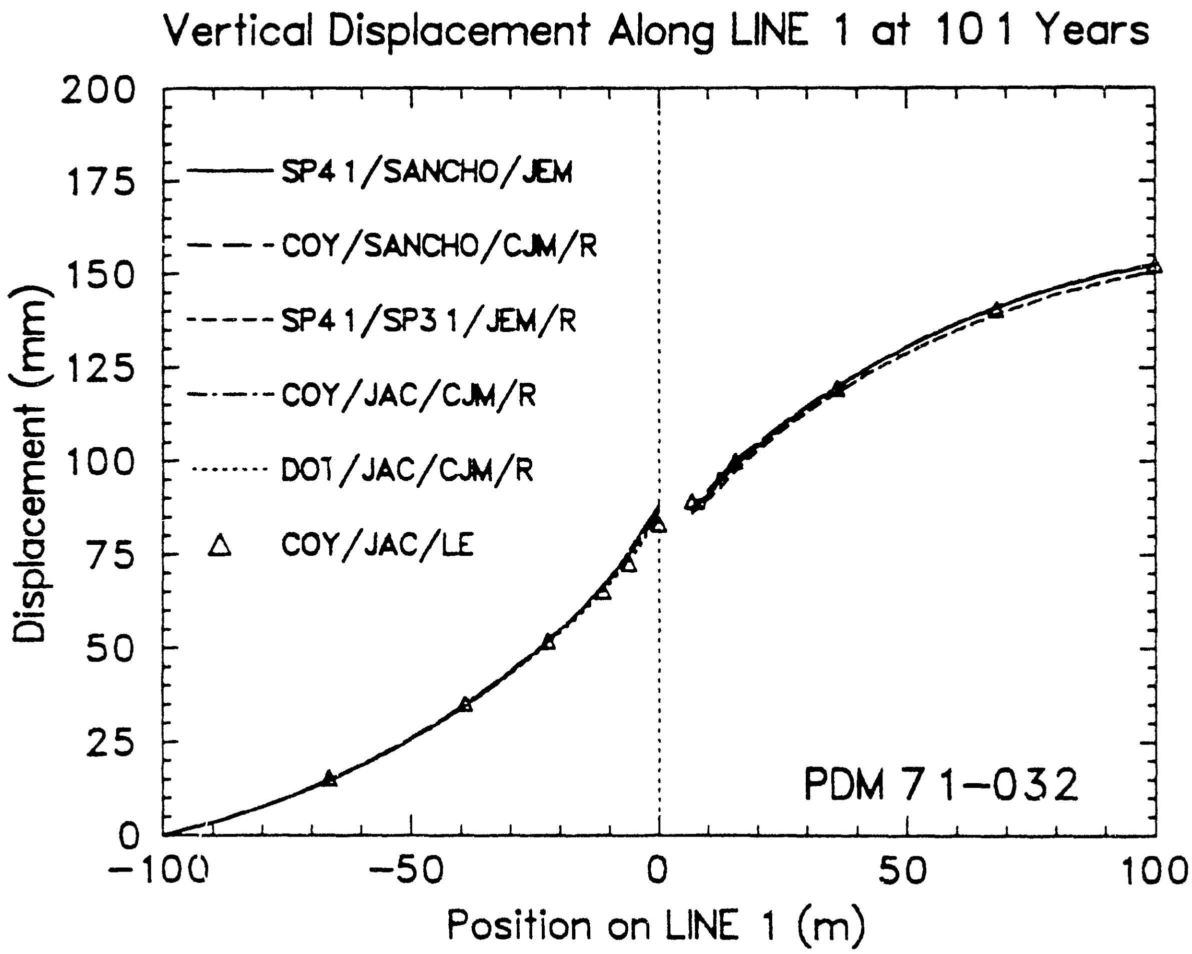

Figure 5-132. Comparison of Results for the Vertical Displacement Along Line 1 (Figure 2-3) at 101 Yr, Third Analysis

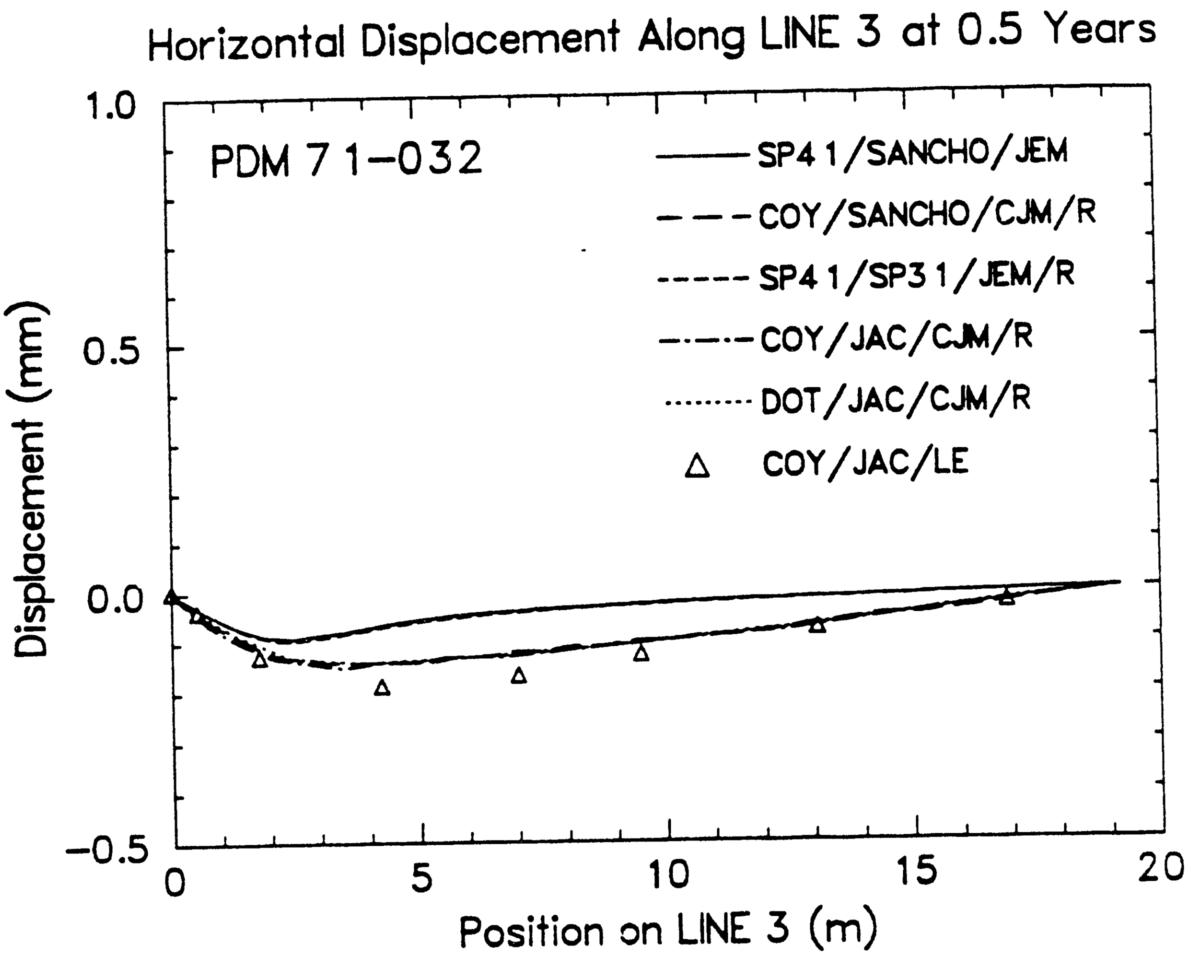

Figure 5-133 Comparison of Results for the Horizontal Displacement Along Line 3 (Figure 2-3) at 0.5 Yr, Third Analysis

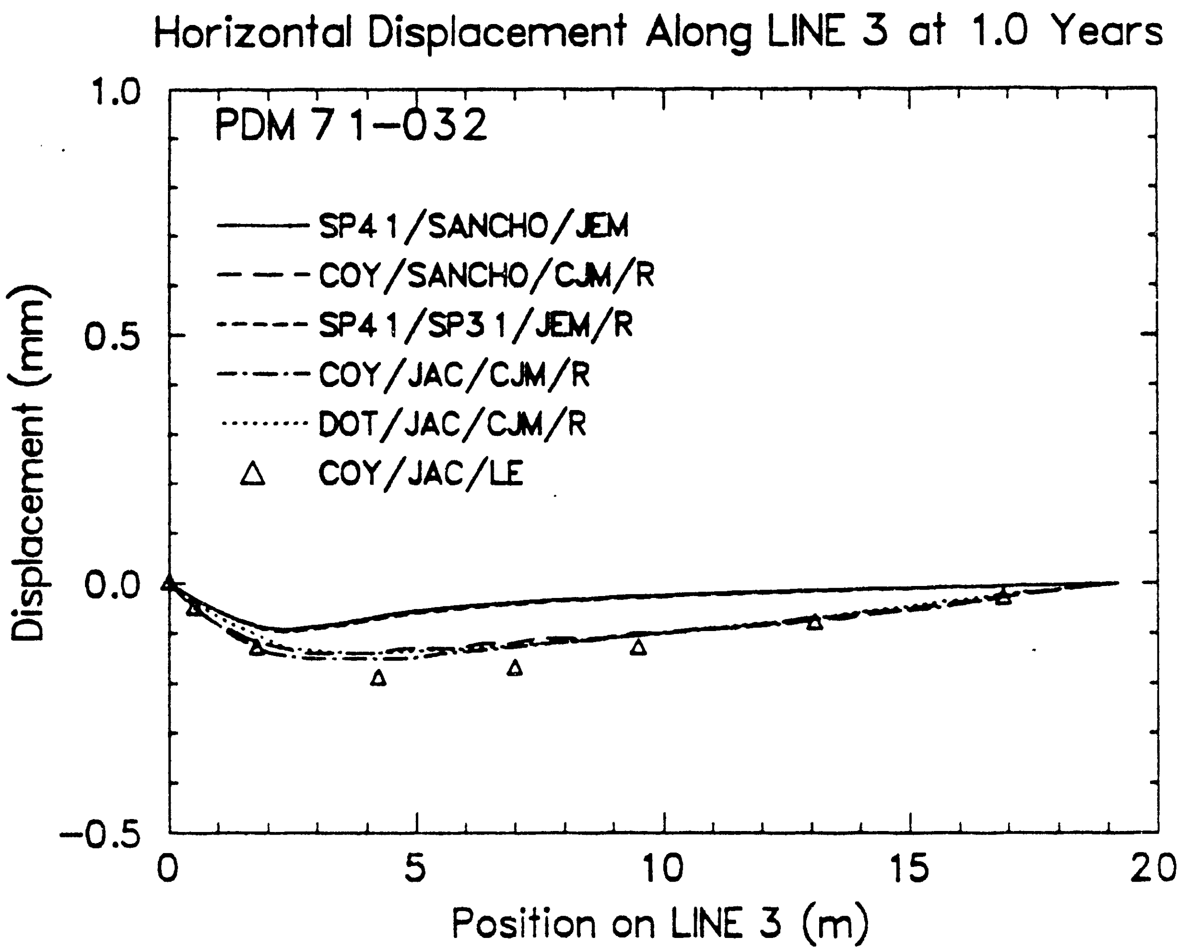

Figure 5-134. Comparison of Results for the Horizontal Displacement Along Line 3 (Figure 2-3) at 1 Yr, Third Analysis

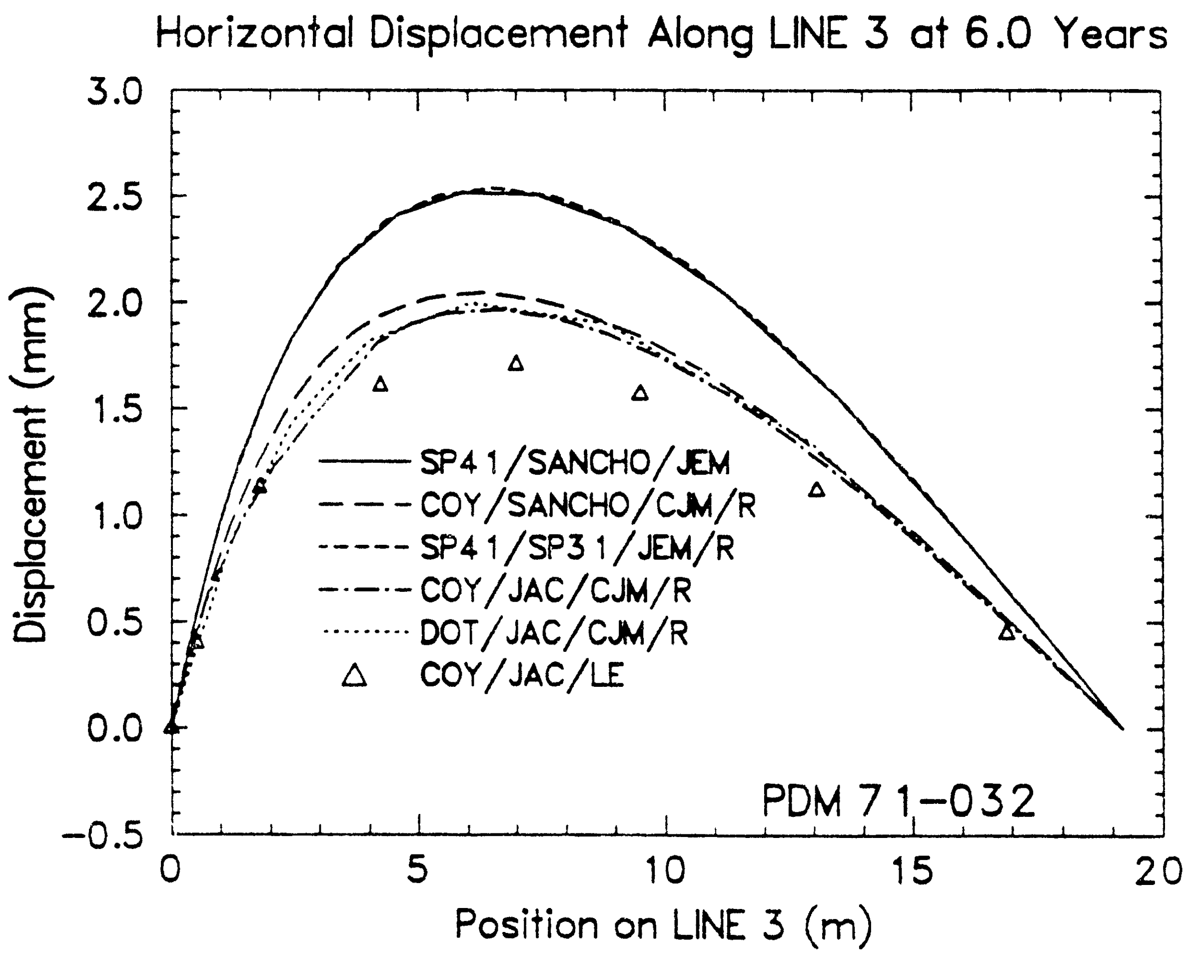

Figure 5-135. Comparison of Results for the Horizontal Displacement Along Line 3 (Figure 2-3) at 6 Yr, Third Analysis

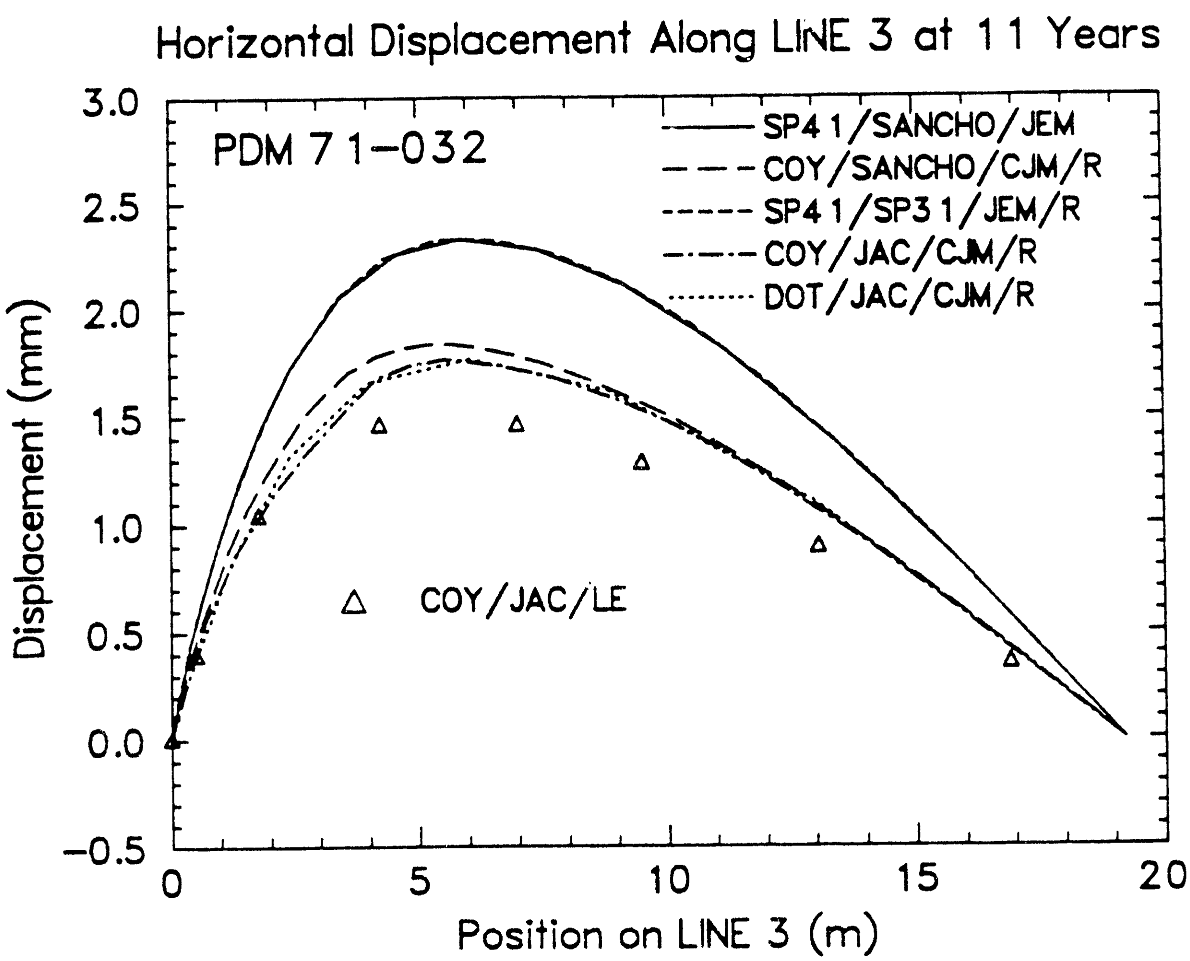

Figure 5-136. Comparison of Results for the Horizontal Displacement Along Line 3 (Figure 2-3) at 11 Yr, Third Analysis

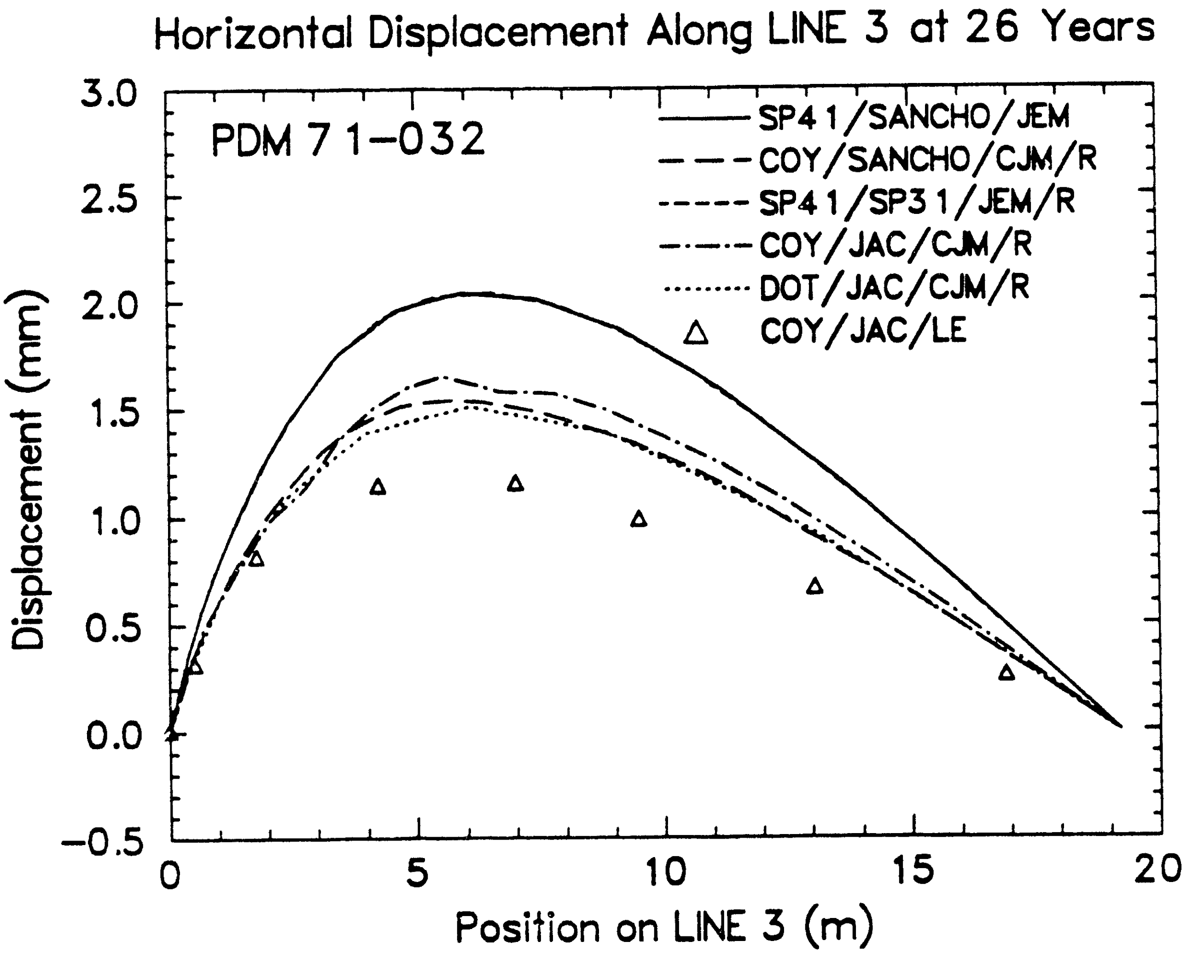

Figure 5-137. Comparison of Results for the Horizontal Displacement Along Line 3 (Figure 2-3) at 26 Yr. Third Analysis

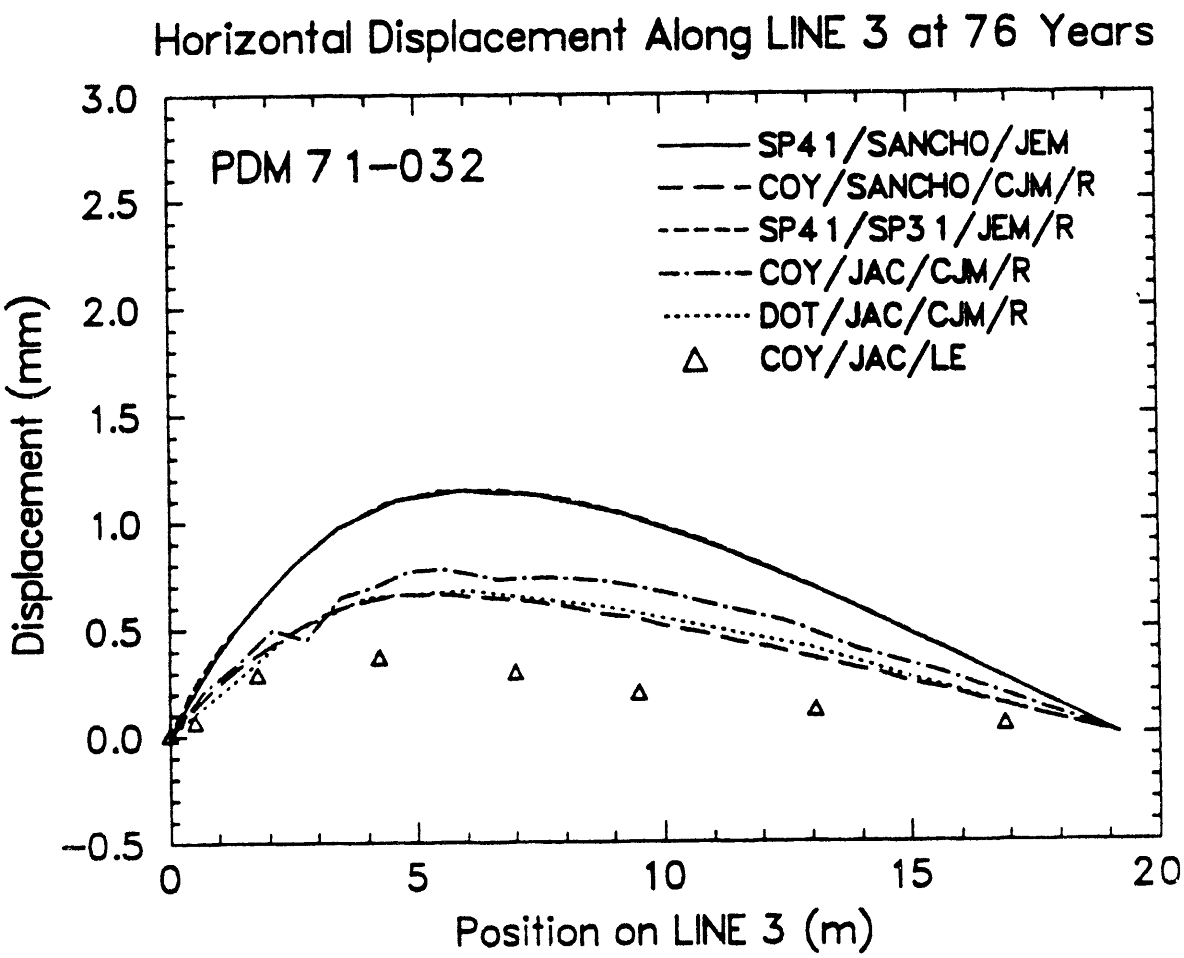

Figure 5-138. Comparison of Results for the Horizontal Displacement Along Line 3 (Figure 2-3) at 76 Yr, Third Analysis

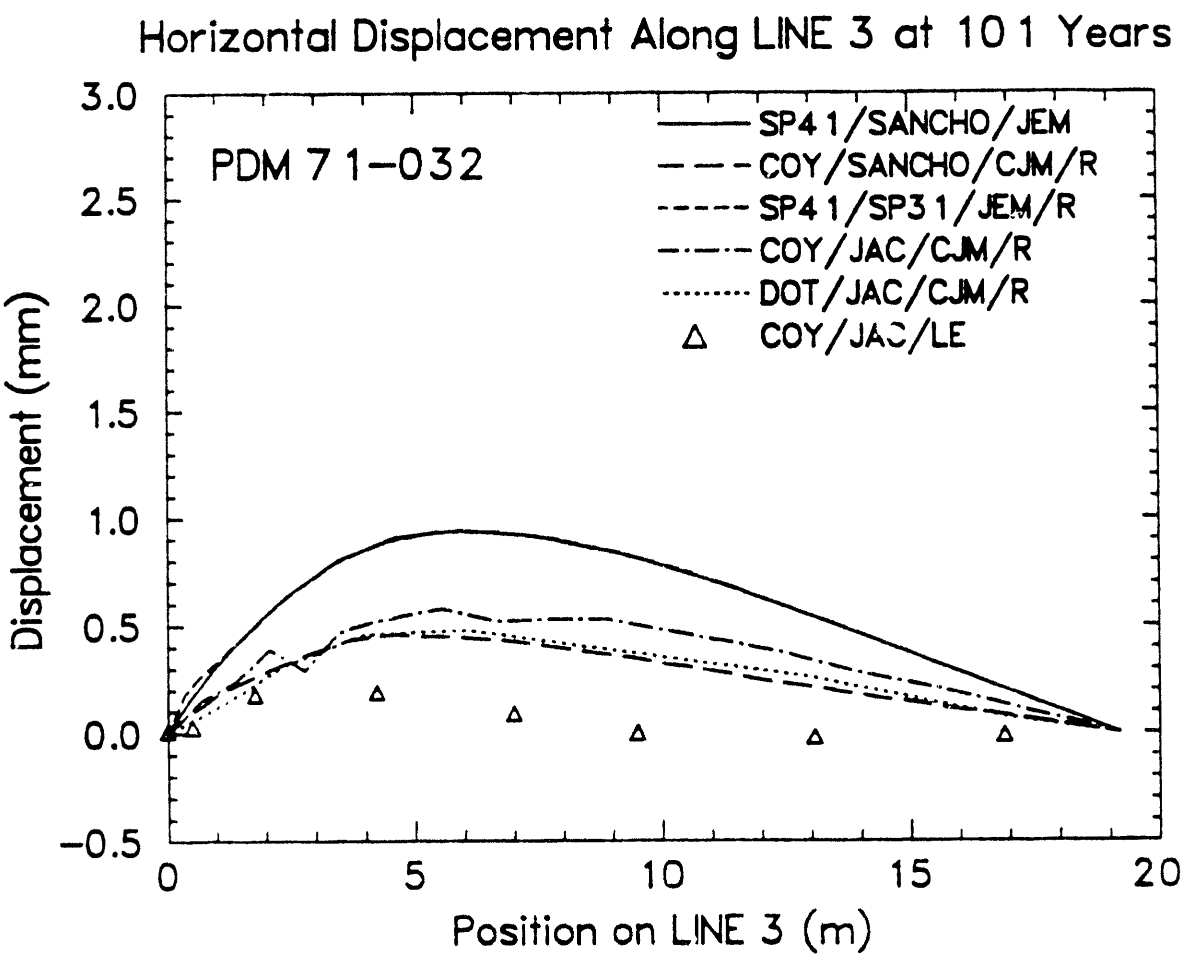

Figure 5-139. Comparison of Results for the Horizontal Displacement Along Line 3 (Figure 2-3) at 101 Yr. Third Analysis

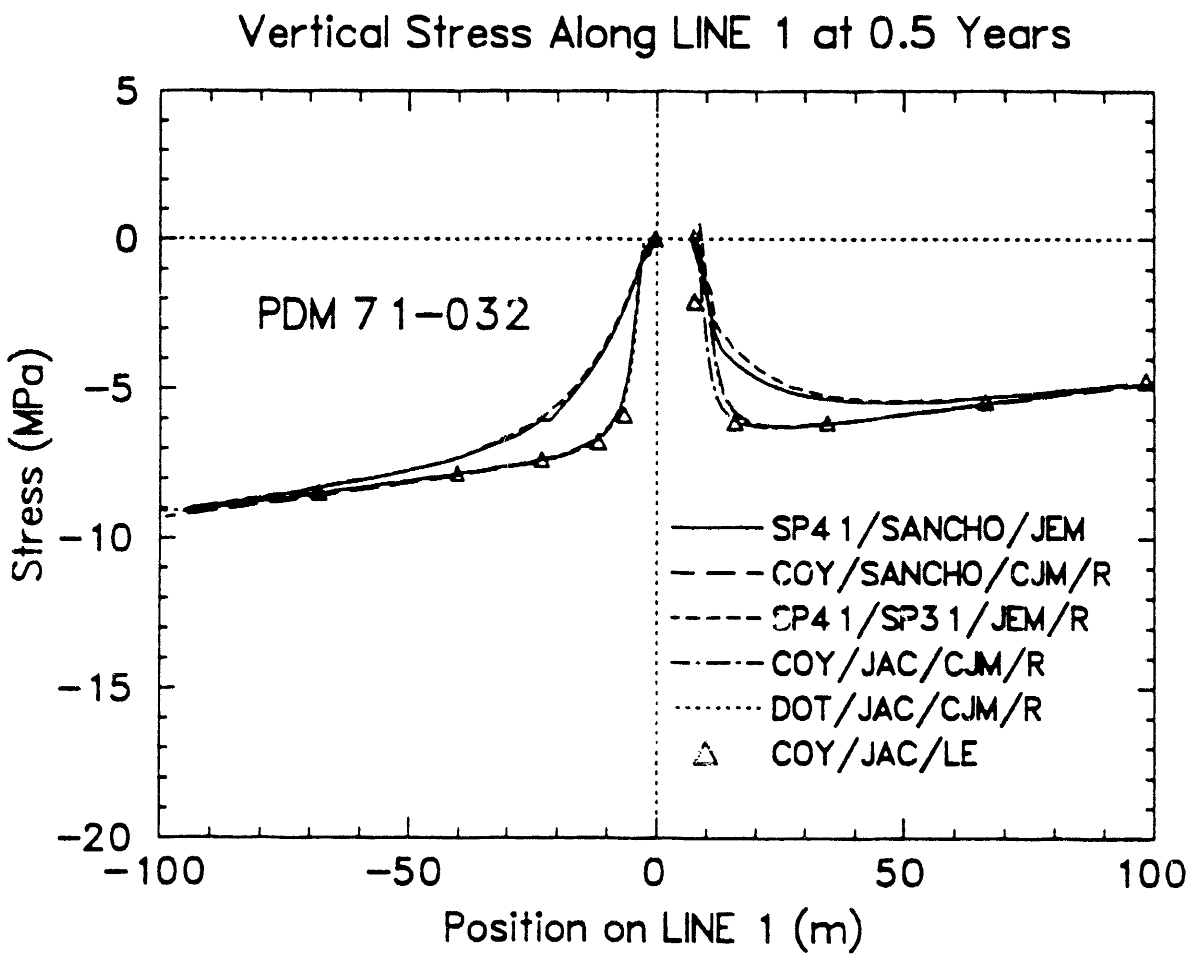

Figure 5-140. Comparison of Results for the Vertical Stress Along Line 1 (Figure 2-3) at 0.5 Yr, Third Analysis

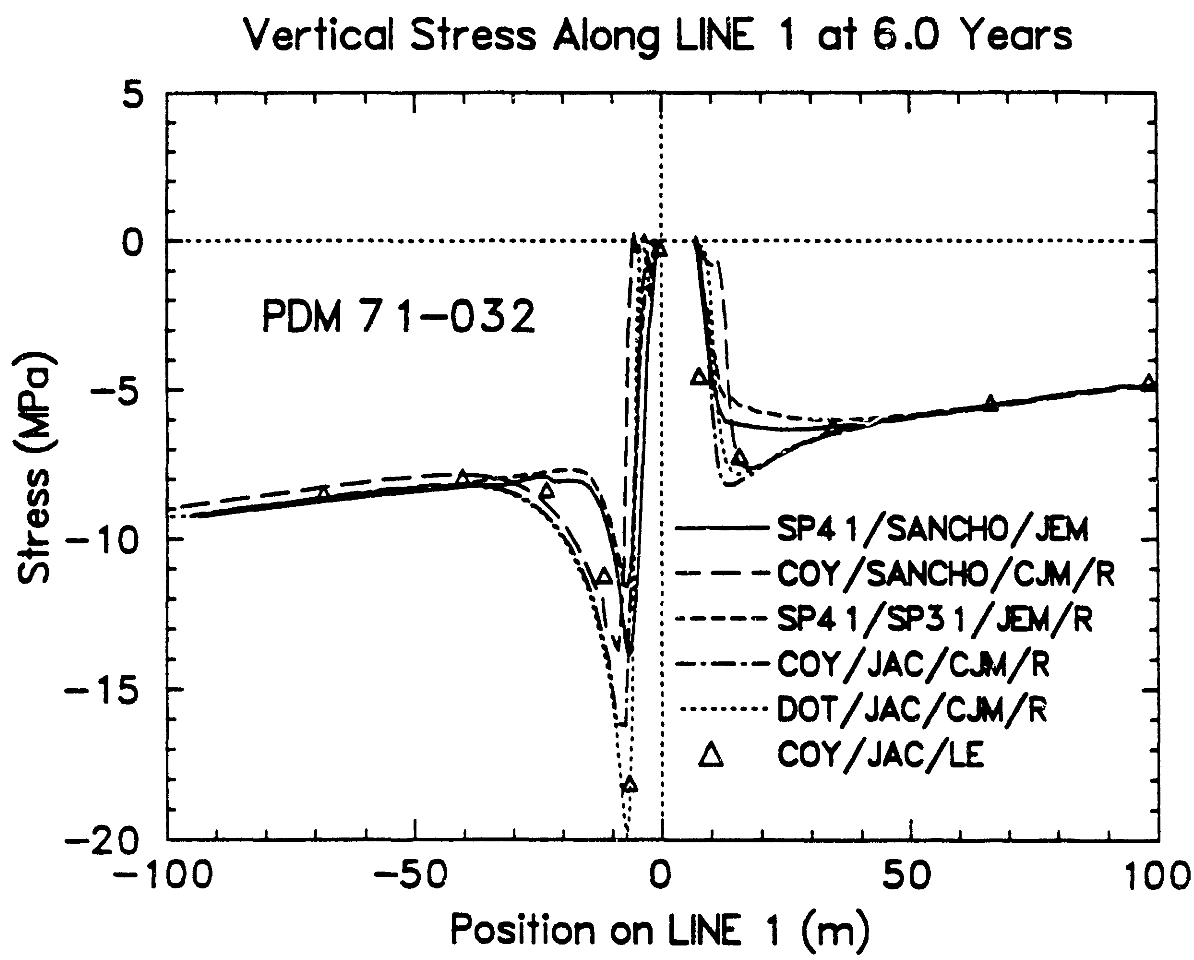

Figure 5-141. Comparison of Results for the Vertical Stress Along Line 1 (Figure 2-3) at 6 Yr, Third Analysis

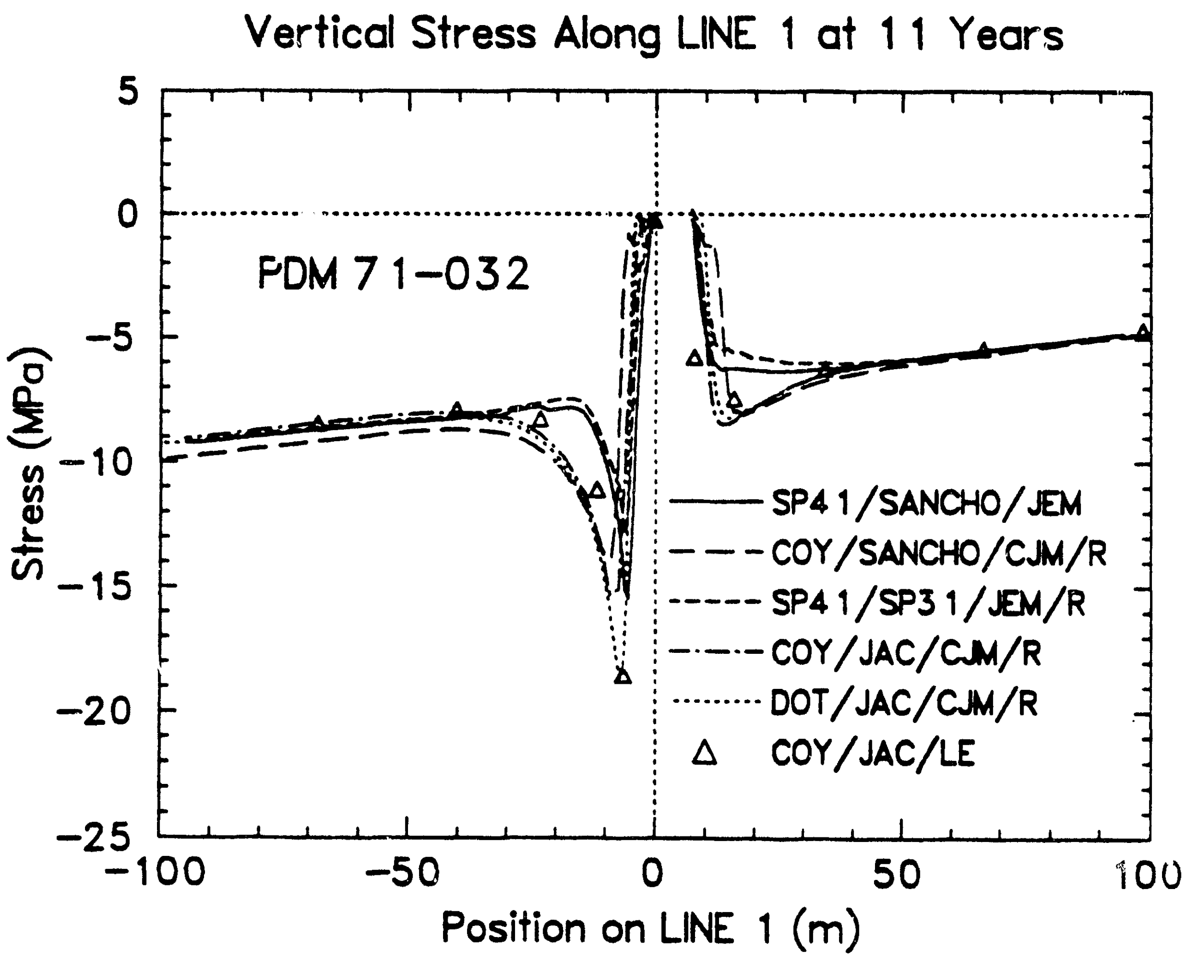

Figure 5-142. Comparison of Results for the Vertical Stress Along Line 1 (Figure 2-3) at 11 Yr, Third Analysis

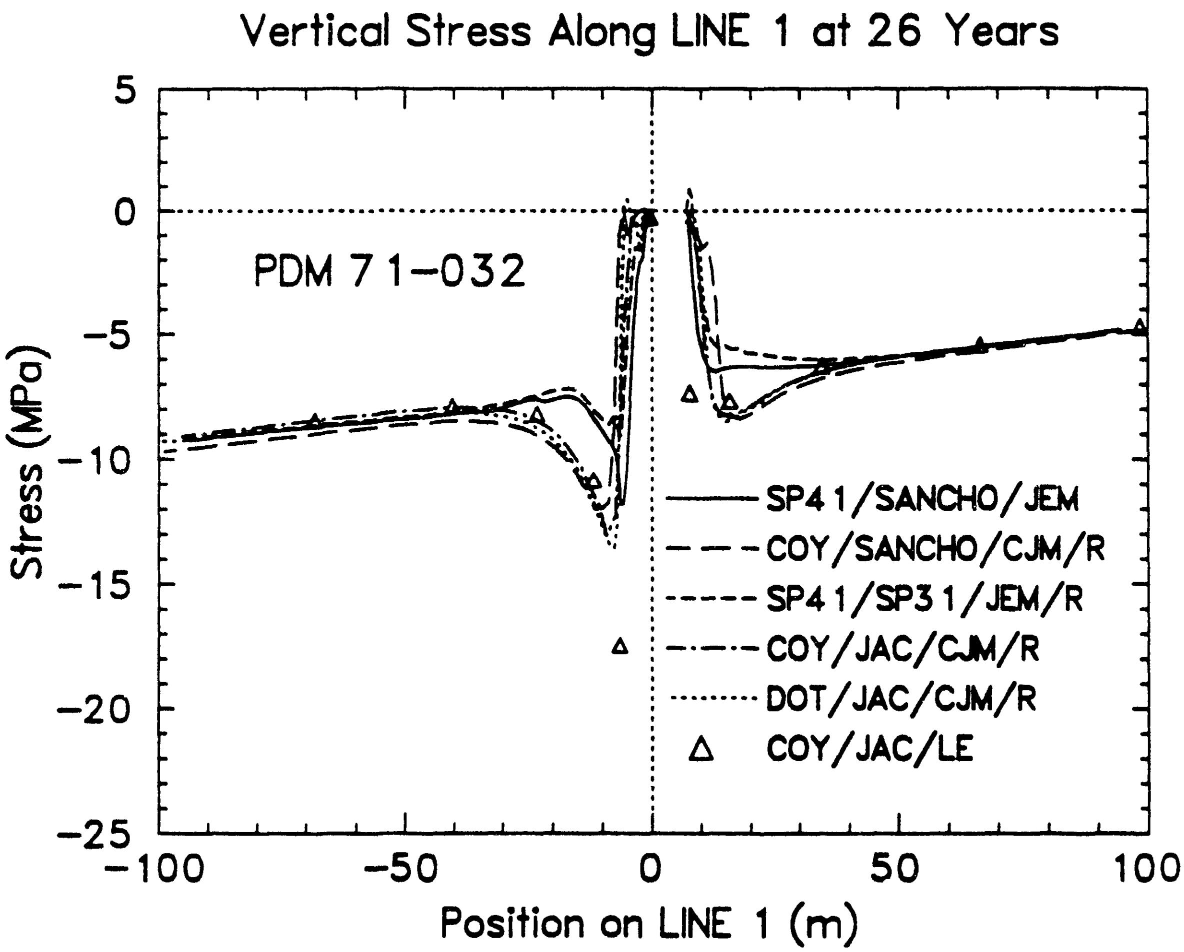

Figure 5-143. Comparison of Results for the Vertical Stress Along Line 1 (Figure 2-3) at 26 Yr, Third Analysis

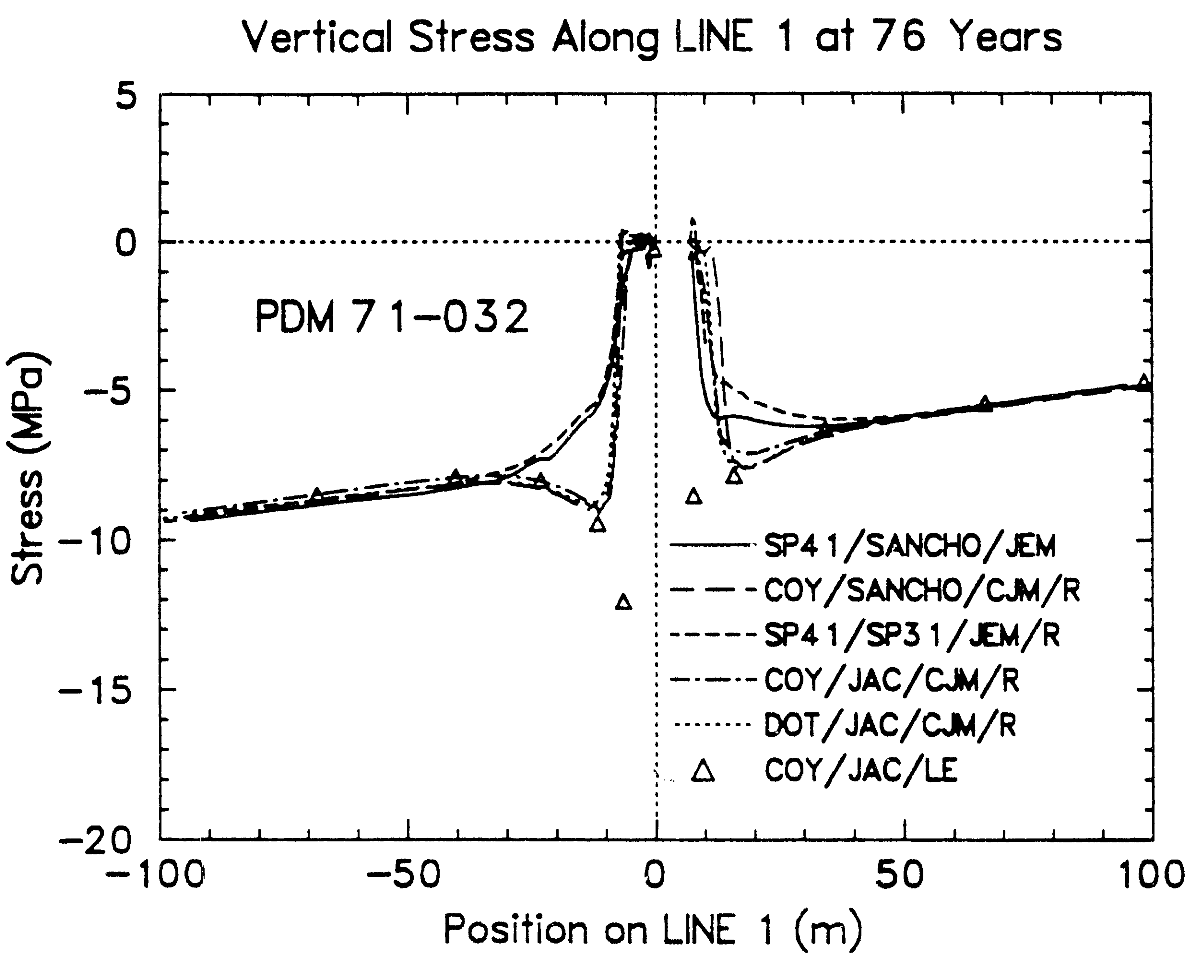

Figure 5-144. Comparison of Results for the Vertical Stress Along Line 1 (Figure 2-3) at 76 Yr, Third Analysis

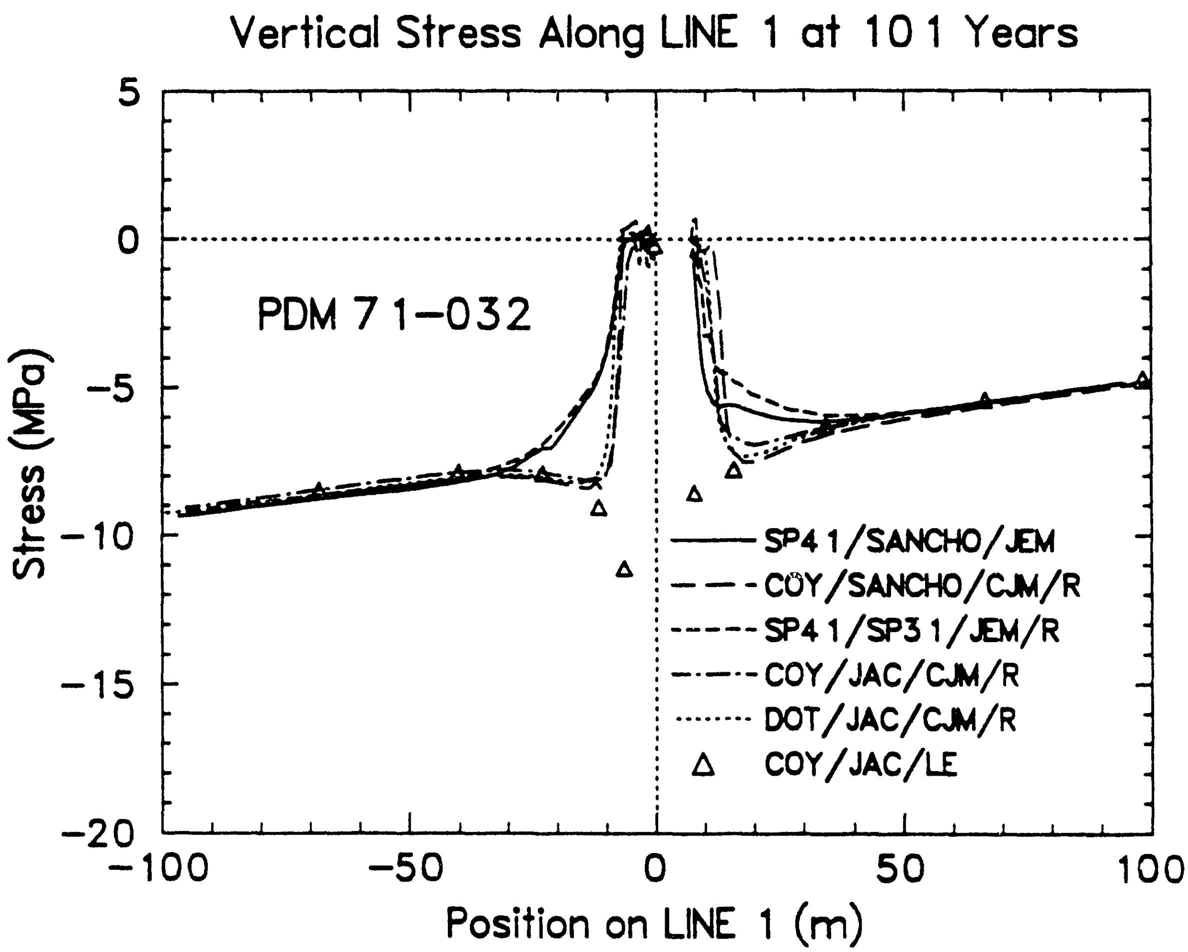

Figure 5-145. Comparison of Results for the Vertical Stress Along Line 1 (Figure 2-3) at 101 Yr, Third Analysis

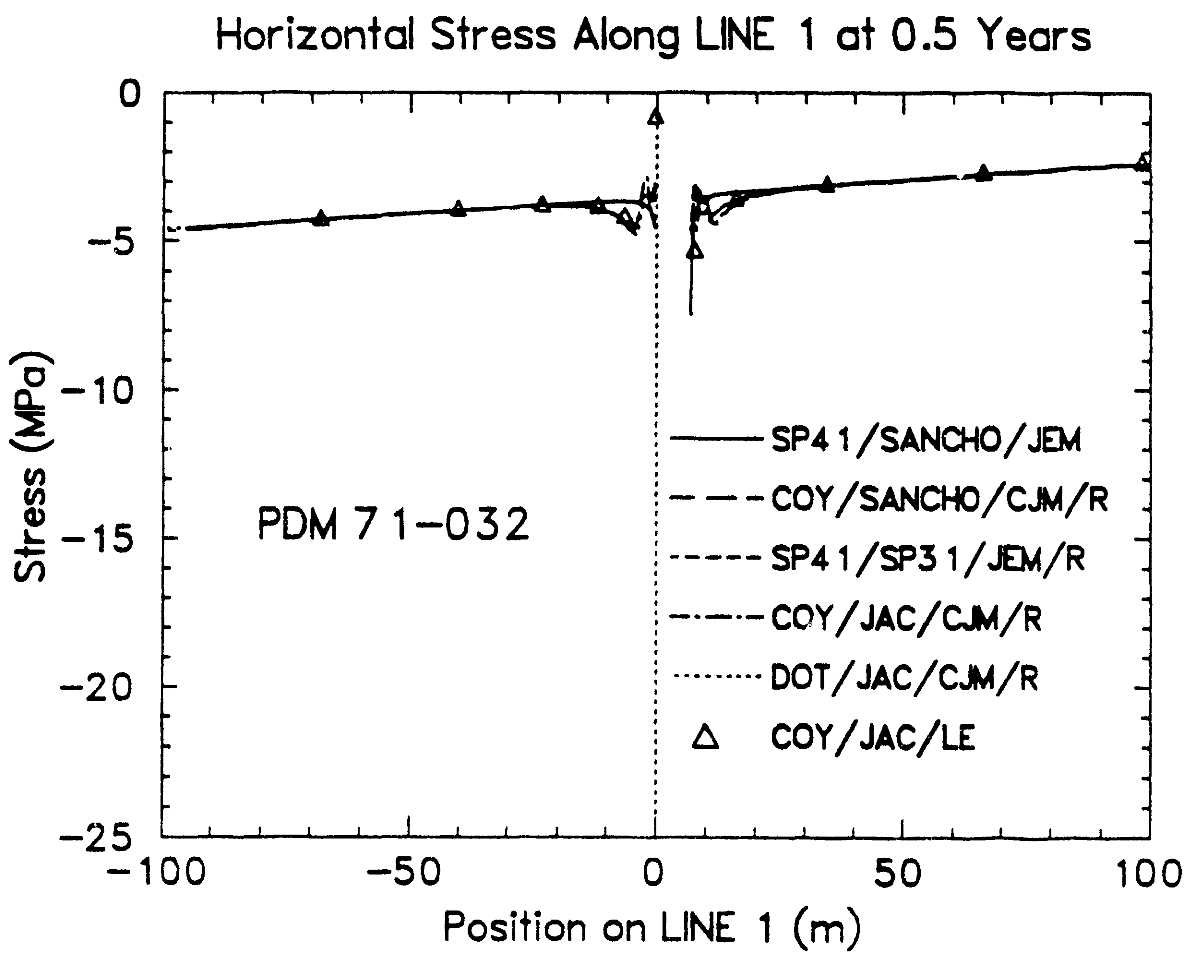

Figure 5-146. Comparison of Results for the Horizontal Stress Along Line 1 (Figure 2-3) at 0.5 Yr, Third Analysis

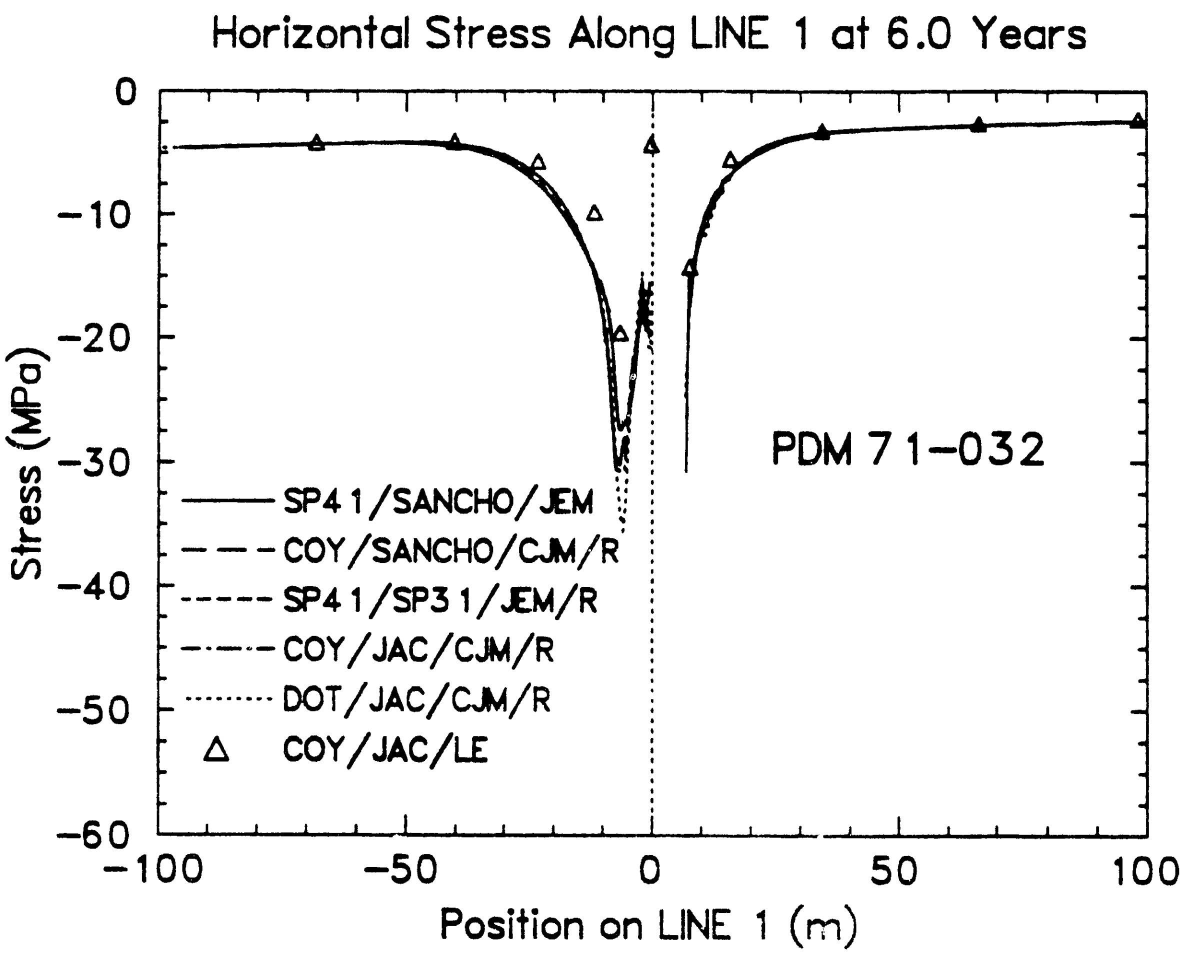

Figure 5-147. Comparison of Results for the Horizontal Stress Along Line 1 (Figure 2-3) at 6 Yr, Third Analysis

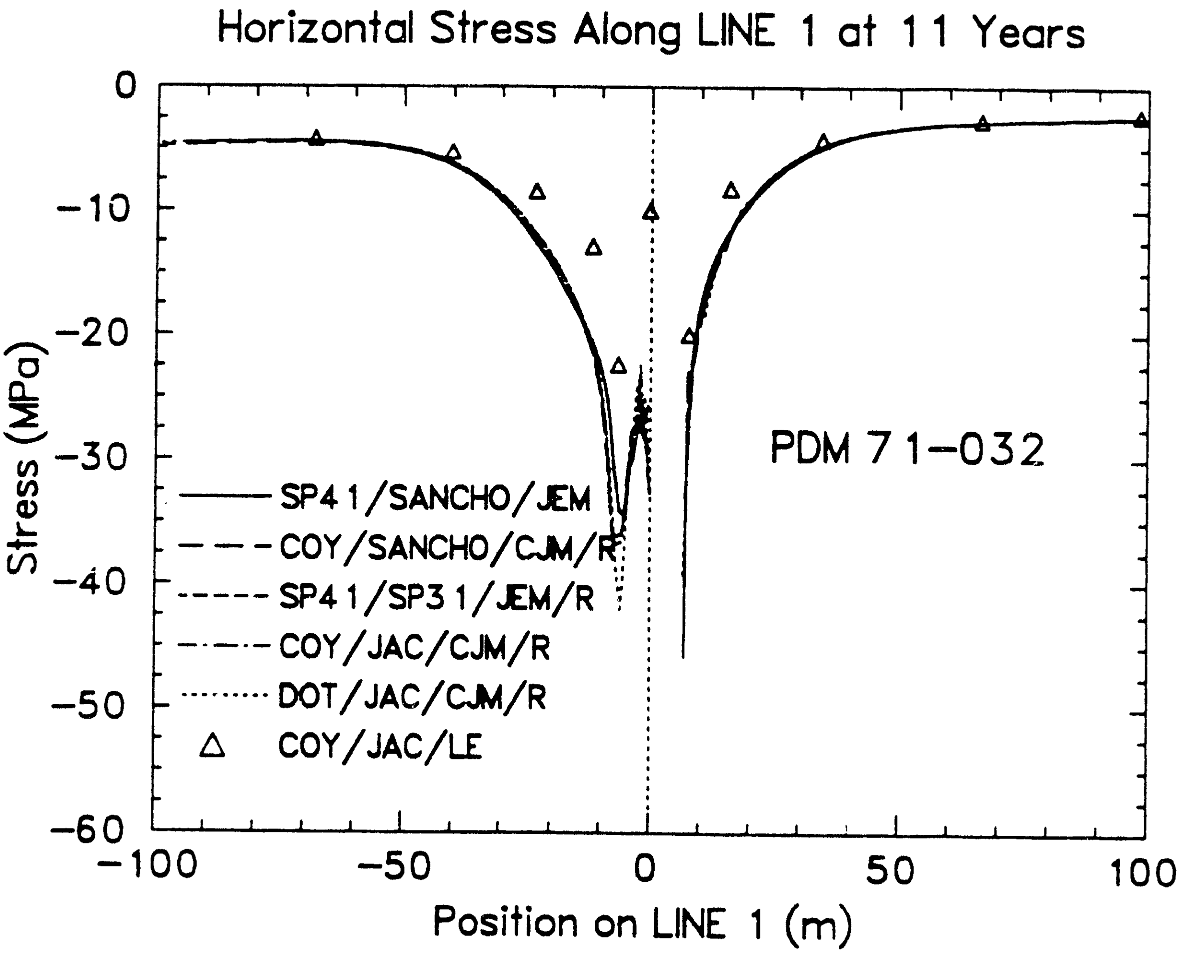

Figure 5-148. Comparison of Results for the Horizontal Stress Along Line 1 (Figure 2-3) at 11 Yr, Third Analysis

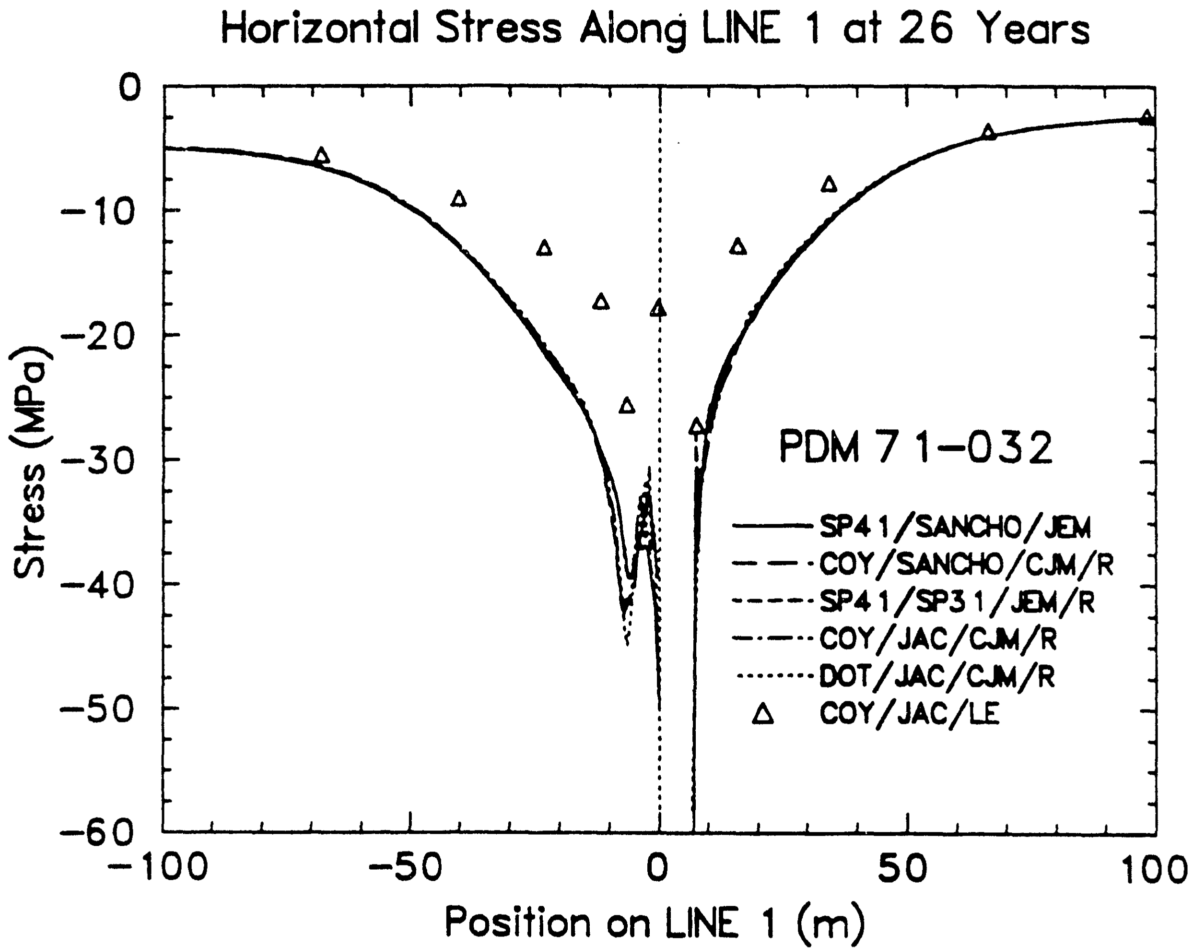

Figure 5-149. Comparison of Results for the Horizontal Stress Along Line 1 (Figure 2-3) at 26 Yr, Third Analysis

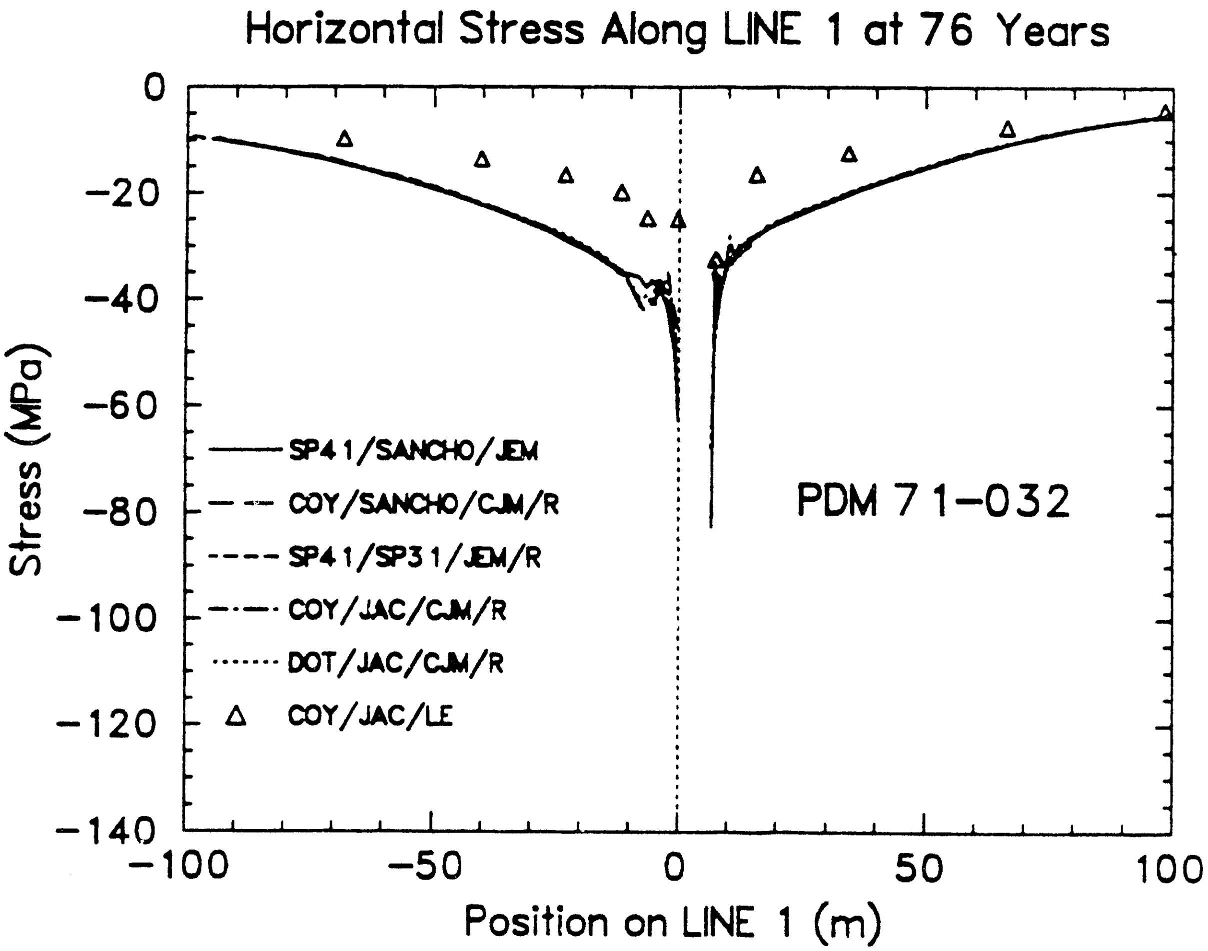

Figure 5-150. Comparison of Results for the Horizontal Stress Along Line 1 (Figure 2-3) at 76 Yr, Third Analysis

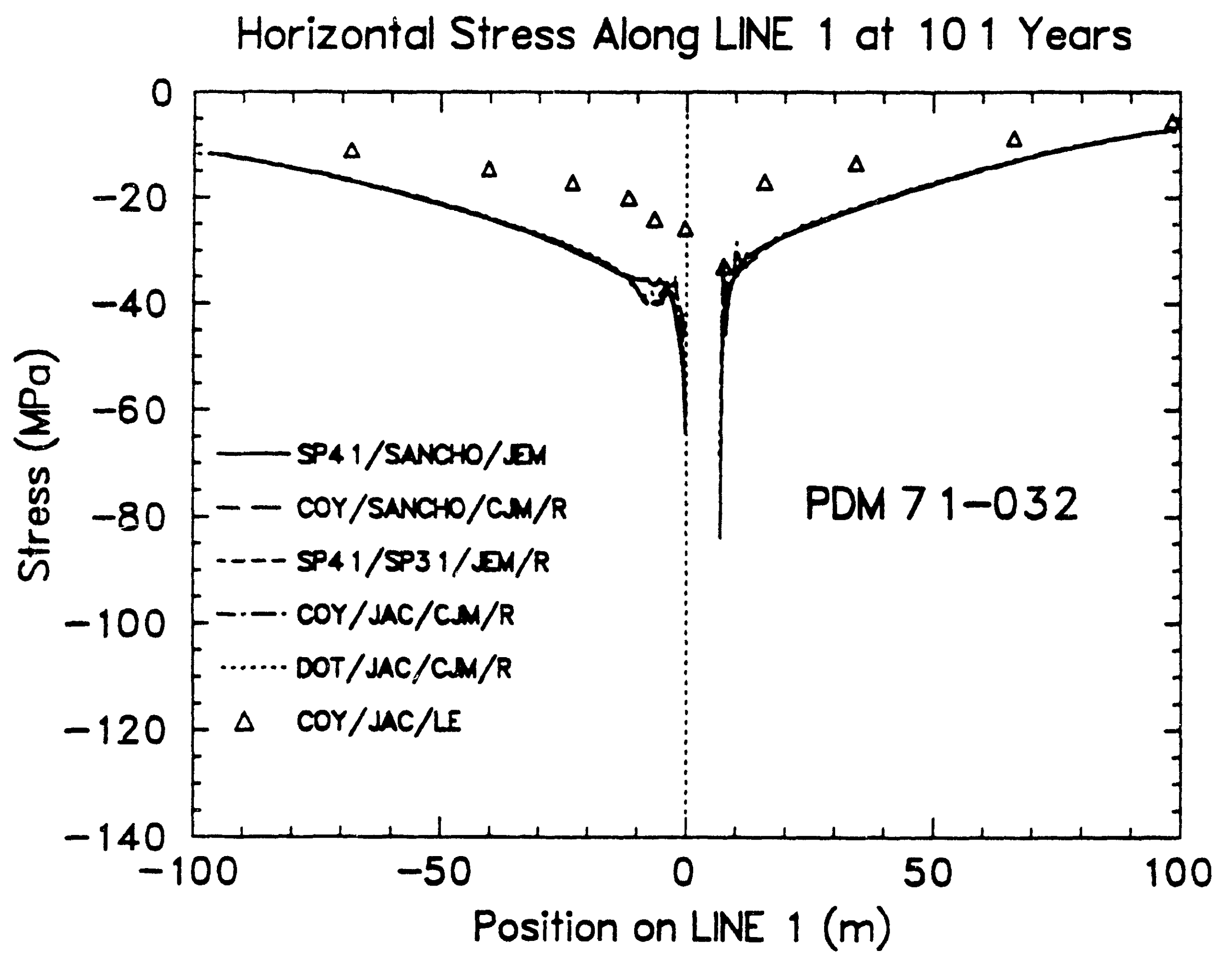

Figure 5-151. Comparison of Results for the Horizontal Stress Along Line 1 (Figure 2-3) at 101 Yr, Third Analysis

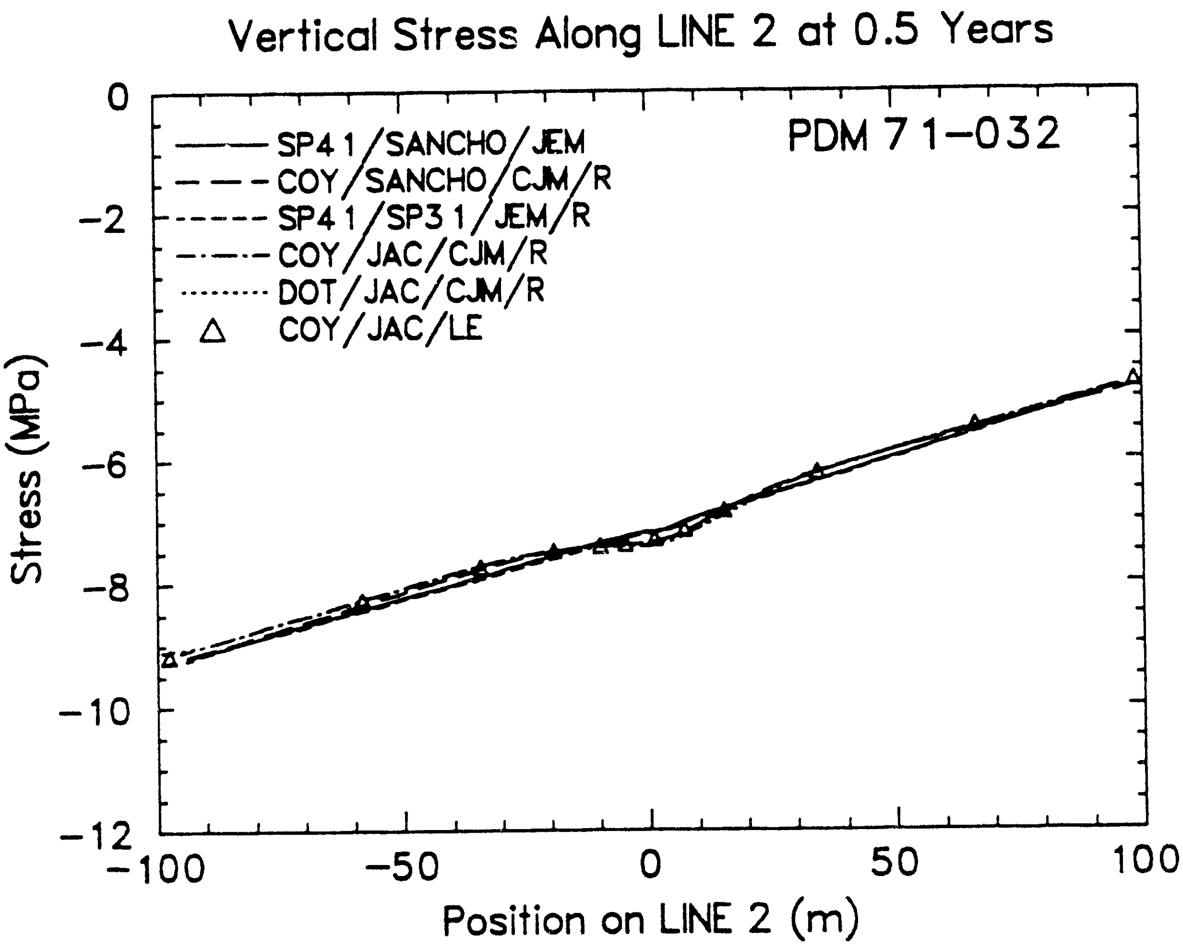

Figure 5-152. Comparison of Results for the Vertical Stress Along Line 2 (Figure 2-3) at 0.5 Yr, Third Analysis

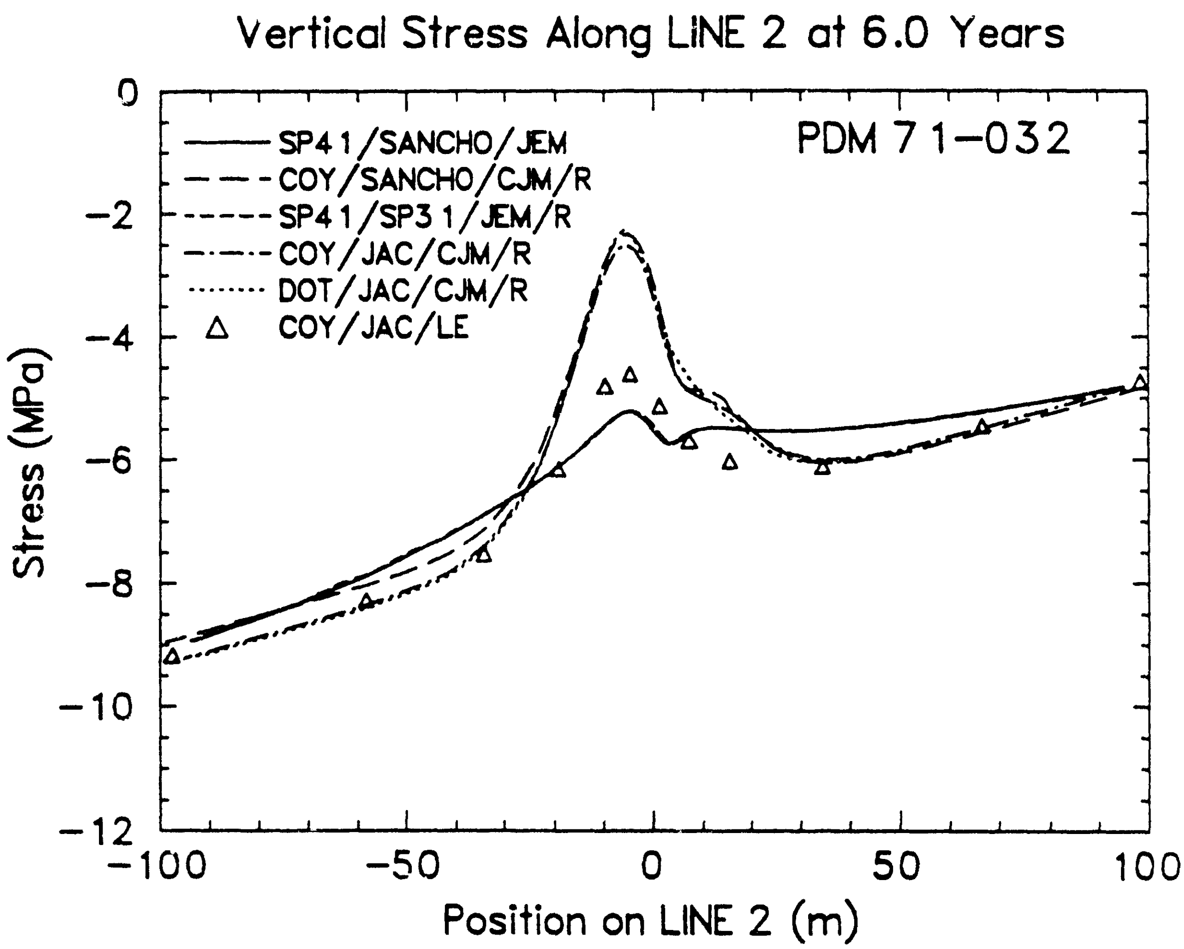

Figure 5-153. Comparison of Results for the Vertical Stress Along Line 2 (Figure 2-3) at 6 Yr, Third Analysis

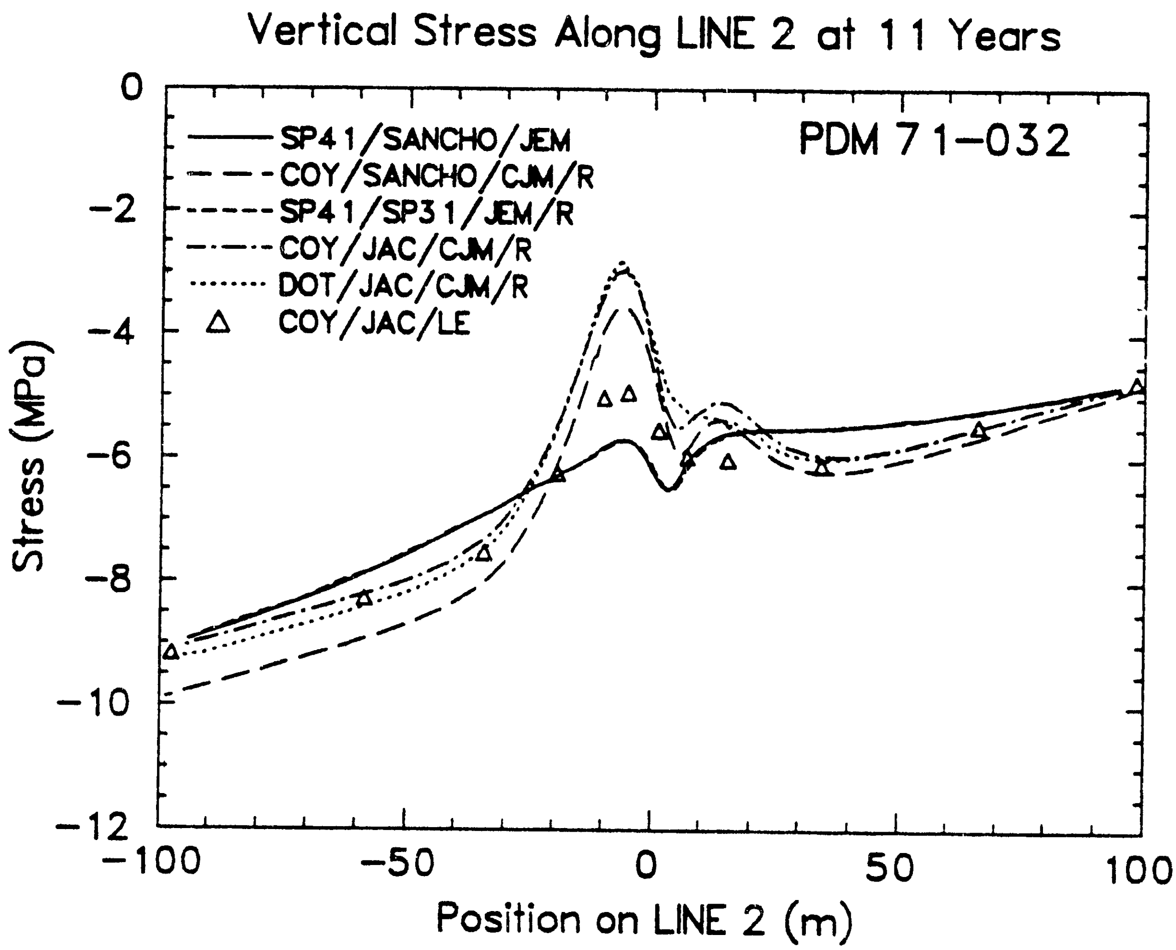

Figure 5-154. Comparison of Results for the Vertical Stress Along Line 2 (Figure 2-3) at 11 Yr, Third Analysis

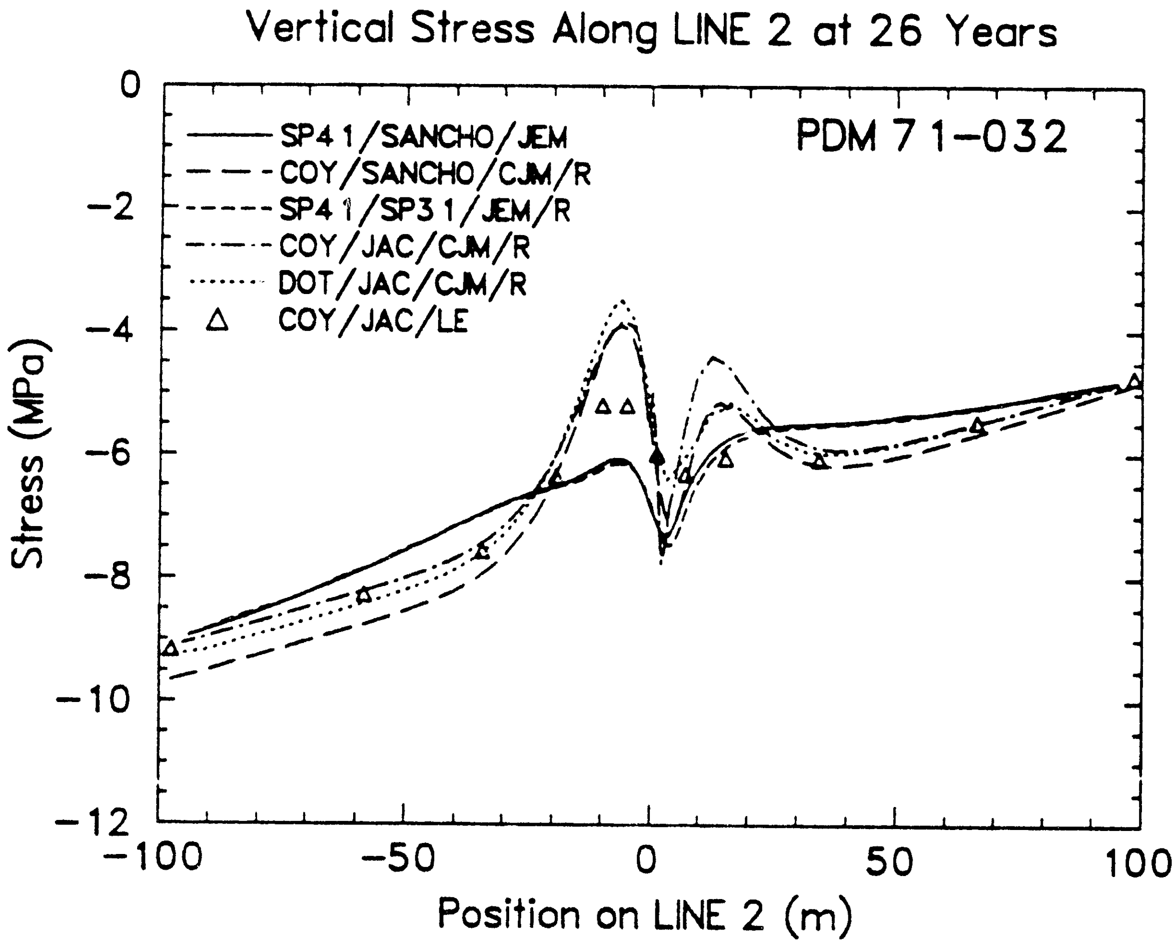

Figure 5-155. Comparison of Results for the Vertical Stress Along Line 2 (Figure 2-3) at 26 Yr, Third Analysis

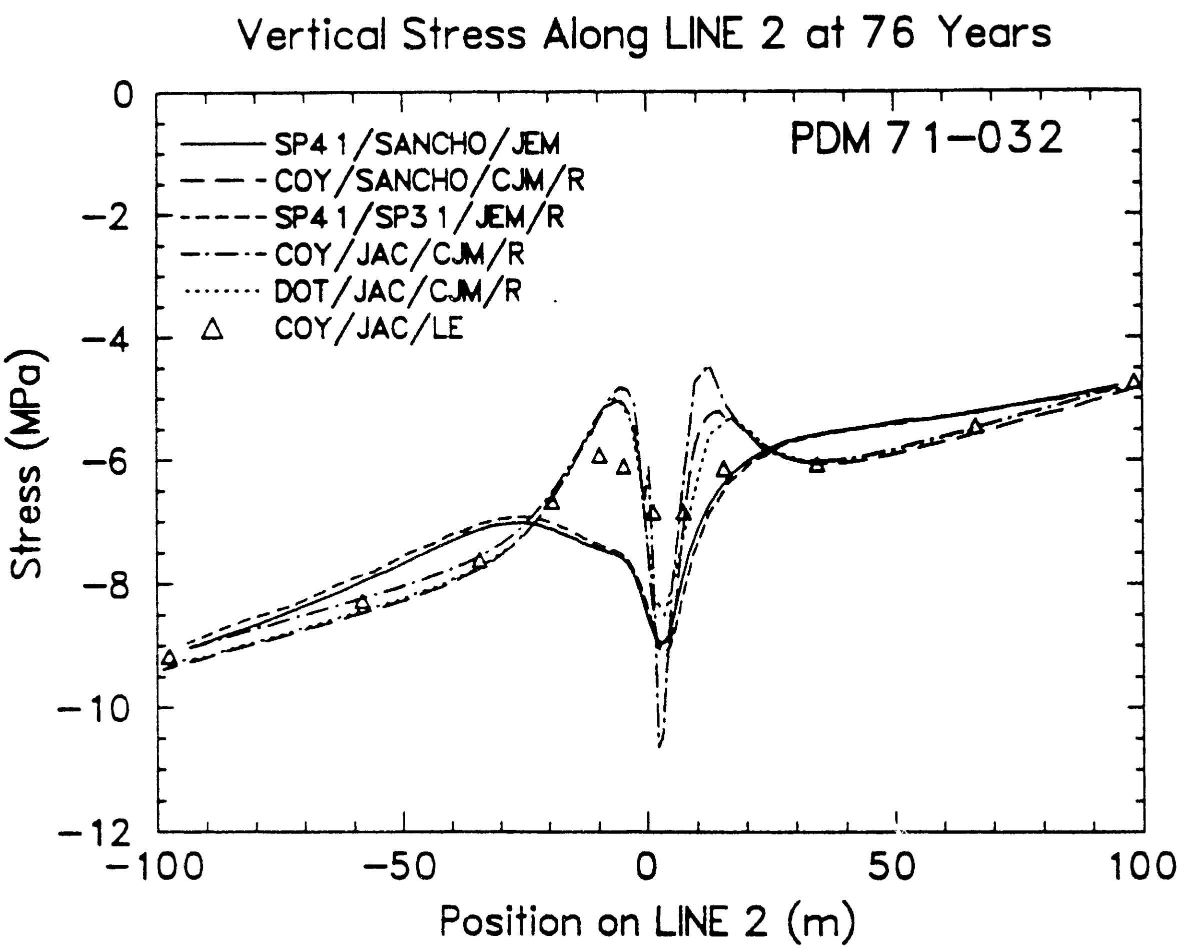

Figure 5-156. Comparison of Results for the Vertical Stress Along Line 2 (Figure 2-3) at 76 Yr, Third Analysis

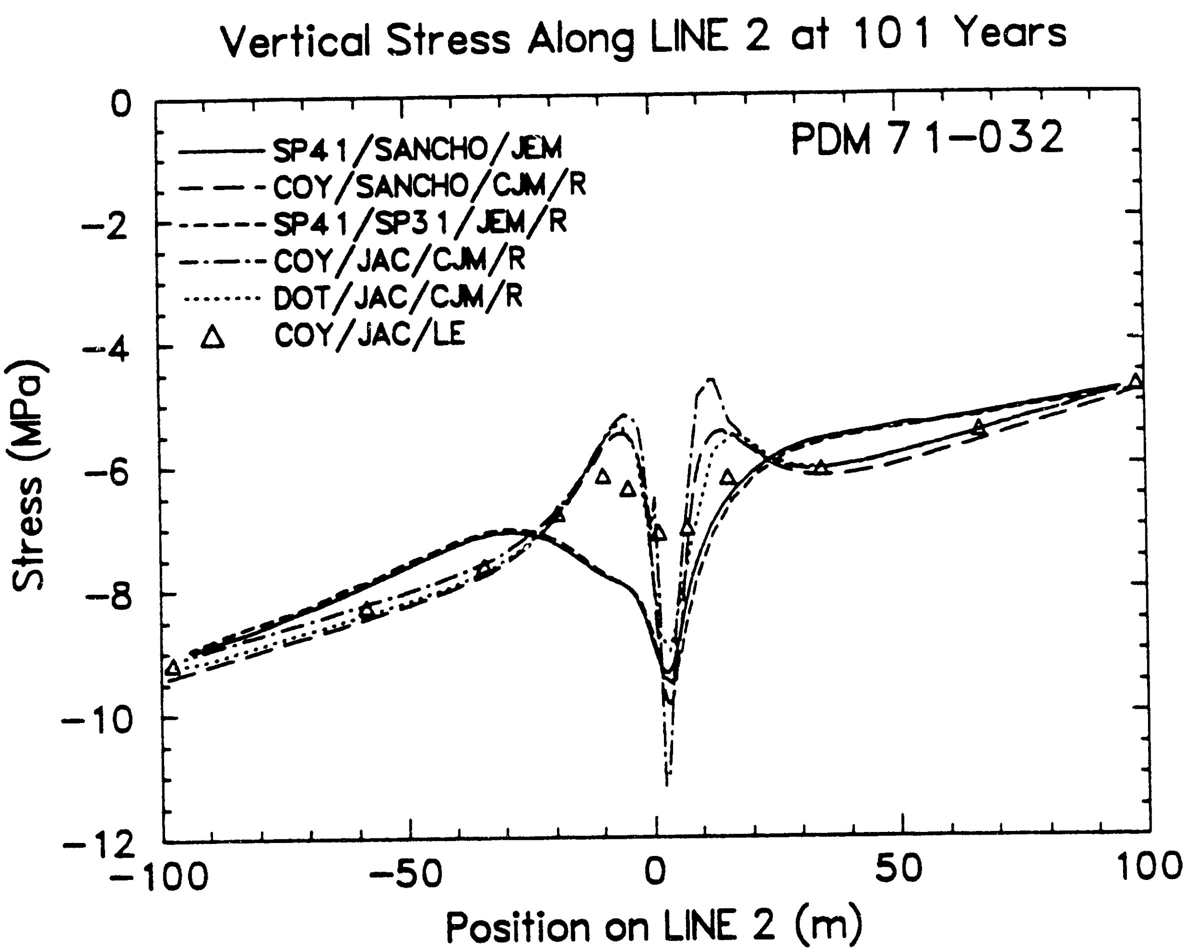

Figure 5-157. Comparison of Results for the Vertical Stress Along Line 2 (Figure 2-3) at 101 Yr, Third Analysis

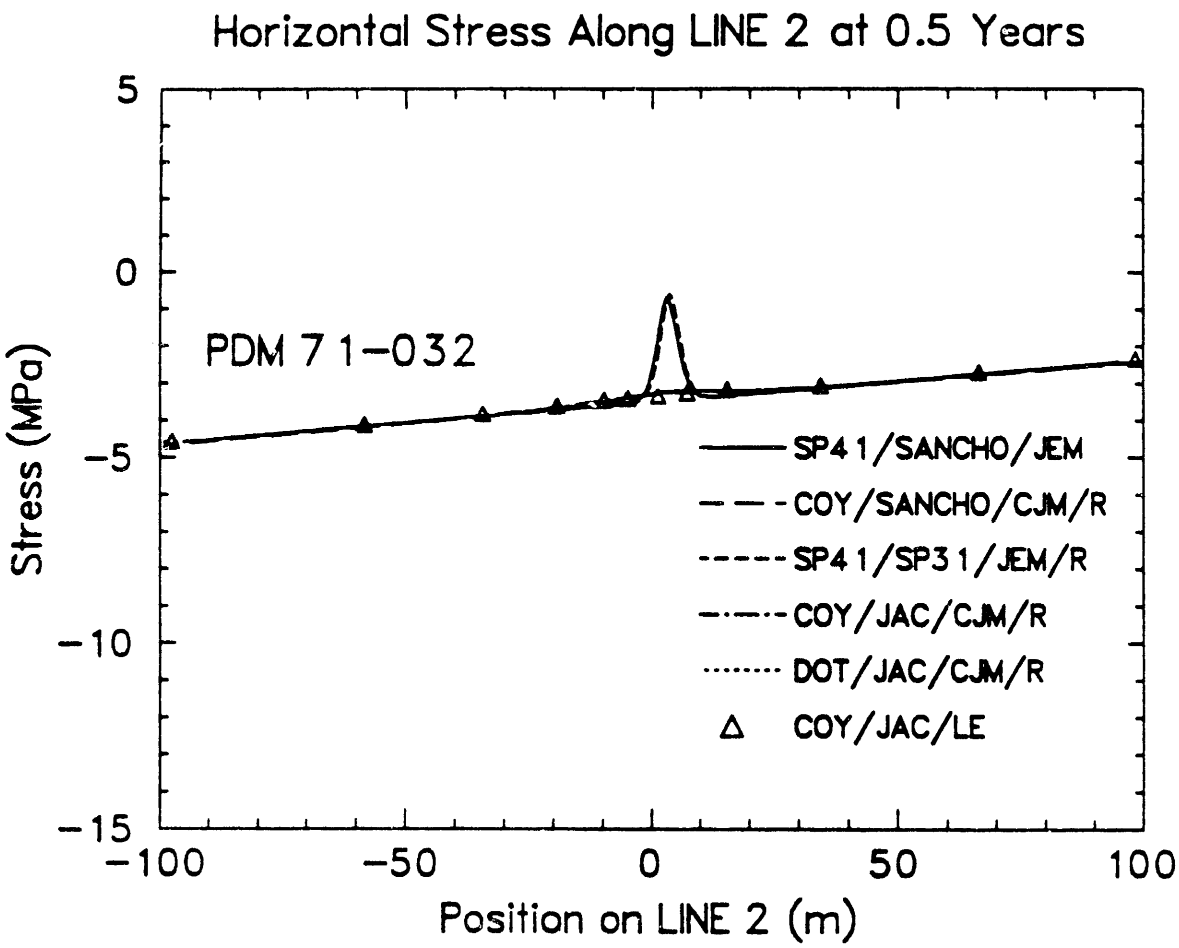

Figure 5-158. Comparison of Results for the Horizontal Stress Along Line 2 (Figure 2-3) at 0.5 Yr, Third Analysis

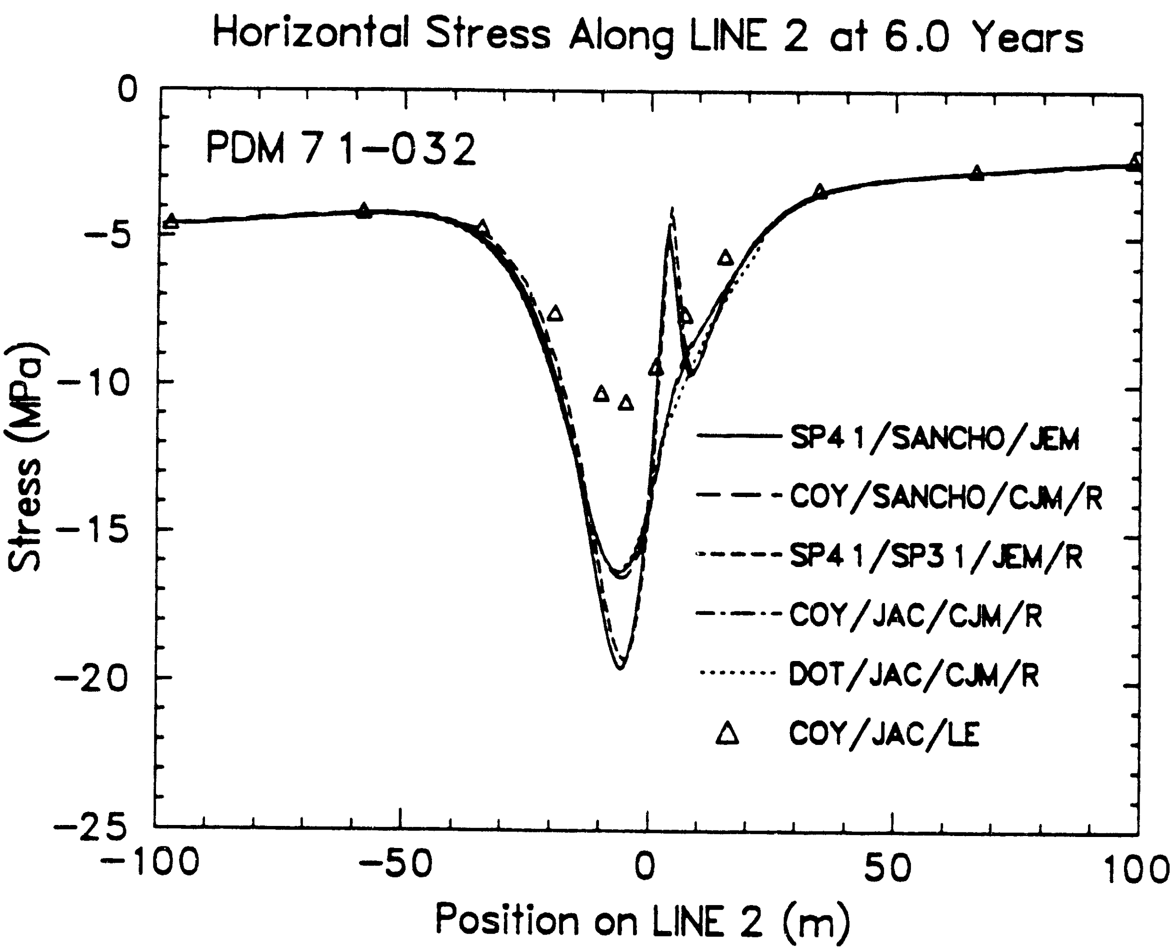

Figure 5-159. Comparison of Results for the Horizontal Stress Along Line 2 (Figure 2-3) at 6 Yr, Third Analysis

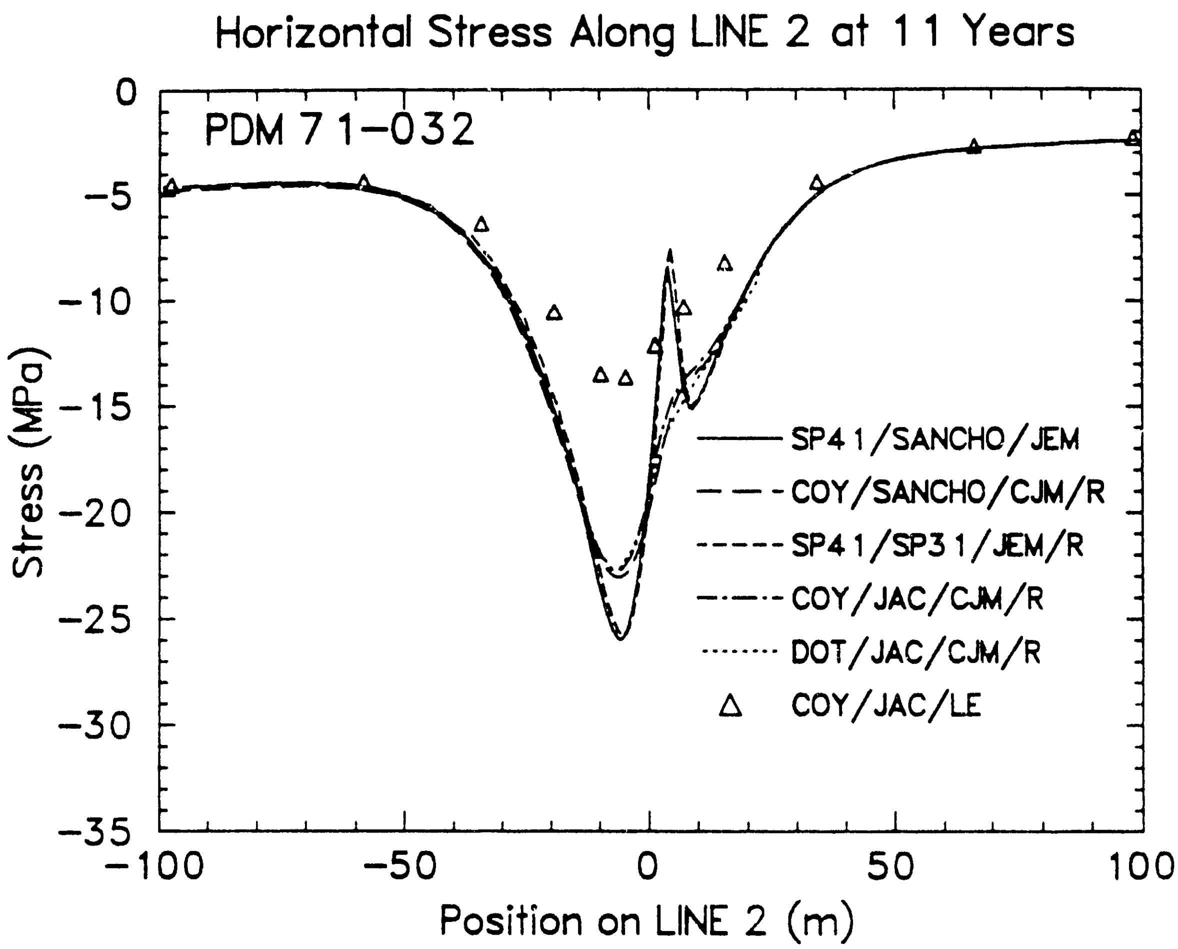

Figure 5-160. Comparison of Results for the Horizontal Stress Along Line 2 (Figure 2-3) at 11 Yr, Third Analysis

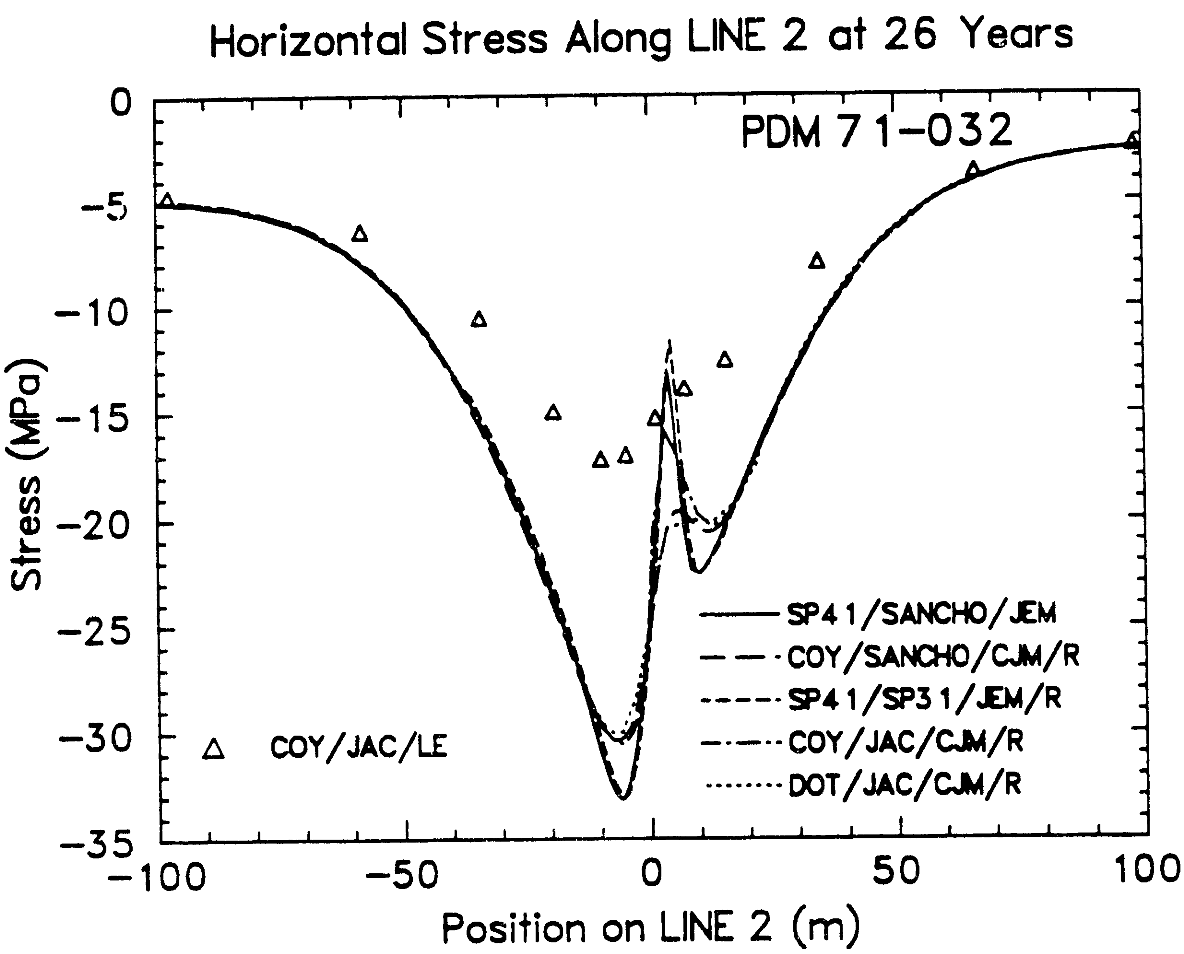

Figure 5-161. Comparison of Results for the Horizontal Stress Along Line 2 (Figure 2-3) at 26 Yr, Third Analysis

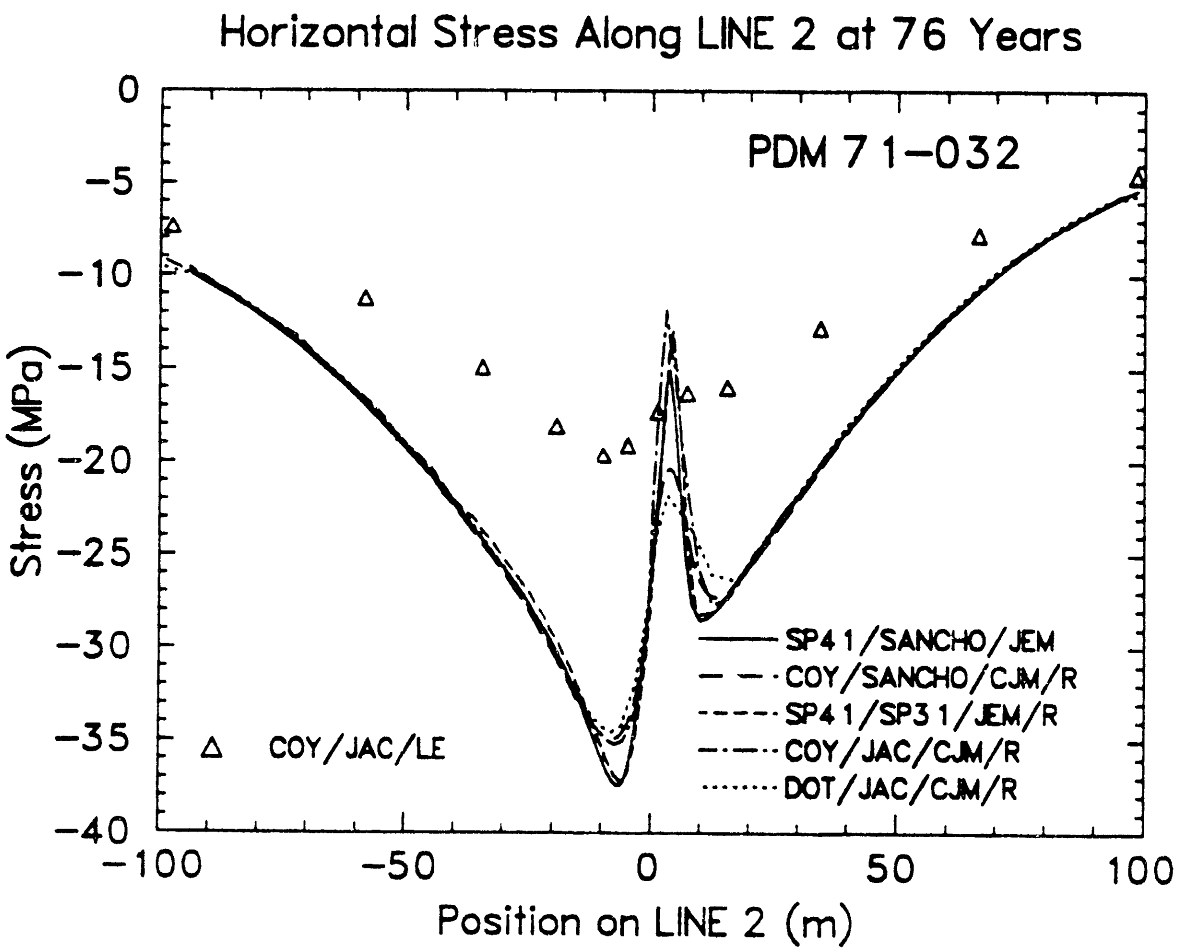

Figure 5-162. Comparison of Results for the Horizontal Stress Along Line 2 (Figure 2-3) at 76 Yr, Third Analysis

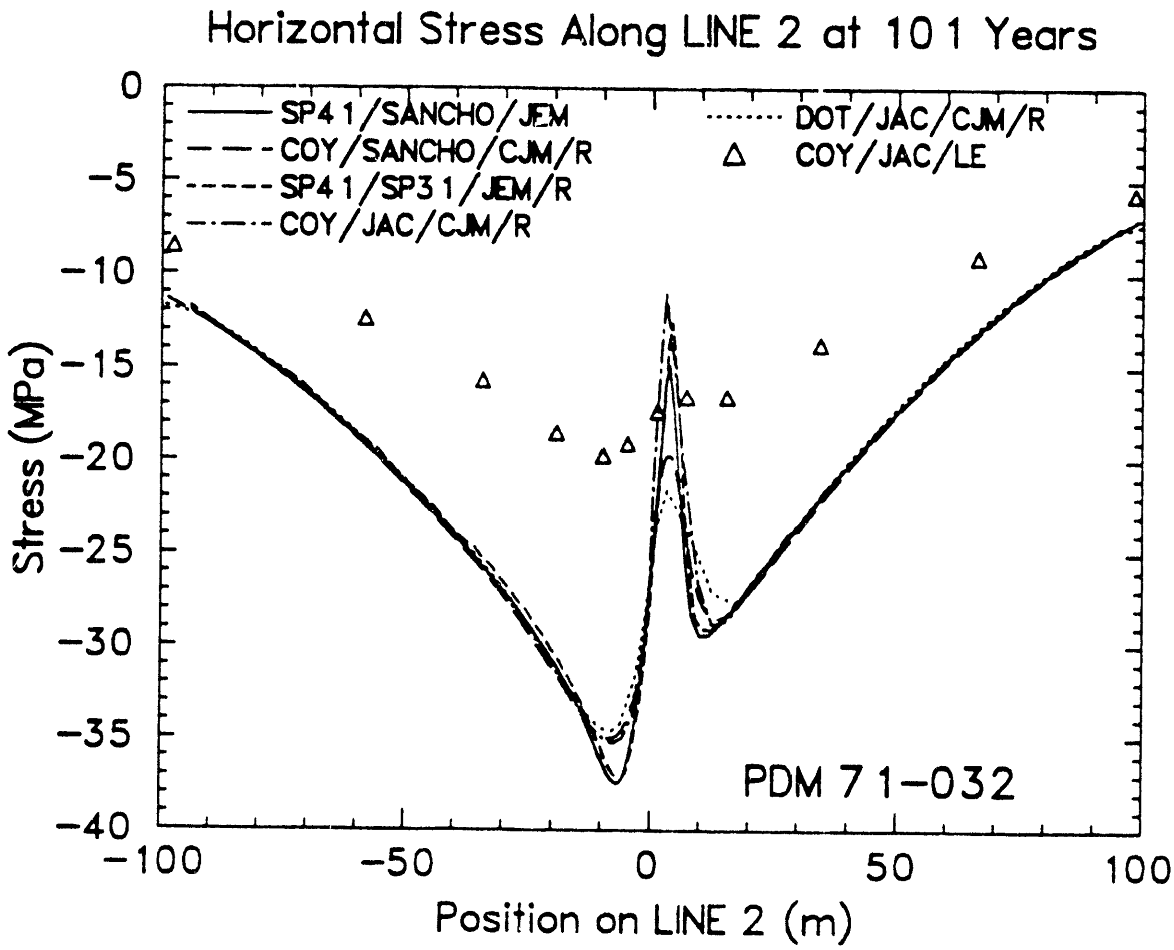

Figure 5-163. Comparison of Results for the Horizontal Stress Along Line 2 (Figure 2-3) at 101 Yr, Third Analysis

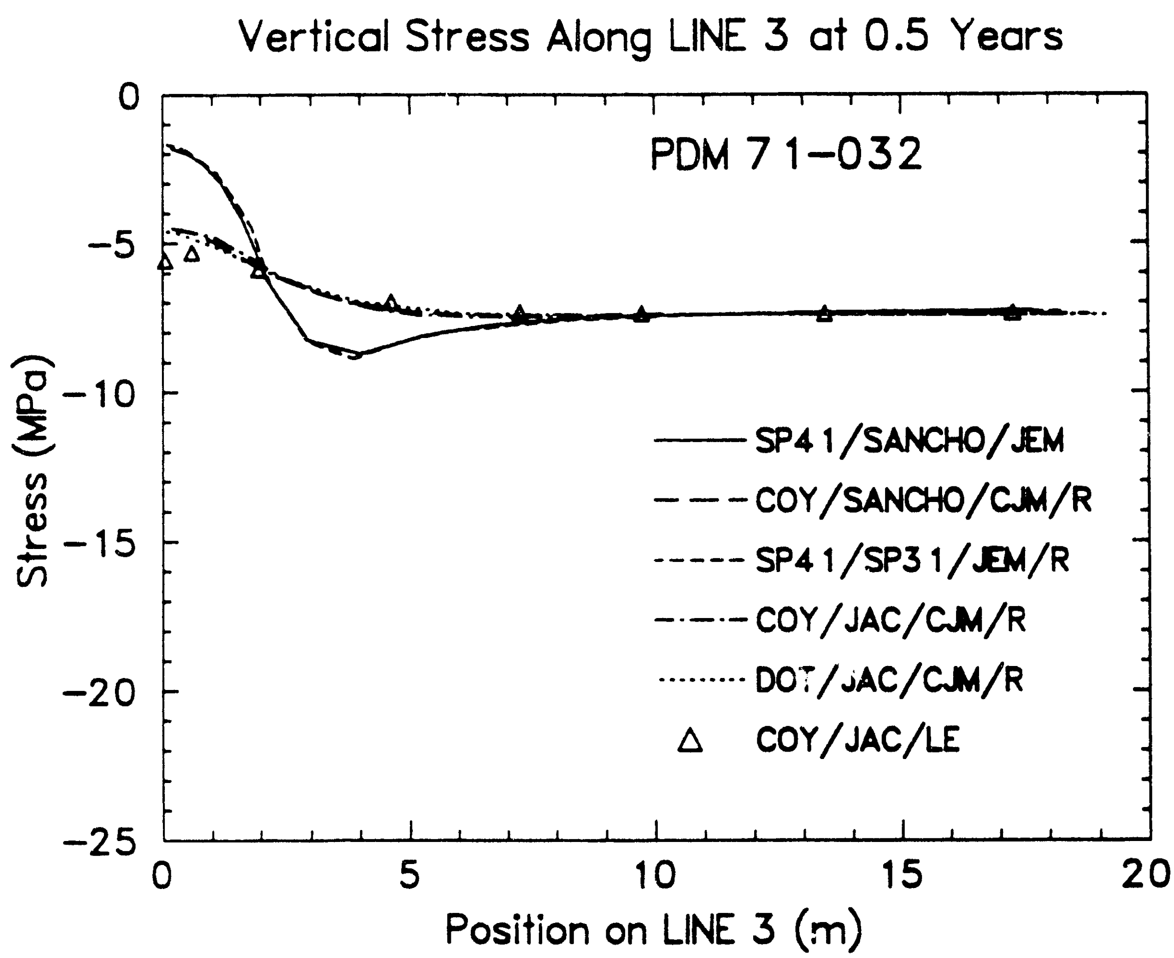

Figure 5-164. Comparison of Results for the Vertical Stress Along Line 3 (Figure 2-3) at 0.5 Yr, Third Analysis

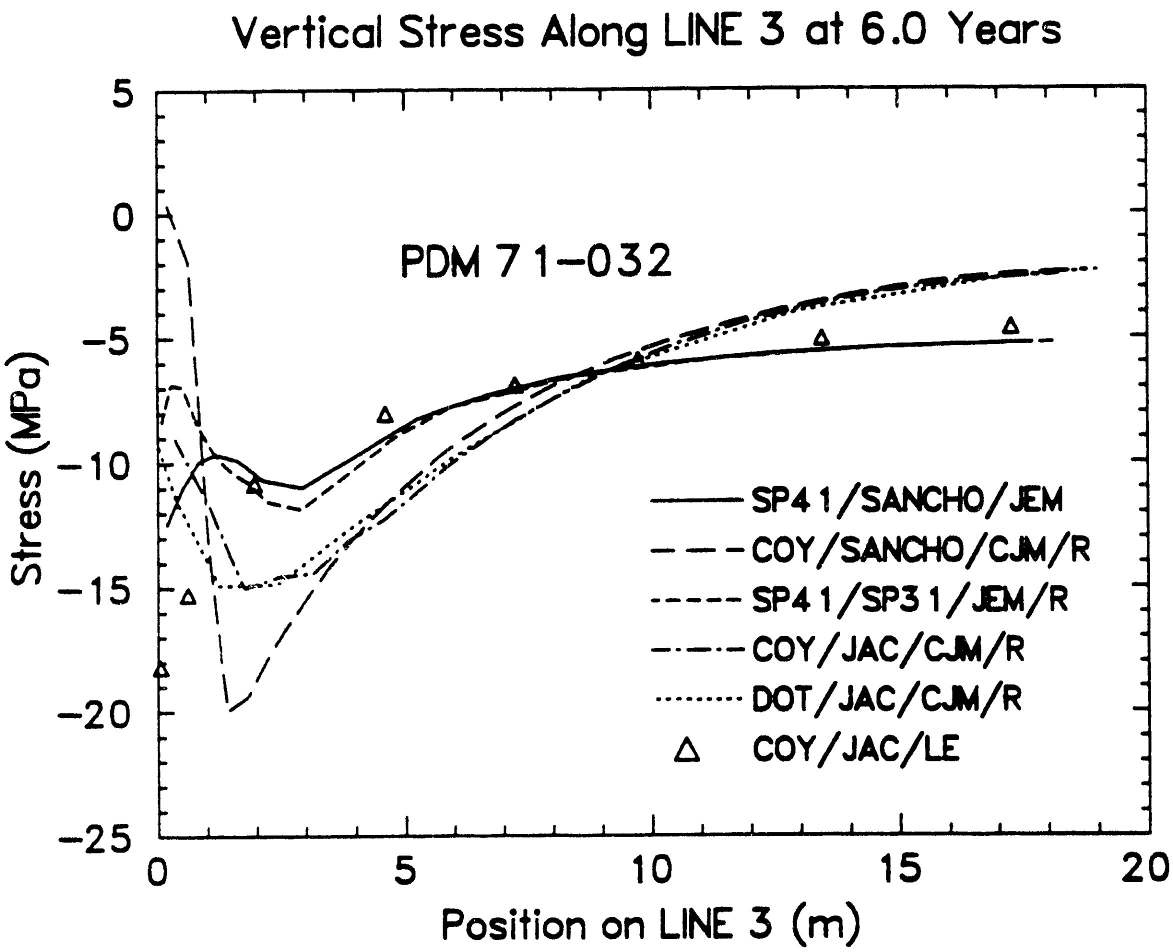

Figure 5-165. Comparison of Results for the Vertical Stres⁻ Along Line 3 (Figure 2-3) at 6 Yr, Third Analysis

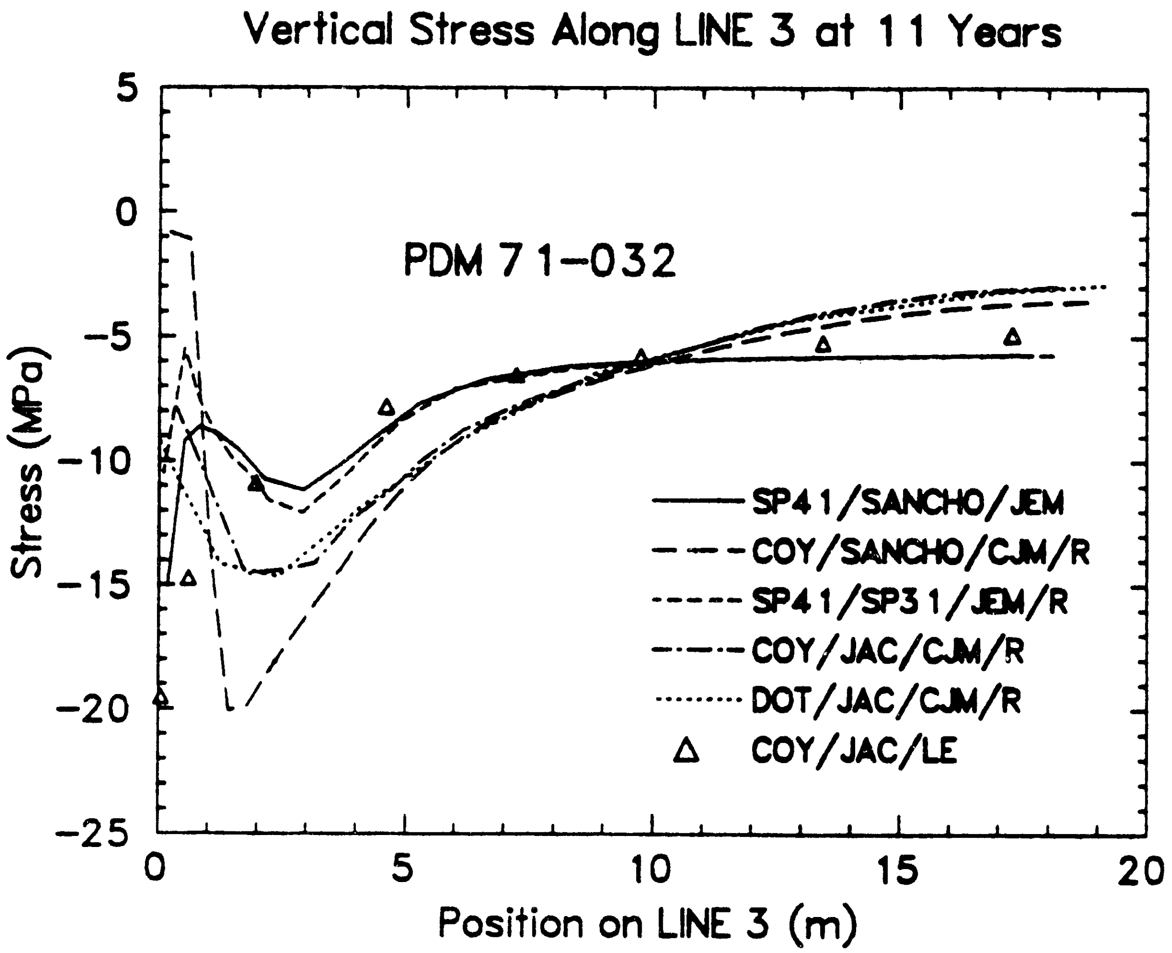

Figure 5-166. Comparison of Results for the Vertical Stress Along Line 3 (Figure 2-3) at 11 Yr, Third Analysis

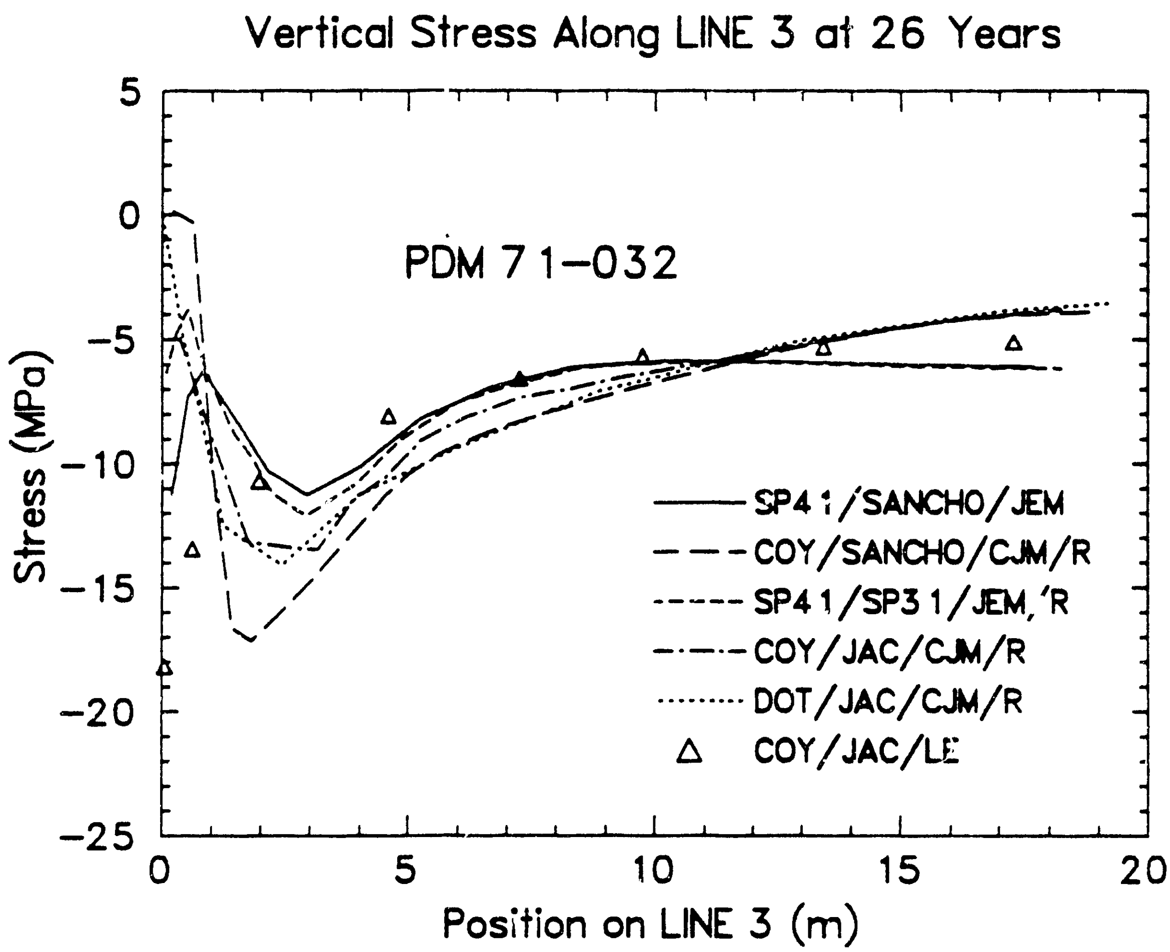

Figure 5-167. Comparison of Results for the Vertical Stress Along Line 3 (Figure 2-3) at 26 Yr, Third Analysis

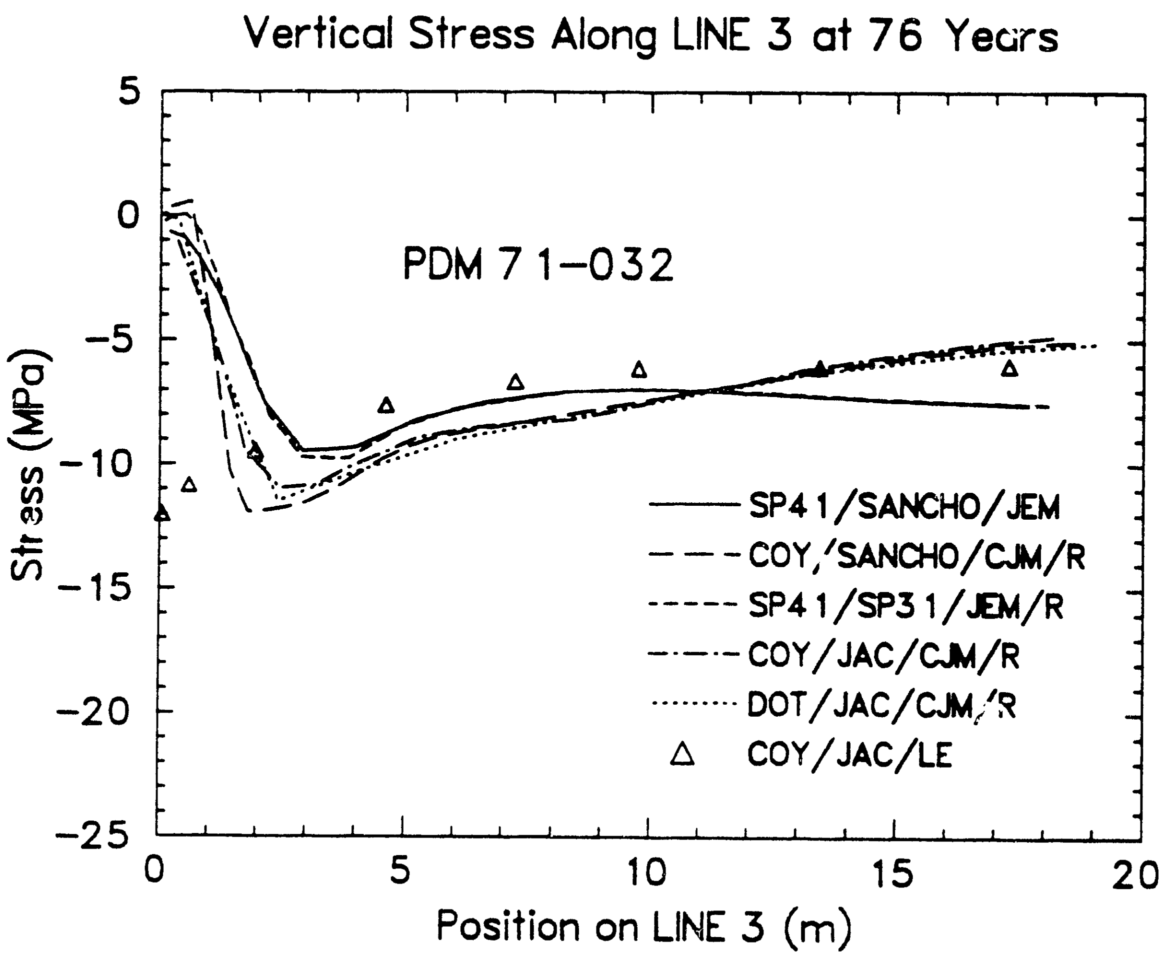

Figure 5-168. Comparison of Results for the Vertical Stress Along Line 3 (Figure 2-3) at 76 Yr, Third Analysis

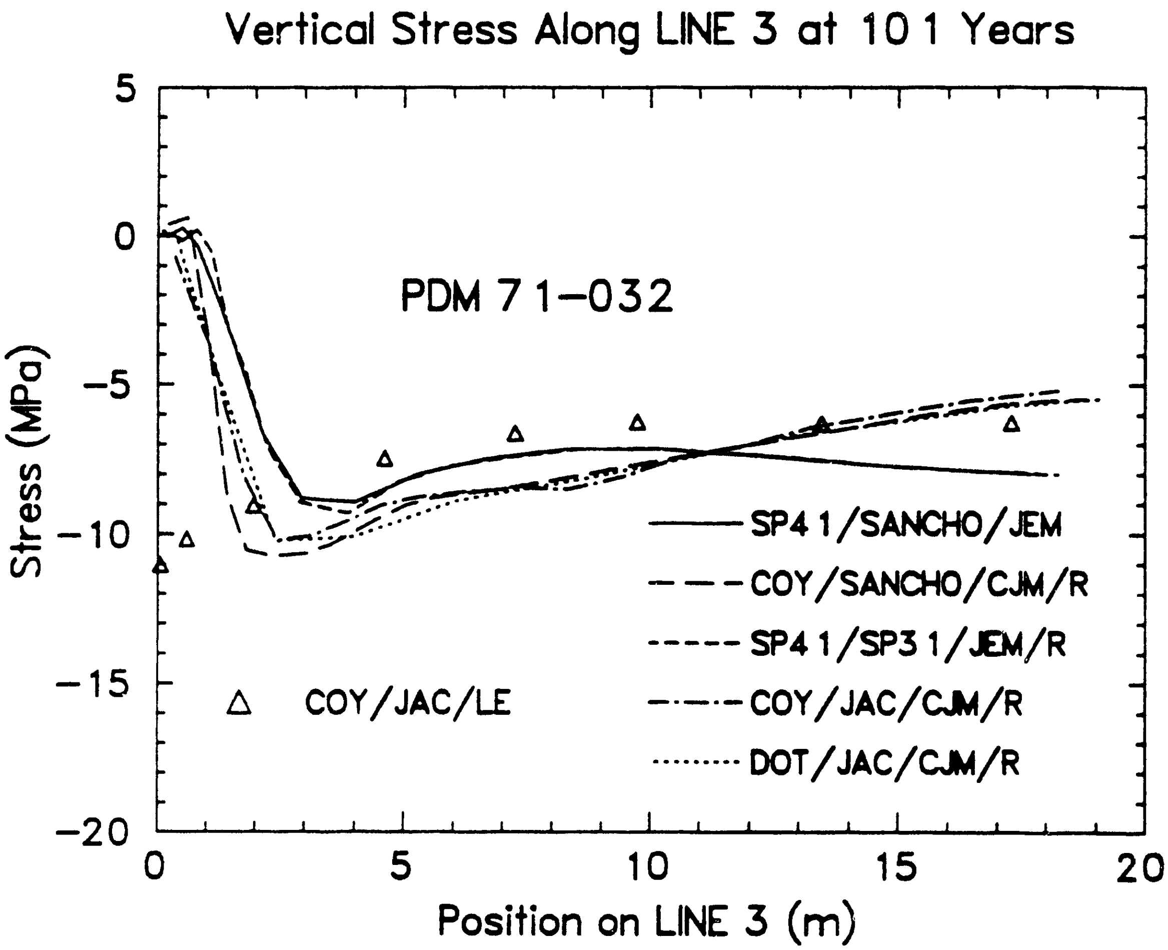

Figure 5-169. Comparison of Results for the Vertical Stress Along Line 3 (Figure 2-3) at 101 Yr, Third Analysis

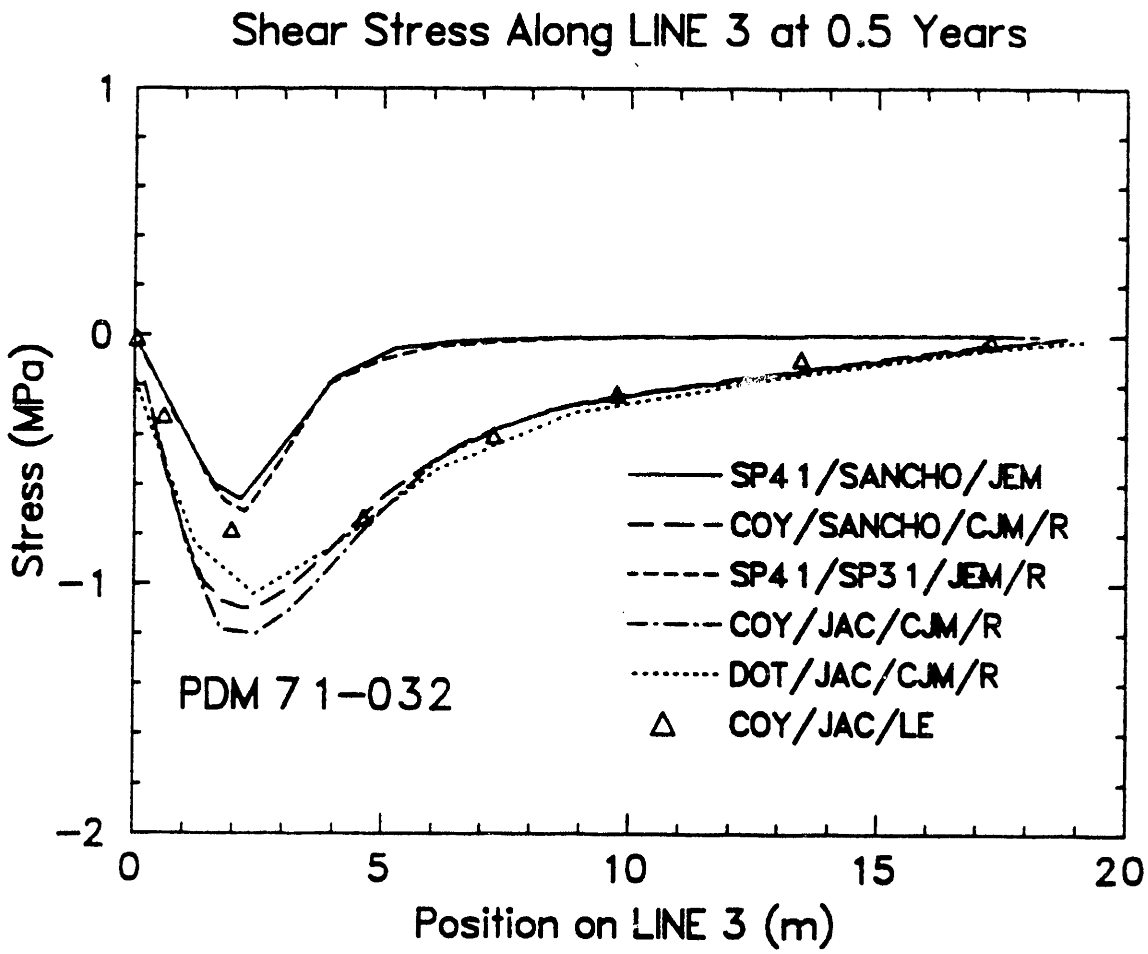

Figure 5-170. Comparison of Results for the Shear Stress Along Line 3 (Figure 2-3) at 0.5 Yr, Third Analysis

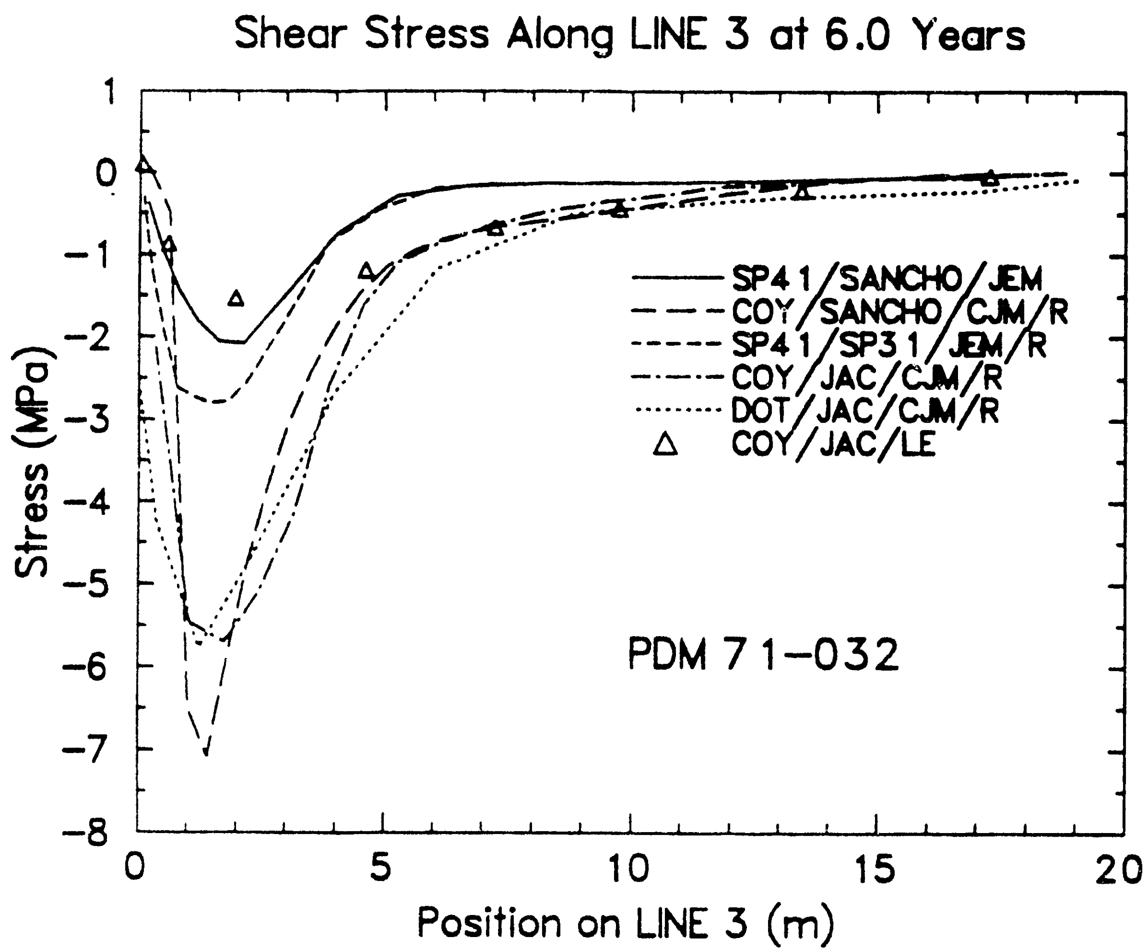

Figure 5-171. Comparison of Results for the Shear Stress Along Line 3 (Figure 2-3) at 6 Yr, Third Analysis

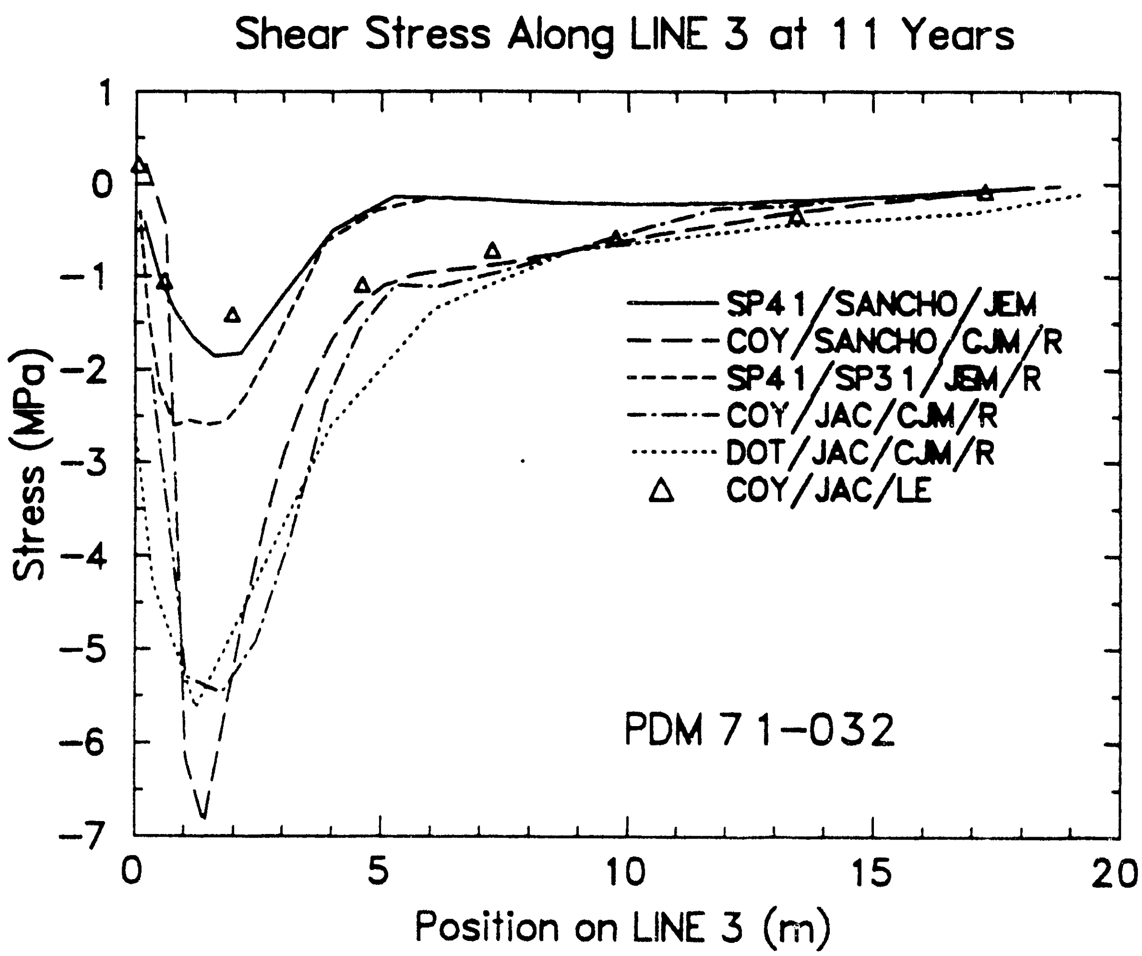

Figure 5-172. Comparison of Results for the Shear Stress Along Line 3 (Figure 2-3) at 11 Yr, Third Analysis

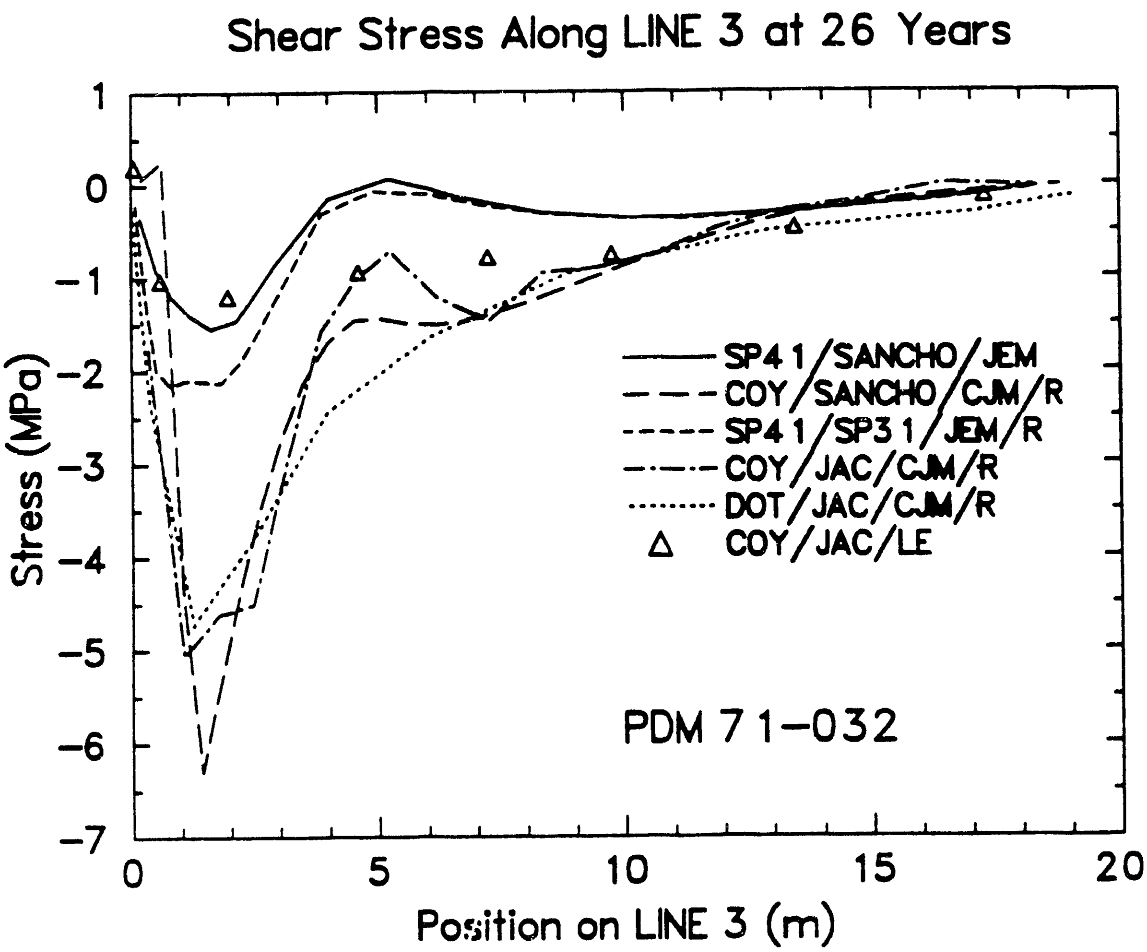

Figure 5-173. Comparison of Results for the Shear Stress Along Line 3 (Figure 2-3) at 26 Yr, Third Analysis

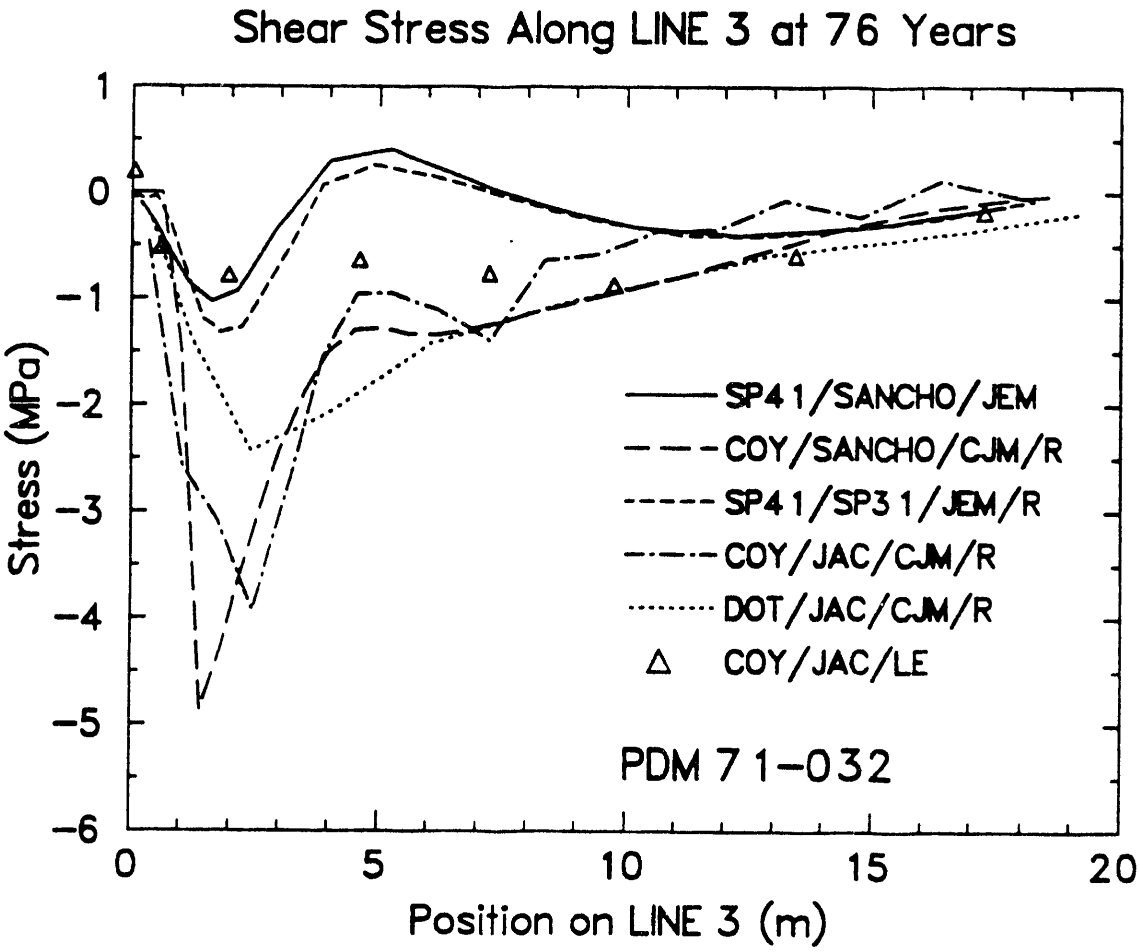

Figure 5-174. Comparison of Results for the Shear Stress Long Line 3 (Figure 2-3) at 76 Yr, Third Analysis

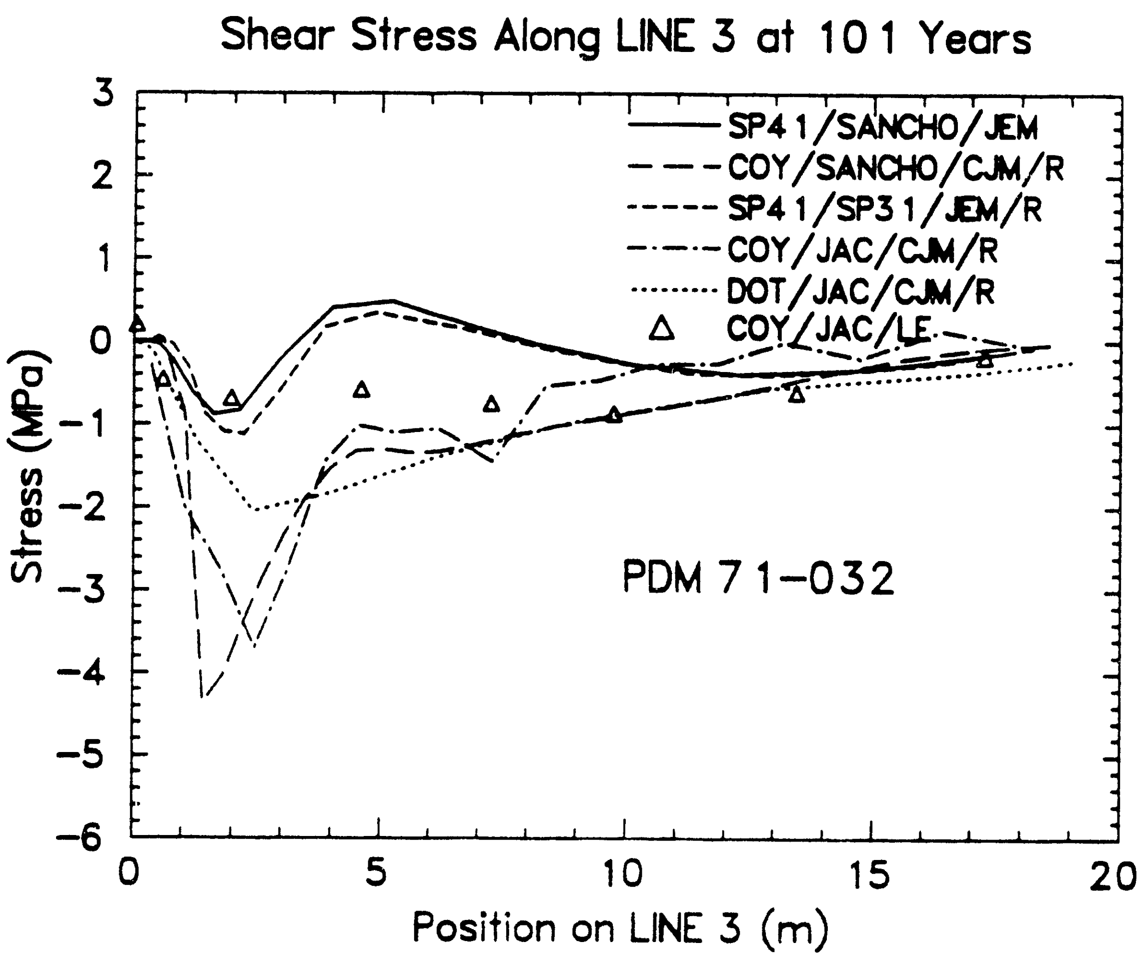

Figure 5-175. Comparison of Results for the Shear Stress Along Line 3 (Figure 2-3) at 101 Yr, Third Analysis

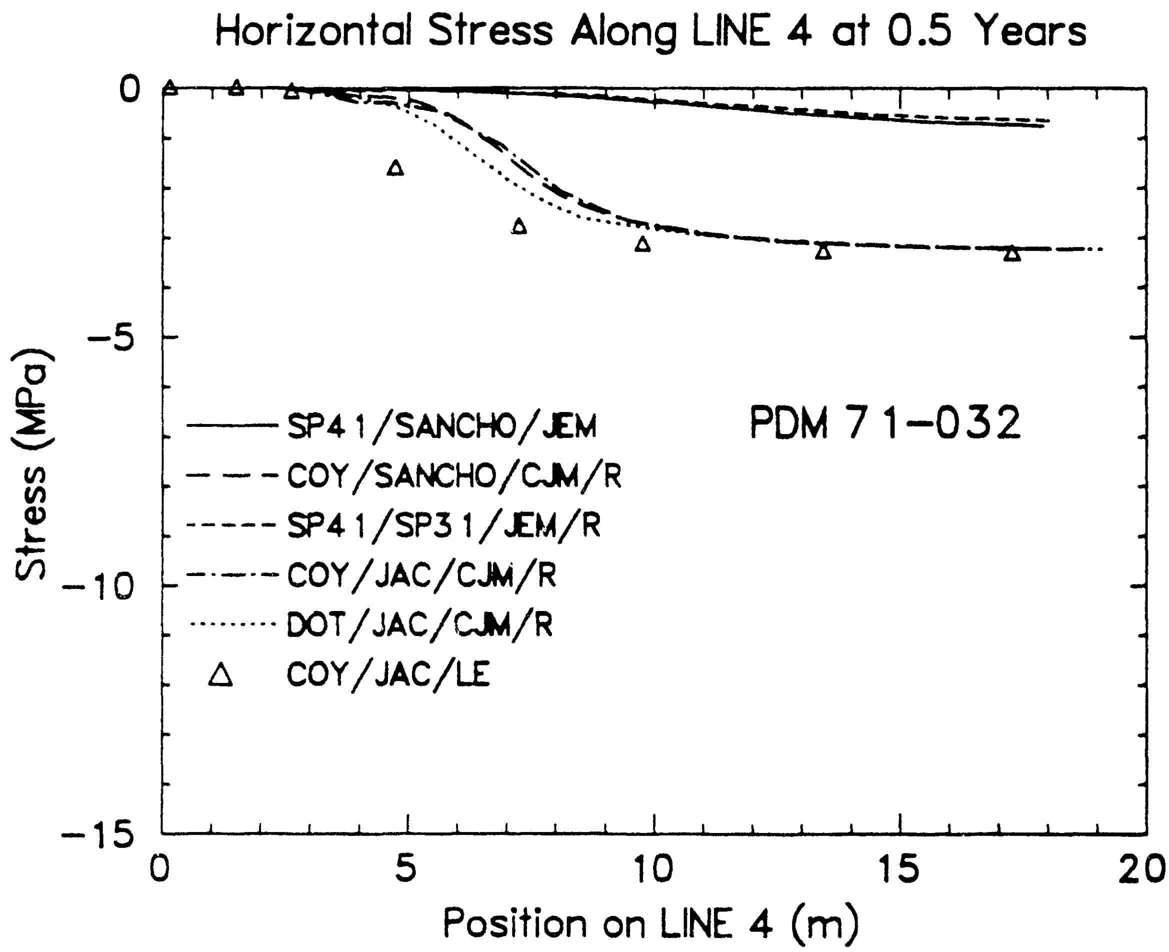

Figure 5-176. Comparison of Results for the Horizontal Stress Along Line 4 (Figure 2-3) at 0.5 Yr, Third Analysis

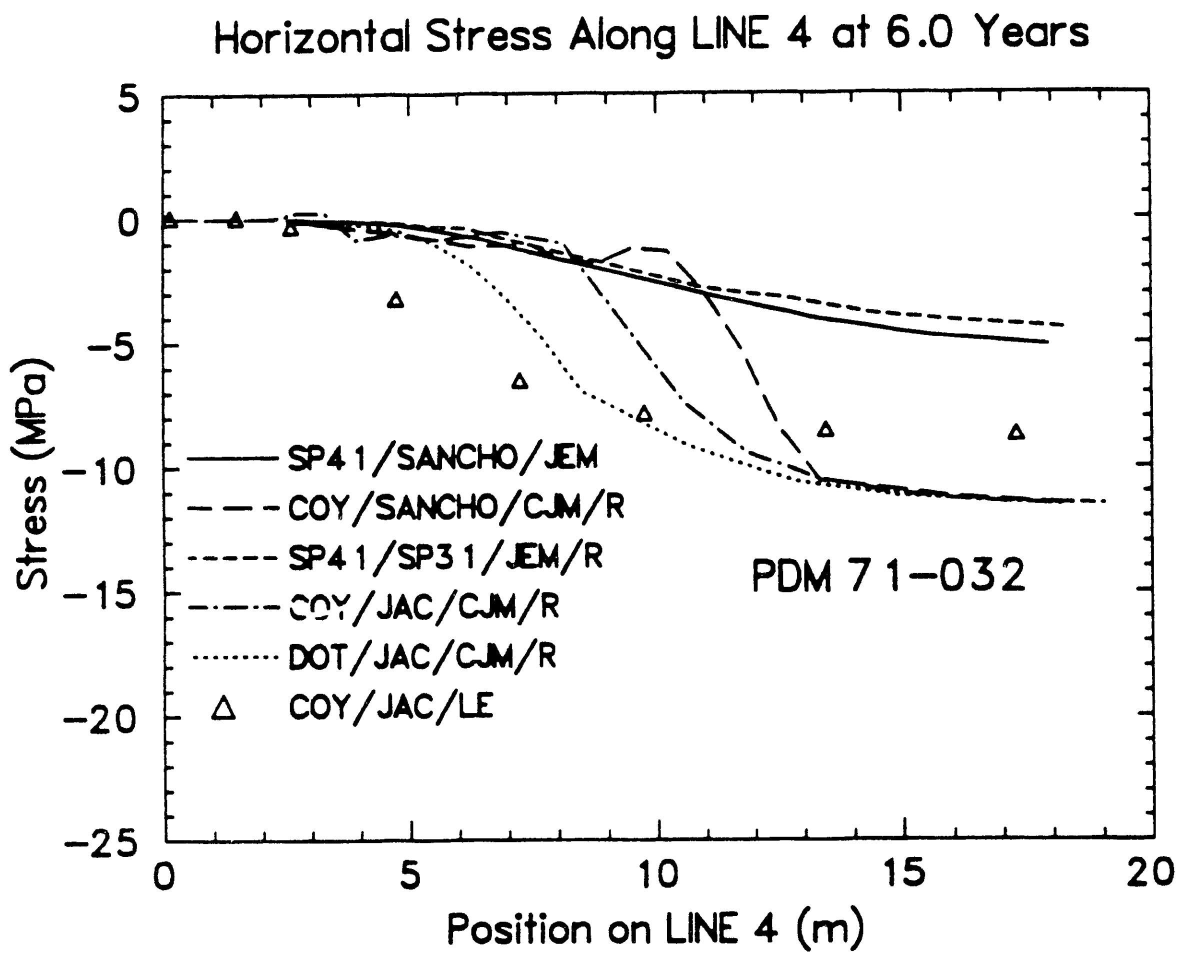

Figure 5-177. Comparison of Results for the Horizontal Stress Along Line 4 (Figure 2-3) at 6 Yr, Third Analysis

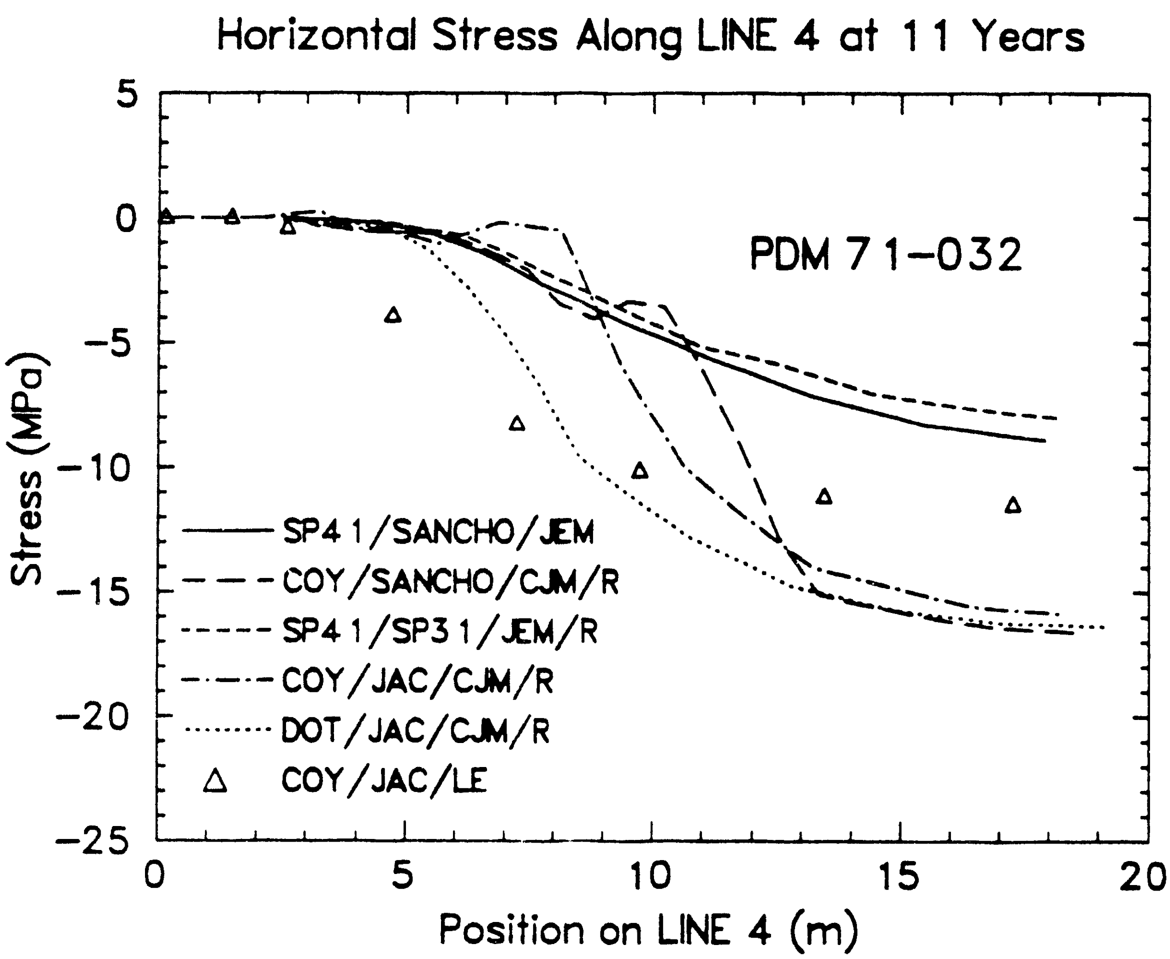

Figure 5-178. Comparison of Results for the Horizontal Stress Along Line 4 (Figure 2-3) at 11 Yr, Third Analysis

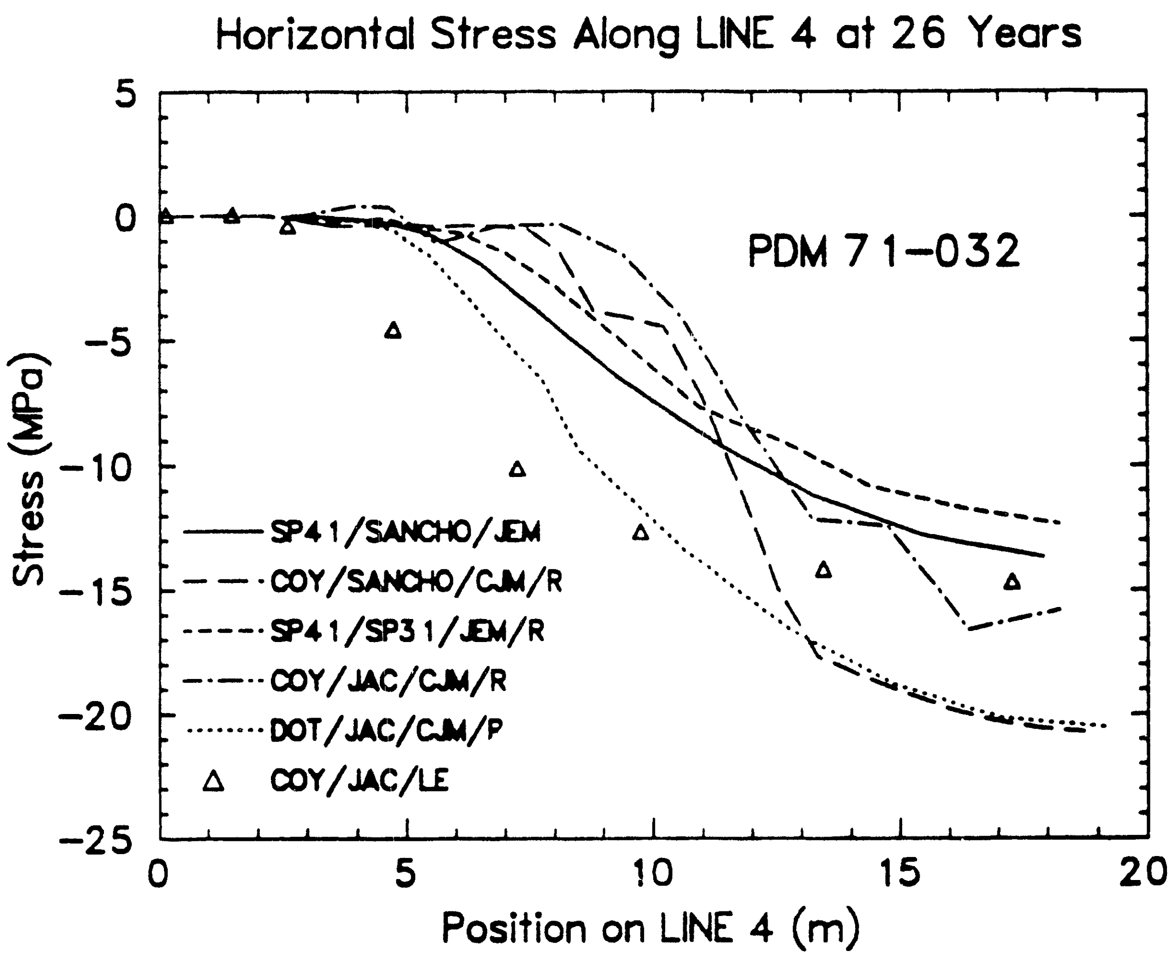

Figure 5-179. Comparison of Results for the Horizontal Stress Along Line 4 (Figure 2-3) at 26 Yr, Third Analysis

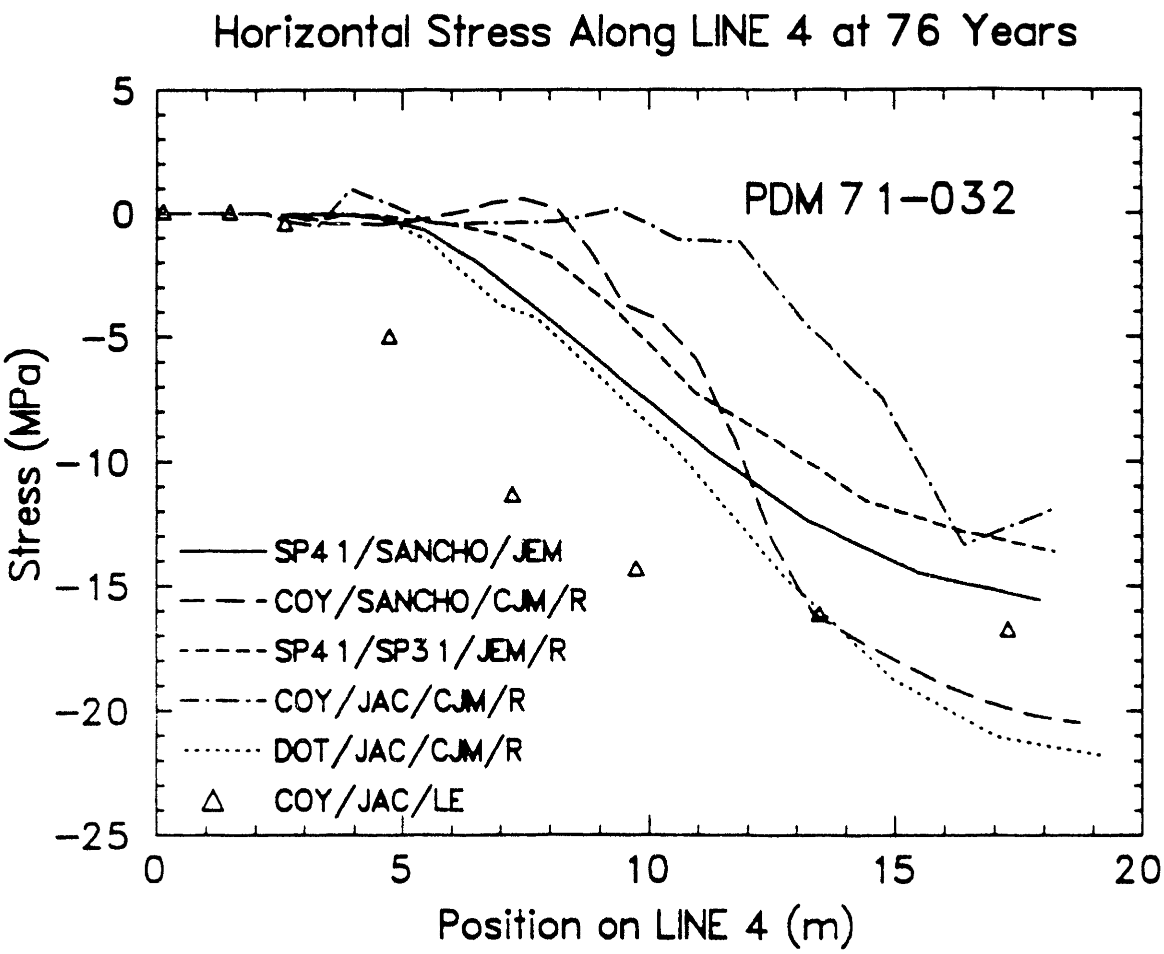

Figure 5-180. Comparison of Results for the Horizontal Stress Along Line 4 (Figure 2-3) at 76 Yr, Third Analysis

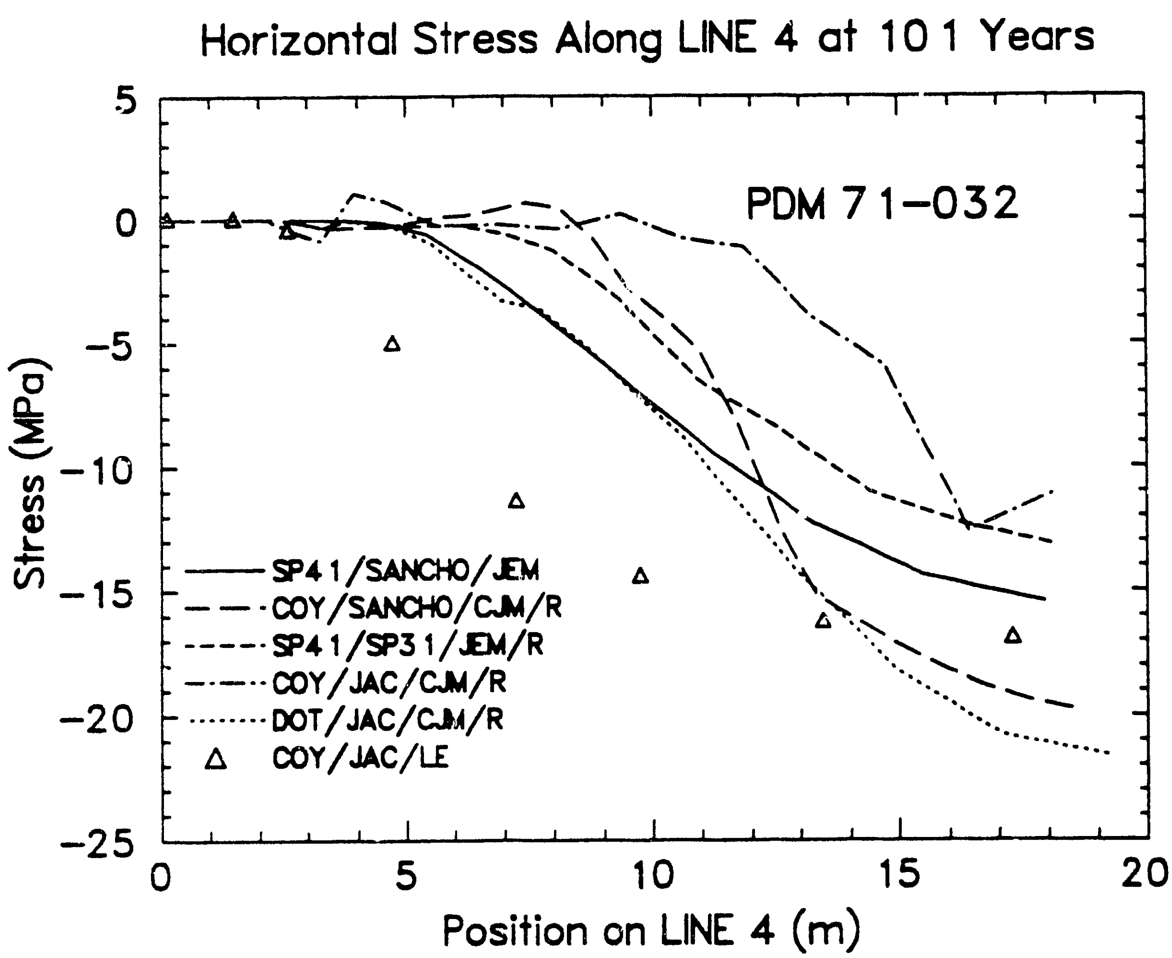

Figure 5-181. Comparison of Results for the Horizontal Stress Along Line 4 (Figure 2-3) at 101 Yr, Third Analysis

6.0 ASSESSMENT OF RESULTS

The final results, obtained after several iterations of analysis, are quite consistent for each model. Based on their review of the results from the second and third analyses, the PIs and the participant analysts have concluded that the small differences remaining in some of the comparisons between the various solutions for a given model are primarily a result of variations in the way the analysts approached the problem. The fact that several iterations of analysis were required to resolve most of the differences points to the fact that analysis using nonlinear material models is a difficult endeavor, and the results are somewhat analyst-dependent. Solving such problems with state-of-the-art numerical methods, requires considerable judgment and experience on the part of the analyst. Differences in the choices of meshing, type of element, number of time steps, and solution control variables (such as solution tolerance), all contribute in subtle ways to differences in the reported solution, even when using identical software. For this benchmark analysis, such differences may never be completely resolved. However, the agreement among the solutions is sufficiently good to conclude that it is highly unlikely that the remaining differences result from errors in the codes used.

The principal purpose of this exercise was to assist in verification of the codes and models for their intended use within the YMP and not to make any judgment regarding the validity of the models used. However, some differences in the behavior of the two jointed rock mass models were noted, and, for completeness, some comment is warranted. Differences are noted as early as upon "excavation". The JEM tends to predict somewhat larger displacements and smaller stresses than does the CJM. This is especially true in regions near the drift where shear stresses are larger. The reason for this is most likely related to the differences in the two models in the way the shear stress versus joint slip relationship is formulated. The normal stress versus joint closure behavior is nearly identical in the two models. The JEM tends to allow slip at lower stresses; thus, the stresses in regions where this occurs are lower, and the displacements are larger than those predicted by the CJM. It is worth noting, however, that this difference tends to be smaller after heating of the rock is well established. This is because the thermal expansion of rock tends to close the joints and prevent further slip.

The results from the calculations using the two jointed rock mass models were compared to those from the previous calculations using the elastic rock mass model. In the elastic model, the rock mass is treated as a homogeneous, isotropic, elastic material with a Young's modulus of one-half that of the intact rock. The reduction in modulus is intended to account for the lower stiffness of the rock mass because of the joints. It is interesting to note that the results from the elastic analysis compared quite favorably with those from the more complex jointed rock analyses, in some respects. For example, when comparing vertical displacements and vertical stresses, the elastic model was in good agreement with both jointed rock models. However, for horizontal stresses and displacements, agreement was not very good. The jointed rock models predicted significantly larger stresses and displacements than those predicted by the elastic model. The specified joint spacing for the jointed rock calculations was 1 m for the horizontal joints and 0.1 m for the vertical joints. Horizontal joints would mostly affect the vertical normal stresses and displacements whereas the vertical joints have a greater effect on the horizontal normal stress and displacement. Thus, it appears that the elastic calculation (using one-half the intact rock modulus) best simulates a rock with a 1-m joint spacing, at least if the joints have properties similar to those assumed for the jointed rock mass analysis. Decreasing the joint spacing by a factor of ten (horizontal to vertical) does not affect the corresponding stresses and displacements by same amount, i.e., there is a nonlinear effect. The horizontal stress and displacements predicted by the jointed rock models are approximately 20-50% larger than the elastic model prediction in regions near the drift. In the far field, at a distance greater than 20-50 m from the drift and heater, the jointed rock solutions agree very well with the elastic solution. This is, for the most part, a result of the imposed symmetry of the problem and the fact that both sets of solutions were required to satisfy the same boundary conditions.

7.0 CONCLUDING REMARKS

The intent of this report is to document the results from the jointed rock mass model analysis portion of the first benchmark exercise to an extent sufficient to support the verification of the codes involved. The results in this report were presented as they were received from the participants and plotted in a form that the authors judged to be convenient for comparisons. Sufficient detail is provided for readers to assess the results and their implications.

Some further observations can be made about the results of this portion of the benchmark exercise. First, one of the objectives of the benchmark exercise is to uncover any errors in the numerical implementation of the codes and models used. As a result of the jointed rock mass analysis portion of the benchmark exercise, one error in the CJM implementation was discovered and corrected. In addition, the initial analyses lead to further improvements in the numerical methods incorporated in the model subroutine. Thus, as a result of the exercise, a significantly more efficient implementation of the model is now available. Second, this portion of the benchmark exercise has lead to a successful demonstration of the capability to perform complex, nonlinear thermomechanical analyses of underground openings under conditions typical of those expected in a nuclear waste repository. While this does not indicate that the models used here are the same as those necessary to model the Yucca Mountain behavior (i.e., exploratory shaft evaluations are planned), it is sufficient to indicate that a variety of codes can be used for thermomechanical analyses of repository behavior. Finally, as noted in the evaluation of the results of this portion of the benchmark exercise (Section 6), the results obtained with nonlinear jointed rock mass models may depend somewhat on the analyst's approach to the problem and their experience with the codes used. This is in contrast to the thermal (Costin and Bauer, 1989) and thermoelastic (Bauer and Costin, 1990) analyses that were performed as the first two parts of this benchmark exercise in which it was shown that the results were not sensitive to the analyst's choice of meshes or numerical control variables. Thus it might be concluded that, when using nonlinear methods, greater attention to the way the problem is addressed is necessary. For critical design or performance calculations, more than one set of independent analyses should be performed, as operator influences upon the results are inherent. Some of the operator influence could possibly be better understood through systematic studies of, for example, mesh refinement, convergence tolerance evaluations, etc. The work done to date does not allow one to prescribe a "correct" analysis procedure which obviates the need for redundant calculations for critical situations.

8.0 REFERENCES

Barton, N., "Modelling Rock Joint Behavior from In Situ Block Tests: Implications for Nuclear Waste Repository Design, ONWI-308, prepared by Terra Tek Engineering, Salt Lake City, UT, for the Office of Nuclear Waste Isolation, Battelle Memorial Institute, Columbus, OH, 1982. (HQS.880517.2252)

Bauer, S. J., and L. S. Costin, "YMP Thermal and Mechanical Codes First Benchmark Exercise Part II: Elastic Analysis," SAND89-0757, Sandia National Laboratories, Albuquerque, NM, 1990. (NNA.900515.0143)

Biffle, J. H., "JAC - A Two-Dimensional Finite Element Computer Program for the Non-Linear Quasistatic Response of Solids with the Conjugate Gradient Method," SAND81-0998, Sandia National Laboratories, Albuquerque, NM, 1984. (HQS.880517.2257)

Blanford, M. L., and S. W. Key, "The Joint Empirical Model - an Equivalent Continuum Model for Jointed Rock Masses," SAND87-7072, Sandia National Laboratories, Albuquerque, NM, 1991. (NNA.910416.0046)

Bowden, F. P., and D. Tabor, Friction and Lubrication of Solids, Oxford University Press, New York, NY, 1954. (NNA.910617.0056)

Chen, E. P., "A Computational Model for Jointed Media with Orthogonal Sets of Joints," SAND86-1122, Sandia National Laboratories, Albuquerque, NM, 1987. (NNA.891020.0180)

Costin, L. S., and S. J. Bauer, "YMP Thermal and Mechanical Codes First Benchmark Exercise Part I: Thermal Analysis," SAND88-1221, Sandia National Laboratories, Albuquerque, NM, 1989. (NNA.900919.0186)

NRC (U.S. Nuclear Regulatory Commission), "Final Technical Position on Documentation of Computer Codes for High Level Waste Management," NUREG-0856, 1983. (NNA.871104.0034)

Stone, C. M., R. D. Krieg, and Z. E. Beisinger, "SANCHO - A Finite Element Computer Program for the Quasistatic, Large Deformation, Inelastic Response of Two-Dimensional Solids, SAND84-2618, Sandia National Laboratories, Albuquerque, NM, 1985. (HQS.880517.2351)

Appendix A: Comparison of Report Data with Those in the RIB and SEPDB

All material property and design configuration data used in the benchmark calculations reported in this document were taken from the NNWSI Reference Information Base, Version 2.002 (draft). For specific values of the data used see Appendix A, Section 4 of Costin and Bauer (1989). This report contains no data taken from or that should be included in the SEPDB.

DISTRIBUTION LIST

1 J. W. Bartlett, Director (RW-1)
Office of Civilian Radioactive
Waste Management
U.S. Department of Energy
1000 Independence Avenue, S.W.
Washington, D.C. 20585

1 F. G. Peters, Deputy Director (RW-2)
Office of Civilian Radioactive
Waste Management
U.S. Department of Energy
1000 Independence Avenue, S.W.
Washington, D.C. 20585

1 T. H. Isaacs (RW-4)
Office of Strategic Planning
and International Programs
Office of Civilian Radioactive
Waste Management
U.S. Department of Energy
1000 Independence Avenue, S.W.
Washington, D.C. 20585

1 J. D. Saltzman (RW-5)
Office of External Relations
Office of Civilian Radioactive
Waste Management
U.S. Department of Energy
1000 Independence Avenue, S.W.
Washington, D.C. 20585

1 Samuel Rousso (RW-10)
Office of Program and Resources
Management
Office of Civilian Radioactive
Waste Management
U.S. Department of Energy
1000 Independence Avenue, S.W.
Washington, D.C. 20585

1 J. C. Bresee (RW-10)
Office of Civilian Radioactive
Waste Management
U.S. Department of Energy
1000 Independence Avenue, S.W.
Washington, D.C. 20585

1 C. P. Gertz (RW-20)
Office of Geologic Disposal
Office of Civilian Radioactive
Waste Management
U.S. Department of Energy
1000 Independence Avenue, S.W.
Washington, D.C. 20585

1 S. J. Brocoum (RW-22)
Analysis and Verification Division
Office of Civilian Radioactive
Waste Management
U.S. Department of Energy
1000 Independence Avenue, S.W.
Washington, D.C. 20585

1 D. D. Shelor (RW-30)
Office of Systems and Compliance
Office of Civilian Radioactive
Waste Management
U.S. Department of Energy
1000 Independence Avenue, S.W.
Washington, D.C. 20585

1 J. Roberts (RW-33)
Office of Civilian Radioactive
Waste Management
U.S. Department of Energy
1000 Independence Avenue, S.W.
Washington, D.C. 20585

1 G. J. Parker (RW-332)
Office of Civilian Radioactive
Waste Management
U.S. Department of Energy
1000 Independence Avenue, S.W.
Washington, D.C. 20585

1 Associate Director (RW-40)
Office of Storage and Transportation
Office of Civilian Radioactive
Waste Management
U.S. Department of Energy
1000 Independence Avenue, S.W.
Washington, D.C. 20585

1 Associate Director (RW-50)
Office of Contract Business
Management
Office of Civilian Radioactive
Waste Management
U.S. Department of Energy
1000 Independence Avenue, S.W.
Washington, D.C. 20585

1 C. G. Russomanno (RW-52)
Office of Civilian Radioactive
Waste Management
U.S. Department of Energy
1000 Independence Avenue, S.W.
Washington, D.C. 20585

1 D. U. Deere, Chairman
Nuclear Waste Technical
Review Board
1100 Wilson Blvd. #910
Arlington, VA 22209-2297

1 Dr. Clarence R. Allen
Nuclear Waste Technical Review Board
1000 E. California Blvd.
Pasadena, CA 91106

1 Dr. John E. Cantlon
Nuclear Waste Technical Review Board
1795 Bramble Dr.
East Lansing, MI 48823

1 Dr. Melvin W. Carter
Nuclear Waste Technical Review Board
4621 Ellisbury Dr., N.E.
Atlanta, GA 30332

1 Dr. Donald Langmuir
Nuclear Waste Technical Review Board
109 So. Lookout Mountain Cr.
Golden, CO 80401

1 Dr. D. Warner North
Nuclear Waste Technical Review Board
Decision Focus, Inc.
4984 El Camino Real
Los Altos, CA 94062

1 Dr. Dennis L. Price
Nuclear Wast Technical Review Board
1011 Evergreen Way
Blacksburg, VA 24060

1 Dr. Ellis D. Verink
Nuclear Waste Technical Review Board
4401 N.W. 18th Place
Gainesville, FL 32605

5 C. P. Gertz, Project Manager
Yucca Mountain Project Office
U.S. Department of Energy
P.O. Box 98608--MS 523
Las Vegas, NV 89193-8608

1 C. L. West, Director
Office of External Affairs
DOE Field Office, Nevada
U.S. Department of Energy
P.O. Box 98518
Las Vegas, NV 89193-8518

12 Technical Information Officer
DOE Field Office, Nevada
U.S. Department of Energy
P.O. Box 98518
Las Vegas, NV 89193-8518

1 P. K. Fitzsimmons, Director
Health Physics & Environmental
Division
DOE Field Office, Nevada
U.S. Department of Energy
P.O. Box 98518
Las Vegas, NV 89193-8518

1 D. R. Elle, Director
Environmental Protection Division
DOE Field Office, Nevada
U.S. Department of Energy
P.O. Box 98518
Las Vegas, Nv 89193-8518

1 Repository Licensing & Quality
Assurance Project Directorate
Division of Waste Management
U.S. Nuclear Regulatory Commission
Washington, D.C. 20555

1 Senior Project Manager for Yucca
Mountain Repository Project Branch
Division of Waste Management
U.S. Nuclear Regulatory Commission
Washington, D.C. 20555

1 NRC Document Control Desk
Division of Waste Management
U.S. Nuclear Regulatory Commission
Washington, D.C. 20555

1 P. T. Prestholt
NRC Site Representative
301 E. Stewart Ave.
Las Vegas, NV 89101

1 E. P. Binnall
Field Systems Group Leader
Building 50B/4235
Lawrence Berkeley Laboratory
Berkeley, CA 94720

1 Center for Nuclear Waste
Regulatory Analyses
6220 Culebra Road
Drawer 28510
San Antonio, TX 78284

3 L. J. Jardine
Technical Project Officer for YMP
Mail Stop L-204
Lawrence Livermore National Laboratory
P.O. Box 808
Livermore, CA 94550

4 R. J. Herbst
Technical Project Officer for YMP
N-5, Mail Stop J521
Los Alamos National Laboratory
P.O. Box 1663
Los Alamos, NM 87545

1 H. N. Kalia
Exploratory Shaft Test Manager
Los Alamos National Laboratory
Mail Stop 527
101 Convention Center Dr.
Suite 820
Las Vegas, NV 89109

1 J. F. Divine
Assistant Director for Engineering Geology
U.S. Geological Survey
106 National Center
12201 Sunrise Valley Dr.
Reston, VA 22092

6 L. R. Hayes
Technical Project Officer
Yucca Mountain Project Branch--MS 425
U.S. Geological Survey
P.O. Box 25046
Denver, CO 80225

1 V. R. Schneider
Asst. Chief Hydrologist--MS 414
Office of Program Coordination & Technical Support
U.S. Geological Survey
12201 Sunrise Valley Drive
Reston, VA 22092

1 R. B. Raup, Jr.
Geological Division Coordinator
MS 913
Yucca Mountain Project
U.S. Geological Survey
P.O. Box 25046
Denver, CO 80225

1 D. H. Appel, Chief
Hydrologic Investigations Program
MS 421
U.S. Geological Survey
P.O. Box 25046
Denver, CO 80225

1 E. J. Helley
Branch of Western Regional Geology
MS 427
U.S. Geological Survey
345 Middlefield Road
Menlo Park, CA 94025

1 Chief
Nevada Operations Office
U.S. Geological Survey
101 Convention Center Drive
Suite 860, MS 509
Las Vegas, NV 89109

1 D. Zesiger
U.S. Geological Survey
101 Convention Center Dr.
Suite 860 - MS509
Las Vegas, NV 89109

1 R. V. Watkins, Chief
Project Planning and Management
U.S. Geological Survey
P.O. Box 25046
421 Federal Center
Denver, CO 80225

1 A. L. Flint
U.S. Geological Survey
MS 721
P.O. Box 327
Mercury, NV 89023

1 D. A. Beck
U.S. Geological Survey
1500 E. Tropicana, Suite 201
Las Vegas, NV 89119

1 P. A. Glancy
U.S. Geological Survey
Federal Building, Room 224
Carson City, NV 89701

1 Sherman S. C. Wu
Branch of Astrogeology
U.S. Geological Survey
2255 N. Gemini Dr.
Flagstaff, AZ 86001

1 J. H. Sass
Branch of Tectonophysics
U.S. Geological Survey
2255 N. Gemini Dr.
Flagstaff, AZ 86001

1 DeWayne A. Campbell
Technical Project Officer for YMP
Bureau of Reclamation
Code D-3790
P.O. Box 25007
Denver, CO 80225

1 S. M. Dash
Science Applications International Corp.
14062 Denver West Parkway, Suite 255
Golden, CO 80401

1 K. W. Causseaux
NHP Reports Chief
U.S. Geological Survey
421 Federal Center
P.O. Box 25046
Denver, CO 80225

1 V. M. Glanzman
U.S. Geological Survey
913 Federal Center
P.O. Box 25046
Denver, CO 80225

1 J. H. Nelson
Technical Project Officer for YMP
Science Applications International Corp.
101 Convention Center Dr.
Suite 407
Las Vegas, NV 89109

2 SAIC-T&MSS Library
Science Applications International Corp.
101 Convention Center Dr.
Suite 407
Las Vegas, NV 89109

1 Elaine Ezra
YMP GIS Project Manager
EG&G Energy Measurements, Inc.
Mail Stop D-12
P.O. Box 1912
Las Vegas, NV 89125

1 R. E. Jackson, Program Manager
Roy F. Weston, Inc.
955 L'Enfant Plaza, Southwest
Washington, D.C. 20024

1 Technical Information Center
Roy F. Weston, Inc.
955 L'Enfant Plaza, Southwest
Washington, D.C. 20024

1 D. Hedges, Vice President,
Quality Assurance
Roy F. Weston, Inc.
4425 Spring Mountain Road, Suite 300
Las Vegas, Nevada 89102

1 D. L. Fraser, General Manager
Reynolds Electrical & Engineering Co.
Mail Stop 555
P.O. Box 98521
Las Vegas, NV 89193-8521

1 R. F. Pritchett
Technical Project Officer for YMP
Reynolds Electrical & Engineering Co.
MS 408
P.O. Box 98521
Las Vegas, NV 89193-8521

1 B. W. Colston
General Manager & President
Las Vegas Branch
Raytheon Services Nevada
Mail Stop 416
P.O. Box 95487
Las Vegas, NV 89193-5487

1 R. L. Bullock
Technical Project Officer for YMP
Raytheon Services Nevada
Suite P250, MS 403
101 Convention Center Dr.
Las Vegas, NV 89109

1 R. E. Lowder
Technical Project Officer for YMP
MAC Technical Services
101 Convention Center Drive
Suite 1100
Las Vegas, NV 89109

1 C. K. Hastings, Manager
PASS Program
Pacific Northwest Laboratories
P.O. Box 999
Richland, WA 99352

1 A. T. Tamura
Science and Technology Division
Office of Scientific and Technical Information
U.S. Department of Energy
P.O. Box 62
Oak Ridge, TN 37831

1 Carlos G. Bell, Jr.
Professor of Civil Engineering
Civil and Mechanical Engineering Department
University of Nevada, Las Vegas
4505 South Maryland Parkway
Las Vegas, NV 89154

1 C. F. Costa, Director
Nuclear Radiation Assessment Division
U.S. Environmental Protection Agency
Environmental Monitoring Systems Laboratory
P.O. Box 93478
Las Vegas, NV 89193-3478

1 ONWI Library
Battelle Columbus Laboratory
Office of Nuclear Waste Isolation
505 King Avenue
Columbus, OH 43201

1 T. Hay, Executive Assistant
Office of the Governor
State of Nevada
Capitol Complex
Carson City, NV 89710

3 R. R. Loux, Jr.
Executive Director
Nuclear Waste Project Office
State of Nevada
Evergreen Center, Suite 252
1802 North Carson Street
Carson City, NV 89710

1 C. H. Johnson
Technical Program Manager
Nuclear Waste Project Office
State of Nevada
Evergreen Center, Suite 252
1802 North Carson Street
Carson City, NV 89710

1 John Fordham
Water Resources Center
Desert Research Institute
P.O. Box 60220
Reno, NV 89506

1 Dr. Martin Mifflin
Water Resources Center
Desert Research Institute
2505 Chandler Avenue
Suite 1
Las Vegas, NV 89120

1 Eric Anderson
Mountain West Research-Southwest Inc.
2901 N. Central Ave. #1000
Phoenix, AZ 85012-2730

1 Department of Comprehensive Planning
Clark County
225 Bridger Avenue, 7th Floor
Las Vegas, NV 89155

1 Planning Department
Nye County
P.O. Box 153
Tonopah, NV 89049

1 Lincoln County Commission
Lincoln County
P.O. Box 90
Pioche, NV 89043

5 Judy Foremaster
City of Caliente
P.O. Box 158
Caliente, NV 89008

1 Economic Development Department
City of Las Vegas
400 East Stewart Avenue
Las Vegas, NV 89101

1 Community Planning & Development
City of North Las Vegas
P.O. Box 4086
North Las Vegas, NV 89030

1 Director of Community Planning
City of Boulder City
P.O. Box 367
Boulder City, NV 89005

1 Commission of the European Communities
200 Rue de la Loi
B-1049 Brussels
BELGIUM

2 M. J. Dorsey, Librarian
YMP Research and Study Center
Reynolds Electrical & Engineering Co., Inc.
MS 407
P.O. Box 98521
Las Vegas, NV 89193-8521

1 Amy Anderson
Argonne National Laboratory
Building 362
9700 So. Cass Ave.
Argonne, IL 60439

1 M. P. Hardy
J.F.T. Agapito & Associates
715 Horizon Dr., Suite 300
Grand Junction, CO 81506

1 S. Petney
RE/SPEC Inc.
4775 Indian School Rd. NE
Suite 300
Albuquerque, NM 87108

1 D. Labreche
RE/SPEC Inc.
4775 Indian School Rd. NE
Suite 300
Albuquerque, NM 87108

1 D. Parrish
RE/SPEC Inc.
4775 Indian School Rd. NE
Suite 300
Albuquerque, NM 87108

1	6300	T. O. Hunter
1	6310	T. E. Blejwas, Actg.
1	6310A	L. E. Shephard
1	6311	A. L. Stevens
1	6312	F. W. Bingham
5	6313	L. S. Costin
1	6313	S. J. Bauer
1	6313	J. Pott
1	6313	E. E. Ryder
1	6315	F. B. Nimick, Actg.
1	6316	R. P. Sandoval
1	6317	S. Sinnock
2	6318	R. J. Macer for 100/124231/SAND89-1639/QA
1	6319	R. R. Richards
1	1420	W. J. Camp
1	1425	J. H. Biffle
1	1425	J. Jung
1	1500	E. H. Barsis
1	1510	J. C. Cummings
1	1514	H. S. Morgan
1	1514	E. P. Chen
1	1514	J. F. Holland
1	1514	J. R. Koteras
1	1514	R. L. Johnson
5	3141	S. A. Landenberger
8	3145	Document Processing for DOE/OSTI
3	3151	G. C. Claycomb
20	6341	WMT Library
1	6410	D. J. McCloskey, Actg.
1	8523-2	Central Technical Files

END

DATE FILMED

01/02/92